A THESIS

FOR THE DEGREE OF DOCTOR OF PHYLOSOPHY

MOLECULAR INSIGHT INTO THE IMMUNE SYSTEM OF THE DISK ABALONE (*Haliotis discus discus*): cDNA MICROARRAY, TRANSCRIPTIONAL PROFILING AND FUNCTIONAL ASPECTS

Mahanama De Zoysa

Department of Aquatic Life Medicine

GRADUATE SCHOOL

JEJU NATIONAL UNIVERSITY

2010-02

MOLECULAR INSIGHT INTO THE IMMUNE SYSTEM OF THE DISK ABALONE (*Haliotis discus discus*): cDNA MICROARRAY, TRANSCRIPTIONAL PROFILING AND FUNCTIONAL ASPECTS

Mahanama De Zoysa

(Supervised by Professor Jehee Lee)

A thesis submitted in partial fulfillment of the requirement for the degree of

DOCTOR OF PHILOSOPHY

2010-02

The thesis has been examined and approved by

Thesis Director, Gi-Young Kim, Professor of Marine Biomedical Sciences

Choon-Bok Song, Professor of Marine Biomedical Sciences

Moon-Soo Heo, Professor of Marine Biomedical Sciences

Joon Bum Jeong, Professor of Marine Biomedical Sciences

Jehee Lee, Professor of Marine Biomedical Sciences

2010-01-01

Date

Department of Aquatic Life Medicine
GRADUATE SCHOOL
JEJU NATIONAL UNIVERSITY
REPUBLIC OF KOREA

CONTENTS

요약문

전복의 초기 면역 시스템은 다른 무척추동물들에서 처럼 주된 방어체계로 사용된다. 따라서, 분자적 수준에서 다양한 미생물의 공격에 대한 면역 응답 및 그 기작을 이해하는 것이 중요하다. 본 연구에서는, 까막전복으로부터 면역에 관련된 유전자들을 분자적 수준에서 이해하기 위해 cDNA microarray, 전사 profiling 및 각각의 단백질들에 대한 기능적 특성 분석을 수행함으로써 전복의 면역 응답 체계를 이해하고자 하였다.

본 연구에서는, 까막전복의 cDNA library로부터 4.2 K의 cDNA chip을 제작하였고, cDNA microarray를 이용한 mRNA 차원에서의 전사 수준 분석은 까막전복에 혼합 박테리아 (*Vibrio alginolyticus, Vibrio parahemolyticus, Listeria monocytogenes*) 50 μL (5x10^7 cells/mL)와 viral hemorrhagic septicemia virus (VHSV) 50 μL (1 X 108 pfu/ml)를 각각 주입하여 면역 공격 실험을 통해 수행하였다. 면역 공격에 대한 전사 응답 반응은 박테리아와 VHSV의 공격 실험 후 24시간째에 아가미, 소화관, 그리고 혈구에서 조사하였다.

박테리아가 공격된 전복에서는, 아가미에서 68개 (1.6%)와 소화관에서112개 (2.7%)의 전사 상의 변화를 확인함으로써 발현 수준의 의미있는 변화(≥2 or **≤2** 배)를 관찰할 수 있었다. 본 연구의 결과에서는 박테리아 공격에 대한 전복의 초기 면역 반응과 관련하여, 전사인자들 또는 그들의 활성인자들 (KLF, NFIL-3, IK-B), 염증과 apoptosis와 관련된 단백질들 (AIF, TNF-α, archeron), cytokine들 (IFN-44-like, SOCS-2)과 항산화 효소들 (glutathione S transferase, TRx-2, TPx)이 활성화 될 수 있다는 것을 보여주었다.

VHSV 공격 실험에서는 PBS를 대조구로 했을 때와 비교하여 아가미와 혈구에서 280개(6.6%)의 의미있는 발현수준의 변화(≥1.5 or ≤1.5배)를 보였다. 아가미와 혈구에서 각각 88개와 65개 유전자의 발현이 증가하였다. 확인된 유전자들은 염증과 apoptosis 관련 유전자 (TNF super family, Fas ligand), IFN 조절 단백질 (IFN-44 like, IFN inducible GTPase), 전사 인자 (C-jun, NFIL-3), 해독 단백질 (glutathione peroxidase)과 같이 면역 기능에 따라 분류하였다. 전사가 조절된 유전자들의 상당수는 기능이 알려져 있지 않거나 GenBank에서 유사한 유전자들을 찾을 수 없었지만, 전복에서의 면역시스템에 관련하는 새로운 유전자들일 가능성을 보인다.

TNF super-family에 속하는 단백질들은 염증 반응 조절, apoptosis 및 면역 조절들에 관여하는 다양한 역할을 한다. 그들 사이에서, TNF-α 와 Fas ligand들은

다양한 기능적 면역 조절자처럼 여겨져 왔다. 까막전복으로부터 TNF-α 와 Fas ligand를 코딩하는 유전자들을 AbTNF-α 와 AbFas ligand로 각각 명칭하였으며, microarray 결과들에서 전사 수준이 증가함을 보였다. AbTNF-α 와 Fas ligand의 아미노산 서열들은 TNF family signature와 N-terminal transmembrane domain들을 가지고 있었다. 계통 분석결과, AbTNF-α 와 Fas ligand는 다른 무척추동물의 것과 가까운 관계를 보였다. qRT-PCR 결과, AbTNF-α 와 AbFas ligand는 전복의 혈구, 아가미, 외투막, 근육, 소화관, 간췌장에서 지속적으로 발현되는 것을 확인할 수 있었으며, 박테리아, VHSV와 LPS 공격 실험에 의한 AbTNF-α 와 AbFas ligand의 전사 수준은 아가미와 혈구에서 의미있는 증가($p<0.05$)를 보였다. AbTNF-α 와 AbFas ligand 를 코딩하는 유전자는 발현 벡터에 재조합하여, *Escherichia coli* 에서 재조합 단백질의 과잉 생산을 유도하였고, pMAL protein fusion system을 이용하여 재조합된 단백질을 정제하였다. 재조합 AbTNF-α 와 AbFas ligand 단백질은 전복의 혈구세포와 인간의 THP-1 세포에서 superoxide anion (O^{-}_{2}) 유도에 의해 생물학적 활성을 나타내었다. 또한, 몇 가지 면역 유전자들은 (defensin, SOCS-2, NF-kB) 전복의 혈구세포에 재조합 AbTNF-α 와 AbFas ligand를 처리했을 때 발현 수준이 다르게 나타나는 것을 볼 수 있었다. 두 재조합 단백질의 생물학적 활성을 통해, 박테리아, 바이러스, LPS의 공격 때와는 반대로 AbTNF-α와 AbFas ligand의 전사 수준이 증가함을 봤을 때, 우리는 미생물 주입했을 때 ROS 처럼 O^{-}_{2} 유도에 의해 전복의 TNF-α 와 Fas ligand가 응답할 수 있다는 것을 제안 할 수 있다.

LPS에 유도되는 TNF-α factor (LITAF)와 Rel family nuclear factor kappa B (Rel/NF-kB)는 염증 cytokine들과 apoptosis, 면역 과련 유전자들의 조절에 있어 두 가지 중요한 작용을 하는 전사 요소들이다. 최근 연구에서는 전복의 LITAF (AbLITAF)와 Rel/NF-kB (AbRel/NF-kB) 상관 관계와 그들의 면역 응답에 대한 연구가 진행되었다. AbLITAF의 염기서열 분석결과 147개의 아미노산으로 구성되고 두 개의 CXXC motifs (^{82}CPHC^{85} and ^{134}CPNC^{137})를 포함하는 LITAF (Zn^{+2}) binding domain이 확인되었다. 그리고, 계통분석 결과 AbLITAF가 LITAF family 단백질에 속하는 것을 확인할 수 있었다. AbRel/NF-kB는 무척추동물과 척추동물의 것과 유사한 Rel homology domain (RHD), Rel protein signature (^{107}FRYECR^{112}), DNA binding motif (^{103}RGLRFFRYEC^{101}), nuclear localization signal (NLS)과 transcription factor immunoglobulin–like fold (TIG) 같은 다수의 domain을 포함하고 있었다. 조직 특이적 분석 결과, AbLITAF와 AbRel/NF-kB의 mRNA 둘 다 모든 선택된 조직들에서 발현이 이루어졌다. 하지만, AbRel/NF-kB보다 AbLITAF에서의 발현 수준이 외

투막을 제외한 모든 조직에서 더 높게 나타났다. 다른 연체동물들과 본 연구의 전복 TNF-α, LITAF, Rel/NF-kB 데이터로부터 종합된 결과들은, 연체동물 문 전체에 걸쳐 일어날 수 있는 LITAF와 NF-kB의 독립적인 방향을 강하게 제시할 수 있다.

본 연구의 4장에서는 병원체 감염에 대한 전복의 초기 면역 반응에 중요한 구성 요소로 알려진 defensin과 histone H2A로 명명된 두 개의 항균펩타이드들을 암호화하는 유전자에 대해서 서술한다. 전복의 defensin (pro-defensin)은 66개의 아미노산을 암호화하는 198 bp의 염기서열로 구성된다. 무척추동물의 최근 연구에서 3차 구조 상에 defensin family domain, 6개의 cysteine 잔기의 배열 그리고 그들의 이황화 결합 (C1-C4, C2-C5, C3-C63), alpha helix 구조가 보여졌고, 우리는 전복의 defensin이 다른 무척추동물 defensin의 새로운 member임을 계통적 관계를 통해 제시하였다.

자극을 주지 않은 전복에서, defensin의 전사 수준은 혈구세포, 아가미, 외투막, 근육, 소화관 그리고 간췌장을 포함하는 모든 실험된 조직들에서 지속적으로 발현되어졌다. 또한, *V. alginolyticus, V. parahemolyticus*와 *L. monocytogenes* 같은 박테리아 공격 실험 상에서도 전복 defensin의 전사 수준은 혈구세포, 아가미, 소화관에서 의미있게 유도되어졌다. 4장의 두 번째 절에서는 전복으로부터 histone H2A cDNA 유전자를 클로닝하였고, 전복의 histone H2A의 N말단 서열로부터 "Abhisin"를 지칭하는 40개의 아미노산 항균펩타이드를 서열을 확인하였다. Abhisin는 net positive charge (+13), 높은 소수성 잔기들(27%)과2.82 Kcal/mol protein binding potential을 가지는 항균펩타이드들의 특징적인 점을 보여준다. 본 연구에서 합성된 abhisin 을 250 μg/mL 처리했을 때 박테리아 계통인 *L. monocytogenes*, *V. ichthyoenteri*와 fungi 계통인 *Pityrosporum ovale*에 대해 성장을 저해하는 것으로 확인되었다. 하지만, 그람 음성균보다 그람 양성균에 대해 더 강한 활성을 나타내는 것으로 보여졌다. 부가적으로, *P. ovale*를 대상으로 abhisin을 처리했을 때의 손상 정도를 주사 전자 현미경 (SEM)을 통해 관찰 하였다. 흥미로운 점은, THP-1 leukemia cancer cell에 abhisin을 50 μg/mL 처리했을 때 생존 능력이 약 25% 감소하는 것을 확인할 수 있었고, 일반 vero cell에는 영향을 나타내지 않았다. 이 결과를 통해 abhisin이 일반 cell보다 cancer cell에 세포 독성을 가진다고 할 수 있다. 그리고, 전복에 박테리아 공격 실험을 수행했을 때 아가미와 소화관에서 Histone H2A 전사 수준이 의미있게 유도되어졌음을 qRT-PCR 결과를 통해 확인할 수 있었다. 종합적인 결과를 봤을 때 defensin과 histone H2A 전구체 또는 그것의 N-말단 아미노산 (abhisin)이 까막 전복에서 강

력한 항균펩타이드들이고, 그들은 감염들에 대한 보호체계를 증가시키는 면역 방어 반응에 포함된다고 할 수 있다.

ROS는 침입된 병원체들에 대한 무척추동물의 가장 중요한 숙주 방어 요소 중 하나이다. 항산화 인자는 과도한 ROS에 의해 생성되는 산화적 스트레스에 대한 잠재적인 indicator이다. 따라서 ROS 수준의 주입 상태에 따른 항산화 효소들의 전사 수준은 산화적 스트레스에 대한 indicator로 사용할 수 있다. 미생물의 주입에 대해 관계하는 항산화 효소들의 변화를 이해하기 위해, 박테리아와 VHSV 공격 실험 후에 전복 항산화 효소들 [Mn-superoxide dismutase (Mn-SOD); CuZn-superoxide dismutase (CuZn-SOD); catalase; thioredoxin peroxidase (TPx); mitochondrial thioredoxin-2 (Mt-TRx-2); Selenium dependant glutathione peroxidases (SeGPx)]의 전사 수준을 분석하였다. 그 결과, Mn-SOD, SeGPx에서 면역 공격 실험 동안 각각 다른 시점에 뚜렷한 변화를 확인할 수 있었다. 더 나아가, 그것은 전복에서 항산화 효소가 박테리아와 VHSV 공격에 대해 식균 작용 활성과 다른 초기 면역 방어 응답으로 유도될 수 있다는 것을 제시할 수 있다.

본 연구에서는 전복의 cDNA microarray 분석 결과를 가지고 ESTs에 결합하여 접근함으로써 박테리아와 VHSV 공격 실험 상에서 방어 작용에 관계되는 전복의 유전자들을 탐색하였다. 이 접근 방식은 다른 병원체들에 대한 전복의 방어 체계에 관계된 유전자들의 확인을 위한 좋은 잠재력을 지닌다. 현재까지 연구에서는 전복의 초기 면역 시스템에 대한 다른 숙주 방어 인자들 하에 다양한 유전자 집단을 보여주었다. 전복의 면역에 관련된 유전자들과 그 단백질들은 염증 및 apoptosis 조절자, 전사 인자들인 NF-kB, LITAF, NFIL-3 C-Jun, cytokine 조절 인자인 SOCS-2와 IFN-44, 항균펩타이드 같은 defensin과 histone H2A 그리고 항산화 효소 등을 포함한다. 결론적으로, 본 연구는 척추동물과 무척추동물간에 면역 기능에 관련된 유전자들의 진화적 관계를 규명하는 단초를 제공한다. 선택된 면역 관련 유전자들에 대해서는 이후에 전복의 면역 방어 기작에 대한 연구를 수행하는데 기여할 수 있다.

Summary

The innate immune system is the main host defense in abalone like invertebrates. Hence, it is important to understand the immune responses and their mechanisms against different microbial challengers at molecular level. In this study, molecular analysis of immune genes in disk abalone, *Haliotis discus discus* was investigated using cDNA microarray, transcriptional profiling and functional properties of respective proteins.

An abalone 4.2 K cDNA microarray (cDNA chip) was manufactured using the abalone cDNA library clones (ESTs). The cDNA microarray analysis was performed with two immune challenge experiments by injecting 50 μL ($5x10^7$cells/mL) of bacteria mixture (*Vibrio alginolyticus, V. parahemolyticus,* and *Listeria monocytogenes)* and 50 μL ($1 X 10^8$ pfu/ml) of viral hemorrhagic septicemia virus (VHSV). Transcriptional response of abalone gills, digestive tract, and hemocytes was investigated at 24 h post challenge of bacteria and VHSV. In bacteria challenged abalone, 68 (1.6%) and 112 (2.7%) transcripts were significantly (≥2 or ≤2 –fold) changed in their expression levels in gills and digestive tract, respectively. There were 46 tissue-specific transcripts that were up-regulated only in digestive tract. In contrast, only 13 transcripts showed gill-specific up-regulation. Our results showed that challenge of bacteria, may activate the transcription factors or their activators (KLF, NFIL-3 and Ik-B), inflammatory and apoptosis-related proteins (AIF, TNF-α, archeron), other cytokines (IFN-44-like, SOCS-2) and antioxidant enzymes (glutathione S transferase, TRx-2 and TPx) as a part of the innate immune responses of abalone.

Upon VHSV challenge, 280 (6.6%) transcripts were significantly (≥1.5 or ≤1.5 –fold) changed in their expression level of gills and hemocytes compared to respective PBS controls. Total of 88 and 65 genes were up-regulated in gills and hemocytes, respectively. Identified genes were grouped under different immune-functional categories such as inflammatory and apoptosis related genes (TNF super family, Fas ligand), IFN regulatory proteins (IFN-44 like, IFN inducible GTPase), transcription factors (C-jun, NFIL-3) and detoxification proteins (glutathione peroxidase). Considerable number of regulated transcripts were matched with either hypothetical (un-known) sequences or showed no GenBank match (no hit) suggesting that those immune responded transcripts may represent novel genes related to immune system in abalone.

Members of TNF super-family play diversified roles in mediating the inflammatory responses, apoptosis and immune regulation. Among them, TNF-α and Fas ligands are considered as multifunctional immune modulators. The gene encoding TNF-α and Fas ligand,

which showed up-regulation in microarray results were isolated from abalone cDNA library, denoted as the AbTNF-α and AbFas ligand, respectively. The AbTNF-α and Fas ligand amino acid sequences showed their characteristic TNF family signature and N-terminal transmembrane domains. Phylogenic analysis results showed that AbTNF-α and Fas ligand were closely related with their invertebrate counterparts. qRT-PCR results showed that AbTNF-α and AbFas ligand transcripts were constitutively expressed in abalone hemocytes, gills, mantle, muscle, digestive tract and hepatopancrease in a tissue-specific manner. Transcription level of AbTNF-α and AbFas ligand was significantly ($p<0.05$) up-regulated in gills and hemocytes by bacteria, VHSV and LPS challenge. The recombinant AbTNF-α and AbFas ligand proteins were over-expressed in *Escherichia coli* (*E. coli*) and purified using a pMAL protein fusion system. Recombinant AbTNF-α and AbFas ligand showed its biological activity by inducing O^{-}_{2} in abalone hemocytes and human THP-1 cells. Also, several immune genes such as defensin, SOCS-2, NF-kB have shown marked differences at transcriptional level when abalone hemocytes treated with recombinant AbTNF-α and AbFas ligand. Correlating the transcriptional up-regulation of AbTNF-α and AbFas ligand against bacteria, virus and LPS challenge with the biological activity of two recombinant proteins, we could suggest that the abalone TNF-α and Fas ligand may response to microbial infection by inducing O^{-}_{2} like ROS.

LITAF and Rel/NF-kB are two important transcription factors which play major role in the regulating inflammatory cytokines, apoptosis and immune related genes. Present study describes the discovery of abalone LITAF (AbLITAF) and Rel/NF-kB (AbRel/NF-kB) homologues and their immune responses. Analysis of AbLITAF sequence shows that it shares characteristic LITAF (Zn^{+2}) binding domain with two CXXC motifs (^{82}CPHC^{85} and ^{134}CPNC^{137}) with putative peptide of 147 aa. Phylogenetic analysis results further confirms that AbLITAF is a member of LITAF family proteins. AbRel/NF-kB shares numerous signature motifs such as RHD, Rel protein signature (^{107}FRYECR^{112}), DNA binding motif (^{103}RGLRFFRYEC^{101}), NLS and transcription factor TIG fold similar to their invertebrate and vertebrate counterparts. Tissue specific analysis results showed that both AbLITAF and AbRel/NF-kB mRNA is expressed ubiquitously in all selected tissues in constitutive manner. However, constitutive expression of AbLITAF was higher than AbRel/NF-kB in all tissues except mantle. Upon immune challenged by bacteria and VHSV, AbLITAF showed the significant up-regulation in gills and hemocytes while AbRel/NF-kB transcription was not change significantly. The cumulative data from other molluscs and our data with reference to

TNF-α, LITAF, Rel/NF-kB from abalone provide strong evidence that LITAF and NF-kB are independent pathways likely to occur throughout the Phylum mollusc.

In the fourth chapter, it describes the gene-encoded two AMPs namely defensin and histone H2A derived AMP as important components of the abalone innate immune response against pathogen invasion. Abalone defensin (pro-defensin) consists of 198-bp coding sequence of putative 66 aa acids which includes the 48 aa mature peptide. The present of invertebrate defensin family domain, arrangement of six cysteine residues and their disulfide linage in C_1-C_4, C_2-C_5, and C_3-C_6, alpha helix in three dimensional structure and phylogenetic relationship suggest that abalone defensin could be a new member of invertebrate defensin family closely related to arthropod defensins. In non-stimulated abalone, defensin transcripts were constitutively expressed in all examined tissues including hemocytes, gills, mantle, muscle, digestive tract and hepatopancreas. Also, abalone defensin transcripts were significantly induced in hemocytes, gills and digestive tract upon bacterial challenge containing *V. alginolyticus, V. parahemolyticus* and *L. monocytogenes.*

In the second section of chapter four, describes a 40-amino acid AMP designated as "Abhisin" identified from the N-terminus of the abalone histone H2A. Abhisin displays characteristic features of AMPs including net positive charge (+13), higher hydrophobic residues (27%) and 2.82 Kcal/mol protein binding potential. Our results showed that growth inhibition of *L. monocytogenes*, *V. ichthyoenteri* bacteria, and fungi (yeast) *Pityrosporum ovale* by synthetic abhisin at 250 µg/mL. However, stronger activity was displayed against the Gram positive than negative bacteria. Additionally, SEM observation results confirmed that *P. ovale* cells were damaged by abhisin treatment. Interestingly, abhisin treatment (50 µg/mL) decreased the viability of THP-1 leukemia cancer cells approximately by 25% but there was no effect on the normal vero cells, suggesting that abhisin has cytotoxicity against cancer cells than normal cells. qRT-PCR results revealed that histone H2A transcription was significantly induced after bacteria challenge in abalone gills and digestive tract. Our overall results suggest that defensin and precursor histone H2A or its N-terminal peptide (abhisin) are potent AMPs in disk abalone that could involve in immune defense reactions to increase protection against infections.

ROS are highly microbicidal and considered as one of the most important components of host defense of invertebrates against invading pathogens. Antioxidants are potential indicators of oxidative stress due to excessive ROS. Hence, transcriptional responses of antioxidant enzymes could be used as an indicator of oxidative stress (ROS

level) as well as infectious status. In order to understand the change of antioxidant enzymes in relation to microbial infection, abalone antioxidant enzymes (Mn-SOD, CuZn-SOD, catalase, TPx, Mt-TRx-2, and SeGPx) transcriptional responses were analyzed after bacteria and VHSV challenge. Results showed that several antioxidant enzymes such as Mn-SOD, catalase, SeGPx, were induced but the responses were shown marked differences at different time points during the immune challenge. Furthermore, it could be suggested that bacteria and VHSV challenge may induce the oxidative stress associated with the activation of phagocytosis and other innate immune defense responses in abalone.

In conclusion, the approach to combine the abalone ESTs with cDNA microarray analysis has been resulted for the screening of abalone genes involved in the defense reaction upon a bacteria and VHSV challenge. This approach has good potential for identifying genes as immune markers involved in abalone defenses against different pathogens. Present study clearly showed abalone innate immune system has a number of diversified gene families under different host defense components. Genes and their proteins involved in the disk abalone immunity include sets of TNF-α, Fas ligand, caspase like inflammatory and apoptosis regulators; NF-kB, LITAF, NFIL-3 C-Jun like transcription factors; SOCS-2 and IFN-44 like cytokine regulators; defensin and histone H2A like AMPs and classical set of enzymatic antioxidant genes. Final outcome of this study provides the linkage of evolutional relationship of immune functional genes between invertebrates and vertebrates with better insight into abalone immune defense as a highly complex and diversified system. Further functional studies on these selected immune response genes involved in the abalone host defense mechanisms have to be initiated in future.

LIST OF FIGURES

LIST OF TABLES

ABBREVIATIONS

Ab	abalone
AIF	allograft inflammatory factor
α	alpha
AMP	antimicrobial peptide(s)
ANOVA	analysis of variance
APD	antimicrobial peptide database
AVG	abalone viral ganglioneuritis
β	beta
BLAST	Basic Local Alignment Tool
bp	base pair(s)
CIP	calf intestinal phosphatase
°C	centigrade
cDNA	complementary deoxyribonucleic acid
Cu,Zn-SOD	copper zinc super oxide dismutase
DEPC	diethyl pyrocarbonate
DIZ	disc inhibition zone
DMEM	Dulbecco's modified eagle medium
DMSO	dimethyl sulfoxide
DNA	deoxyribonucleic acid
dNTP	deoxynucleotide-triphosphate
DTT	dithiothreitol
E.coli	*Escherichia coli*
EDTA	ethylene diamine tetra acetic acid
EST	expressed sequence tag(s)
FBS	fetal bovine serum
ɣ	gama
x g	gravity
G+	Gram positive
G-	Gram negative
GO	gene ontology
GSH	glutathione
GTPase	guanosine triphosphatase
HE	hydroethidium
H_2O_2	hydrogen peroxide
HSC	hematopoietic stem cell

IFN	interferon
I-kB	inhibitor of kappa B
IL	interleukin
IPTG	isopropyl-beta-D-thiogalactopyranoside
K	kilo
Kb	kilobase(s)
Kcal	kilo calorie
KDa	kilo dalton
KLF	krüppell-like factor
L	liter
LB	Luria-Bertani
LITAF	lipopolysaccharide-induced tumor necrosis factor alpha factor
LPS	lipo polysaccharide
LT- α	lymphotoxin alpha
MBP	maltose binding protein
mg	mili gram(s)
mL	miilliliter(s)
MnSOD	managanese super oxide dismutase
mol	mole
MTT	3-(4,5-dimethylthiazol-2-yl)-2,5-diphenyltetrazolium bromide
Mt-Trx-2	mitoocondrial thioredoxin 2
mRNA	messenger RNA
Mx	myxovirus myxovirus-resistance protein
MW	molecular weight
μL	microlitre(s)
NADPH	nicotinamide adenine dinucleotide phosphate
NCBI	National Center for Biotechnology Information
NFIL-3	nuclear factor interleukin-3
NF-kB	nuclear factor kappa B
NK cells	natural killer cells
NLS	nuclear localization signal
nm	nanometer(s)
NOX	NADPH oxidase
O^-_2	superoxide anion
$^1O_2$	singlet oxygen
OD	optical density
ORF	open reading frame
PAGE	polyacrylamide gel electrophoresis

PBS	phosphate buffered saline
PCR	polymerase chain reaction
pfu	plaque forming units
p*I*	isoelectri point
PMN	polymophonuclear leukocytes
PMT	photo-multiplicator
PRD	proline rich domain
PRR	pattern-recognition receptors
proPO	prophenoloxidase-activating system
PRx	peroxiredoxin
qRT-PCR	quantitative real time polimerase chain reaction
Rel/NF-kB	rel family nuclear factor kappa B
ROS	reactive oxygen species
rpm	revolutions per minutes
RT-PCR	reverse transcription-polymerase chain reaction
SD	standard deviation
SDS	sodium dodecyl sulphate
SeGPx	selenium dependent glutathione peroxidase
SEM	scanning electron microscope
SOCS-2	supressor of cytokine signaling 2
TACE	TNF alpha converting enzyme
Taq	*Thermus aqaticus*
THP-1	human acute monocytic leukemia cell line
TIG	transcription factor immunoglobulin
TNF	tumor necrosis factor
TNF- α	tumor necrosis factor-alpha
TPx	thioredoxin peroxidase
TRxR	thioredoxin reductase
TRx-2	thioredoxin 2
U	unit
UTR	untranslated region
VHSV	viral hemoragic septicemia virus

GENERAL INTRODUCTION

Abalone biology and taxonomy

Abalone (from Spanish word `Abulón`) belongs to Phylum Mollusk one of the largest phyla in the animal kingdom. The phylum takes its name from Latin word "mollus" meaning of "soft". A significant characteristic of mollusks is their soft body which is generally protected by a hard, calcium- containing shell except in some forms such as in slugs and octopuses which their shell has been lost in the course of evolution. Mollusks are a highly diverse group of animals that include three major classes namely Class bivalve (oysters, mussels, scallops, and clams), Class gastropod (abalone, snails, limpets, sea hares and slugs), and Class cephalopod (cuttlefish, squids, and octopuses). Abalone includes in class gastropod, the largest and most successful class of mollusks containing over 60,000-75,000 known living species and 15,000 fossil forms. All abalones belong to the Family Haliotidae and Genus Haliotis (http://simple.wikipedia.org/wiki/Gastropoda). There are over 70 species of halitosis species, which all of are marine. The most important species with regard to aquaculture in North America is the red abalone, *Haliotis rufescens,* while in Asia, *H. discuss hannai, H. discus discus* and *H. diversicolor supertexta* are predominantly cultured (McBride, 1998).

Abalone Aquaculture and diseases

The emergence of new pathogens, particularly intracellular bacteria and viruses represent serious risks for the health of aquatic animals (Villena, 2003). A mass mortality has been reported from of marine mollusks including abalone due to pathogenic infections in different parts of the world resulting massive economic loss (Hooper at al., 2007). Recently reported abalone disease infections and causative agents are listed in table 1.

Major innate immune defense components in invertebrate mollusks

A correctly functioning immune system is vital to efficient aquaculture for both defense against invading pathogens and response to different stress (Villena, 2003). Innate immunity is the first line of defense against infection and invertebrates including abalone. Under the intensive conditions of aquaculture, some of the innate defenses are easily compromised and can allow pathogens more easily gain access to tissues and cells for infecting the host. The high immune specificity is usually considered as an exclusive property of vertebrate adaptive immunity which has been assumed that invertebrates lack of highly

specific immune defense (Loker at al., 2004).

To identify genetic diversity in genome scale and their phylogenetic as well as functional relationships “model organism concept” has been adapted from long time in different invertebrates including *Drosophila* (insect) and *Caenorhabditis elegans* (nematode). Genome sequencing projects of those two invertebrates have been already completed and genomic data are available to the public. Hence, it facilitates the unlimited genetic base to research community for understanding the immune defense mechanisms of those model species. From invertebrate model systems, we have learnt that the primary components of innate immunity fall into three categories that define the effectiveness of an immune response. First, the organism distinguishes between self and nonself; second, the organism mounts a defensive response that can kill or disable the invader; and finally, the organism recognizes and can eliminate its own damaged or diseased cells. These requirements lead to the three essential components of innate immunity: phagocytosis (cell-mediated); activation of humoral responses leading to opsonization, melanization, and coagulation (cell-free); and the production of humoral antimicrobial compounds (cell-free). Invertebrate immune defense against pathogens mainly occurs by major innate immunity systems or components and pathways which include; PRRs, hemolymph coagulation, AMP, respiratory burst activity, proPO, phagocytosis activity, lectin agglutinin system, antiviral, antifungal, antibacterial systems (Iwanaga et al., 2005).

The mechanisms underlying these host defense components depend on the presence of functional proteins in appropriate quantities, within a crucial time window. These proteins are encoded by genes whose transcription is tightly coordinated by complex programs of gene expression. As a summery, each of above individual immune defense systems consist functional genes under specific signaling pathways. In many occasions pathways are interrelated and work coordinately. Based on the several previous studies, researchers have described the important fact that the invertebrate’s immune defense mechanisms are heterogeneous, complex and poorly understood. In order to understand the entire immune defense mechanism in a whole organism, we need to know the regulatory mechanism and specific function of individual genes of each immune system. In general, it believes that molecular understanding of the genes and pathways regulating the mollusk immune system has lagged behind compared to that reported for other invertebrates such as insects and nematodes. Transcriptional analysis is one of the basic steps which could be applied to understand the immune functions and components at molecular level.

Table 1: Diseases in abalone aquaculture; a summery of recent reports

Disease name	Abalone species	Causative agents	Country
Virus infections			
Crack shell disease	*Haliotis diversicolor*	Different virus strains	China/Japan
Amyotrophia	*H. discus hannai*	Spherical virus	Australia
	H. discus discus	Virus like partials	South Africa
Viral mortality	*H. rubra, Haliotis hannai*	Herpes-like virus	Australia
Viral ganglioneuritis	*Haliotis diversicolor*	Spherical type virus	Australia
Bacterial infections			
Abalone vibriosis	*H. discus hannai*	*V. aliginolyticus*	Korea
	H. diversicolor supertexta	*V. parahaemolyticus*	Taiwan
	Haliotis spp	*Vibrio spp*	China /Japan
		V. fluvialis, V. campbellii,	Australia
		Pseudomonas fluoresces	South Africa
White spots in necrotic muscle	*H. diversicolor supratexta*	*Candidatus xenohaliotis* *Pakinsus olseni/atlanticus*	China
Blister disease	*H. discus hannai*	*V. carchariae/V. fluvialis II*	Japan/China
Fungal infection			
Foot tubercles	*H.sieboldii*	*Haliphthorous milfordensis*	Japan
Parasite infections			
Kidney Coccidia	*H. midae/H. spadicea*	Ciliates-*Margolisiella haliotis*	USA
		Sabellid polychaetes	China/Australia
		Trematode metacercariae	USA
Withering disease	*H. cracheridii*	Rickettsiales-like prokaryote	Mexico
Perkinsus	*H. rubra/H. laevigata*	*Perkinsus olseni/P. atlanticus*	Australia

DNA microarray for global expression profiling

The recent increase in availability of gene expression technologies has the potential to dramatically expand our understanding of cellular immunology in molecular detail. By studying the gene expression of genes in various cellular contexts, it is possible to assign putative function to protein encoded by genes. Moreover, level of gene expression reflects the cellular activity and physiology. Analysis of gene expression at mRNA level (transcriptional) could be performed in several ways such as northern blot, RT-PCR etc. Alternatively, DNA microarray or DNA chip is a one of the latest high-throughput method used to analyze the large scale gene expression profiles of biologic samples which technology began in 1995 (Lamartine, 2006). Also, DNA microarray technology has given rise to the study of functional genomics. The entire set of genes of an organism can be microarrayed on an area as small as a fingernail and the expression levels of thousands of genes are simultaneously studied in a single experiment. DNA microarray technology allows comparisons of gene expression levels on a genomic scale in all kinds of combinations of samples derived from normal and diseased tissues, treated and nontreated time courses, and different stages of differentiation or development. Further computational analysis of microarray data allows the classification of known or unknown genes by their mRNA expression patterns. Global gene expression profiles in cells or tissues will provide us with a better understanding of the molecular basis of phenotype, pathology, or treatment.

Microarray manufacturing technology

The measurement of mRNA abundance is based on the capacity of every nucleic acid strand to recognize complementary sequences through base pairing. In 1995, Pat Brown et al., used glass support associated with fluorescence detection and robotically spotted 10,000 DNA probes onto a microscope slide and hybridized with a double-labeled mRNA population. This approach is now largely used in large-scale transcriptome analysis and called “cDNA microarray.” Its principle is described in fig. 1: A microarray is a solid substrate, such as a silicon wafer or glass slide, on which DNA or oligonucleotides from either host or pathogen could be attached. These nucleic acids are complementary to thousands of genes of both known and unknown function. There are two main types of microarray: spotted DNA and oligonucleotide arrays (Schena et al., 1995).

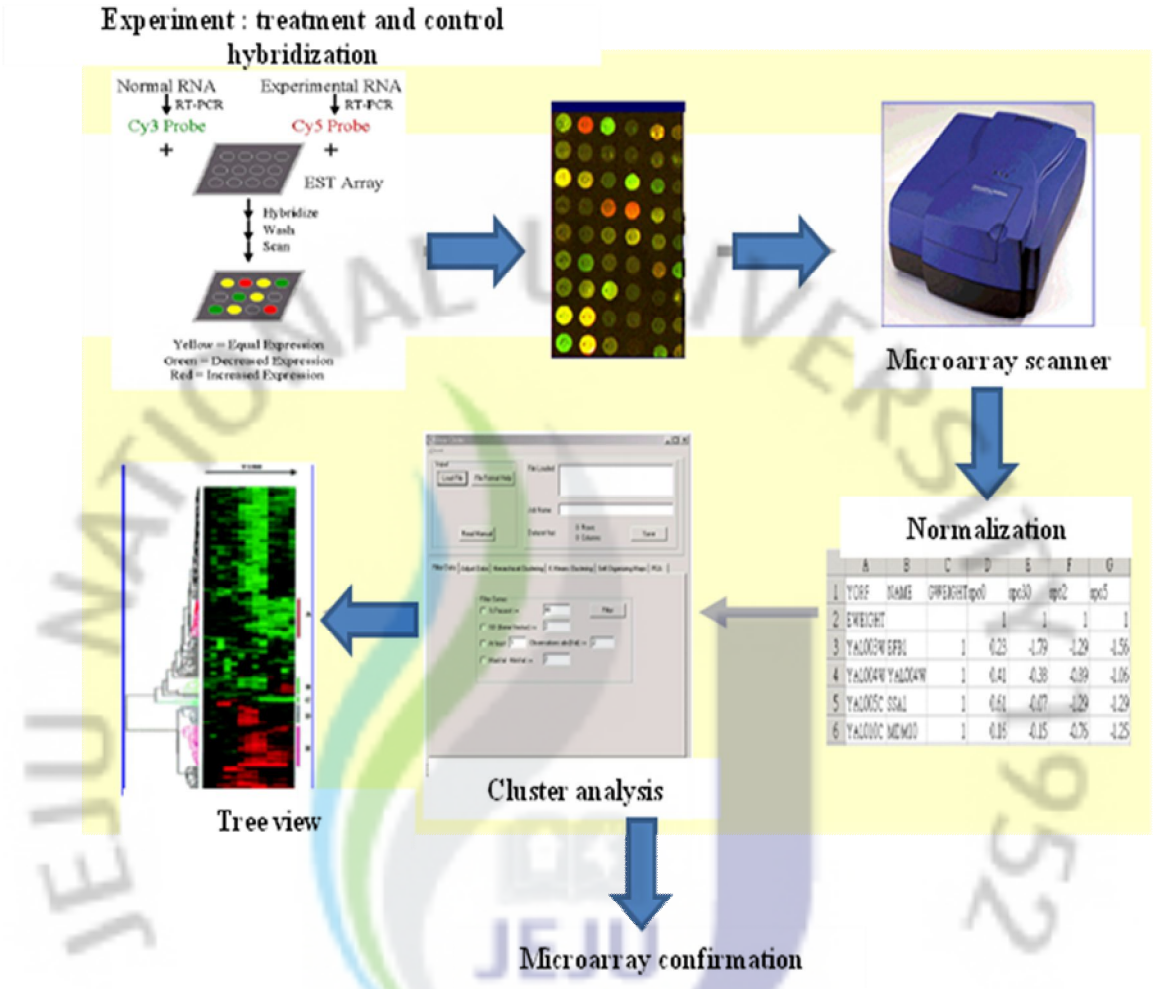

Fig.1. Schematic diagram of cDNA microarray principle for gene expression

Spotted DNA arrays

The spotted DNA method entails attaching single-strand or disassociated double-strand DNA (from a cDNA library or genomic products amplified by PCR) to the slide. In most slides, duplicate spots are attached as controls, either next to or distant from the first spot, with up to 20 000 spots per slide. RNAs are extracted from two cell cultures from which expression level needs to be compared. Messenger RNAs are then transformed into cDNA by reverse transcription. At this stage, cDNA from the first culture is labeled with a red dye (Cy5), whereas cDNA from the second culture is labelled with a green dye (Cy3). Green-labeled and red-labeled cDNAs are mixed together (called the target), put on the matrix of spotted single-strand DNA (called the probe) and incubated for one night. The fluorescent cDNA will then hybridize on the probe DNA spots. For slide scanning, a laser excites each spot and the fluorescent emission is gathered through a PMT coupled to a confocal microscope. Two images are obtained where green and red scales represent fluorescent intensities read. By superimposing these two images, one image composed of spots going from red (where only DNA from the first culture is fixed) to green (where only DNA from the second culture is fixed) passing through the yellow color (where DNAs from the two cultures are fixed in equal amounts) is obtained. Since the amount of fluorescent DNA fixed is proportional to the amount of mRNA present in each cell at the beginning, the red/green fluorescence ratio can be calculated. If this ratio is greater than 1 (red on the image), the gene expression is greater under the first experimental condition; if this ratio is smaller than 1 (green on the image), the gene expression is greater in the second condition (Schena et al., 1995).

Oligonucleotide arrays

Oligonucleotides can either be spotted as above or directly synthesized in situ on to the solid substrate, negating the need for attachment methods. Each oligonucleotide is usually about 50–70 nucleotides long rather than a whole gene. Over the slide there are several different oligonucleotide sequences from the same gene. This range produces more robust results because the same gene can be probed independently several times in the same experiment. A refinement of this method-Affymetrix microarrays (Affymetrix, CA, USA)-allows even greater specificity and may have up to 600 000 oligonucleotides per chip. For each approximately 20 nucleotide sequence there is a duplicate sequence with a single base change, called a mismatch. The mismatch sequences allow comparison between hybridization

to a specific sequence and background hybridization to non-specific sequences and “true” quantification. Another advantage of oligonucleotidearrays is that they can be designed to include different alleles and splicing variants. The main disadvantage if there is hybridization with a single sample only is that more detailed data processing is needed to determine changes in the abundance of each transcript in two populations. The vast quantity of data generated from microarray experiment is only useful if it can be interpreted. The knowledge that a gene is expressed under a particular condition is not an answer in itself but only the first step in understanding. For example, whether expression of a gene is vital for host defense or involved in tissue injury requires further investigation. In addition, expression of a gene does not always translate into production of a protein. Although gene expression reveals nothing directly about translational and post-translational events, protein activation status alterations can and do frequently alter the expression of downstream target genes. These transcriptional consequences of protein activation can result in reproducible signatures of gene expression, specific to such an activation pathway. Microarrays therefore provide a stepping-off point for a wide range of further biological investigations (Bryant et al., 2004).

OUTLINE OF THE STUDY

Previous studies on pathogenic infections and immune challenge revealed that several genes involved in the immune defense response of disk abalone. These studies have been mainly conducted with a single or very few genes at a time. Since immune response reactions are highly complex and interrelated in the cellular level, DNA microarray based approaches allow researchers to interrogate host and pathogen genomes. It enables the investigation of entire transcriptional responses, biological pathways as well as previously unknown genes and their functions. No information is available reference to the immune response genes of abalone upon bacterial and viral challenge in a large scale gene expression using cDNA microarray technique.

Chapter one of this study has been focused on the construction of 4.2 K cDNA microarray using disk abalone cDNA library clones (ESTs) and analysis of transcriptional response in gills, digestive tract and hemocytes upon immune modulation (challenge) of abalone with bacteria (*Vibrio alginolyticus, Vibrio parahemolyticus,* and *Listeria monocytogenes*) and VHSV. This chapter further describes the identification of novel immune response genes from disk abalone and their functional categories under different host defense components of invertebrate immune defense systems including antimicrobial, inflammatory, apoptosis, antioxidant, protease inhibitory, cytokines regulatory genes and immune regulatory transcription factors. Based on the resulted microarray gene expression profiles, it was possible to select and grouped immune potential genes for further characterization which provides molecular insights of host immune defense systems against pathogens.

Chapter 2, 3, 4, and 5 have been focused to molecular characterization, transcriptional analysis (expression profiling) and functional aspects of genes and their respective proteins selected from microarray analysis and abalone cDNA library. Inflammatory and apoptosis related genes such as TNF-α, Fas ligand have been discussed in chapter 2. Also, two important transcription factors namely Rel/NF-kB and LITAF have been characterized in chapter 3. Chapter 4 describes the role of two AMP namely defensin and histone H2A derived AMP called “abhishin”. Additionally, immune responses of other genes such as antioxidant enzymes, cytokine regulators (SOCS-2), protease inhibitors have been discussed. Finally, the results presented in all chapters are summarized and discussed with suggesting (hypothesis) possible mechanisms, pathways and other potential immune relevant genes which may exist in abalone as host defense system.

CHAPTER 1

cDNA microarray analysis of bacteria and virus (VHSV) challenged disk abalone

ABSTRACT

In this study, cDNA microarray technology has been used to analyze the transcriptional profiles of immune-challenged disk abalone using bacteria (*Vibrio alginolyticus, V. parahemolyticus,* and *Listeria monocytogenes*) and VHSV to select potential genes as immune-markers as well as to screen novel immune response genes. An abalone 4.2 K cDNA microarray was manufactured using the abalone ESTs, which has been constructed in our laboratory.

In bacteria challenged microarray, 68 (1.6%) and 112 (2.7%) transcripts changed their expression levels significantly (≥2 or ≤2 –fold) in gills and digestive tract tissues, respectively. There were 46 tissue-specific transcripts that were up-regulated only in digestive tract tissue. In contrast, only 13 transcripts showed gill-specific up-regulation. Verification of microarray results was done by selecting six candidate genes namely KLF, lachesin, muscle Lim protein, TRx-2, NFIL-3, abalone protein 38 using qRT-PCR. Our results indicate that post challenge of bacteria (at 24 h), may activate the transcription factors or their activators (KLF, inhibitor of NF-kB or Ik-B), inflammatory and apoptosis-related proteins (NFIL-3, AIF, TNF-α, archeron), cytokines (IFN-44-like, SOCS-2) and antioxidant enzymes (glutathione S transferase, TRx-2 and TPx) as a part of the innate immune responses in abalone.

Upon VHSV challenge, 280 (6.6%) transcripts were significantly (≥1.5 or ≤1.5 –fold) changed their expression level in gills and hemocytes against VHSV challenge compared to respective PBS controls. Total of 88 and 65 genes were up-regulated in gills and hemocytes, respectively. These genes included under various immune-functional categories such as KLF, inflammatory and apoptosis related genes (TNF super family members, Fas ligand), IFN regulatory proteins (IFN-44 like protein, IFN inducible GTPase) and detoxification proteins (glutathione peroxidase). In contrast to up-regulated responses, 25 and 102 genes were shown down-regulation in gills and hemocytes, respectively.

Considerably higher number of ESTs was matched to hypothetical (unknown) proteins while several ESTs that had no GenBank match (no hit). These significantly responded unknown and no hit transcripts may be novel genes involving immune defense role. Based on the microarray results, we selected TNF-α, Fas ligand, AIF, SOCS-2 and as potential immune-markers in abalone against bacterial and viral infection which required investigating further with different type of microorganisms. Additionally, the identification of immune-relevant genes and their expression profiles in this microarray will permit detailed investigation of the host defense mechanisms of abalone.

1.1. INTRODUCTION

Abalones are frequently infected by a wide range of pathogens including bacteria, viruses and parasites resulting huge economic losses (table 1). Bacterial infection is one of the serious threats to abalone aquaculture among the wide range of pathogens. It is generally known that bacterial pathogencity is associated with structural components of their cell wall, such as LPS or active secretions of substances that either damage host tissue or protect the bacteria from host defense (Paillard et al., 2004). Bacterial infections into abalone lead to major diseases such as abalone vibriosis (Elston et al., 1983), blister or white spot necrosis (Li et al., 1997), and brown ring disease (Shepheerd et al., 1997). Additionally, high mortality outbreaks have been reported in abalone *Haliotis tuberculata* by pathogenic *V. carchariae* (Nicolas et al., 2002) at elevated seawater temperature. It was reported that abalones are frequently infected by Vibrio species (Li et al., 1997).

Various types of viruses have been reported from mollusk species associated with specific types of infection or disease conditions (Renault and Novoa 2000). However, only few viral diseases were reported from abalone species. Nakatsugawa et al., (1990) identified the virus in a primary culture of hemocytes of Japanese black abalone *Nordotic discus discus* which virus caused to "amyotrophia" disease. Later, amyotrophia infection was identified in *H. discus hannai* (Yu et al., 2007), *H. discus discus*, *H. madaka* species (Momoyama et al., 1999). Also, a spherical enveloped virus related to disease called "crack shell" was identified in *Haliotis discus hannai*, (Wang Li 1997) and *Haliotis diversicolor* Reeve (Wang et al., 2004). Furthermore, this virus was mainly detected in the cytoplasm of hemocytes, connective tissues of other organs such as digestive gland and intestine. Fang et al., (2002) identified the DNA virus in the cytoplasm of the digestive gland, kidney, and intestine of *H. diversicolor supertexta*. Abalone viral mortality is caused by several spherical viruses which could be grouped mainly into four virus types (type I, II, III, IV). Type I is the least virulent while types II, III and IV are highly virulent, resulting in mass mortalities. A herpes-like virus which caused infectious disease named as abalone viral ganglioneuritis (AVG) was identified from *H. diversicolor supertexta* (Chang et al., 2005; Hooper et al., 2007). However, very little is known about the immune responses of abalone against virus challenge at a molecular level.

McGuire and his group (McGuire et al., 1998) emphasized that greater understanding of the complex interactions between host, pathogen and environmental factors could lead to the identification of the host defense strategies. Therefore, a better understanding of interrelated immune defense responses may help in developing strategies

and tools to reduce infectious diseases in abalone. To address this goal, a wide screening program of immune-response genes and their interactions in abalone is necessary. To date, most of the abalone immune defense systems have been studied at the molecular level based on the functions of individual genes "single gene research", no studies have utilized the "whole genome approach". To overcome the limitations, barriers and misinterpretations of "single gene" analysis approaches, scientists are increasingly concentrating on large-scale gene expression studies using genomic techniques associated with bioinformatics.

A DNA microarray is a high-throughput tool that allows the transcriptional analysis of large number of genes simultaneously to expand our understanding of cellular immunology in molecular level. There are several reports on microarray analysis to investigate transcriptional responses of pathogen-infected or immune-stimulated invertebrate animals such as *Drosophila* (Pal et al., 2008; Johansson et al., 2005), the moth *Plutella xylostella* (Eum et al., 2007), mosquito (Aguilar et al., 2005), and shrimp (Dhar et al., 2003). So far, only a few microarray studies have been conducted in mollusk species such as the oyster *Crassostrea gigas*, and *C. virginica* (Jenny et al., 2007; Lang et al., 2009). However, there is no report on large-scale gene expression study using cDNA microarray to identify immune response genes and their functional groups of disk abalone or other mollusks. Therefore, the construction of large-scale transcriptome profiling using a cDNA microarray against bacteria and virus challenge would provide much needed information for identification and characterization of different components of the abalone immune system.

The first chapter of the present study describes the application of a cDNA microarray technique for investigating immune-related genes, their transcriptional responses and possible interactions in abalone. For that, 4.2 K cDNA chip was constructed by adding 4188 transcripts from disk abalone ESTs, and described the microarray transcriptional profiling in gills and digestive tract tissues of bacterial (*V. alginolyticus, V. parahemolyticus and L. monocytogenes*) as well as gills and hemocytes of VHSV challenged abalones.

1.2. MATERIALS AND METHODS

1.2.1. Disk abalone cDNA library and 4.2 K microarray construction

An abalone cDNA library was constructed using mRNA isolated from whole tissues of disk abalone and cDNA library construction kit (Creator™ SMART™, Clontech, USA). The cDNA library was normalized using Trimmer-Direct cDNA normalization kit according to the manufacturer's protocol (Evrogen, Russia). Then, the cDNA clones were ligated into the pDNR-LIB vector at *SfiI* restriction site. After obtaining the plasmids with different cDNA inserts, 6700 clones were sequenced from the 5' end with M13 forward vector primer utilizing a Big Dye Terminator sequencing kit and ABI 3700 sequencer (Macrogen, Korea). Finally, disk abalone normalized cDNA library ESTs were obtained and used to select cDNA sequences for microarray construction. The disk abalone microarray platform was produced by GenomicTree Inc (Daejon, Republic of Korea). Briefly, a set of cDNA clones representing 4188 genes were selected from abalone ESTs to construct the cDNA microarray. In order to construct the cDNA region of each clone, PCR amplification was carried out using M13 forward and reverse universal primers (Table 2) under the following conditions: initial denaturation at 94 ^{o}C for 5 min, followed by 30 cycles of 94 ^{o}C for 1 min, 55 ^{o}C for 1 min and 72 ^{o}C for 90 s, and a final extension step at 72 ^{o}C for 10 min. The PCR-amplified products were examined by 1% agarose gel electrophoresis, purified using Sephadex G-50 columns, air-dried and resuspended in 50% DMSO solution. Purified DNA samples were spotted using an OmniGrid^{TM} Microarrayer (GeneMachines, San Carlos, CA) onto silanized glass slides (GAPS-II^{TM}, Corning, Charlotte, NC). Each slide was crosslinked with 300 mJ of short wave ultraviolet (UV) irradiation (Stratalinker, Stratagene, La Jolla, CA) and stored in humidity and light-controlled conditions until use. Finally, a total of 4188 amplicons were spotted in a total of 16 sub arrays in a 17 x 16 raw-column arrangement.

1.2.2. Abalone culture

Healthy disk abalones *(H. discus discus*) with an average body weight of 50-60 g were obtained from the Youngsoo abalone farm (Jeju Island, Republic of Korea). Abalones were maintained in flat-bottomed fiberglass tanks (60 L) with aerated and sand-filtered seawater at 18–20 °C during the experiment. Animals were acclimatized for a one week prior to the experiment. They were fed daily with fresh seaweed (*Undaria pinnatifida*) diet. A maximum of 20 animals per tank were maintained during the experiment.

1.2.3. Isolation of abalone tissues and hemocytes

Healthy animals were selected to examine the tissue specific expression profile of selected genes. Abalones were carefully dissected on ice and tissues (gills, mantle, muscle, digestive tract and hepatopancreas) were collected and pooled from three abalones. The abalone hemolymph was withdrawn from the cephalic arterial sinus, accessed anteriorly at the angle between the foot and the head using a syringe fitted with a 22-gauge needle. Collected hemolymph was immediately transferred into micro tubes and kept on ice. Then, hemolymph was centrifuged at 1500 g for 10 min at 4 ^{o}C. The supernatant was removed and hemocytes were collected. All the tissue samples were snap-frozen in liquid nitrogen immediately after obtained from abalone and stored at -80 ^{o}C until used for RNA isolation.

1.2.4. Bacterial challenge for microarray

Abalones were immune-challenged using two Gram negative (G-) bacteria *V. alginolyticus* (KCTC2472), *V. parahemolyticus* (KCTC2729); and, Gram positive (G+) *L. monocytogenes* (KCTC3710). All three bacteria were obtained from the Korean Collection for Type Cultures. The three bacteria mixture was intramuscularly injected into the abalone. Briefly, *V. alginolyticus* and *V. parahemolyticus* were cultured in marine broth for 16-20 h at 25^{o} C, while shaking at 200 rpm. *L. monocytogenes* was cultured in LB broth for 16 h at 30^{o} C. Then all three bacterial cultures (1.5 mL) were centrifuged at 7000 x g for 5 min at 4^{o} C. The supernatant fluid was removed and the bacterial pellets were re-suspended in PBS and an equal volume of each bacterial media was mixed to make bacterial stock with a cell density of 1.0 at 600 nm absorbance. Three abalones (n=3) were injected intramuscularly with 50 µL/animal (5x10^{7} cells/mL) of bacterial stock. Three control abalones (n=3) were injected with the same amount of sterile PBS and treated identically as the bacteria-injected group. Gills and digestive tissues were harvested at 24 h post challenge of bacteria and PBS control groups for microarray analysis.

1.2.5. Virus challenge for microarray

For the virus challenge experiment, abalones were intramuscularly injected with 50 µL VHSV solution (1 X 10^{8} pfu/mL per abalone). The control group was injected with same volume of PBS. Abalone gills and hemocytes were isolated after 24 h of VHSV challenge for microarray analysis. To analysis the transcriptional up-regulation of immune relevant genes digestive tract also has been selected from VHSV challenged abalones.

1.2.6. RNA isolation

An equal amount (50 mg) of gills, digestive tract or hemocytes samples were obtained from immune-challenged and un-induced or PBS-injected abalones (n=3) separately. RNA was extracted from pooled tissue of three replicate tissue samples using the Tri Reagent™ Kit (Sigma, USA) according to manufacturer's protocol. RNA quality was assessed by spectrophotometer using a Nanodrop ND-1000 (Nanodrop, USA) and run on a Bioanalyzer 2100 (Agilent, USA) for microarray analysis.

1.2.7. Microarray hybridization

RNA labeling, array hybridization and scanning were carried out by GenomicTree Inc (Daejon, Republic of Korea). Briefly, for bacteria-infected (test) and control RNAs, the synthesis of target cDNA probes and hybridization were performed using Agilent's Low RNA Input Linear Amplification Kit PLUS (Agilent Technologies, USA) according to the manufacturer's instructions. Briefly, 1 μg of each disk abalone total RNA was mixed with dT-promoter primer and M-MLV-reverse transcriptase, followed by incubation at 40 ^{o}C for 2 h. The reverse-transcribed samples were linear-amplified using T7 polymerase with 2 h incubation at 40 ^{o}C. During amplification, control cRNAs and test (from bacteria-infected tissues) cRNAs were labeled with Cy3-CTP and Cy5-CTP, respectively. Both fluorescent-labeled control and test samples were combined and resuspended in 80 μL of hybridization buffer (3X SSC and 0.3% SDS, 50% formamide). After 3 min boiling at 95 ^{o}C and 3 min cooling in ice, the hybridization mixtures were directly introduced to disk abalone 4.2K cDNA microarray. For hybridization, the microarray slide was incubated in a humidified hybridization chamber at 42^{o} C for 16 h with mild agitation to perform competitive hybridization reactions between labeled probes and targets on microarray. Washing of hybridized arrays was performed with gentle agitation to eliminate the nonspecific binding as follows: 5 min at 42 ^{o}C in 1×SSC and 0.2% SDS, 5 min at room temperature in 1×SSC and 0.2% SDS, and 2 min at room temperature in 0.1×SSC (twice). Finally, microarrays were spin-dried and stored in dark condition until scanned.

1.2.8. Microarray data analysis

The hybridization images were visualized with Axon GenePix 4000B scanner (Axon Instruments, CA) and analyzed by GenePix Pro 6.0 program (Axon Instruments, USA). The

average fluorescence intensity of each spot was calculated and local background was subtracted. All data normalization and selection of the fold-changed genes were performed using GeneSpring 7.3.1 (Agilent Technologies, USA). Intensity-dependent normalization (LOWESS) was performed, where the ratio was reduced to the residual of the Lowes fit of the intensity vs. ratio curve. The averages of normalized ratios were calculated by dividing the average of normalized test channel intensity by the average of normalized control channel intensity. Up-down regulated genes were analyzed using the algorithms BLASTX and BLASTN that are available at NCBI to identify similar (homology) sequences. When the expected value (E) was less than 1.E-05, an EST was considered as a significant match to a specific homology sequence. Then, the identified sequences were classified into functional groups using a GO web based application and manual adjustments.

1.2.9. Bacteria and VHSV challenge for microarray validation

To validate the microarray results, two independent time course experiments were conducted by applying same method of bacterial and VHSV challenge, as described for the microarray experiments. Briefly, abalones were challenged with bacteria mixture and VHSV. Tissue samples of gills, digestive tract (from bacterial challenged) and gills and hemocytes (VHSV challenged) were isolated at 3, 6, 12, 24, and 48 h. Selected tissues were collected from three individuals at every time point while control samples were collected from PBS-injected abalones.

1.2.10. cDNA synthesis

RNA isolation was done as previously described method and purified RNA was diluted up to 1 μg/μL concentration before synthesis of cDNA. A sample of 2.5 μg RNA was used to synthesize cDNA from each tissue using a Superscript III first-strand synthesis system for RT-PCR kit (Invitrogen, USA). Briefly, RNA was incubated with 1 μL of 50 μM oligo $(dT)_{20}$ and 1 μL of 10 mM dNTP for 5 min at 65 °C. After incubation, 2 μL of 10× cDNA synthesis buffer, 2 μL of dithiothreitol (DTT, 0.1 M), 1 μL of RNaseOUT™ (40 U/μL) and 1 μL of SuperScript III reverse transcriptase (15 U/μL) were added and incubated for 1 h at 50 °C. The reaction was terminated by adjusting the temperature to 85 °C for 5 min. Then, 1 μL of RNase H was added to each cDNA and incubated at 37 °C for 20 min. Finally, synthesized cDNA was diluted 10 fold (total 200 μL) before storing at -20 °C.

1.2.11. Quantitative real-time PCR (qRT-PCR)

In order to validate the microarray results we selected several candidate genes and designed the gene-specific primers. Selected genes are KLF, lachesin, muscle LIM protein, TRx-2, NFIL 3, abalone protein 38, HSC protein, IFN-44 like protein and C-Jun super family protein. The gene coding for the abalone ribosomal protein was selected as a reference gene. Gene specific primers designed from candidate genes are listed in table 1. Immune challenge was done using the same bacteria with similar treatment conditions as described for the microarray. The main difference was the isolation of tissue samples at 3 h, 6 h, 12 h, 24 h and 48 h after bacteria and VHSV challenge. The transcriptional expression was determined by qRT-PCR (TaKaRa Japan). qRT-PCR was carried out in a 20 μL reaction volume containing 5 μL of 1:10 diluted original cDNA, 10 μL of 2× SYBR Green Master Mix, 1.0 μL of each primer (20 pmol/μL), and 3.0 μL of PCR grade water using Thermal Cycler Dice^{TM} Real Time System (TaKaRa, Japan). The qRT-PCR cycling protocol was as follows: one cycle of 94 °C for 3 min, amplification for 35 cycles (95 °C, 20 s; 58 °C, 20 s; 72 °C, 30s). The baseline was set automatically by Thermal Cycler Dice^{TM} Real Time System Software (version 2.00). The expression was determined by the $2^{-\Delta\Delta CT}$ method (Livak et al., 2001). The resultant relative expression level was compared with respective PBS control to determine the expression-fold of each gene.

1.2.12. Bioinformatics tools used for sequence analysis and characterization

BLAST program was used to search similar nucleotide and protein sequences used in this study (Altschul et al., 1990). Characteristic domains or motifs were identified using PROSITE profile database (Bairoch et al., 1997). Prediction of abhisin AMP properties and similar peptide sequences were identified and compared using an antimicrobial peptide database (Wang et al., 2004). The signal peptide was predicted through a SignalP worldwide P server (http://www.cbs.dtu.dk/). The N-terminal transmembrane portion sequence domains were determined by DAS transmembrane prediction (http://www.sbc.su.se/~miklos/DAS/) and motif scan programs (http://myhits.isb-sib.ch/cgi-bin/motif_scan), respectively. The α-helix secondary structure of abhisin was predicted by the Schiffer-Edmundson helical wheel modeling using DNAstar program. Pair-wise and multiple sequence alignments were analyzed using ClustalW version 1.8 program (Thompson et al., 1994). The phylogenic relationship was determined using the neighbor-joining (NJ) method and MEGA 3.1 program (Kumar et al., 2004).

1.2.13. Statistical analysis

For RT-PCR analysis, all data represent means ± standard deviation and were subjected to a one-way ANOVA followed by Duncan's Multiple Range test using the SPSS 11.5 program. Differences were considered statistically significant at $P<0.05$.

Table 2: Description of the primers used in this study.

Primer name	Target	Orientation	Primer sequence (5'- 3')
M13	cDNA amplification	Forward	GTTTTCCCAGTCACGAC
M13	cDNA amplification	Reverse	CAGGAACAGCTATGAC
KLF-1F	Real time PCR	Forward	GTCACATGCAGCGGAATTCTAAGG
KLF-1-R		Reverse	AAGCTATCCCTAGCGGCCGTTTAT
Lachesin-1-F	Real time PCR	Forward	ACGGCAGTAGTGTCAACGAAGGA
Lachesin-1-R		Reverse	A AGGCGTAAGTGGGATGTTCCATGT
Muscle LIM protein-1F	Real time PCR	Forward	AA TACCACTATGGCCATGCACGAGAT
Muscle LIM protein-1R		Reverse	TACCACTATGGCCATGCACGAGAT
Mt-TRx-2-1F	Real time PCR	Forward	CTATCATTGCTGGCAAAGCAGGCA
Mt-TRx-2-1R		Reverse	CCCACAACTGTTGGCACGGAATTT
NFIL-3-1F	Real time PCR	Forward	AGAATAATGAGTCCGCACGACGGT
NFIL-3-1R		Reverse	TCAGAGCTGCTAGCTCATGCTTCA
Abalone protein 38-1F	Real time PCR	Forward	GTTTGTCGTCTGTGTTCAGACACTGGT
Abalone protein 38-1R		Reverse	AACGGGTTTGGCGTGTGCTTA
HSC protein-1F	Real time PCR	Forward	GCGCCAAATACAGATGCAGAACCA
HSC protein-1R		Reverse	AGGCCAGTGTGTAGAAGGAACCAA
IFN-44 like protein-1F	Real time PCR	Forward	TGACATGGCTGGCGTGTTTGAATC
IFN-44 like protein-1R		Reverse	TCGGACAAAGCTGATGGAAGACGA
C-Jun superfamily-1F	Real time PCR	Forward	ATCATTCAGGCAAACGGCATGGTC
C-Jun superfamily-1R		Reverse	GAAGTTCGGCCAAAGCATCCACAA
TNF-1F	Internal sequencing	Forward	ACAGAAGGGAATCGTCGTGGAGAT
Fas ligand -1F	Internal sequencing	Forward	ACACGACTGGTGGCGTCAGATATT
TNF-2F	Real time PCR	Forward	TGAACAGAAAGGTGCAAGGCAACC
TNF-2R		Reverse	AAGAGTTGTCTCCCTGGTCCAACA
Fas ligand -2F	Real time PCR	Forward	ACACGACTGGTGGCGTCAGATATT
Fas ligand -2R		Reverse	ACAGTGAACAATGCCAAGGCCATC
TNF- α-3F	Cloning of ORF	Forward	(GA)3GAATTCATTGCGGTTATTTGCCTTGTTGTA (*Eco*R I)
TNF- α-3R		Reverse	(GA)3AAGCTTTAAATCATATATACACCAAAGTAAT (*Hind*III)
Fas ligand -3F	Cloning of ORF	Forward	(GA)3GAATTCATGTCTTCCTCTGTGTGTGAGAGG (*Eco*R I)
Fas ligand -3R		Reverse	(G)3AAGCTTCTACAGACGATGCAGCCCAAAATG (*Hind*III)
LITAF-1F	Internal sequencing	Forward	GTTTACTGTGCTGTGCTGTTCGCT
LITAF-2F	Internal sequencing	Forward	GTCACAAGGAGCACAATGTAGAAC
Rel/NF-kB-1F	Internal sequencing	Forward	CACCCACATTCACTTGTGGGGAAAGA
Rel/NF-kB-F2	Cloning of ORF	Forward	TCAGGAAGGTCGCGCACATCATC

Rel/NF-kB-R1	Cloning of ORF	Reverse	TCAAGAGTTCTCACTTAG CCCCTG
LITAF-3F	Real time PCR	Forward	ACAGATCGTCACGGCAACTCACTA
LITAF-3R		Reverse	AAATCACACCCAACAAGGCACAGG
Rel/NF-kB-F3	Real time PCR	Forward	AATGTTCTCCAGTGCTGCTCTGAC
Rel/NF-kB-R2		Reverse	AGCAGATCTTCCCTCACACTCGTA
Defensin-1F	Real time PCR	Forward	TTATCGCCTTTGTTGGCATGTCCG
Defensin-1R		Reverse	ACAGGCAGAATCACCGAAGGAGTT
Histone H2A-F1	Internal sequencing	Forward	AACACCAGGTCATCCGTTGA
Histone H2A-F2	Real time PCR	Forward	GCAAAGGTGGAAAAACGAAGGC
Histone H2A-R1		Reverse	CGCTGCGGATTTCTTAGGCAACAA
MnSOD-1F	Real time PCR	Forward	ATGTTGTCTGCTACGCTCTCTGCT
MnSOD-1R		Reverse	GCGTTGTGATGCTTCTTGTGGTGA
Cu,ZnSOD-1F	Real time PCR	Forward	TGCTGACGCATCAGGAGTAGCAAA
Cu,ZnSOD-1R		Reverse	TCAGGCTTTCTTCATTGCCTCCCT
Catalase-1F	Real time PCR	Forward	CTACCTGCAACTTCCCGTCAACT
Catalase-1R		Reverse	AGAGAGCTTGAAAGGGCACTCCAT
TPx-1F	Real time PCR	Forward	TCATTGATGACAAGGCCAACCTGC
TPx-1R		Reverse	ACAAACTTCTCCGTGCTTGTCAGT
SeGPx-1F	Real time PCR	Forward	TATACCGCCACCTGGTGAAAGGAA
SeGPx-1R		Reverse	CCACATTGACGATCAGCAGCACAT
TRx2-1F	Real time PCR	Forward	CTATCATTGCTGGCAAAGCAGGCA
TRx-2-1R		Reverse	CCCACAACTGTTGGCACGGAATTT
Abalone ribosomal-1F	Internal control/	Forward	T CAGGAGGAGTCCAGTGCAGTATG
Abalone ribosomal-1R	Housekeeping gene	Reverse	CACCAACAAGGACATCATTTGTC

The number of the same base pair repeats is indicated within the bracket with the subscripted number. Restriction enzyme sites of the cloning primers are underlined.

1.3. Results and discussion

1.3.1. *Microarray analysis differently expressed genes in abalone gills and digestive tract after bacteria challenge*

Transcriptional responses in gills and digestive tract tissues of abalone were assayed using a cDNA chip at 24 h post challenge of *V. alginolyticus, V. parahemolyticus,* and *L. monocytogenes*. The threshold significance for the microarray was chosen at $P< 0.05$, with a signed expression change (≥2 or ≤2 –fold) of both up- and down-regulated genes. Up and down regulated transcripts in bacteria challenge vs control (PBS) groups in were visualized using heat map (fig 2). Number of genes significantly up and down –regulated based on the tissue type and their GO analysis results are shown in fig 3. The challenge with the three bacterial species has resulted in distinct and partially overlapping transcript profiles for gills and digestive tract genes compared to PBS-injected control abalones. Among the 4188 genes analyzed, 68 (1.6%) and 112 (2.7%) had altered expression levels (≥2 or ≤2 –fold) upon challenge with bacteria mixture in gills and digestive tract, respectively (Fig. 3A). Based on significance and gene selection criteria, 51 and 84 genes were up-regulated (≥2-fold) in gills and digestive tract tissues, respectively. In addition, 38 genes were commonly up-regulated (overlap) in gills and digestive tract tissues. In contrast to up-regulation, a total of 17 and 38 genes were down-regulated (≤2 –fold) in gills and digestive tract, respectively, and only 4 genes were down-regulated commonly in both tissues after bacterial challenge. Microarray results showed that a relatively lower number of genes were down-regulated in gills and digestive tract compared to the number of up-regulated genes at 24 h post challenge with bacteria. Interestingly, a higher number of genes exhibited significant expression changes in digestive tract, compared to gills. There were 46 tissue-specific transcripts that were up-regulated only in digestive tract. In contrast, 13 transcripts showed a gill-specific up-regulation response.

Clustering of differentially expressed genes in disk abalone gills and digestive tract

Abalone genes that had a significantly altered expression level (≥2 or ≤2 –fold) by bacterial challenge were categorized into 4 main clusters. Clusters 1 and 2 consisted of genes that were up-regulated in gills and digestive tract, respectively, while clusters 3 and 4 were down-regulated in gills and digestive after bacterial challenge, respectively. The lists of genes and details on exact fold changers of 4 different clusters are given in table 3, 4, 5 and 6. GO analysis results of differentially expressed abalone genes belonging to the four different clusters are shown in figure 4.

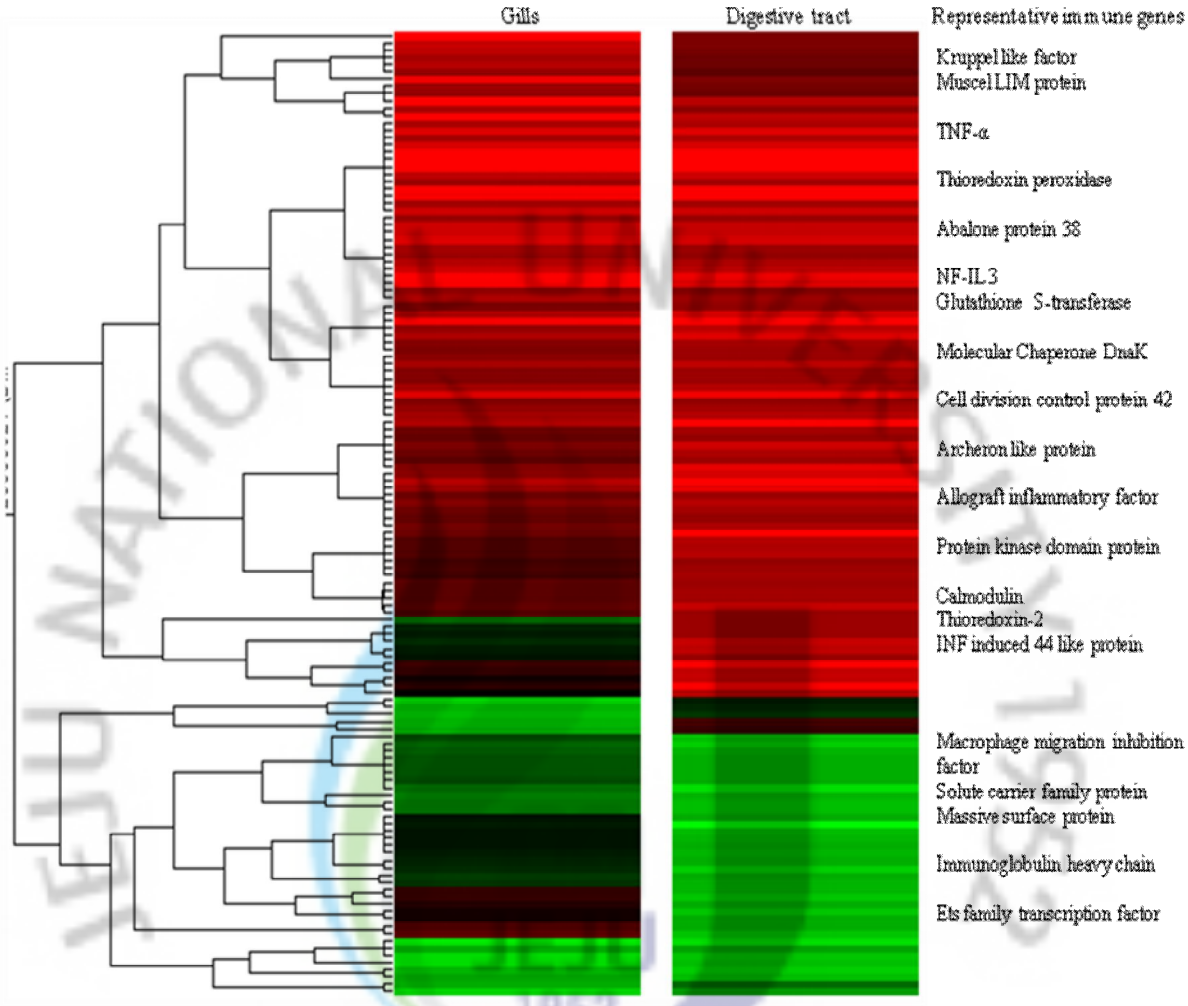

Fig. 2. Gene expression profiles of significantly regulated transcripts (≥2 or ≤2 –fold change) in abalone gills and digestive tract at 24 h post challenge of *V. alginolyticus, V. parahemolyticus*, and *L. monocytogenes*. Each row represents a cDNA clone that was expressed at a statistically significant level in bacterial challenged animals relative to control individuals in each tissue. Selected immune response clones are labeled at either side of each tissue. The quantitative changes in gene expression are represented in colors: red indicated that gene is more highly expressed (up-regulated) than its respective control, and green indicates repressed (down-regulated) genes.

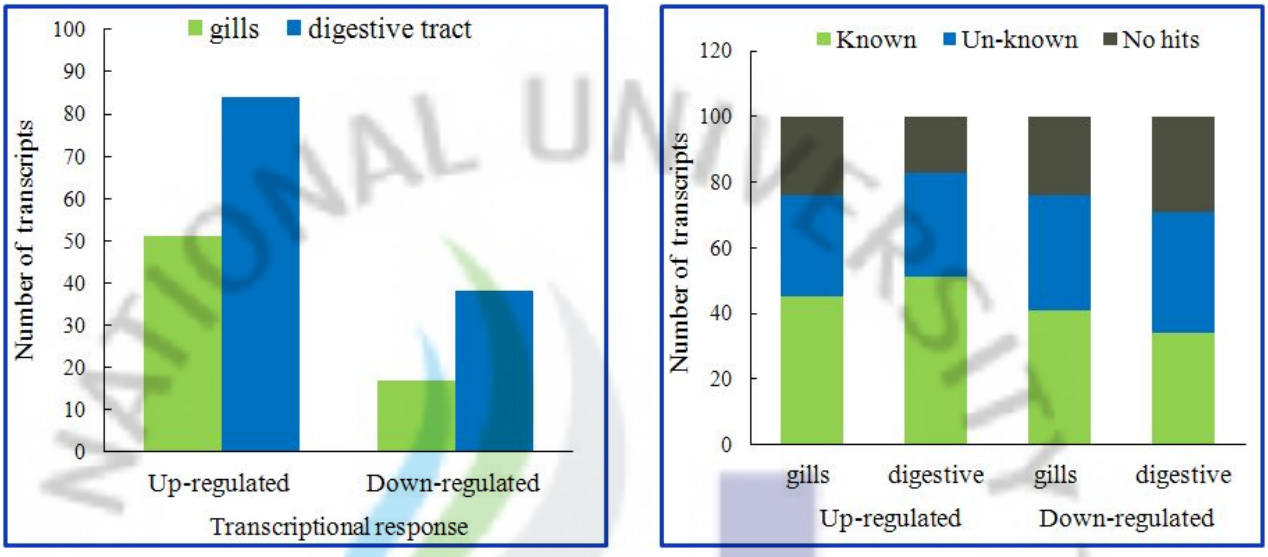

Fig.3. Classification of significantly (≥2 or ≤2 –fold change) responded transcript numbers in abalone at 24 h post challenge of *V. alginolyticus, V. parahemolyticus, L. monocytogenes.* A) number of up-and down-regulated transcripts in gills and digestive tract; B) Blast and GO analysis of significantly up and down-regulated transcripts in gills and digestive tract.

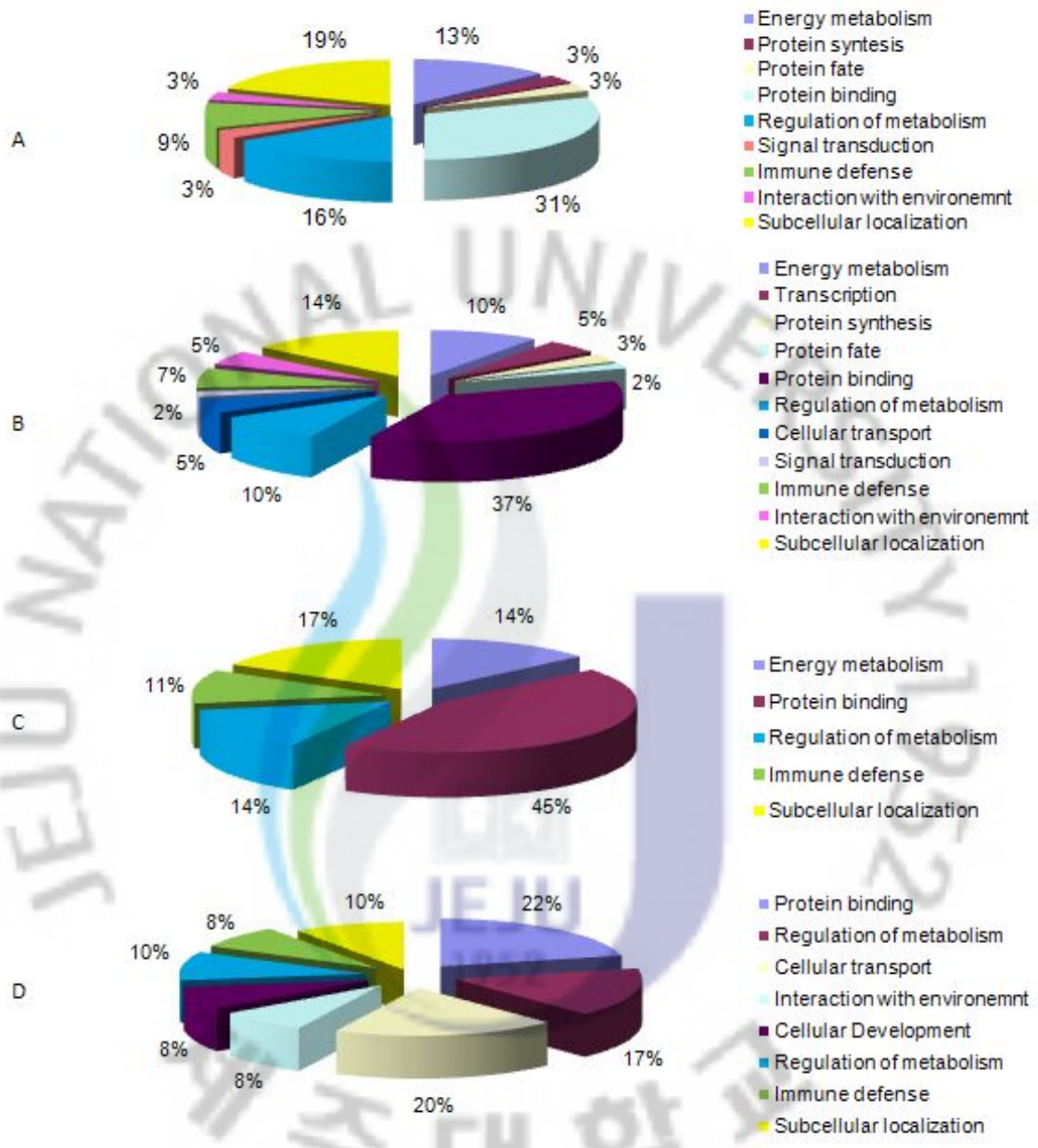

Fig. 4. Gene Ontology (GO) analysis of significantly regulated transcripts (≥2 or ≤2 -fold) in abalone after *V. alginolyticus, V. parahemolyticus* and *L. monocytogenes* challenge at 24 h. A) up-regulated transcripts in gills; B) up-regulated transcripts in digestive tracts; C) down-regulated transcripts in gills; D) down-regulated transcripts in digestive tract. The legend describing the color-coded GO categories is shown with each figure.

Cluster 1: up-regulated (≥2–fold) genes in gills

A total of 51 genes up-regulated in gills are listed in Table 3 with their respective microarray expression levels, and the most similar homology identification in NCBI. Sequence homology and GO analysis results revealed that 45%, 31% and 24% of sequences were exhibited as known, unknown (unclassified function), and "no hit" categories using BLASTx cutoff *E*-value at 10^{-5} (fig. 3B). Significantly up-regulated genes were categorized by different putative functions including metabolism, protein synthesis, protein fate, protein binding, regulation of metabolism, signal transduction, immune defense, interaction with environment and sub-cellular localization (fig. 4). In abalone gills, 9% of the up-regulated genes were grouped into the immune defense category. A broad range of immune-relevant genes were identified in this category, which are involved in transcriptional regulation (KLF), cell adhesion (Ependymin-related protein), regulators of apoptosis and immune modulation (TNF-α; Baculoviral IAP repeat protein), IFN-related cytokines (IFN-induced 44-like protein), antioxidant enzyme (Glutathione-S-transferase) and other indirect immune relevant genes (muscle LIM protein).

Cluster 2: up-regulated (≥2–fold) genes in digestive tract

Up-regulated genes in digestive tract after the bacterial challenge are shown Table 4. BLAST and GO analysis results based on the digestive tract microarray, 51% and 32% up-regulated genes were belonged to known and unknown groups, respectively (Fig. 3B). Also, 17% gene sequences have not shown any BLAST hit. Results shown that 7% of the up-regulated genes were represented by immune defense category belong to abalone digestive tract. Interestingly, immune-relevant genes such as KLF, TNF-α, baculoviral IAP repeat protein, glutathione-S-transferase, IFN-induced 44-like proteins were commonly up-regulated in gills and digestive tract by bacterial challenge. Moreover, GO analysis results showed the presence of additional immune potential genes in cluster 2. These were classified under signal transduction (protein kinase domain protein), inflammatory responses (AIF; NFIL-3), cell adhesion (ras suppressor protein), stress response (TRx-2 and TPx), immune regulation (calmodulin), and apoptosis (archeron-like protein). Our results further demonstrated that 37% of the up-regulated genes were involved in protein binding function in abalone digestive tract. Most of other up-regulated genes in digestive tract could be assigned to different functional groups such as energy metabolism, protein synthesis, cellular transport and regulation of metabolism reflecting different aspects of abalone physiological status.

Cluster 3: down-regulated (≤2 –fold) genes in gills

Significantly down-regulated genes in gills after the bacterial challenge are shown in Table 5. BLAST and GO analysis results showed that 41% known and 35% unknown genes were down-regulated while 24% of the transcripts had no BLAST hit (Fig. 3B). GO analysis results showed that only four immune-relevant genes were down-regulated in gills including macrophage migration inhibitory factor, Ets-family transcription factor, merozoite surface protein, and immunoglobulin heavy chain protein. Go results further demonstrated that 14%, and 46% of down-regulated genes were grouped into energy metabolism and protein binding, respectively (4C).

Cluster 4: down-regulated (≤2 –fold) genes in digestive tract

Significantly down-regulated genes in abalone digestive tract after the bacterial challenge are shown in Table 6. Among 38 down-regulated genes in the digestive tract, 34% and 37% were identified as known and unknown categories, respectively (Fig. 3B). A relatively higher number of down-regulated genes (29%) did not show homology to known sequences. A down-regulated gene cluster of the digestive tract is shown in fig 4D. Results show that these genes were classified under different functional systems in abalone, such as energy metabolism, transcriptional regulation, protein synthesis, and cellular transport, and signal transduction, interaction with the environment, sub-cellular localization and immune defense. In the immune category, two important genes were down-regulated namely macrophage migration inhibitory factor and programmed cell death.

Additionally, there were four transcripts significantly down-regulated in both gills and digestive tract. Among these four, three sequences exhibited homology to macrophage migration inhibitory factor, proton/sodium-glutamate symport protein, similar to egg binding protein while other only could be described as a hypothetical protein.

Table 3. List of genes significantly up-regulated in abalone gills after bacterial challenge

Number	EST number	Putative gene name	Expression fold (+)	Accession number of similar sequence	Blast X *E*- value
1	cDNA_19-G11	Kruppel-like factor	6.2	EF587285.1	6.00E-101
2	cDNA_13-E01	Iodothyronine deiodinase 3	6.2	DQ888896	6.00E-28
3	cDNA_01-H07	Ependymin related protein-1	5.1	ABO26653.1	4.00E-49
4	cDNA_01-F07	Muscle LIM protein	5.0	ACJ65685.1	1.00E-94
5	cDNA_26-F11	similar to Cat Eye Syndrome protein	4.7	XP_416390.2	5.00E-36
6	cDNA_50-E06	Baculoviral IAP repeat protein	4.6	EEB10965.1	3.00E-41
7	cDNA_04-A07	Extracellular ligand-binding receptor	4.6	YP919708.1	2.00
8	cDNA_01-H08	Myo-insitol oxygenase	4.0	NP_064361.2	1.00E-59
9	cDNA_19-F01	No hit	4.0	-	-
10	cDNA_27-H06	Hypothetical protein	3.9	XP_001659791.1	2.00E-46
11	cDNA_27-B03	Hypothetical protein	3.8	XP_002224975.1	0.008
12	cDNA_46-G06	Hypothetical protein	3.7	XP_002235967.1	5.00E-18
13	cDNA_01-F06	Cell wall surface family protein	3.7	NP_816151.1	0.87
14	cDNA_52-A03	Sulfatase 1 precursor	3.3	AAF30402.1	1.00E-85
15	cDNA_01-G08	No hit	3.3	-	-
16	cDNA_27-D03	Family 10 cellulase	3.1	AAP31839.2	1.00E-47
17	cDNA_70-A09	Tumor necrosis factor alpha	3.1	ACF75368.1	1.00E-116
18	cDNA_21-F10	Hypothetical protein	3.0	XP_392183.1	5.00E-34
19	cDNA_19-G10	No hit	3.0	-	-
20	cDNA_35-A12	Eukaryotic translation initiation factor 3	3.0	ACI68356.1	1.00E-72
21	cDNA_19-H10	Hypothetical protein	3.0	XP_001368094.1	3.00E-73
22	cDNA_13-D01	Type I iodothyronine deiodinase	2.8	O42449.3	1.00E-24
23	cDNA_04-B07	Hypothetical protein	2.7	XP_001906452.1	3.8
24	cDNA_58-C07	No hit	2.6	-	-
25	cDNA_50-G09	No hit	2.6	-	-
26	cDNA_67-G08	Cyano fluorescent protein	2.6	ABZ11027.1	7.00E-04
27	cDNA_44-B08	Hypothetical protein	2.5	XP_002237731.1	2.00E-37
28	cDNA_26-A12	No hit	2.5	-	-
29	cDNA_09-C05	No hit	2.4	-	-
30	cDNA_22-E01	Interferon-induced 44-like protein	2.4	ACJ12608.1	0.004
31	cDNA_13-D04	No hit	2.4		
32	cDNA_44-A09	Hypothetical protein	2.4	XP_001374394.1	6.00E-10
33	cDNA_51-A12	Glutathione-S-transferase isoform 1	2.3	ABF67506.1	1.00E-120
34	cDNA_30-E11	Hypothetical protein	2.3	XP_002219320.1	9.00E-23
35	cDNA_01-G07	Abalone protein 38	2.3	ABY87432.1	2.00E-24
36	cDNA_04-E02	Hypothetical protein	2.3	XP_002206531.1	2.00E-10
37	cDNA_66-H09	Molecular chaperone DnaK	2.3	YP_015810.1	3.00E-67
38	cDNA_24-G09	Hypothetical protein	2.2	XP_001636064.1	6.00E-39
39	cDNA_01-E07	No hit	2.2	-	-
40	cDNA_14-E10	Beta-galactosidase like protein	2.2	CAA18137	4.2
41	cDNA_69-E09	Cell division control protein 42	2.2	XP_957345.2	8.00E-30
42	cDNA_56-A09	Hypothetical protein	2.2	XP_001744503.1	3.00E-18
43	cDNA_12-B04	Transposase	2.1	NP_061389.1	1.00E-157
44	cDNA_47-D02	DNA primase	2.1	ZP_02425989.1	0.82
45	cDNA_23-F03	Hypothetical protein	2.1	YP_164729.1	0.033
46	cDNA_19-G12	No hit	2.1	-	-
47	cDNA_03-B01	No hit	2.1	-	-
48	cDNA_47-C02	Hypothetical protein	2.1	YP_002499530.1	4.00E-10
49	cDNA_48-F04	No hit	2.1	-	-

50	cDNA_13-D03	Hypothetical protein	2.0	XP_001621740.1	2.00E-09
51	cDNA_63-C05	Hypothetical protein	2.0	XP_002235005.1	1.00E-25

Expression folds of up-or down regulation is shown as a measure of normalized bacterial challenge/PBS control.

Table 4. List of genes significantly up-regulated in abalone digestive tract after bacterial Challenge

Serial number	EST number	Putative gene name	Expression Fold (+)	Accession number of similar sequence	Blast X *E*- value
1	cDNA_19-G11	Kruppel-like factor	6.9	EF587285.1	6.00E-101
2	cDNA_27-H06	Hypothetical protein	6.0	XP_001659791.1	2.00E-46
3	cDNA_09-C05	No hit	5.6	-	-
4	cDNA_01-H07	Ependymin related protein-1	5.1	ABO26653.1	4.00E-49
5	cDNA_01-F07	Muscle LIM protein	4.8	ACJ65685.1	1.00E-94
6	cDNA_44-B08	Hypothetical protein	4.6	XP_002237731.1	2.00E-37
7	cDNA_04-A07	Extracellular ligand-binding receptor	4.5	YP919708.1	2.00
8	cDNA_69-D10	Hypothetical protein	4.2	XP_002210288.1	5.00E-05
9	cDNA_27-B03	Hypothetical protein	4.0	XP_002224975.1	0.008
10	cDNA_37-H07	Hypothetical protein	4.0	YP_002535627.1	4.00E-11
11	cDNA_22-G12	Motile sperm domain containing protein	4.0	XP_538179.1	0.038
12	cDNA_52-A03	Sulfatase 1 precursor	3.7	AF109924.1	1.00E-85
13	cDNA_50-E06	Baculoviral IAP repeat-containing protein	3.7	EEB10965.1	3.00E-41
14	cDNA_47-D02	DNA primase	3.5	ZP_02425989.1	0.82
15	cDNA_01-D07	No hit	3.5	-	
16	cDNA_01-G08	No hit	3.3	-	
17	cDNA_01-H08	Myo-insitol oxygenase	3.3	NP_064361.2	1.00E-59
18	cDNA_51-A12	Glutathione-S-transferase isoform 1	3.2	ABF67506.1	1.00E-120
19	cDNA_44-A09	Hypothetical protein	3.2	XP_001374394.1	6.00E-10
20	cDNA_27-D03	Family 10 cellulase	3.1	AAP31839.2	1.00E-47
21	cDNA_01-F06	Cell wall surface family protein	3.1	NP_816151.1	0.87
22	cDNA_63-C05	Hypothetical protein	3.1	XP_002235005.1	1.00E-25
23	cDNA_19-H11	Ras suppressor protein 1	3.0	XP_694901.3	4.00E-16
24	cDNA_32-F02	Hypothetical protein	3.0	XP_002227539.1	1.00E-17
25	cDNA_70-A09	Tumor necrosis factor alpha	2.9	ACF75368.1	1.00E-116
26	cDNA_04-B07	Hypothetical protein	2.9	XP_001906452.1	3.8
27	cDNA_24-D12	No hit	2.9		
28	cDNA_34-F12	*Mg-PIXM ester cyclae	2.9	ZP_01447969	5.1
29	cDNA_21-F10	Hypothetical protein	2.8	XP_392183.1	5.00E-34
30	cDNA_63-G12	V-type proton ATPase	2.8	XP_002165747.1	1.00E-53
31	cDNA_19-G10	No hit	2.8	-	-
32	cDNA_18-B09	No hit	2.8	-	-
33	cDNA_24-E12	Hypothetical protein	2.7	XP_002211649.1	6.00E-07
34	cDNA_19-G12	No hit	2.7	-	-
35	cDNA_35-A12	Eukaryotic translation initiation factor 3	2.7	ACI68356.1	1.00E-72
36	cDNA_19-F01	No hit	2.7	-	-
37	cDNA_04-E02	Hypothetical protein	2.6	XP_002206531.1	2.00E-10
38	cDNA_50-B06	Thioredoxin peroxidase 2	2.6	ABO26635.1	1.00E-111
39	cDNA_26-F11	similar to Cat Eye Syndrome protein	2.5	XP_416390.2	5.00E-36
40	cDNA_56-G10	Hypothetical protein	2.5	XP_002227365.1	8.00E-28
41	cDNA_24-C12	Hypothetical protein	2.5	XP_001631546.1	7.00E-23
42	cDNA_14-E10	Beta-galactosidase like protein	2.5	CAA18137	4.2
43	cDNA_26-C07	Archeron-like protein	2.5	ACJ65686.1	1.00E-116
44	cDNA_66-H09	Molecular chaperone DnaK	2.5	YP_015810.1	3.00E-67
45	cDNA_07-F05	Glycogen synthase kinase	2.4	ACJ65687.1	5.00E-74
46	cDNA_13-D04	No hit	2.4	-	-
47	cDNA_68-H04	Transitional endoplasmic reticulum ATPase	2.4	XP_966692	1.4
48	cDNA_01-C07	SJCHGC00821 protein	2.4	AAW26951.1	1.00E-48

49	cDNA_50-G09	No hit	2.4	-	-
50	cDNA_30-E11	Hypothetical protein	2.3	XP_002219320.1	9.00E-23
51	cDNA_01-E07	No hit	2.3	-	-
52	cDNA_63-E10	Solute carrier family 6, member 9	2.3	XP_002208721.1	5.00E-38
53	cDNA_48-F04	No hit	2.3	-	-
54	cDNA_41-H11	Allograft inflammatory factor	2.3	ACJ65689.1	1.00E-80
55	cDNA_09-B05	Hypothetical protein	2.3	NP_297916.1	4.00E-07
56	cDNA_25-C10	Cubilin	2.3	NP_001088914.1	1.00E-12
57	cDNA_60-D08	Hypothetical protein	2.3	XP_418270.2	0.004
58	cDNA_26-G11	Protein kinase domain protein	2.2	XP_001028019	4.1
59	cDNA_23-F03	Hypothetical protein	2.2	YP_164729.1	0.033
60	cDNA_26-A12	No hit	2.2	-	
61	cDNA_63-B05	Hypothetical protein	2.2	XP_001629111.1	3.00E-31
62	cDNA_39-G11	Sodium-neurotransmitter symporter	2.2	EEC18529.1	1E-74
63	cDNA_37-A06	Hypothetical protein	2.2	XP_311178.3	6.00E-06
64	cDNA_67-E08	Calmodulin 2	2.2	ABY87354.1	2.00E-68
65	cDNA_01-G07	Abalone protein 38	2.2	ABY87432.1	2.00E-24
66	cDNA_63-F12	Hypothetical protein	2.1	AAW26951.1	4.00E-49
67	cDNA_15-A01	Hypothetical protein	2.1	XP_002229586.1	2.00E-45
68	cDNA_52-H12	Putative ribosomal protein S13	2.1	ABW90418.1	4.00E-24
69	cDNA_69-E09	Cell division control protein 42	2.1	XP_957345.2	8.00E-30
70	cDNA_37-D03	Chloride cannel activated protein	2.1	XP_796840.1	5.00E-37
71	cDNA_21-B05	CDH1-D	2.1	AAL31950.1	4.00E-32
72	cDNA_05-G01	Stanniocalcin-like protein	2.1	ABY87355.1	1.00E-11
73	cDNA_42-H01	Hypothetical protein	2.1	XP_002215013.1	4.00E-30
74	cDNA_39-F12	Integral membrane protein	2.1	YP_001598233	8.3
75	cDNA_30-G11	Solute carrier family 3, member 1	2.1	XP_782131.1	2.00E-33
76	cDNA_22-F12	No hit	2.1	-	-
77	cDNA_09-D05	Hypothetical protein	2.1	XP_001626032.1	2.00E-09
78	cDNA_63-B06	Sodium channel protein	2.1	AAP13992	9
79	cDNA_56-A09	Hypothetical protein	2.0	XP_001744503.1	3.00E-18
80	cDNA_22-D05	Hypothetical protein	2.0	XP_001501860.2	1.00E-10
81	cDNA_32-H12	Hypothetical chloroplast RF1	2.0	YP_740709.1	0.081
82	cDNA_39-G03	Thioredoxin 2	2.0	XP_001969325.1	4.00E-18
83	cDNA_18-F01	Interleukin 3 regulated protein	2.0	ACJ65688.1	1.00E-128
84	cDNA_22-E01	Interferon-induced 44-like protein	2.0	ACJ12608.1	0.004

* Mg-protoporphyrin IX monomethyl ester cyclase is abbreviated as Mg-PIXM ester cyclase

Table 5. List of genes significantly down-regulated in abalone gills after bacterial challenge.

Serial number	EST number	Putative gene name	Expression fold (-)	Accession number of similar sequence	Blast X *E*- value
1	cDNA_42-D01	Proton/sodium-glutamate symport protein	2.9	ZP_01723331	5.2
2	cDNA_42-E09	No hit	2.8	-	-
3	cDNA_30-H03	Hypothetical protein	2.7	XP_002224539.1	3.00E-15
4	cDNA_13-A09	Hypothetical protein	2.5	XP_002210123.1	5.00E-27
5	cDNA_48-C01	Merozoite surface protein 1	2.3	ABS84417.1	5.1
6	cDNA_22-G07	No hit	2.2	-	-
7	cDNA_55-F07	Similar to egg binding receptor	2.2	XP_791820.2	0.002
8	cDNA_07-H11	No hit	2.2	-	-
9	cDNA_51-H04	Macrophage migration inhibitory factor	2.1	ACJ65690.1	1.00E-62
10	cDNA_56-F02	No hit	2.1	-	-
11	cDNA_48-C10	Massive surface protein	2.1	YP_002000023.1	0.006
12	cDNA_38-F10	ETS-family transcription factor	2.1	AAU11487.2	2.00E-50
13	cDNA_41-D02	Hypothetical protein	2.0	XP_314226.4	0.059
14	cDNA_17-G02	Hypothetical protein	2.0	NP_506781.1	4.00E-25
15	cDNA_38-E08	Hypothetical protein	2.0	XP_002309564.1	4.00
16	cDNA_48-A09	Immunoglobulin heavy chain	2.0	XP_002082027.1	0.07
17	cDNA_41-C08	Hypothetical protein	2.0	NP_001106593.1	8.00E-16

Table 6. List of genes significantly down-regulated in abalone digestive tract after bacterial challenge.

Serial number	EST number	Putative gene name	Expression fold (-)	Accession number of similar sequence	Blast X *E*- value
1	cDNA_15-A05	No hit	3.7	-	
2	cDNA_41-F03	Hypothetical protein	2.8	XP_002094704.1	4.00E-07
3	cDNA_69-B09	similar to Headcase protein	2.6	XP_001607251.1	7.00E-50
4	cDNA_55-F07	similar to egg binding receptor 1	2.6	XP_791820.2	0.002
5	cDNA_16-E12	Myosin essential light chain	2.5	ABO26638.1	4.00E-87
6	cDNA_42-E09	Proton/sodium-glutamate symport protein	2.5	ZP_01723331	5.2
7	cDNA_65-E01	Hypothetical protein	2.4	XP_001024860	0.83
8	cDNA_09-D07	Hypothetical protein	2.4	XP_001321169.1	5.00E-05
9	cDNA_16-E05	Carboxypeptidase A-like protein	2.4	ABV44738.1	8.00E-15
10	cDNA_11-B10	Hypothetical protein	2.3	XP_002237001.1	2.00E-66
11	cDNA_38-E08	Hypothetical protein	2.3	XP_002309564.1	4.00
12	cDNA_42-D01	No hit	2.3	-	-
13	cDNA_47-E09	Hypothetical protein	2.2	XP_001614410	7.8
14	cDNA_51-D06	Hypothetical protein	2.2	XP_001717648	4.3
15	cDNA_54-A12	Na-dependent Cl/HCO3 exchanger	2.2	AAN75454.1	3.00E-63
16	cDNA_09-E07	similar to solute carrier family 16	2.2	XP_543918.1	1.00E-21
17	cDNA_60-B01	No hit	2.2	-	
18	cDNA_03-B07	Mip2 protein	2.2	AAI55723.1	1.00E-08
19	cDNA_53-E11	Predicted protein	2.1	XP_001382080.1	1.00E-16
20	cDNA_23-E03	S-layer domain protein	2.1	ZP_02169523	4.7
21	cDNA_09-B09	No hit	2.1	-	
22	cDNA_05-G09	Hypothetical protein	2.1	NP_001090151	7.5
23	cDNA_62-B11	Hypothetical protein	2.1	XP_001349986	7.8
24	cDNA_09-H09	Predicted protein	2.1	XP_002125356.1	8.00E-26
25	cDNA_60-H07	No hit	2.1	-	-
26	cDNA_05-H09	Parafibromin	2.0	NP_001016031.2	2.00E-76
27	cDNA_29-B01	No hit	2.0	-	-
28	cDNA_40-F11	No hit	2.0	-	-
29	cDNA_62-H02	No hit	2.0	-	-
30	cDNA_45-B09	Hypothetical protein	2.0	XP_001424468	9.6
31	cDNA_07-A10	Hypothetical protein	2.0	XP_002230082.1	1.00E-08
32	cDNA_03-G05	Hypothetical protein	2.0	XP_001716613	0.2
33	cDNA_32-F12	Hypothetical protein	2.0	XP_001683321	0.51
34	cDNA_60-H04	No hit	2.0	-	-
35	cDNA_52-D11	No hit	2.0	-	-
36	cDNA_49-G07	Programmed cell death 2a	2.0	XP_002222564.1	8.00E-81
37	cDNA_26-H10	Phenol sulfotransferase	2.0	NP_998930.1	1.00E-30
38	cDNA_51-H04	Macrophage migration inhibitory factor	2.0	ACJ65690.1	1.00E-62

Confirmation of bacterial challenge microarray results by qRT-PCR

In order to confirm our microarray results, we selected six candidate genes from the significantly up-regulated genes from gills (KLF, lachesin and muscle Lim protein) and digestive tract (TRx-2, NFIL-3 and abalone protein 38). Additionally, we have done full-length sequencing of several genes for further characterization. QRT-PCR result of gene expression profiles are shown in figure 5. The first gene corresponded to KLF, a representative transcription factor involved in the activation of immune-relevant genes under different immune modulation. Results showed that abalone KLF transcripts were significantly up-regulated in gills with the highest induction (4.4-fold) at 24 h post infection of bacteria (fig. 5-A). In microarray analysis, one EST clone showed a 2-fold up-regulation in gills that corresponds to lachesin, a protein of an immunoglobulin superfamily. However, confirmation of results showed that lachesin was induced in gills with 3.8-fold at 24 h, which was higher than the level observed on the microarray (Fig. 5-B). The third candidate gene was represented by muscle Lim protein, which has shown significant up-regulation in both gills (5.0-fold) and digestive tract (4.8-fold) in microarray analysis. In the gills, muscle Lim transcripts were shown to have a lower transcriptional induction (2.3-fold) at 24 h (fig. 5-C) than microarray results, however; it was significantly induced during 3-48 h post bacterial challenge in the time course experiment. Another set of clones namely TRx-2, NFIL-3 and abalone proteins 38 were selected from the genes from digestive tract. TRx-2 is represented as an important antioxidant enzyme in disk abalone which showed significant induction (1.6-fold) at 12 h (fig. 5-D). We observed that expression (1.4-fold) at 24 h in time course analysis was lower than that of in microarray expression (2.0-fold) in digestive tract. The NFIL-3 (Fig. 5E) showed significant enhancement of transcripts over the 48 h bacterial challenge compared to microarray results at 24 h (2.0-fold). The final candidate gene was designated as abalone protein 38 since it matched to sequence identified from bacteria-challenged abalone *Haliotis diversicolor* (ABY87432). Abalone protein 38 has shown significant induction during the course of bacteria treatment (fig. 5F), showing greater expression (24-fold) at 24 h than that observed for the microarray data. Overall results revealed that our microarray data could be validated based on the candidate gene expression profiles with induced levels obtained by qRT-PCR. However, it is important to note that most of the up-regulated expression levels (in qRT-PCR) at 24 h post challenge do not exactly match the microarray data, which may be due to variation among the individual animals.

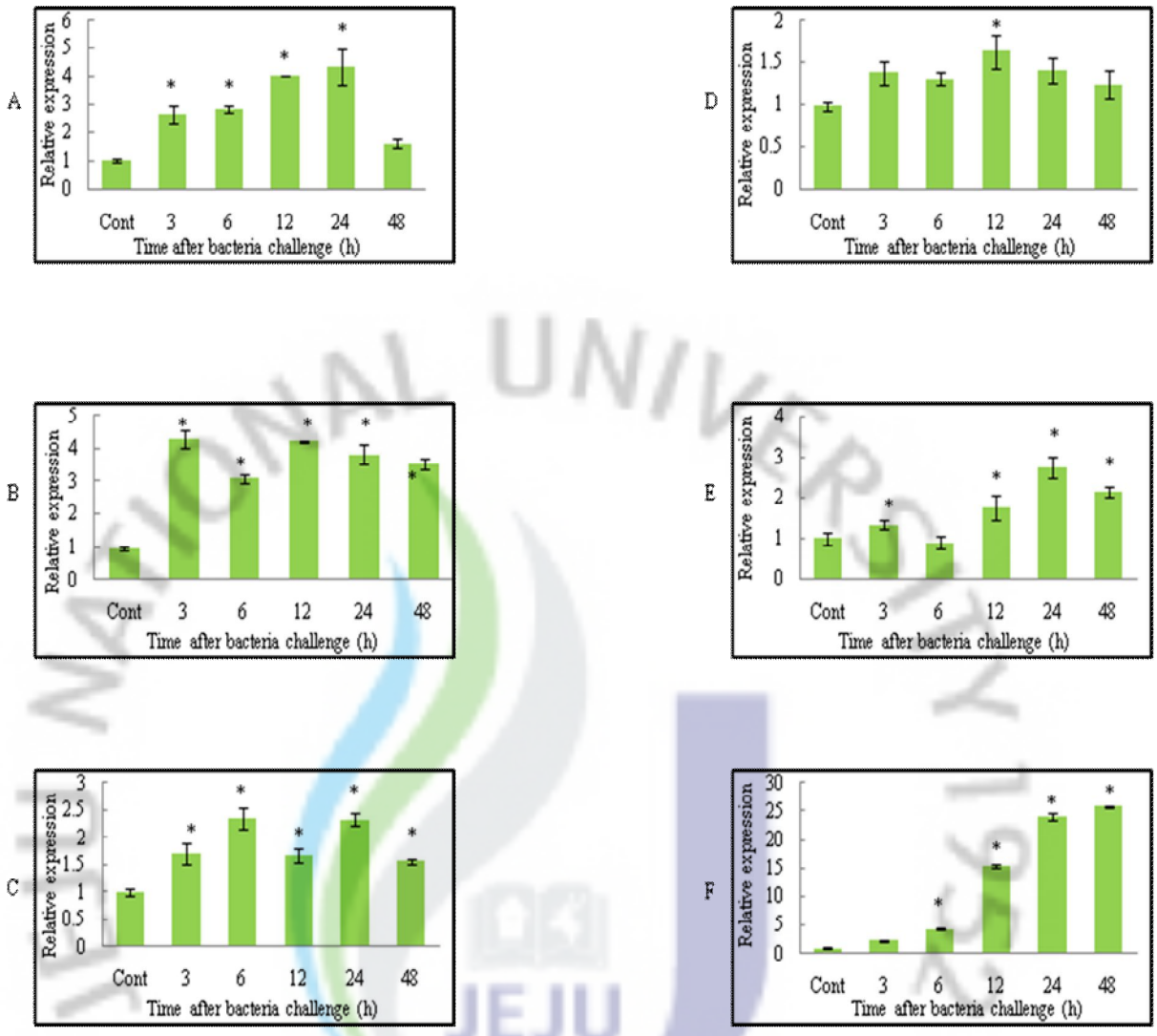

Fig. 5. qRT-PCR analysis of six potential (candidate) immune genes identified from the bacterial challenged microarray analysis of abalone gills and digestive tract. A) KLF (gills); B) lachesin (gills); C) muscle Lim protein (gills); D) TRx-2 (digestive); E) NFIL-3 (Digestive tract); F) abalone protein 38 (digestive). The relative mRNA expression was calculated by a $2^{-\Delta\Delta CT}$ method using abalone ribosomal protein as a reference gene and relative to control (PBS). Data are presented as mean relative expression ± standard deviation (SD) for three replicate real-time reactions from pooled tissue of three individual abalones at each time point. Statistical analysis was performed by one-way ANOVA followed by Duncan's Multiple Range test using the SPSS 11.5 program. Differences were considered statistically

significant at P<0.05 and an asterisk (*) is used to indicate the significant induction compared to control.

Identification of other immune-relevant genes after bacterial challenge

Expression levels of several immune-related genes did not exceed 2.0-fold in abalone gills and digestive tract by *V. alginolyticus, V. parahemolyticus,* and *L. monocytogenes* challenge (data not shown). Although, not significant at ≥2–fold level these genes have shown higher expression level ranging from 1.5-1.9-fold. These genes included IFN induced microtubular aggregate (1.9-fold), IL-2 (1.9-fold), SOCS-2 (1.8-fold), I-kB (1.8-fold), protein kinase (1.7-fold), cytochrome oxidase 450 (1.7-fold), heat shock protein (1.7-fold), macrophage stimulating factor (1.6-fold), melanocortin receptor (1.6-fold) and cytochrome oxidase III (1.6-fold). These genes may be expressed constitutively in gills and digestive tract or less transcriptional activation against bacterial challenge used in this study.

1.3.2. *Microarray analysis differently expressed genes in abalone gills and hemocytes after VHSV challenge*

In this study, effect of VHSV challenge on the transcriptional responses was analyzed in gills and hemocytes of abalone using cDNA microarray. The threshold significance for the microarray was chosen at $P< 0.05$, with a signed expression change (≥1.5 or ≤1.5 –fold) of both up- and down-regulated genes. Up and down regulated transcripts after VHSV challenge vs control (PBS) groups in were visualized using heat map (fig 6). Number of genes significantly up and down –regulated based on the tissue type and their GO analysis results are shown in fig 7. Among the 4188 genes analyzed, 113 (2.7%) and 167 (4.0%) had altered expression levels (≥1.5 or ≤1.5–fold) upon VHSV challenge in gills and hemocytes, respectively.

Based on significance and gene selection criteria, 88 and 65 genes were up-regulated in gills and hemocytes, respectively at 24 h. In contrast to up-regulation, a total of 25 and 102 genes were down-regulated in gills and hemocytes, respectively (fig. 7A). Microarray results showed that a number of up-regulated genes were higher than down-regulated genes in only in gills while hemocytes showed higher down –regulated genes than up-regulated. Sequence homology analysis was performed for each significantly responded clone using BLAST program (fig. 7B). Among up-regulated genes, 31% gills and 39% hemocytes sequences were matched with known functional genes while 24% gills and 26% hemocytes sequences were shown no significant similarity to known genes from other organisms and considered as unknown genes (BLASTx e value of $1X\ 10^{-5}$ as threshold to define significant similarity). Remaining up-regulated transcripts in gills (45%) and hemocytes (35%) did not hit any of sequence available at the data base. Among down-regulated transcripts, high number of transcripts in gills (52%) and hemocytes (63%) were not hit to any data base sequence and only 32% of gills and 20% of hemocytes transcripts showed significant similarity to known sequences. Remaining portion of each tissue (gill-16%, hemocyte-17%) exhibited no significant similarity to known sequence.

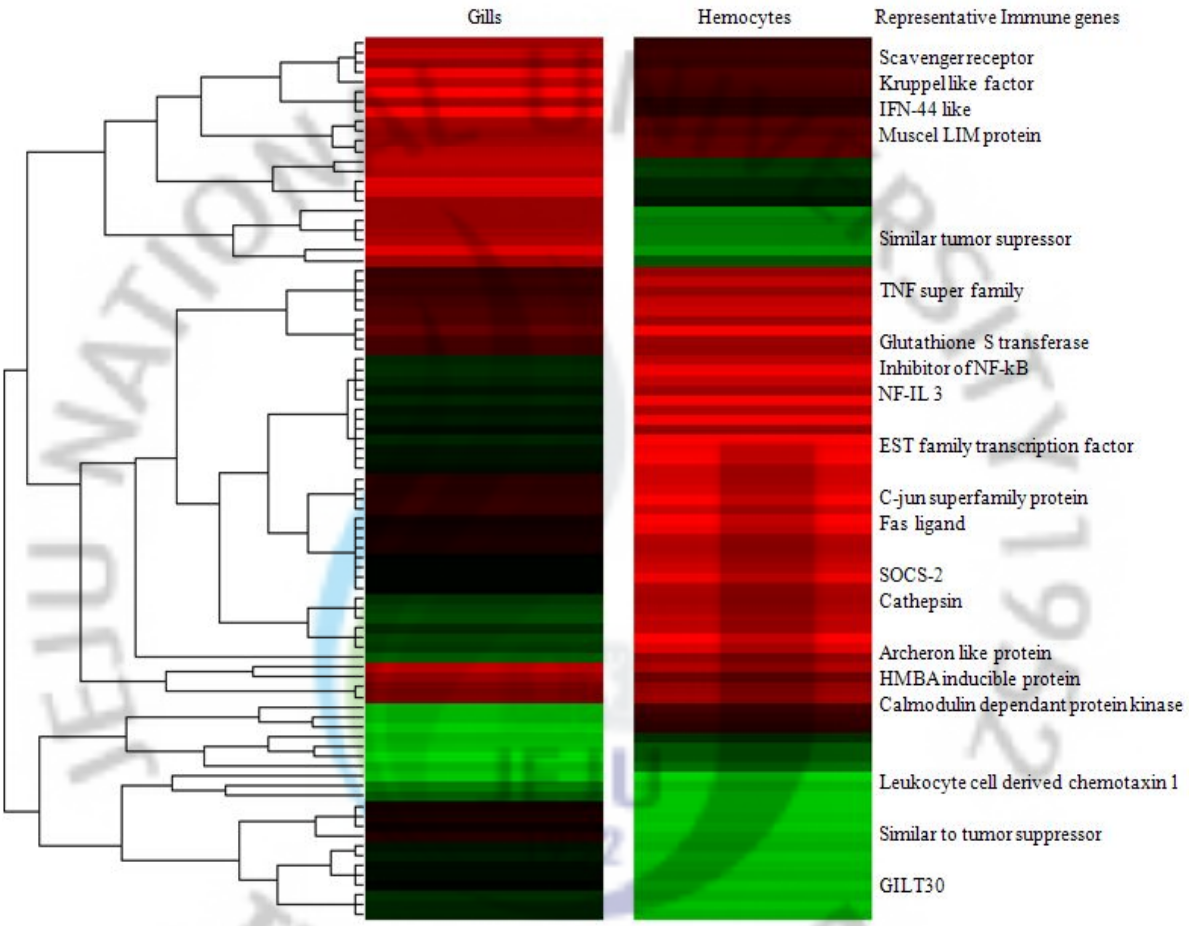

Fig. 6. Gene expression profiles of significantly regulated transcripts (≥1.5 or ≤1.5 –fold change) in disk abalone gills and hemocytes at 24 h post challenge of VHSV. Each row represents a cDNA clone that was expressed at a statistically significant level in VHSV challenge relative to control individuals in each tissue. Selected immune response clones are labeled at either side of each tissue. The quantitative changes in gene expression are represented in colors: red indicated that gene is more highly expressed (up-regulated) than its respective control, and green indicates repressed (down-regulated) genes.

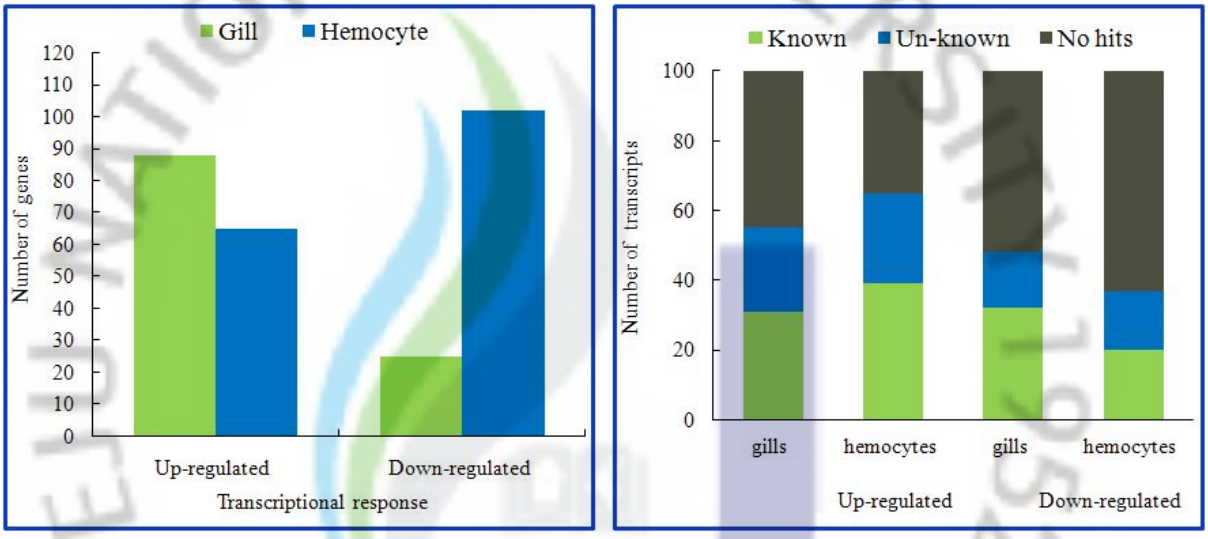

Fig.7. Classification of significantly (≥1.5 or ≤1.5 –fold change) responded transcripts abalone at 24 h post challenge of VHSV. A) number of up-and down-regulated transcripts in gills and hemocytes; B) Blast and GO analysis of significantly up and down-regulated transcripts in gills and hemocytes.

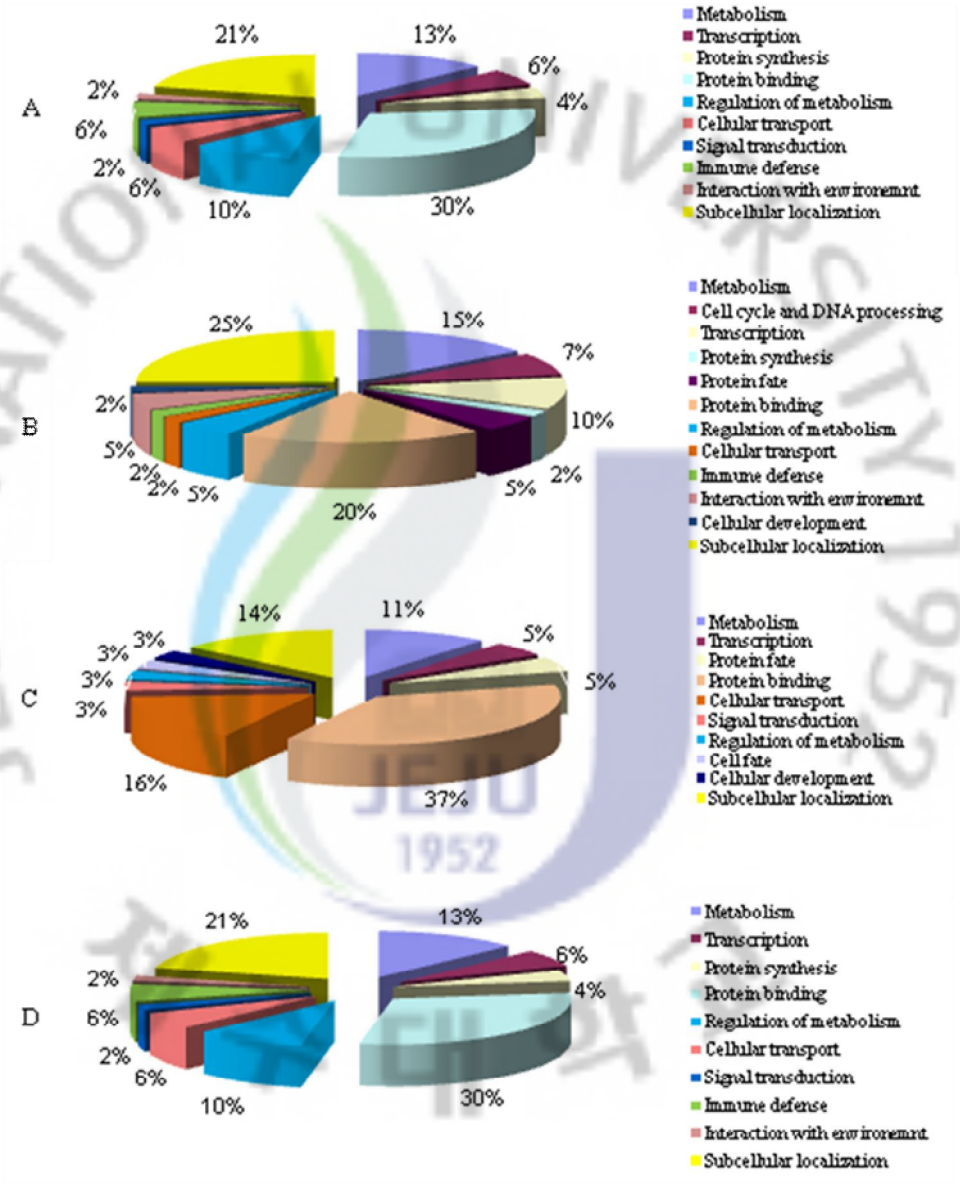

Fig 8. Gene Ontology (GO) analysis of significantly regulated transcripts (≥1.5 or ≤1.5 -fold) in disk abalone at 24 h after VHSV challenge

Clustering of differentially expressed genes in disk abalone gills and hemocytes

Abalone genes that had a significantly altered expression level (≥1.5 or ≤1.5 –fold) by VHSV challenged were categorized into 4 main clusters. Clusters 1 and 2 consisted of genes that were up-regulated in gills and hemocytes, respectively, while clusters 3 and 4 were down-regulated in gills and hemocytes, respectively. The lists of genes belongs to four different clusters are shown in tables 1, 2, 3 and 4, respectively. GO analysis results of differentially expressed abalone genes belonging to the four different clusters are shown in figure 8.

Cluster 1: up-regulated (≥1.5–fold) genes in gills

A total of 88 genes up-regulated in gills are listed in Table 7 with their respective microarray expression fold values, and the most similar homology identification in NCBI. Significantly up-regulated genes were categorized by different putative functions including metabolism, protein synthesis, protein fate, protein binding, regulation of metabolism, signal transduction, immune defense, interaction with environment and sub-cellular localization (8A-2). In abalone gills, 6% of the up-regulated genes were grouped into the immune defense category. Several immune-relevant genes were identified in this category, which are involved in transcriptional regulation (KLF, NFIL3, C-Jun superfamily member), regulators of apoptosis and immune modulation (TNF-α; Fas ligand), IFN-related cytokines (IFN-induced 44-like protein), antioxidant enzyme (Glutathione-S-transferase).

Cluster 2: up-regulated (≥1.5–fold) genes hemocytes

Significantly up-regulated genes in hemocytes after the VHSV challenge is shown Table 8. Results shown that 2% of the up-regulated genes were classified as immune defense category. Immune-relevant genes such as IFN inducible GTPase, low density lipoprotein receptor, SOCS-2, calmodulin dependant protein kinase, archeron like protein and HMBA inducible protein were included among the hemocyte up-regulated genes. Most of other up-regulated genes in hemocytes could be assigned to different functional groups such as energy metabolism, protein synthesis, cellular transport and regulation of metabolism reflecting different aspects of abalone physiological status.

Cluster 3: down-regulated (≤1.5 –fold) genes in gills

Genes which showed significant down-regulation in abalone gills after the VHSV challenge is shown in Table 9. Results showed that totally 25 gene transcripts were down regulated and majority of them are either unknown or no hit sequences. Chromosome segregation protein, leukocyte cell derived chemotaxin and protein kinase-like protein was among the down regulated genes in gills.

Cluster 4: down-regulated (≤1.5 –fold) genes in hemocytes

Significantly down-regulated genes in abalone hemocytes after the VHSV challenge are shown in Table 5. Compared to number of genes down regulated in gills (25), hemocytes have shown higher number of down regulated genes (102) against VHSV challenge. Calmodulin, cathepsin, serpin peptidase inhibitor, interferon gamma-inducible protein 30 were the important immune related genes which down regulated in hemocytes.

Confirmation of VHSV challenge microarray results by qRT-PCR

In order to confirm our microarray results, we selected six candidate genes including hematopoietic stem cell, KLF, muscle Lim, C-Jun (Ap-1) super family and NFIL3 regula ted proteins from the significantly up-regulated genes from gills and hemocytes. Additionally, we have done full-length sequencing of several candidate genes for further characterization. qRT-PCR result of gene expression profiles are shown in figure 9. Overall results revealed that our microarray data could be validated based on the candidate gene expression profiles with induced levels obtained by qRT-PCR. However, it is important to note that most of the up-regulated expression levels (in qRT-PCR) at 24 h p.i. do not exactly match the microarray data, which may be due to variation among the individual animals.

Table 7. List of genes significantly up-regulated in gills after VHSV challenge

Serial number	EST number	Putative gene name	Expression fold (+)	Accession number of similar sequence	Blast X *E*- value
1	cDNA_46-G06	Scavenger receptor	4.6	NP_001100492	5.00E-8
2	cDNA_24-G0	Hematopoietic stem/progenitor cells protein	4.4	ACO10100	7e-41
3	cDNA_01-A02	similar to Gamma-crystallin N	3.7	XP_597249.4	1.00E-05
4	cDNA_30-E09	Translation elongation factor	3.4	XP_002401272	4e-90
5	cDNA_19-G11	Kruppel-like factor	3.3	EF587285.1	6.00E-101
6	cDNA_22-E01	Interferon-induced 44-like protein	3.2	ACJ12608.1	0.004
7	cDNA_67-G08	Cyano fluorescent protein	2.9	ABZ11027.1	0.0007
8	cDNA_14-E10	Beta galactosidae like protein	2.8	CAA18137	4.20
9	cDNA_13-E01	No hit	2.7	-	-
10	cDNA_05-F04	Hypothetical protein	2.6	NP_001088235.1	8.00E-12
11	cDNA_29-B08	TNF superfamily ligand TL1A	2.5	XP_001368166.1	6.00E-05
12	cDNA_27-B03	Hypothetical protein	2.4	XP_002224975.1	0.008
13	cDNA_58-C07	No hit	2.3	-	-
14	cDNA_09-C05	No hit	2.3	-	-
15	cDNA_14-A06	RNA-binding protein Nova-1	2.2	EEF40472.1	0.01
16	cDNA_46-D06	Hypothetical protein	2.2	XP_002201046.1	2E-20
17	cDNA_19-H10	similar to Thymidylate synthase	2.2	XP_001368094.1	3E-73
18	cDNA_44-B08	Hypothetical protein	2.2	XP_002237731.1	2E-37f
19	cDNA_19-G10	No hit	2.2	-	-
20	cDNA_47-F05	similar to TNF superfamily ligand TL1A	2.1	XP_001368166.1	0.022
21	cDNA_51-A12	Glutathione-S-transferase isoform 1	2.1	ABF67506.1	1E-120
22	cDNA_01-H02	No hit	2.1	-	-
23	cDNA_52-A03	Sulfatase 1 precursor	2.0	AAF30402.1	1E-85
24	cDNA_27-D03	Family 10 cellulase	2.0	AAP31839.2	1E-47
25	cDNA_02-F07	similar to TNF superfamily ligand TL1A	2.0	XP_001368166.1	0.007
26	cDNA_69-E09	Cell division control protein 42 (CDC42)	2.0	XP_957345.2	8.00E-30
27	cDNA_13-H02	No hit	2.0	-	-
28	cDNA_13-D01	Type I iodothyronine deiodinase	2.0	O42449|IOD1_ORENI	1E-24
29	cDNA_01-B02	No hit	2.0	-	-
30	cDNA_12-H11	DCMP deaminase	2.0	NP_001040508.1	8E-50
31	cDNA_56-F05	Neurofilament medium tail domain	2.0	ACJ64830.1	0.019
32	cDNA_27-H06	Hypothetical protein	1.9	XP_001659791.1	2E-46
33	cDNA_52-H12	Putative ribosomal protein S13	1.9	ABW90418.1	4E-24
34	cDNA_30-E11	Hypothetical protein	1.8	XP_002219320.1	9E-23
35	cDNA_63-C05	Hypothetical protein	1.8	XP_002235005.1	1E-25
36	cDNA_47-D02	No hit	1.8	-	-
37	cDNA_19-B08	Hypothetical protein	1.8	XP_002249132.1	2E-23
38	cDNA_32-F02	Hypothetical protein-Similar to Acheron	1.8	XP_002227539.1	1.00E-17
39	cDNA_23-E12	Hypothetical protein	1.8	XP_001635305.1	1E-61
40	cDNA_07-E02	NADH dehydrogenase subunit 3	1.7	YP_026067.1	6E-30
41	cDNA_04-A07	No hit	1.7	-	-
42	cDNA_15-G06	No hit	1.7	-	-
43	cDNA_14-E09	No hit	1.7	-	-
44	cDNA_09-D05	Hypothetical protein	1.7	XP_001626032.1	2.00E-09

45	cDNA_46-A09	No hit	1.7	-	-
46	cDNA_18-F01	Nuclear factor interleukin 3 regulated protein	1.7	ACJ65688.1	1E-128
47	cDNA_19-F02	No hit	1.7	-	-
48	cDNA_04-F06	Hypothetical protein	1.7	XP_002242171.1	1E-83
49	cDNA_23-H10	Inhibitor of nuclear factor-kappaB protein	1.7	ACF93446.1	0.42
50	cDNA_01-F07	Muscle LIM protein	1.7	ACJ65685.1	1E-94
51	cDNA_14-D10	Hypothetical protein	1.7	CAF89235.1	5E-21
52	cDNA_62-D06	Psimilar to Iduronate 2-sulfatase precursor	1.7	XP_002123020.1	1.00E-32
53	cDNA_01-H08	Mouse Myo-Inositol Oxygenase	1.7	AAV65817.1	1e-59
54	cDNA_01-H07	DEAD (Asp-Glu-Ala-Asp) box polypeptide 56	1.7	NP_001003876	4e-80
55	cDNA_28-F07	No hit	1.7	-	-
56	cDNA_19-G12	No hit	1.7	-	-
57	cDNA_50-G07	Methyltransferase	1.6	ZP_01448465.1	0.001
58	cDNA_61-H03	Hypothetical protein	1.6	XP_002122447.1	2.00E-14
59	cDNA_13-G03	Hypothetical protein	1.6	ABY87425.1	1.00E-05
60	cDNA_14-E08	Hypothetical protein	1.6	XP_001626348.1	0.009
61	cDNA_06-F09	Hypothetical protein	1.6	ABK21458.1	8.00E-42
62	cDNA_63-B05	Hypothetical protein	1.6	XP_001629111.1	3.00E-31
63	cDNA_59-A11	No hit	1.6	-	-
64	cDNA_13-A08	Actin	1.6	AAQ92368.1	2.00E-68
65	cDNA_17-B06	Selenoprotein	1.6	O19097|SELW_SHEEP	6.00E-11
66	cDNA_26-H10	Phenol sulfotransferase	1.6	NP_998930.1	1E-30
67	cDNA_15-C10	No hit	1.6	-	-
68	cDNA_26-G12	No hit	1.6	-	-
69	cDNA_16-H06	Hypothetical protein	1.6	XP_002220600.1	1.00E-15
70	cDNA_01-F06	No hit	1.6	-	-
71	cDNA_24-F05	Sigma class glutathione-s-transferase	1.6	ABO26604.1	1.00E-105
72	cDNA_16-A05	Heparanase	1.6	NP_001038470.1	3E-43
73	cDNA_01-G08	No hit	1.6	-	-
74	cDNA_50-H08	No hit	1.6	-	-
75	cDNA_69-E12	Hypothetical protein	1.5	XP_002131562.1	6.00E-06
76	cDNA_44-D08	No hit	1.5	-	-
77	cDNA_38-G04	Hypothetical protein	1.5	XP_001622513.1	2.00E-17
78	cDNA_47-E05	No hit	1.5	-	-
79	cDNA_67-H07	ETS-family transcription factor	1.5	AAU11487	1e-45
80	cDNA_16-E08	Hypothetical protein	1.5	XP_001485101.1	5.00E-06
81	cDNA_65-A05	Similar to solute carrier family 5	1.5	XP_002131513	1e-46
82	cDNA_15-A09	No hit	1.5	-	-
83	cDNA_24-E05	Regulator of chromosome condensation	1.5	EER05288	0.017
84	cDNA_28-F04	Fas ligand-like protein	1.5	ACJ12607.1	1E-147
85	cDNA_43-A02	No hit	1.5	-	-
86	cDNA_27-A03	Hypothetical protein	1.5	NP_001089561.1	2.00E-62
87	cDNA_26-F11	similar to Cat Eye Syndrome protein	1.5	XP_416390.2	5.00E-36
88	cDNA_03-F09	Cathepsin L	1.5	AAP49831.1	2.00E-42

Table 8. List of genes significantly up-regulated in hemocytes after VHSV challenge

Serial number	EST number	Putative gene name	Expression Fold (+)	Accession number of similar sequence	Blast X *E*- value
1	cDNA_38-H09	Cyclin B	4.1	ABO26668.1	1E-124
2	cDNA_16-H05	C2H2-type Zn finger protein	3.7	XP_002237418.1	0.006
3	cDNA_09-D04	Interferon-inducible GTPase	3.6	ABW94983.1	3.00E-18
4	cDNA_18-C05	Vitelline envelope zona pellucida domain 10	3.3	ABE72954.1	4E-48
5	cDNA_24-G02	Vitelline coat protein B	3.0	ABO26627.1	1E-154
6	cDNA_09-E04	Hypothetical protein	3.0	XP_863776.1	1E-93
7	cDNA_19-A03	Fatty acid synthase	3.0	ACE00290.1	1.00E-07
8	cDNA_26-G03	Low density lipoprotein receptor	2.7	To be checked	
9	cDNA_09-C04	Hp: similar to protein phosphatase 2	2.7	XP_973546.1	5.00E-09
10	cDNA_02-A01	Histone 1	2.6	CAA11816.1	2.00E-21
11	cDNA_12-G09	Hypothetical protein	2.6	XP_002211844.1	2.00E-13
12	cDNA_02-B01	Hypothetical protein	2.4	XP_002212329.1	8.00E-14
13	cDNA_64-F02	No hit	2.4	-	-
14	cDNA_12-D09	Similar to pol polyprotein	2.4	XP_002166647.1	8.00E-21
15	cDNA_41-E02	No hit	2.4	-	-
16	cDNA_23-B01	Hypothetical protein	2.1	CAF93083.1	8.00E-13
17	cDNA_12-H10	Hypothetical protein	2.1	XP_002204676.1	1.00E-55
18	cDNA_01-A06	Hypothetical protein	2.0	AAH93430.1	2.00E-06
19	cDNA_21-B05	CDH1-D	2.0	AAL31950.1	4E-32
20	cDNA_19-F02	No hit	2.0	-	-
21	cDNA_69-D11	No hit	2.0	-	-
22	cDNA_05-C11	Vetelline envelope zona pellucida domain 10	2.0	ABE72951.1	1E-21
23	cDNA_16-H03	Vitelline coat protein 41	2.0	BAB15843.1	1E-154
24	cDNA_52-H12	Putative ribosomal protein S13	2.0	ABW90418.1	4E-24
25	cDNA_19-A07	Hypothetical protein	1.9	XP_002211072.1	1E-25
26	cDNA_59-A11	No hit	1.9	-	-
27	cDNA_15-H11	Nuclear pore-targeting complex component	1.9	XP_788859.1	1E-91
28	cDNA_18-B01	No hit	1.9	-	-
29	cDNA_53-H07	No hit	1.8	-	-
30	cDNA_55-E10	No hit	1.8	-	-
31	cDNA_23-D08	No hit	1.8	XP_002244974.1	7E-88
32	cDNA_22-B10	Glutaredoxin 5	1.8	ABO26655.1	2E-78
33	cDNA_02-C01	Hypothetical protein	1.7	ZP_03207365.1	2.00E-13
34	cDNA_12-C06	Hypothetical protein	1.7	XP_001179515.1	5E-23
35	cDNA_16-H09	SOCS-2	1.7	-	-
36	cDNA_15-C10	No hit	1.7		
37	cDNA_49-F06	Aldehyde reductase 1	1.7	XP_001844836.1	4E-64
38	cDNA_46-G12	similar to mannosidase	1.7	XP_001363427.1	0.006
39	cDNA_18-D05	Hypothetical protein	1.7	XP_393282.3	3.00E-11
40	cDNA_03-E07	No hit	1.7	-	-
41	cDNA_19-G02	Hypothetical protein	1.6	XP_001716072.1	3.00E-.04
42	cDNA_19-G01	X-box binding protein	1.6	ABO26643.1	2E-41
43	cDNA_09-D05	Hypothetical protein	1.6	XP_001626032.1	2.00E-09
44	cDNA_38-C03	Hypothetical protein	1.6	XP_002201284.1	9.00E-19
45	cDNA_21-C09	Hypothetical protein	1.6	XP_002225541.1	1.00E-51
46	cDNA_12-C09	Hypothetical protein	1.6	XP_001629265.1	3.00E-18
47	cDNA_30-G11	Hp; similar to Solute carrier family 3	1.6	XP_782131.1	2E-33
48	cDNA_05-D11	Hypothetical protein	1.6	XP_001986848.1	0.005
49	cDNA_23-F12	Hypothetical protein	1.6	NP_001001208.1	1E-117
50	cDNA_08-E10	No hit	1.6	-	-
51	cDNA_19-B06	No hit	1.6	-	-
52	cDNA_62-D06	Similar to Iduronate 2-sulfatase precursor	1.6	XP_002123020.1	1E-32
53	cDNA_09-F01	No hit	1.6	-	-
54	cDNA_43-A06	Sterol regulatory element binding transcription factor 1	1.6	NP_001098599.11E-58	

55	cDNA_08-E02	Giardia variant-specific surface protein	1.6	XP_001023022.1	0.034
56	cDNA_02-G08	Calmodulin-dependent protein kinase	1.6	ABY87388.1	8.00E-62
57	cDNA_09-F12	Similar to Proteasome	1.6	XP_793302.2	1E-77
58	cDNA_26-C07	Archeron-like protein	1.5	ACJ65686.1	1E-116
59	cDNA_14-B09	Similar to alpha(1,2) fucosyltransferase	1.5	XP_001362194.1	
60	cDNA_20-A10	Ubiquitin C-terminal hydrolase	1.5	EEC02305.1	1E-101
61	cDNA_64-H10	Hypothetical protein	1.5	XP_972204.1	2E-31
62	cDNA_12-E06	No hit	1.5	-	-
63	cDNA_69-C05	No hit	1.5	-	-
64	cDNA_12-D08	HMBA-inducible protein	1.5	XP_002225541.1	1E-51
65	cDNA_08-D09	Hypothetical protein	1.5	XP_002215300.1	0.004

Table 9. List of genes significantly down-regulated in gills after VHSV challenge

Serial number	EST number	Putative gene name	Expression fold (-)	Accession number of similar sequence	Blast X *E*- value
1	cDNA_16-F07	Chromosome segregation protein SMC	2.8	YP_001734374.1	0.042
2	cDNA_28-G10	Leukocyte cell derived chemotaxin 1	2.5	CAQ14216	4.1
3	cDNA_28-E10	Similar to protein kinase	2.3	XP_002156911.1	1E-70
4	cDNA_22-G07	No hit	2.3	-	-
5	cDNA_42-H12	No hit	2.2	-	-
6	cDNA_13-A09	Hypothetical protein	2.2	XP_002210123.1	5E-27
7	cDNA_32-F11	Transcription factor with NAC and TSN motifs	2.1	EEC16446.1	3E-53
8	cDNA_42-E09	No hit	2.1	-	-
9	cDNA_55-F07	Similar to egg binding receptor 1	2.0	XP_791820.2	0.002
10	cDNA_28-D10	Hypothetical protein	1.8	XP_002108587.1	2.00E-18
11	cDNA_27-B09	No hit	1.7	-	-
12	cDNA_54-H04	No hit	1.7	-	-
13	cDNA_34-H10	No hit	1.7	-	-
14	cDNA_55-C10	Hypothetical protein	1.6	XP_002223422.1	3.00E-11
15	cDNA_17-F04	Ribosomal protein S14	1.6	ABO26682.1	7E-72
16	cDNA_50-B10	No hit	1.6	-	-
17	cDNA_17-E04	Hypothetical protein	1.6	XP_002235967.1	2.00E-15
18	cDNA_03-D12	Hypothetical protein	1.6	XP_002217403.1	2.00E-76
19	cDNA_23-E01	Similar to sidekick 1	1.6	XP_594486.4	2.00E-06
20	cDNA_26-D10	No hit	1.6	-	-
21	cDNA_45-D05	Hypothetical protein	1.6	EEE65753.1	3.00E-09
22	cDNA_03-A08	NAD(+) ADP-ribosyltransferase-3	1.5	XP_002119648.1	1.00E-14
23	cDNA_54-H05	Hypothetical protein	1.5	XP_001623938.1	1.00E-19
24	cDNA_58-E12	Mitochondrial 28S ribosomal protein S5	1.5	XP_001865121.1	3E-42
25	cDNA_48-C01	No hit	1.5	-	-

Table 10. List of genes significantly down-regulated in hemocytes after VHSV challenge

Serial number	EST number	Putative gene name	Expression fold (-)	Accesion number of similar sequence	Blast X *E* value
1	cDNA_33-F06	No hit	2.4	-	-
2	cDNA_64-G07	Hypothetical protein	2.4	XP_001749112.1	2.00E-04
3	cDNA_60-G12	No hit	2.3	-	-
4	cDNA_31-D05	No hit	2.3	-	-
5	cDNA_44-H01	No hit	2.2	-	-
6	cDNA_28-F09	Similar to stearoyl-CoA desaturase	2.2	XP_001086993.1	1E-73
7	cDNA_39-C12	No hit	2.1	-	-
8	cDNA_31-C05	Hypothetical protein	2.1	XP_001638334.1	4E-38
9	cDNA_46-D10	Lipophorin receptor isoform 1	2.1	NP_001104808.1	1.00E-31
10	cDNA_62-F08	Hypothetical protein	2.0	XP_001626341.1	2.00E-05
11	cDNA_18-C04	No hit	2.0	-	-
12	cDNA_41-D09	No hit	1.9	-	-
13	cDNA_67-E08	Calmodulin 2	1.9	ABY87354.1	2E-68
14	cDNA_17-G05	Hypothetical protein	1.9	ABY87367.1	3E-37
15	cDNA_64-F07	No hit	1.9	-	-
16	cDNA_36-H12	Angiopoietin-like 1	1.9	NP_001103417.1	1E-29
17	cDNA_18-D04	Hypothetical protein	1.8	XP_001641553.1	3E-49
18	cDNA_29-C06	No hit	1.8	-	-
19	cDNA_06-G10	Keratin-associated protein 4-3	1.8	EEC17204.1	0.004
20	cDNA_32-A02	Lysosomal aspartic protease	1.8	XP_001867326.1	5E-82
21	cDNA_60-A11	Hp; similar to cathepsin L	1.8	XP_780713.1	2.00E-59
22	cDNA_09-A10	Hypothetical protein	1.8	XP_002251340.1	0.05
23	cDNA_22-D05	Hypothetical protein	1.8	XP_001501860.2	1.00E-10
24	cDNA_60-D08	Hypothetical protein	1.8	XP_418270.2	0.004
25	cDNA_38-E08	No hit	1.8	-	-
26	cDNA_19-G11	No hit	1.8	-	-
27	cDNA_43-F09	No hit	1.8	-	-
28	cDNA_28-C11	Hypothetical protein	1.8	XP_001602687.1	1.00E-17
29	cDNA_61-E07	Hypothetical protein	1.7	XP_002226490.1	6.00E-11
30	cDNA_70-C04	Similar to serpin peptidase inhibitor	1.7	XP_002119928.1	6.00E-05
31	cDNA_03-H05	Similar to tumor suppressor	1.7	XP_001370166.1	5.00E-18
32	cDNA_32-G12	No hit	1.7	-	-
33	cDNA_33-B04	Gelsolin-like protein	1.7	CAD43405.1	1E-20
34	cDNA_69-G12	No hit	1.7	-	-
35	cDNA_05-A11	Cytochrome c oxidase subunit III	1.7	YP_026066.1	3E-53
36	cDNA_41-C09	Hypothetical protein	1.7	CAN61314.1	2.00E-04
37	cDNA_33-H02	Similar to Ras suppressor protein 1	1.7	XP_002193437.1	2E-88
38	cDNA_38-C05	No hit	1.7	-	-
39	cDNA_56-D12	Interferon gamma-inducible protein 30	1.7	AAQ83892.1	8E-48
40	cDNA_18-D10	No hit	1.7	-	-
41	cDNA_17-G07	Similar to receptor protein Notch1	1.7	XP_797229.2	1.00E-07
42	cDNA_03-A09	Tissue inhibitor of metalloproteinase	1.7	ABY87360.1	3.00E-67
43	cDNA_52-A02	Sulfatase 1 precursor	1.7	AAF30402.1	1.00E-85
44	cDNA_03-C05	No hit	1.6	-	-
45	cDNA_30-G05	No hit	1.6	-	-
46	cDNA_33-A11	No hit	1.6	-	-
47	cDNA_30-C05	No hit	1.6	-	-
48	cDNA_67-D08	Transcription factor 21	1.6	ACI68100.1	2.00E-17
49	cDNA_08-A03	No hit	1.6	-	-
50	cDNA_36-H07	No hit	1.6	-	-
51	cDNA_03-B01	No hit	1.6	-	-
52	cDNA_36-A09	No hit	1.6	-	-
53	cDNA_17-G02	Hypothetical protein	1.6	NP_506781.1	4E-25
54	cDNA_23-B06	No hit	1.6	-	-
55	cDNA_30-G02	Hypothetical protein	1.6	CAG06361.1	8.00E-06
56	cDNA_40-C02	No hit	1.6	-	-

57	cDNA_44-G07	No hit	1.6	-	-
58	cDNA_42-F06	Hypothetical protein	1.6	AAH74217.1	8E-93
59	cDNA_27-B03	Hypothetical protein	1.6	XP_002224975.1	0.008
60	cDNA_65-G12	Hypothetical protein	1.6	XP_002228902.1	1.00E-10
61	cDNA_58-D04	No hit	1.6	-	-
62	cDNA_22-G07	No hit	1.6	-	-
63	cDNA_49-D01	Hypothetical protein	1.6	EEC13269.1	6E-43
64	cDNA_16-B01	Hypothetical protein	1.6	XP_002209233.1	1.00E-51
65	cDNA_61-G01	No hit	1.6	-	-
66	cDNA_19-G10	No hit	1.6	-	-
67	cDNA_32-H02	No hit	1.6	-	-
68	cDNA_21-E07	Cell surface flocculin (cell wall adhesin)	1.6	CAX44143.1	9.00E-13
69	cDNA_22-G01	No hit	1.6	-	-
70	cDNA_61-D02	Hypothetical protein	1.6	XP_796139.1	1.00E-39
71	cDNA_62-E08	No hit	1.6	-	-
72	cDNA_61-H02	No hit	1.6	-	-
73	cDNA_40-A02	Mitochondrial inner membrane translocase	1.6	EEC16324.1	5.00E-21
74	cDNA_22-H11	Hypothetical protein	1.6	XP_002241546.1	2.00E-63
75	cDNA_31-D04	No hit	1.6	-	-
76	cDNA_02-A07	No hit	1.6	-	-
77	cDNA_38-E01	No hit	1.6	-	-
78	cDNA_02-B06	No hit	1.6	-	-
79	cDNA_39-F06	Hypothetical protein	1.6	XP_315123.4	6.00E-10
80	cDNA_37-D12	No hit	1.6	-	-
81	cDNA_35-D04	Hypothetical protein	1.6	XP_001634403.1	3E-61
82	cDNA_29-C03	Hydroxyprostaglandin dehydrogenase	1.6	XP_694331.3	8E-46
83	cDNA_40-F09	No hit	1.6	-	-
84	cDNA_55-E02	similar to adaptin	1.6	XP_971073.1	5E-57
85	cDNA_14-E08	Hypothetical protein	1.6	XP_001626348.1	0.009
86	cDNA_16-H06	Hypothetical protein	1.6	XP_002220600.1	1.00E-15
87	cDNA_28-B12	No hit	1.5	-	-
88	cDNA_69-D08	No hit	1.5	-	-
89	cDNA_33-C11	No hit	1.5	-	-
90	cDNA_47-F11	No hit	1.5	-	-
91	cDNA_42-H10	No hit	1.5	-	-
92	cDNA_22-G12	Mortile sperm domain containing protein	1.5	XP_538179.1	.038
93	cDNA_20-G12	No hit	1.5	-	-
94	cDNA_38-E03	No hit	1.5	-	-
95	cDNA_41-C04	No hit	1.5	-	-
96	cDNA_18-D09	Hypothetical protein	1.5	EEB11102.1	0.00003
97	cDNA_20-F02	No hit	1.5	-	-
98	cDNA_27-D03	Family 10 cellulase	1.5	AAP31839.2	1E-47
99	cDNA_36-H08	No hit	1.5	-	-
100	cDNA_04-H04	No hit	1.5	-	-
101	cDNA_47-A12	No hit	1.5	-	-
102	cDNA_30-A07	No hit	1.5	-	-

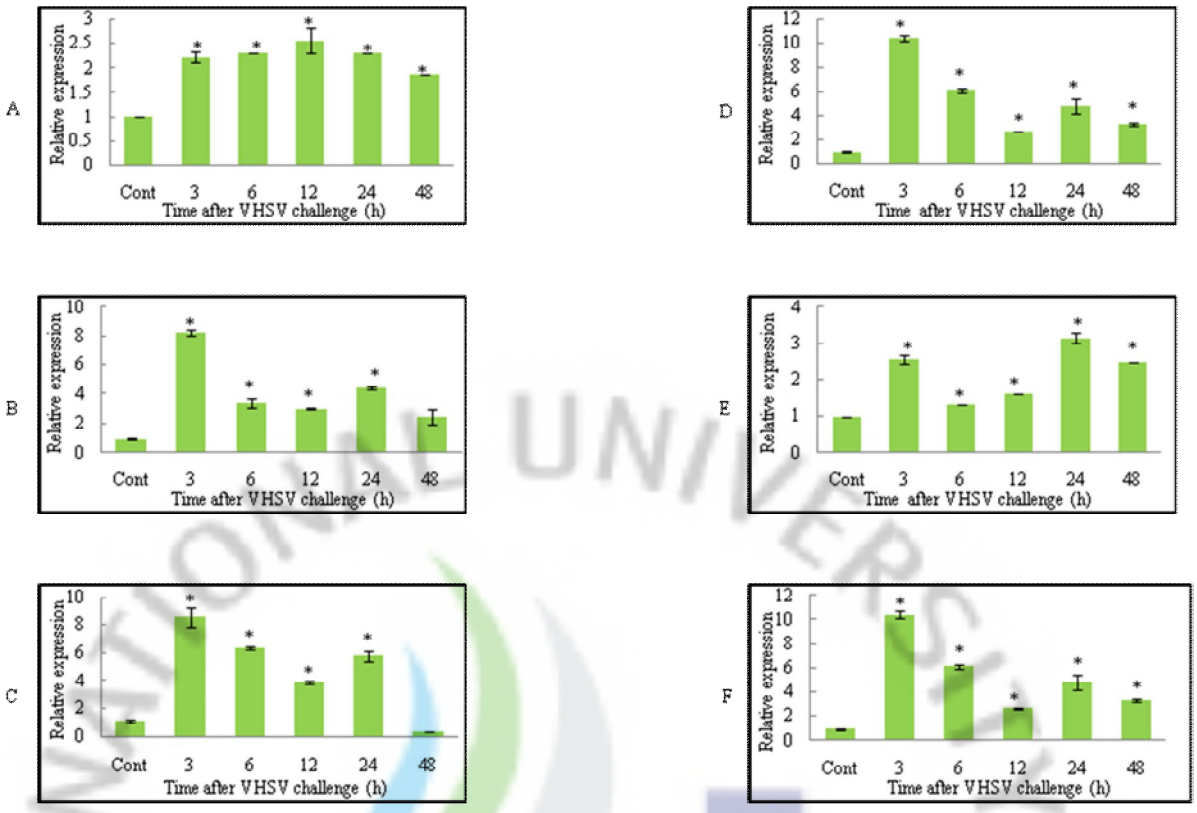

Figure 9. qRT-PCR analysis of six potential (candidate) immune genes identified from the VHSV challenged microarray analysis of disk abalone gills and hemocytes. A) Hematopoietic stem cell protein; B) KLF; C) IFN-44 like protein; D) muscle Lim protein; E) C-jun sperfamily protein; F) NFIL-3. The relative mRNA expression was calculated by a $2^{-\Delta\Delta CT}$ method using abalone ribosomal protein as a reference gene and relative to control (PBS). Data are presented as mean relative expression ± SD for three replicate real-time reactions from pooled tissue of three individual abalones at each time point. Statistical analysis was performed by one-way ANOVA followed by Duncan's Multiple Range test using the SPSS 11.5 program. Differences were considered statistically significant at $P<0.05$ and an asterisk (*) is used to indicate the significant induction compared to control.

1.4. Discussion

The complex interaction between a microbial pathogen and a host is the fundamental basis of infectious disease. DNA microarrays can simultaneously detect changes in transcriptional level for every single gene that may play a role in the host-immune interactions. Therefore, information of highly specific gene expression, as well as sequence homology to a known gene or its family can provide a convenient way to identify immune activation pathways (Dhiman et al., 2001). In this study, a cDNA microarray was designed specifically to discover immune potential genes and analyze transcriptional profiles for better understanding of the abalone immune system at a molecular level. The microarray analysis was assessed using three abalone tissues represented by gills, digestive tract and hemocytes, after bacterial and VHSV challenge compared to respective controls. In invertebrates including mollusks, hemocytes are considered as the main immune cells which involve in functions of immune response, nutrient transport, and digestion, and tissue and shell formation, maintenance of homeostasis (Cheng, 1996). However, the main function of hemocytes is well documented as a cellular defense against foreign biological substances. Cellular defense of hemocytes are involved in several cellular process such as chemotaxix, opsonization, recognition of non-self particles, phagocytosis and intracellular degradation of foreign materials. Therefore, abalone hemocyte is selected for this microarray analysis. The gills and digestive tract tissues were chosen due to their important role in activating immune systems following bacterial challenge. Oxygen transfer occurs at the surface of the gills, where hemolymph (body fluid) is circulating via abalone gills continuously. The pathogen could easily contact gills during hemolymph circulation. Therefore, it has a greater potential to activate cellular defense systems immediately. On the other hand, the mollusk digestive tract is under constant assault by a wide variety of microbial pathogens, and it is considered a prime location for potentially harboring bacteria. It has been identified that an abundance of *Vibrio halioticoli* population in *H. discus hannai*, *H. discus discus*, *H. diversicolor aquatilis*, and *H. diversicolor diversicolor* exists in digestive tract tissue (Sawabe et al., 2003). Hence, we selected those as potential candidate cells and tissues to determine how abalone genes respond to bacterial challenge. Similarly, gills and digestive tract have been used in the first mollusk microarray conducted using ESTs from *C. gigas* and *C. virginica* (Jenny et al., 2007). One of the important outcomes of this study is identification of a higher number of up-regulated genes compared to down-regulated genes in hemocytes, gills and digestive tract, which is an indicator of immune activation in bacteria and VHSV-challenged abalone

(compared to control) as a host defense mechanism.

Immune-relevant genes identified in this study could be grouped into transcription factors, inflammatory cytokines, antioxidant enzymes, apoptosis, and IFN-regulatory genes. Among them, mammalian KLFs are zinc finger-containing transcription factors that appear to exert important regulatory functions on many biological processes, such as growth, development, differentiation and apoptosis. LPS is a membrane glycolipid of Gram-negative bacteria, which could increase the mRNA and protein levels of certain KLFs (Dang et al., 2000). Furthermore, it was reported that KLF-like factor 5 is an important mediator for pro-inflammatory response by increasing TNF-α and IL-6 in intestinal cells with LPS induction (Chanchevalp et al., 2006). Interestingly, the strongest up-regulation was recorded for a transcript encoding a Krüppell-like factor in both gills (6.2-fold) and digestive tract (6.9-fold) alone with TNF-α and IL-3 regulated protein after 24 h bacterial challenge of disk abalone. Similarly, Wang et al., (2008) have identified the partial sequence of KLF and shown its up-regulation of expression in bacteria-induced abalone *H. diversicolor supertexta* hemocytes. Furthermore, our results revealed that elevated I-kB transcripts with 1.8-fold in gills and digestive tract (data not shown). It was reported that enhanced I-kB mRNA after LPS or bacterial stimulation in fish is an indicator of activation of NF-kB pathway (Yazawa et al., 2007). Therefore, strongly up-regulated KLF and moderately elevated I-kB may activate the part of cellular signaling pathways relevant to immune systems in abalone. Furthermore, we identified E26 transformation-specific (Ets) family transcription factor which was down-regulated in bacterial infected gills. It was reported that most Ets family proteins are nuclear targets for activation of RAS-MAP kinase signaling pathway and some of them affect cell proliferation and regulate the apoptosis (Oikawa et al., 2003). Examples of the cytokine or growth factor controlled by Ets family proteins include the Toll-like receptor in myeloid cells (Friedman et al., 2002), immunoglobulin heavy and light chain in B cells, T cell receptors, IL-2 receptor (Bassuk et al., 1997). Furthermore, LPS stimulates the binding of Ets-1 to TNF-α promoter in macrophages (Tsai et al., 2000). On the other hand, some Ets family members have been shown to be involved in the apoptosis process, where many of them exhibit anti-apoptotic responses (Oikawa et al., 2003). Overall, induce or prevention of apoptotic cell death by Ets family proteins may depend on several factors such as transcriptional levels and cellular contests. Based on the present results response of Ets against bacterial challenge gives clues for immune role in abalone which required investigating in future.

In response to microbes and cytokines, endothelial cells rapidly increase the surface

protein such as selectins at the site of infection. The most important cytokines for activating the endothelium are TNF-α, IFN-γ and IL-1 (Abbas et al., 2007). In our study, we identified that apoptosis-related cytokines such as TNF-α, archeron-like protein, and programmed cell death protein demonstrated significant responses against the bacterial challenge at 24 h. TNF-α was significantly induced in both abalone gills and digestive tract while programmed cell death gene was down-regulated only in digestive tract. TNF-α is considered as a multifunctional immune modulator that plays an important role in the innate and adaptive immune systems in vertebrates. In our previous study, we characterized the full-length sequence of disk abalone TNF-α and have shown that its transcriptional inducibility against bacteria, (VHSV) and LPS (De Zoysa et al., 2009). On the other hand, activation of cellular apoptosis by bacteria infection may play an important role in pathogenesis since the apoptosis of immune cells may facilitate favorable conditions to bacteria invasion (Shao et al., 2004). Therefore, induction of apoptosis-related genes could be indicator of inflammatory and apoptosis responses in gills and digestive tissues after bacterial challenge.

Yang et al., (Yang et al., 2005) reported that allograft inflammatory factor 1 (AIF-1) plays important role in mediating the survival, migration and pro-inflammatory properties of macrophages. Additionally, activation of AIF-1 was directed by two pro-inflammatory cytokines namely IL-1b and TNF-α. In a mouse macrophage cell line, production of IL-6, -10, and -12 has driven the enhancement of AIF-1 (Watano et al., 2001). In abalone microarray analysis, two pro-inflammatory cytokines namely TNF-α, and NFIL-3 were shown at higher expression together with AIF in the digestive tract after bacterial challenge. Our results are supported by the recent finding of bacteria-induced AIF-1 in hemocytes of abalone *H. diversicolor* (Wang et al., 2008).

IFN are cytokines that play a crucial role in the defense against virus infection of vertebrates. More recently, it was reported that IFNs have multiple functions in innate and adaptive immune systems. For an example, Furnes et al., (Furnes et al., 2009) demonstrated that Atlantic cod (*Gadus morhua*) IFN-γ expression was increased in head kidney after injection of formalin-killed *Vibrio angullarum*. Bacterial challenge conducted in this study induced the IFN 44-like expression in both gills and digestive tract. Two other IFN regulatory genes such as Mx (De Zoysa et al., 2006) and IFN-γ inducible lysosomal thiol reductase (GILT) (De Zoysa et al., 2007) were recently sequenced and analyzed in disk abalone even though IFN has not been identified in invertebrates yet. In our previous study, we showed that abalone GILT was induced in gills and digestive tract by the single bacterium *V. alginolyticus*

by injection (De Zoysa et al., 2007). However, in these microarray results it was induced only by 1.1-fold at 24 h using the three bacteria mixture containing *V. alginolyticus, V. parahemolyticus* and *L. monocytogenes* (data not shown). The reduced fold-expression changes in microarray results may be due to time point differences of tissue collection, and use of a G+ and G- bacteria mixture in the microarray experiment. Bartee et al., (2008) summarized that synergy between TNF and IFN occurs mainly at the level of gene transcription, suggesting that stimulation of cytokine could activate signal transduction pathways and transcription factors. In this study, we clearly identified the elevated TNF-α and IFN-44-like transcripts in both gill and digestive tract that could be an indicator for activation of cytokine-related immune components in disk abalone. Activation of cytokine-related transcripts could be correlated with the considerably higher SOCS-2 expression detected in this study since excessive cytokine production is controlled by SOCS family proteins. Additionally, activation of SOCS-2 in bacteria-challenged abalone has been described previously (De Zoysa et al., 2008).

Three important antioxidant genes glutathione S transferase, TRx-2 and thioredoxin peroxidase have shown significant up-regulation in abalone after bacterial challenge. All three genes were functionally characterized with reference to their sequence and mRNA expression profiles in our previous studies (Wan et al., 20008; De Zoysa et al., 2008; Wickramaarachchilage et al., 2008). Phagocytosis is one of the important immune defenses in invertebrates during the microbial infection. During the process of phagocytosis, the membrane-bound enzymes and host NADPH-oxidase become activated, which leads to up-regulation of the glycolytic reactions with high oxygen consumption. As a result of that the molecular oxygen reduces to the $O_2^{\cdot-}$ anion, subsequently leading to the production of other forms of ROS to kill or inactivate foreign invaders (Roch et al., 1999). Transcriptional activation (≥2–fold) of glutathione S transferases and four thioredoxin domain-containing proteins has been detected in an *Anopheles gambiae* microarray analysis against *Salmonella typhimurium*, *Staphylococcus aureus* and *Beauveria bassiana* bacteria infection (Aguilar et al., 2005). However, our microarray results did not show significant induction of abalone antioxidant enzymes such as catalase, SOD and SeGPx. The reason for no induction of those antioxidant genes is difficult to explain for data derived from a single time point microarray and their interrelated functions, but time course arrays may be able to provide detailed profiles of these abalone genes.

In order to validate our microarray results, we selected six representative genes for

real-time PCR analysis by conducting an independent time course bacteria challenge experiment. The mRNA expression of candidate genes was not identical, when microarray results were compared with those from quantitative RT-PCR (at 24 h p.i). However, overall expression results have shown that there is transcriptional induction of selected candidate genes. Abalone TNF-α and SOCS-2 are two important genes that were identified from this microarray analysis. We already characterized the full length sequences of SOCS-2 (De Zoysa et al., 2009) and TNF-α (De Zoysa et al., 2009) with transcriptional inducibility against bacteria challenge showing their important role in the immune system. Additionally, we have obtained the full-length sequences of several immune potential genes identified from the present microarray, and respective sequences have been submitted to NCBI. These genes included NFIL-3 (accession: ACJ65688), muscle Lim protein (ACJ65685), allograft inflammatory factor (ACJ65689), archeron-like protein (ACJ65686), macrophage migration inhibitory factor (ACJ65690), calmodulin (EF103391) and IFN 44-like protein (FJ380205). Functional characterization of above identified genes may help to further the understanding of abalone immune system.

Interestingly, no genes encoding AMP have been detected with a higher expression level based on abalone microarray analysis. The disk abalone cDNA library was not constructed using immune-challenged abalone. Hence, ESTs that used to make the microarray may have many immune response genes such as AMPs not represented, where transcriptional expression is at zero or low levels in un-induced abalones. However, expressions of some existing immune-related genes also appear to be less affected by bacterial challenge (data not shown). These genes include pattern recognition receptors (beta 1,3 glucan binding protein; C-type lectin, variable lymphocyte receptor), several inflammatory cytokines (IL-1 receptor, IL-9), transcription factor Rel/NF-kB, and other antioxidant enzymes (MnSOD, CuZnSOD, catalase, SeGPx, peroxiredoxin 6). Furthermore, we observed that bacterial injection has shown relatively small numbers of regulated genes in this microarray. These results can be attributed to several possibilities: i) lower dose of bacteria injection or their opposite interactions due to mixture of 3 pathogenic species; ii) the short duration (24 h) of challenge; iii) high constitutive expression of immune genes in healthy (un-induced) abalones as a preventive measure of pathogens; and, iv) presence of several isoforms (multicopy genes) for a specific function and those can elicit the immune response without expression at higher expression level.

In summary, microarray analysis revealed that bacteria and VHSV-challenged abalone

can activate part of its innate immune responses in gills, digestive tract and hemocytes as a host defense mechanism. More specifically, our results support our hypothesis that bacterial challenge (at 24 h) may activate components of innate immune systems including transcription factors or their activators (KLF, I-kB, NFIL-3), pathogen recognition receptors, inflammatory and apoptosis cytokines (TNF-α, archeron-like protein), other cytokines (SOCS-2, IFN-44-like protein), and antioxidant enzymes (glutathione S transferase, TRx-2 and TPx). Our results further suggest that abalone gills and digestive tract play an important role in host defense against bacteria by activating some of the immune components. The identification of immune-relevant genes and their expression profiles in this microarray will make a foundation for functional studies for understanding host defense mechanisms, complex interactions between host-pathogen and finally, and developing effective ways to control bacterial diseases in abalone.

This is the first report of large scale immune-related gene expression profiling of disk abalone using microarray analysis. The study shows the stimulatory effect of bacteria and virus (VHSV), on abalone genes in gill, digestive and hemocytes. Differently expressed genes were identified as depend on different immune stimulation of this study. However, the microarray analysis revealed only, which genes were altered in expression. To answer the question why they are expressed differently, further studies on particular genes are needed. In that, we have already characterized few important immune related genes such as, TNF-α, Fas ligand, SOCS-2 and NF-kB several other genes have been selected for future study.

In general, around 50% of genes either up or down regulated are known genes. Other genes, which showed significant immune responses, are of course worthy of further investigation in terms of their characteristics and function of the immune response. Notably, the “proteins of unknown function” category contained higher number of genes in all the stimulation experiments; these genes could also make interesting targets for future study, as they may have novel functions in abalone like mollusk immunity. Therefore, the elucidation of the expression and functional roles of immune related genes in abalone constitute a crucial step towards understanding the mollusk immune system and evolution.

CHAPTER 2

Molecular and functional characterization of molluscan TNF-α and Fas ligand genes from disk abalone

ABSTRACT

Members of TNF super-family play diversified roles in mediating the inflammatory responses, apoptosis and immune regulation. Among them, TNF-α and Fas ligands are considered as multifunctional immune modulators. The gene encoding TNF-α and Fas ligand, which showed up-regulation in microarray results were isolated from abalone cDNA library, denoted as the AbTNF-α and AbFas ligand, respectively. The AbTNF-α and Fas ligand amino acid sequences showed their characteristic TNF family signature and N-terminal transmembrane domains. Phylogenic analysis results showed that AbTNF-α and Fas ligand were closely related with their invertebrate counterparts.

qRT-PCR results showed that AbTNF-α and AbFas ligand transcripts were constitutively expressed in abalone hemocytes, gills, mantle, muscle, digestive tract and hepatopancrease in a tissue-specific manner. Transcription level of AbTNF-α and AbFas ligand was significantly ($p<0.05$) up-regulated in gills and hemocytes by bacteria, VHSV and LPS challenge.

The recombinant AbTNF-α and AbFas ligand proteins were over-expressed in *Escherichia coli* (*E. coli*) and purified using a pMAL protein fusion system. Recombinant AbTNF-α and AbFas ligand showed its biological activity by inducing superoxide anion (O^-_2) in abalone hemocytes and human THP-1 cells. Also, several immune genes such as defensin, SOCS-2, NF-kB have shown marked differences at transcriptional level when abalone hemocytes treated with recombinant AbTNF-α and AbFas ligand. Correlating the transcriptional up-regulation of AbTNF-α and AbFas ligand against bacteria, virus and LPS challenge with the biological activity of two recombinant proteins, we could suggest that the abalone TNF-α and Fas ligand may response to microbial infection by inducing O^-_2 like ROS.

2.1. Introduction

Apoptosis is a common physiological process that occurs during embryonic development, tissue turnover and the maintenance of tissue homeostasis (Kerr et al., 1972). It is accelerated by pathogenic infections, as an immune response in the host defense system (Zhang et al., 2005). TNF-α and Fas ligand belongs to a large family of structurally related proteins named the "TNF ligand superfamily". TNF-α is a multifunctional soluble cytokine that can regulate many cellular processes such as immune function, inflammation, apoptosis, cell differentiation, proliferation, and the stimulation of various aspects within the immune system in vertebrates (Goetz et al., 2004). Also, TNF has been called a sentinel or "the body's fire alarm" as it initiates the defense responses to local injury (Feldmann et al., 2005). In that TNF can activate other immune cells or induce apoptosis in infected cells. Beside mammals, the genes encoding TNF-α (or TNF-like) have been recently cloned from several fish species (Laing et al., 2001; Morrisonet al., 2007). In invertebrates, there are few evidences on the presence of TNF-α like molecule. Hughes and his group detected TNF-α immunoreactivity against a monoclonal antibody specific to TNF-α in bivalve mollusks including *Mytilus edulis* hemocytes (Hughes et al., 1990), *Planorbarius corneus* and *Viviparus ater* hemocytes (Ottaviani et al., 1993).

Fas is a type I transmembrane glycoprotein that mediates apoptosis and its biological ligand (Fas ligand) induces apoptosis through the binding to Fas antigens (Curtin et al., 2008). Fas ligand is a type II transmembrane cytokine and expressed mainly in NK cells, cytotoxic T lymphocytes and it plays a critical role in activation-induced cell death of T and B cells (Dhein et al., 1995; Rothstein et al., 1995). Although, many data are available concerning the role of TNF-α and Fas ligand in mammalian apoptosis, little is known about its presence and function in other lower order vertebrates, and invertebrates. Considering the invertebrates, *Drosophila*, a single TNF ligand (Eiger) and its associated receptor (Wengen) have been identified and their role in the apoptosis pathway is well documented (Igaki et al., 2002; Kanda et al., 2002). However, no homologue of TNF-α and Fas ligand have been identified from mollusks previously. Also, there is very little information on the inflammatory and immune responses against these bacterial, virus and other parasite infections at the molecular level in the abalone. Therefore, functional characterization of inflammatory, apoptosis and immune system regulated genes such as TNF-α and Fas ligand are important for further understanding the apoptotic cascade as well as their role in the immune system in abalone-like mollusks.

2.2. Materials and Methods

2.2.1. Identification and sequence characterization of AbTNF-α and AbFas ligand cDNA

Initially, two nucleotide sequences (partial) homologues to TNF-α and Fas ligand counterparts were identified from abalone cDNA library during homology screening using NCBI BLAST. These sequences were denoted as AbTNF-α and AbFas ligand, respectively. The full- length sequence of AbTNF-α and AbFas ligand were obtained by internal sequencing using a terminator reaction kit, Big Dye, and the ABI 3700 sequencer (Macrogen, Korea) with sequencing primers of TNF-1 and Fas ligand -1.

2.2.2. Sequence characterization and phylogenetic analysis

Bioinformatics tools and methods used for sequence characterization and phylogenetic analysis were described in section 1.2.12.

2.2.3. Experimental abalone and immune challenge

Abalone used for this study was described in section 1.2.2. To determine the immune responses of *AbTNF-α and AbFas* ligand, three pathogenic bacteria mixture, VHSV and LPS were used as immunostimulants in time course experiments. Experimental conditions of abalone challenged with bacteria, VHSV and LPS have been described under the sections of 1.2.3, 1.2.4, 1.2.5, 1.2.9 and 1.2.10.

2.2.4. Transcriptional analysis of AbTNF-α and AbFas ligand by qRT-PCR

For this total RNA was extracted from hemocytes, gills and digestive tract using Tri Reagent™ Kit (Sigma, USA) according to manufacturer's protocol (section 1.2.6). Sample of 2.5 µg RNA was used to synthesize cDNA from each tissue using a Cloned AMV first-strand cDNA synthesis kit (Invitrogen, USA) as described in section 1.2.10. Transcriptional analysis was analyzed by qRT-PCR using gene-specific primers of AbTNF-α (TNF-2F and TNF-2R) and AbFas ligand (Fas ligand-F3 and Fas ligand-R1) as shown in table 2. qRT-PCR was carried using a Chromo4^{TM} real-time PCR detector (TaKaRa Japan) as described in section 1.2.11.

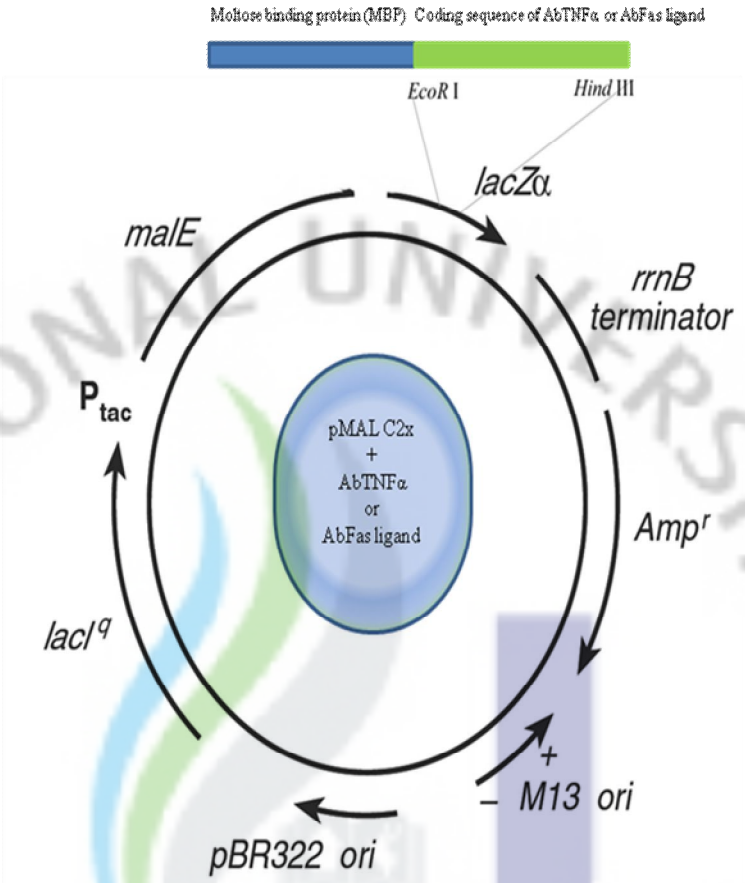

Fig. 10. Schematic diagram of cloning of AbTNF-α or AbFas ligand coding sequences into pMAL-c2X

2.2.5. Cloning of the AbTNF-α and AbFas ligand coding sequences into pMAL-c2X

Two primer sets TNF-α-3F, TNF-α-3R and Fas ligand-3F, Fas ligand-3R were designed after checking the restriction enzyme sites of coding sequences of AbTNF-α and AbFas ligand (table 2). Then, AbTNF-α and AbFas ligand coding sequences were cloned into into pMal-c2x (New England Biolabs, USA) without including signal peptide sequence (Fig. 10). A total of 50 µL of PCR reaction was performed with 5 units of Ex Taq polymerase (TaKaRa, Japan), 5 µL of 10 X Ex Taq buffer, 8 µL of 2.5 mM dNTP, 50 ng of template (cDNA clone of AbTNF-α and AbFas ligand) and 50 pmol of each primer. The reaction was carried out with an initial incubation at 94 ^{o}C for 2 min, 30 cycles (94 ^{o}C, 30 s; 55 ^{o}C, 30 s; 72 ^{o}C; 60 s), followed by a final extension at 72 ^{o}C for 5 min. The PCR product was analyzed on a 1% agarose gel and ethidium bromide staining. Thereafter, PCR product was purified using the Accuprep^{TM} gel purification kit (Bioneer Co., Korea) and digested with respective restriction enzymes. The expression vector, pMAL-c2X, was digested with the same restriction enzymes as the PCR product, and the vector was dephosphorylated with calf intestine phosphates (NEB, USA) in accordance with the vendor's protocol. Then, the vector and PCR product were purified by a 1% agarose gel using the QIAEX II Gel Extraction Kit (QIAGEN Inc., USA). Ligation was carried out at 16 ^{o}C, overnight with 100 ng of pMAL-c2X vector, 70 ng of PCR product, 1 µL of 10 X ligation buffer and 0.5 µL 1 X T4 DNA ligase (TaKaRa, Japan). The ligated product was transformed into XL1 blue cells, followed by *E. coli* BL21 (DE3) cells for protein expression.

2.2.6. Over-expression and purification of recombinant AbTNF-α and AbFas ligand

The recombinant protein of each gene (AbTNF-α, AbFas ligand) was over-expressed in *E. coli* BL21 (DE3) cells by IPTG induction. Briefly, 10 mL volume of *E. coli* BL21 (DE3) starter culture was inoculated in 100 mL Luria broth with 100 µL ampicillin (100 mg/mL) and 10 mM glucose (2% final concentration). The culture was incubated at 37 ^{o}C with shaking at 200 rpm until the cell count reached 0.5 at 600 nm optical density. The culture was shifted to 12 ^{o}C for 15 min and induced by 1 mM IPTG (final concentration) for 16 h. Cells were cooled on ice for 30 min, and harvested by centrifugation at 3000 x g for 30 min at 4 ^{o}C. The cells were re-suspended with 5 mL column buffer (Tris-HCl, pH 7.4, 200 mM NaCl, 0.5 M EDTA) and stored at -20 ^{o}C overnight. Recombinant AbTNF-α or AbFas ligand were purified in the form of fusion protein with MBP by pMAL^{TM} protein fusion and purification system (NEB, USA). Briefly, the re-suspended *E. coli* BL21 (DE3) cells were placed in an

ice-water bath and sonicated 5-6 times in short pulses for 1-2 min. Then the sonicated cell suspension was centrifuged at 9000 x g for 30 min at 4 ^{o}C and resulted supernatant considered as crude protein extract. In the final purification step, amylose resin was poured into a 1 x 5 cm size column and washed with 8 X volumes of column buffer. The crude extract was loaded onto the column and allowed to settle for 10 min followed by washing with 12 X volumes of column buffer. Finally, the AbTNF-α or AbFas ligand fusion protein was eluted by applying the total 2 mL elution buffer (column buffer + 10 mM maltose) in 500 µL aliquots. To determine the protein induction, solubility level, purity state and molecular weight, the AbTNF-α or AbFas ligand samples were collected from different purification steps and then subsequently analyzed on a 12% SDS-PAGE. The gel was stained with 0.05% Coomassie blue R-250, followed by a standard de-staining procedure. Protein markers were obtained from Bio Rad (USA).

2.2.7. Hemocyte culture

The abalone hemolymph was collected as described under the section 1.2.3. Collected hemolymph was immediately transferred into micro tubes and kept on ice. Hemolymph from individuals was pooled and diluted with filtered sterile seawater (v:v) for flow cytometric assays.

2.2.8. Human cell line and culture

Human monocytic leukemia THP-1 cell line was obtained from the American Type Culture Collection (Manassas, VA). The cells were cultured in RPMI 1640 culture medium containing 10% heat inactivated FBS at 37 °C in a 5% CO_2 humidified incubator. Additionally, cell medium was supplemented with 100 U/mL penicillin and 100 µg/mL streptomycin.

2.2.9. Analysis of recombinant AbTNF-α and AbFas ligand-induced ROS in hemocytes and THP-1 cells by flow cytometry

Biological activity of the recombinant AbTNF-α and AbFas ligand was evaluated based on the induction of intracellular ROS (O_2^-) in hemocytes and THP-1 cells by using flow cytometry. Briefly, 300 µL diluted hemolymph was placed in micro tube at 18 ^{o}C while 2 mL of THP-1 cells (1 x 10^5 cells/mL) were seeded in 6-well plates and maintained at 37 ^{o}C in 5% CO_2 incubator. Then, both hemolymph and exposed THP-1 cells were treated with different concentrations (0, 0.5, 2 and 3 µg/mL) of recombinant AbTNF-α or AbFas ligand.

Cells were maintained with MBP as well as without recombinant proteins as controls. After 2 h of incubation with recombinant protein or MBP control, cells were stained with 2 μM HE at respective temperature for 30 min. The HE is used for specific detection of O_2^-. Then, the cells were collected and fluorescence was analyzed using a FACSCalibur flow cytometer (Becton Dickenson; San Jose, CA) in 10,000 events. CellQuest software (Becton Dickenson; San Jose, CA) was used to calculate the O_2^- percentages based on the level of fluorescence.

2.2.10. Analysis of recombinant AbTNF-α and AbFas ligand induced immune gene transcription in hemocytes by qRT-PCR

Transcriptional response of various immune response genes in hemocytes were analyzed by addition recombinant TNF-α or Fas ligand protein using qRT-PCR. Briefly, hemocyte suspensions were allowed to adhere for 20 min before adding TNF-α or Fas ligand (final concentration 2 μg/mL) in 6-wellplates. After 1 h and 3 h incubation with recombinant protein (TNF-α or Fas ligand) at 18 ^oC, hemocytes were collected for RNA isolation as described in 1.2.3. Gene specific primers of selected genes are shown in table 2. cDNA synthsis and qRT-PCR was performed according to the methods described in 1.2.10 and 1.211 sections.

2.3. Results and discussion

2.3.1. Abalone TNF-α (AbTNF-α)

2.3.1.1. Cloning and characterization of AbTNF-α cDNA sequence

AbTNF-α partial sequence was identified from abalone cDNA library and then full length was obtained by internal sequencing reaction. AbTNF-α amino acid sequence showed that characteristic motif to known TNF protein family members at ^{132}IIIPATGVYAVYS^{144}. Therefore, it was named as an abalone TNF-α (AbTNF-α). The full-length of AbTNF-α consisted 930-bp with a 717-bp coding sequence encoding 239 amino acids (fig.11). It contains 124-bp 5' UTR and an 89-bp 3' UTR. The AbTNF-α has a putative molecular mass of 26.5 kDa with an isoelectric point (p*I*) of 7.1. The signal peptide was identified at the N-terminal sequence with the cleavage site at 21 amino acid position. Additionally, a characteristic transmembrane domain was predicted at the 4-27 amino acid range by DAS prediction according to the method described by Cserzo et al. (1997). Also, N-terminal amino acids from 1-26 were shown as a high hydrophobic amino acid cluster. Importantly, AbTNF-α is highly conserved with three main TNF family signature profiles i) TNF family profile I (86-239); ii) TNF family profile II (115-239); iii) TNF family profile III (111-239), which were identified using motif scan under PROSITE program (http://kr.expasy.org/prosite/). Also, a highly conserved cell attachment motif ^{155}RGD^{157} was presented in AbTNF-α. Furthermore, N-glycosylation sequence ^{158}NETD^{161} and one cysteine residue at C^{25} were shown in the mature peptide of AbTNF-α. In ClustalW pairwise comparison, AbTNF-α showed the highest amino acid identity (22%) to the *Drosophila* "Eiger" TNF homologue protein. However, Eiger contains 415 amino acids, which is exceptionally long amino acids protein to all known TNF ligand superfamily members (230-250 amino acids). Additionally, AbTNF-α showed 21% amino acid identity to *Ciona savignyi* TNF member (CsTL), which also contains 289 amino acids. In general, AbTNF- α showed 17-21% amino acid identity ranges to fish and mammalian TNF-αs.

2.3.1.2. Phylogenic analysis

Different TNF superfamily members were included in the phylogenetic analysis to determine the ancestral relationship of AbTNF-α, since it showed lower identity to known TNF-α family member (fig. 12). The *Drosophila* "Eiger" protein was used as the out-group. The results indicated that two main clusters were grouped as vertebrate and invertebrate TNF superfamily members. The vertebrate cluster has divided in to three sub-clusters as i) mammalian TNF-α; ii) mammalian LT-α; iii) teleosts TNF-α members. Ab AbTNF-α was positioned with *Ciona savigny* TNF-α in the invertebrate main cluster.

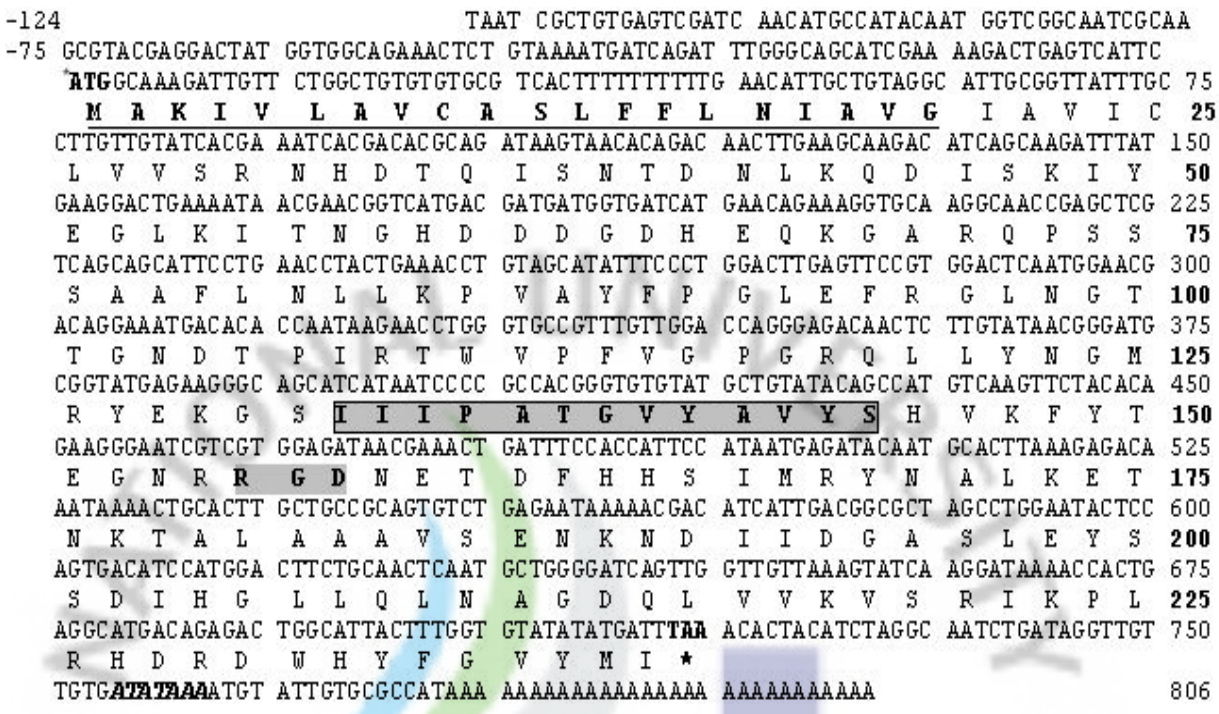

Fig. 11. The complete nucleotide and deduced amino acid sequences of the abalone TNF-α cDNA (GenBank accession **EU863217)**. The start (ATG) and stop (TGA) codons are in bold and high-lighted with an asterisk (*). The predicted transmembrane region is underlined with bold face. The TNF-α signature is boxed. The cell attachment motif ^{155}RGD^{157} is bold shaded. The poly (A) tail is underlined at the end of sequence.

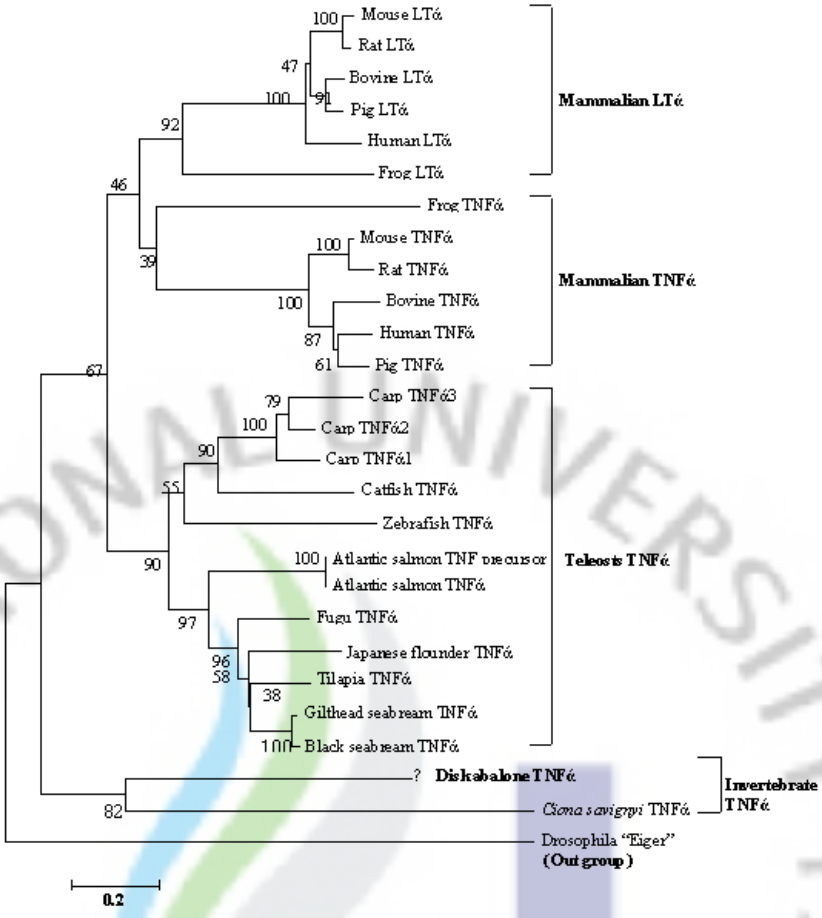

Fig. 12. Phylogenic analysis of abalone TNF-α. Drosophila "Eiger" TNF superfamily ligand was used as the out-group. Numbers indicate the bootstrap confidence values of 1000 replicates. The accession numbers of the selected TNF sequences are disk abalone *Haliotis discus discus* TNF-α, (EU863217); mouse *Mus musculus* TNF-α (AAB65593); LT-α (AAA18593); rat *Rattus norvegicus* TNF-α (CAA47146); LT-α (NP_542947); bovine *Bos taurus* TNF-α (NP_776391); LT-α (CAA78510); pig *Sus scrofa* TNF-α (CAA40591); LT-α (NP_999618); human *Homo sapiens* TNF-α (AAA61198); LT-α (CAA25649); frog *Xenopus tropicalis* TNF-α (AM041993); LT-α (AM041994); carp *Cyprinus carpio* TNF-α1 (AJ311800);TNF-α2 (AJ311801); TNF-α3 (AB112424); channel catfish *Ictalurus punctatus* TNF-α (CAD10389); zebrafish *Danio rerio* TNF-α (AB183467); Atlantic salmon *Salmo salar* TNF-α1 (NP_001117061); TNF precursor (AAX24118); fugu *Takifugu rubripes* TNF-α (NP_001033074); Japanese flounder *Paralychthys olivaceys* TNF-α (AB040448); Nile tilapia *Oreochromis niloticus* TNF-α (AAR88097); black seabream *Acanthopagrus schlegelii* TNF-α (AAP94278); gilthead seabream *Sparus aurata* TNF-α, (Q8JFG3); sea squirts *Ciona savignyi* TNF-α (EU216599); fruit fly *Drosophila melanogaster* Eiger (BAC00950).

2.3.1.3. Tissue specific expression of AbTNF-α

To determine the TNF-α expression profile, qRT-PCR was carried out using gene specific primers designed from the AbTNF-α coding sequence. Constitutive expression of AbTNF-α was detected in all selected tissues namely gill, mantle, muscle, digestive tract, hepatopancreas and hemocytes (fig. 13A). The AbTNF-α mRNA expression in the gill and mantle was statistically ($p<0.05$) higher than in the hemocytes. In contrast muscle, digestive tract and hepatopancreas showed the lower expression than hemocytes. Furthermore, it was revealed that the highest constitutive expression in gill tissue was 1.5-fold higher than hemocytes expression fold. Overall, AbTNF-α expression in all tissues was significantly ($p<0.05$) different from the hemocyte expression.

2.3.1.4. Transcriptional regulation of AbTNF-α expression after bacteria, VHSV and LPS challenge

The immune response of AbTNF-α mRNA was monitored in hemocytes and gills after challenge with bacteria mixture (*V. alginolyticus, V. parahemolyticus,* and *L. monocytogen*), VHSV and LPS. The AbTNF-α mRNA expression levels in bacteria infected gills showed an immediate induction with a 3-fold significant ($p<0.05$) increase at 3 h compared with the PBS control (fig. 13B). Then, the expression level decreased at 6 p.i. and again gradually increased to a peak level of 5.2-fold at 24 h. Furthermore, AbTNF-α expression was declined to 3.0-fold at 48 h p.i. (compared to 24 h). In gills, AbTNF-α expression was significantly ($p<0.05$) increased following bacterial infection in all the time points except at 6 h. In bacteria challenged hemocytes AbTNF-α transcription level was only induced at 12 and 48 h of bacteria challenge while all other time it was decreased compared to control (fig. 13C). In the VHSV infected gills, AbTNF-α was significantly ($p<0.05$) induced at all time points compared to control animals (fig. 13D). There was an immediate response with a 1.6-fold induction of AbTNF-α at 3 h. The highest relative expression was observed at 48 h with a 2.8-fold increase compared to the PBS control group. In VHSV challenged hemocytes, AbTNF-α was significantly up-regulated until 12 h and then decreased below to basal level of control (fig. 13E). In the LPS injected abalone, the level of AbTNF-α was slightly but not significantly ($p<0.05$) increased at 3 h and then decreased at 12 h p.i when compared with the PBS control group (data not shown). However, AbTNF-α expression was significantly ($p<0.05$) induced in the gill tissue only at 48 with a 3.3-fold increase compared to the control animals. In general, AbTNF-α was induced in gills and hemocytes by the bacteria mixture, VHSV and LPS immune challenge undertaken in this study.

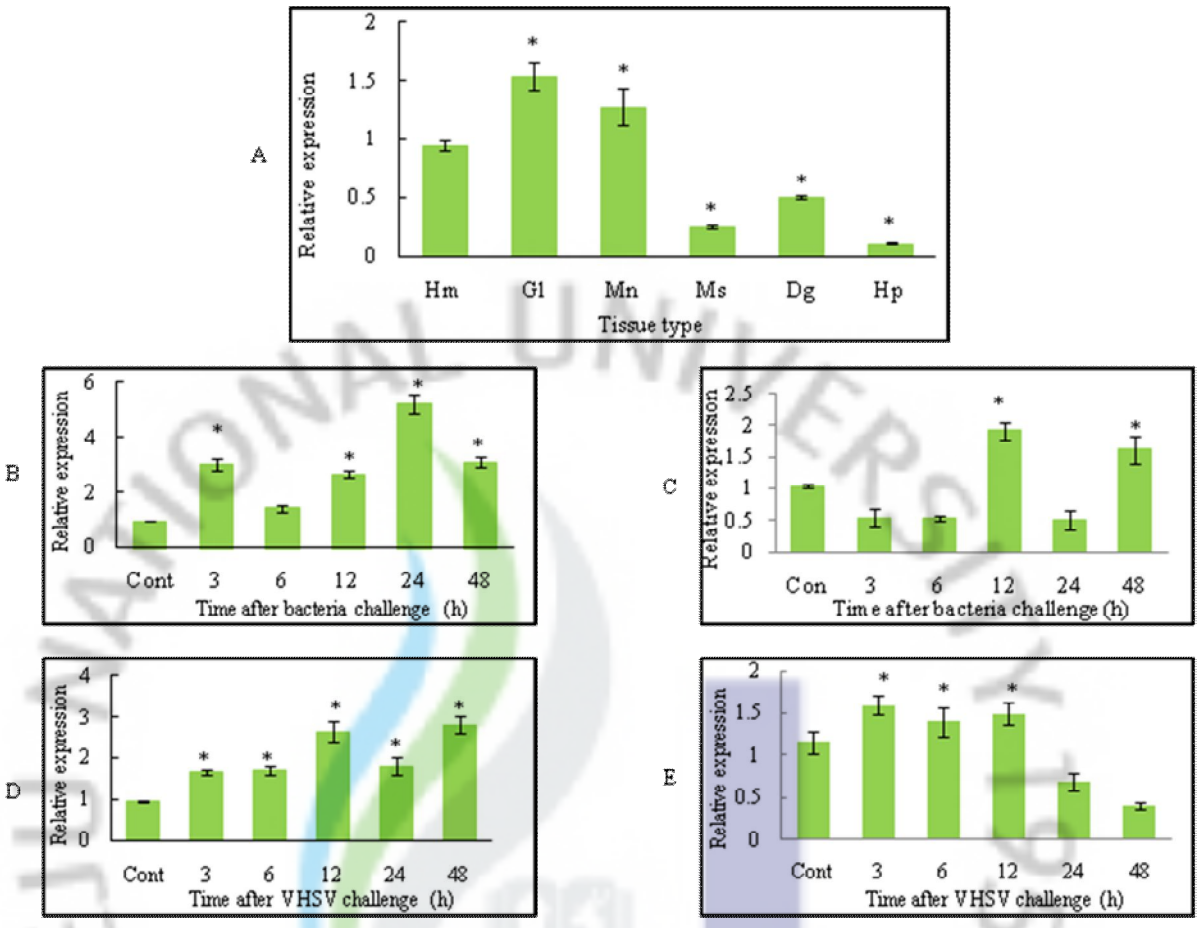

Fig. 13. Tissue expression profile and transcriptional responses of AbTNF-α after bacteria and VHSV challenge by qRT-PCR. The relative AbTNF-α expression fold was calculated by the $2^{-\Delta\Delta CT}$ method using abalone ribosomal protein as a reference gene. Relative expression fold of each tissue was compared to that of hemocyte to determine the tissue specific expression. A) tissue expression profile; B) bacteria challenged gills; C) bacteria challenged hemocytes; D) VHSV challenged gills; E) VHSV challenged hemocytes. Data are presented as mean relative expression ± SD for three replicate real-time reactions from pooled tissue of three individual abalones at each time point. The bars represent the standard deviation (n=3). Gl-gill; Mn-mantle; Ms-muscle; Dg-digestive tract; Hp-hepatopancreas; Hm-hemocyte; Cont-control (PBS).

2.3.1.5. Overexpression and purification of recombinant AbTNF-α

The cloned AbTNF-α coding sequence was inserted into the *malE* gene, which encodes the MBP under the strong tac promoter and *malE* translation initiation signal of pMAL-c2X. The recombinant AbFas ligand protein was produced in the *E. coli* BL21 strain (DE3) by IPTG-driven induction. Aliquots of different fractions during the purification process were analyzed by SDS-PAGE gel with Coomassie Brilliant Blue (Fig. 14). Data indicated a prominent band of approximately 66.5 kDa from the induced cells. Crude soluble protein fraction was obtained after cell lysis using sonication, followed by centrifugation. We observed a strong band in the crude protein extract (soluble) corresponding to the expected protein size. Thereafter, the recombinant TNF-ά fusion protein was purified from the crude protein extract that showed this single protein band in the gel analysis. The molecular mass of the recombinant AbTNF-α (fusion) was around 66.5 kDa, as determined by SDS-PAGE, which is in agreement with our predicted molecular mass (24 kDa) of mature peptide used to purifiy recombinant protein (molecular mass of the MBP is 42.5 kDa).

2.3.1.6. Biochemical properties of the recombinant AbTNF-α

In preliminary tests, the biological activity of the recombinant AbTNF-α was measured by evaluating its ability to induce apoptosis, and generate intracellular ROS such as O^-_2 in abalone hemocytes and human leukemia THP-1 cells using flow cytometry. We examined whether the AbTNF-α could induce apoptosis in THP-1 cells by analyzing the phosphatidylserine on the cell surface using annexin-V staining. However, AbTNF-α treatment did not induce the apoptosis pathway in THP-1 cells (data not shown). Then, we next analyzed the intracellular ROS generation by recombinant AbTNF-α in hemocytes and THP-1 cells, since involvement of ROS in apoptosis activation is well established. As shown in fig. 15, intracellular O^-_2 level was increased in both hemocytes and THP-1 cells in concentration-dependant manner after 2 h treatment of recombinant AbTNF-α ranging from 0.5 μg/mL to 3μg/mL. Furthermore, results showed induction of O^-_2 in abalone hemocytes was greater than THP-1 cells. Cells without recombinant AbTNF-α or only with maximum amount of MBP showed the almost similar intracellular O^-_2 levels lower than that of recombinant AbTNF-α.

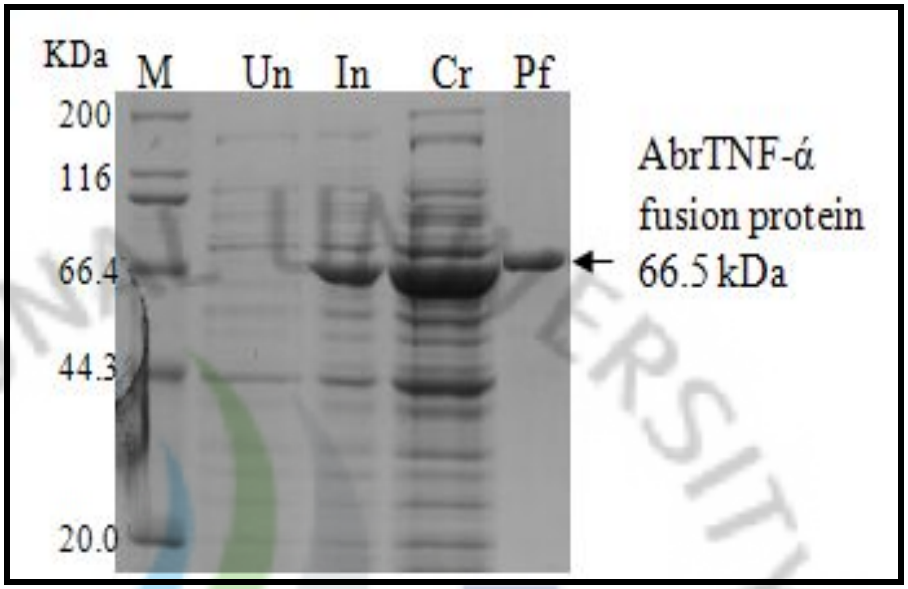

Fig. 14. Over expression and purification of recombinant TNF-ά fusion protein. Protein samples are separated by 12% SDS-PAGE and stained with Coomassie brilliant blue. M: protein marker (TaKaRa, Japan). Un: total cellular extract from *E. coli* BL21(DE3) before induction; In: total cellular extract after induction with 1 mM IPTG at 12 ^{o}C for 16 hr; Cr: soluble crude extract after induction; Pf: purified recombinant TNF-ά ligand fusion protein.

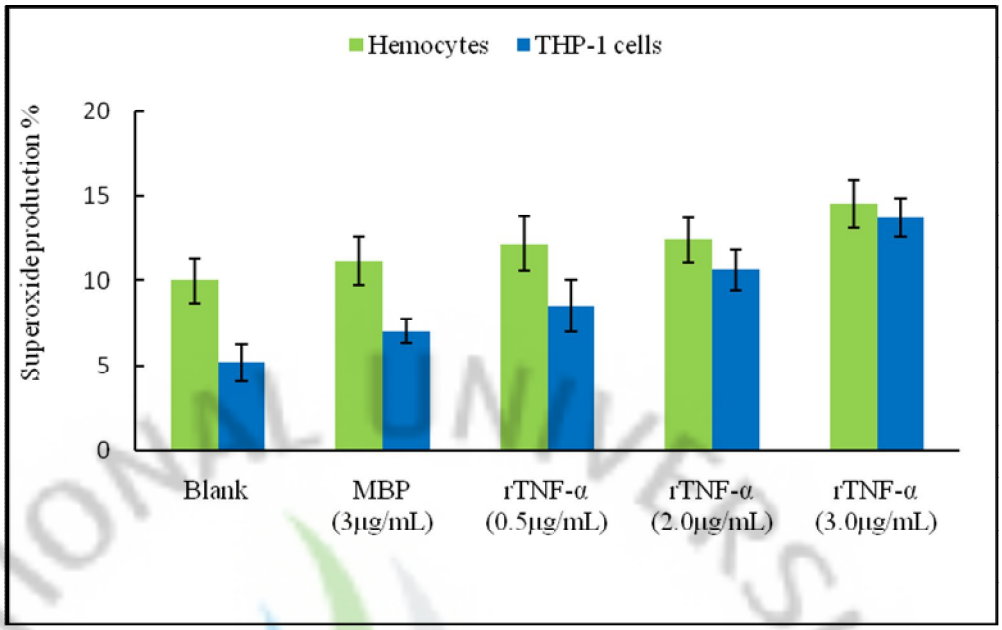

Fig.15. Analysis of intracellular ROS generation (represented by O^{-}_{2}) by recombinant abalone TNF-ά. Abalone hemocytes or THP-1 cells were treated with different concentration of recombinant AbTNF-α for 2 h followed by addition of 2 μM HE for 30 min at 18°C (hemocytes) or 37°C (THP-1 cells). Cells were analyzed for flow cytometry considering 10000 events for each sample. The fluorescence intensity percentage (%) of cells stained by HE (FL2-H) are represented in X axis.

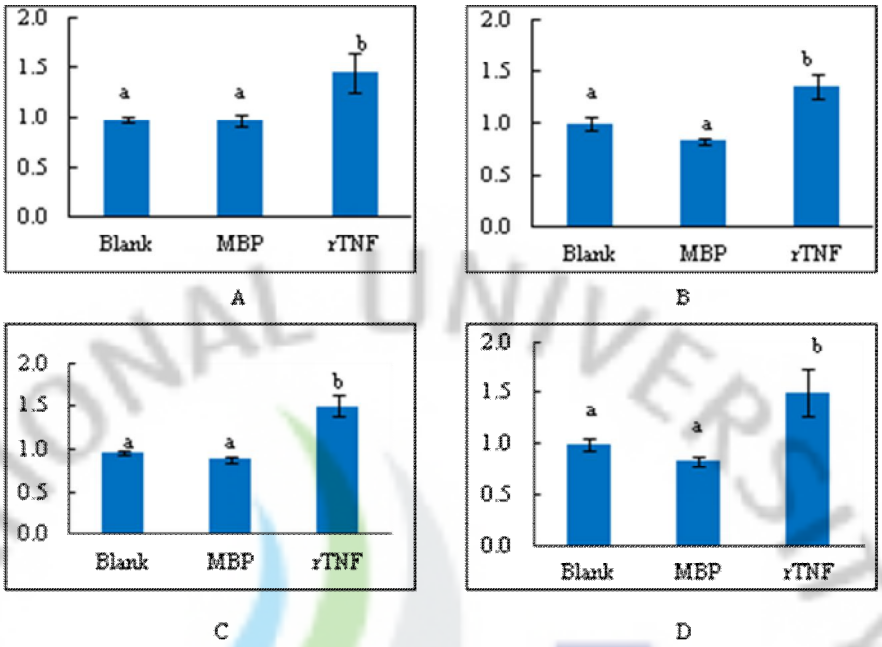

Fig.16. Transcriptional analysis of different immune-relavant genes in abalone hemocytes after treatment of rTNF-ά by qRT-PCR. Abalone hemocytes were treated with 2.5 μg/mL rTNF-ά and incubated for 3 h at 18 ^{o}C. The relative expression fold was calculated by the $2^{-\Delta\Delta CT}$ method using abalone ribosomal protein as a reference gene. Relative expression fold of each gene was compared to that of blank (no protein) and MBP. A) NF-kB; B) caspase 8; C) catalase; D) SOCS-2. Data are presented as mean relative expression ± SD for three replicate real-time reactions from pooled tissue of three individual abalones at each time point. The bars represent the standard deviation (n=3).

.

2.3.1.7. Discussion

Present study, describes the molecular cloning and expression analysis of a TNF-ά homologue from disk abalone as a first report of a mollusk TNF-α member belonging to the TNF superfamily ligand. The average size of the mammalian TNF-α is 234 amino acids with a range between 233 and 235, while the average size of TNF-α in fish is 242, with a range between 226 and 256 amino acids (Goetz et al., 2004). AbTNF-α consists of 239 amino acids, which is similar to range of both mammalian and fish TNF-α. The fish and mammalian TNF share several conserved features. Among them the TNF family signature ([LV]-x-[LIVM]-x_3-G-([LIVMF]-Y-([LIVMFY]$_2$-x_2-([QEKHL]) is highly conserved but varies wi th alternative amino acids (Goetz et al., 2004). Within this signature motif, three cons istent amino acid differences have been observed previously; i) at position 1; isoleucin e and leucine ii) at position 3; isoleucine and valine iii) at position 10; phenylalanine and leucine. In fact fish do not completely follow this signature. Although, AbTNF-α has a conserved TNF signature motif the leucine at position 1 and valine at position 3 are replaced by isoleucine in both locations as previously reported in several fish (Go etz et al., 2004). Therefore, the amino acid residues in the AbTNF-α signature motif is in accordance with the general residue changes in the mammalian and fish TNF signatures.

Mammalian TNF-α is a type II transmembrane glycoprotein having a single transmembrane domain and cleavage site for releasing of the mature soluble protein after proteolysis by TNF-α converting enzyme (TACE) (Ordas et al., 2007; Kruys et al., 1992). Also, the transmembrane domain comprises a cluster of hydrophobic amino acid residues from the N-terminus [9]. Interestingly, a similar transmembrane domain with relatively high hydrophobic amino acid residues is present in AbTNF-α from the 4-27 amino acid region. Therefore, it could be suggested that AbTNF-α is a membrane bound precursor protein, and is released as a mature protein after propeptide proteolysis by TACE or a similar protein in the abalone. Many cytokines and other protein involved in inflammation have the 3' UTR mRNA instability motifs (ATTTA) (Kruys et al., 1992; Caput et al., 1986). These elements are required to attach various ARE binding proteins, which leads to suppress the transport of mRNA out of the nucleus and facilitate the correct expression (Han et al., 1990). However, AbTNF-α did not show any conserved ATTTA in the 3' UTR of cDNA. Although, slightly modified mRNA instability motif (ATATA) was identified at the 3' UTR.

Uenobe and his group showed that Ayu fish TNF has 32-41% amino acid identity to other fish and 30% with mammals (Goetz et al., 2004; Uenobe et al., 2007). We also

observed low identity of AbTNF-α with fish and mammalian TNF-α ranging from 17-22%. A bTNF-α identity with *Drosophila* "Eiger" TNF superfamily member was the highest observed in this study. Both sequences show the predicted transmembrane domain and TNF family signature. In contrast, the "Eiger" protein has exceptionally longer amino acid sequence (415 aa) compared to AbTNF-α and other known TNF-α proteins. The C-terminal domain of "Eiger" shows comparability with human TNF family members with 20-25% identity [17]. Also, AbTNF-α showed low identity (21%) to recently identified TNF-α from invertebrate sea squirts *Ciona savignyi*. Zhang and his group commented that it is difficult to identify TNF ligand superfamily molecules of non-mammals only by sequence due to low identity values (Zhang et al. 2008). Therefore, we have included the different TNF ligand superfamily members in the phylogenic tree to find out possible evolutional relationship of abalone TNF-α. The phylogenic analysis confirmed that invertebrate TNF ligand family is separated from vertebrate TNFs. Also, it was showed that mammalian has a distinct type of TNF-α and TN F-β. However, it is clear that the divergence of abalone TNF-α from a common ancestor with other invertebrate species. Although, the exact position of the AbTNF-α in the evolution could be clarified in detail only after including other invertebrate's TNF superfamily members.

TNF-α mRNA expression in distinct tissues has been previously reported in several fish species. For instance, constitutive TNF-α expression was detected in the head kidney and gill tissues of the rainbow trout (Laing et al., 2001), the head kidney and liver of the catfish (Zou et al., 2003), the head kidney, liver, and macrophages of the gilthead seabream (Garci a-Castillo et al., 2002); and the liver and head kidney of the rainbow trout (Bridle et al., 2 006). In the present study, our results indicates that TNF-α is expressed in main immune related cells (hemocyte) as well as non immune tissues such as gill, mantle, muscle, digestive, and hepatopancreas in abalone. More similarly, the transcripts of CsTL were detected in heart, gonad, digestive gland, intestine, pharynx, neural complex and hemocytes in the invertebrate sea squirts *Ciona savignyi* (Zhang et al., 2008). The TNF-α mRNA expression in fish showed differential expression profile during viral (Tafalla et al., 2005), bacterial [Ordas et al., 2007), parasitic infections (Sigh et al., 2004) and LPS stimulation (Hirono et al., 200 0). Therefore, the study of TNF-α and it's specific transcriptional regulation in terms of cellular activation with different types of pathogens would greatly facilitate the understanding of the mechanism of pathogenesis in abalone disease. Thus, we selected a gram negative and positive bacteria mixture (*V. alginolyticus, V. parahemolyticus, and L. monocytogen*), VHSV

and LPS to study TNF-α responses in the abalone gill. *Vibrio pelagius* strain Hq222 induced TNF-α expression in liver of the turbot at 24 h p.i, while cytokine induction by VHSV was identified at 8 h p.i. (Ordas et al., 2007).

Also, it has been shown that expression of TNF-α is induced by LPS in Japanese flounder (Hirono et al., 2000); in head kidney leucocytes and the macrophage cell line (RTS11) of the rainbow trout (Laing et al., 2001); in head kidney phagocytes of the carp (Sa eij et al., 2003); in liver, spleen, and head kidney of the ayu fish (Uenobe et al., 2007). It was reported that different pathogens induce the expression of pro-inflammatory cytokines in different ways (Thanawongnuwech et al., 2004). Similarly, we also observed that AbTNF-α was significantly induced in the gill after bacteria, VHSV and LPS stimulation. However, the induction levels and highest induction time p.i. varied with the type of induction in this study. Further studies are required to elucidate the expression variation specific to the type of induction.

In conclusion, the first evidence of a TNF-α homologue in the mollusk has been demonstrated in the disk abalone. We could confirm that the cloned TNF homologue from abalone is a subset of the TNF-α superfamily ligands based on the characteristic features presence in the sequence; i) TNF family signature motif; ii) N-terminal transmembrane domain with highly hydrophobic amino acid residues; iii) similar molecular mass (26.5 kDa) to mammalian and fish TNF-α counter parts; iv) grouped with invertebrate TNF-α clade in the phylogenic tree. Also, it indicates that TNF-α is expressed in diversified abalone tissues in a tissue specific manner and was able to induce specific expression profiles of mRNA in response to bacteria mixture of *V. alginolyticus, V. parahemolyticus, and L. monocytogen*, VHSV and LPS induction in the abalone gill. Therefore, the discovery of TNF-α in the mollusk abalone will be supported more detailed investigation into the immunological and inflammatory responses of invertebrate animals.

2.3.2. Abalone *Fas ligand (AbFas ligand)*

2.3.2.1. Characterization of the AbFas ligand cDNA sequence

The cloned full-length AbFas ligand (GenBank ACJ12607) consists of 1832 bp (fig. 17). The open reading frame was composed of 945 bp that translate into a putative peptide of 315 amino acid residues. Sequence analysis indicated a 32 bp long 5' untranslated region (5' UTR) and 859 bp 3' UTR, which contains two RNA instability motifs (^{1407}ATTTA^{1411} and ^{1449}ATTTA^{1453}) with a typical polyadenylation signal (^{1756}AATAAA^{1761}). The AbFas ligand has a putative molecular mass of 35 kDa with 8.9 isoelectric point (p*I*). Additionally, a characteristic transmembrane domain was predicted in the 55-77 amino acid range by the DAS prediction program. Importantly, the AbFas ligand showed three TNF family signature domains in the amino acid sequence: i) profile I (177-315); ii) profile II (192-315); and, iii) profile III (216-232), which were identified using the motif scan of the PROSITE program. Moreover, it was identified one N-glycosylation sequence at ^{213}NGTL^{217}. Signal peptide prediction results showed that there was no putative signal peptide in the AbFas ligand.

We analyzed the AbFas ligand sequence identity with TNF superfamily members including Fas ligand, TNF-α, LT-α from human, bovine, mouse, rat, zebrafish and Japanese flounder FASTA program (Table 11). Results showed that the AbFas ligand has higher identity and similarity to the Fas ligands compared to the TNF- α and LT- α selected in this study. Also, the gap percentages of the AbFas ligand in the alignment were lower among the Fas ligands, compared to the TNF-α, and LT-α sequences. As it is shown in Table 2, the AbFas ligand demonstrated the highest identity (22%) and similarity (34.6%) to human and zebrafish Fas ligands, respectively. Furthermore, results yielded on the variation of AbFas ligand identity in comparison to other proteins, from 22-19.1% compared to other Fas ligands, 20-15% to TNF-α and 14.7-10.4% to LT- α. Moreover, the AbFas ligand amino acid sequence has only 20.5% identity and 31.6% similarity to disk abalone TNF-α. In addition, AbFas ligand was aligned with human, pig, mouse, zebrafish and Japanese flounder sequences in Clustal W multiple analyses. The results revealed that the AbFas ligand has the longest amino acid sequence (315 aa), and very few conserved amino acids among the other comparable sequences. However, the C-terminal region showed that there were more conserved amino acids than observed in the N-terminal region. The AbFas ligand putative transmembrane region was not aligned with other species respective transmembrane regions. Only five proline (P) residues with a 9% proline ratio (5/54) were observed in the AbFas ligand cytoplasmic region, although all other species showed comparatively higher proline residues.

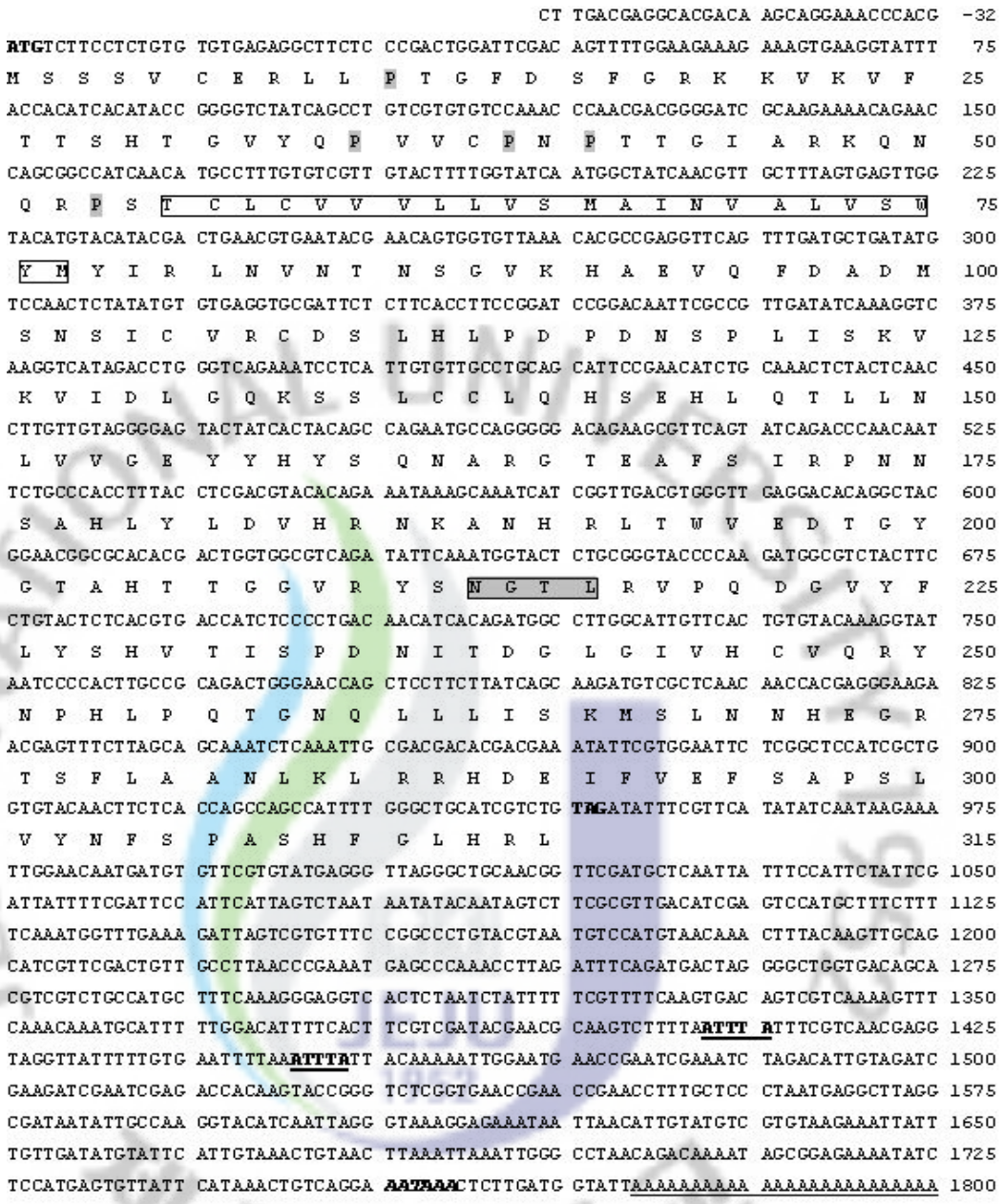

Fig.17. The complete nucleotide and deduced amino acid sequences of the disk abalone Fas ligand cDNA. This nucleotide sequence has been deposited in GenBank under accession number **ACJ12607**. The start (ATG) and stop (TGA) codons are in boldface. The predicted transmembrane domain is boxed. A potential N-linked glycosylation site is in the shaded box. Two predicted RNA instability motifs (ATTTA) are underlined in bold italics. The polyadenylation signal (AATAAA) is in bold italics and the poly-(A) tail is underlined at the end of the nucleotide sequence.

Table 11: Percentage of identity, similarity and gaps of the abalone Fas ligand to other Fas ligand, TNF-α and LT-α sequences.

Gene	Fas ligand			TNF-ά			LT- ά		
Species	Identity	Similarity	Gaps	Identity	Similarity	Gaps	Identity	Similarity	Gaps
Human	22.0	32.5	38.5	16.1	26.8	42.1	14.5	22.4	22.4
Bovine	21.4	32.8	35.6	15.0	27.0	44.0	14.7	20.6	55.8
Mouse	20.7	31.1	38.1	16.2	27.6	39.1	14.3	21.3	54.8
Rat	21.7	31.6	37.1	17.0	27.6	38.7	14.7	24.2	51.0
Zebrafish	20.0	34.6	32.0	20.0	31.6	37.1	10.4	18.0	54.5
Japanese flounder	19.1	32.5	37.3	16.9	29.4	42.6	-	-	-

Dash (-) indicates an unavailable sequence.

2.3.2.2. Phylogenetic analysis of abalone Fas ligand

We were interested to determine the phylogenetic relationship of the AbFas ligand with known TNF superfamily members, since it showed lower identity to known Fas ligands. Representatives (26) from Fas ligand, TNF-α and LT- α were analyzed to construct an un-rooted phylogenetic tree by neighbor-joining method using Human TRAIL, fruit fly Eiger sequences as an out-group (Fig. 18). Our results showed that all investigated TNF superfamily members were divided mainly into the Fas ligand, TNF-α and LT-α sub groups. The AbFas ligand (▲) was isolated as a single branch. However, it was originated from the main branch of invertebrate TNF of abalone and *Cioana*. The mammalian Fas ligand sequences were grouped as a separate cluster while the Japanese flounder Fas ligand was originated as a single branch without connecting to mammalian Fas ligand origin.

Fig. 18. Phylogenetic analysis of abalone Fas ligand amino acid sequence with other known Fas ligand, TNF-α and Lymphotoxin- α sequences. Phylogenetic analysis was done by the 'neighbor-joining' method using the MEGA program version 3.1 based on sequence alignment using ClustalW (1.81). It was bootstrapped 1000 times. Human TNF-related apoptosis inducing ligand denoted as TRAIL (P50591) and fruit fly (*Drosophila melanogoster*) TNF named "Eiger" (BAC00950) sequences were used as out-groups. The accession numbers are disk abalone *Haliotis discus discus* TNF-α (EU863217); AbFas ligand (ACJ12607); pig *Sus scrofa* TNF-α (CAA40591); LT-α (NP_999618); FasL (BAB64291); bovine *Bos taurus* TNF-α (NP_776391); LT-α (CAA78510); human *Homo sapiens* TNF-α (AAA61198); LT-α CAA25649); FasL (NP_000630); mouse *Mus musculus* TNF-α (AAB65593); LT-α (AAA18593); FasL (NP_034307), rat *Rattus norvegicus* TNF-α (CAA47146); LT-α (NP_542947); FasL (NP_037040); frog *Xenopus tropicalis* TNF-□ (AM041993); LT-α (AM041994); Channel catfish *Ictalurus punctatus* TNF-α (CAD10389); Atlantic salmon *Salmo salar* TNF-α (NP_001117061); tilapia *Oreochromis niloticus* TNF-α (AAR88097); Japanese flounder *Paralichthys olivaceus* TNF-α (AB040448); FasL (BAD99014); monkey *Macaca mulatta* FasL (BAA90295); *Ciona savignyi* TNF-ά (EU216599).

2.3.2.3. Tissue specific expression of abalone Fas ligand

To determine the tissue-specific transcriptional profile of AbFas ligand, qRT-PCR was carried out using gene-specific primers designed from the AbFas ligand coding sequence. The relative mRNA expression of each tissue was calculated using abalone ribosomal protein as a reference gene and result was further compared with hemocytes expression level to determine the relative tissue-specific expression profile (Fig. 19A). AbFas ligand was constitutively expressed in all six selected tissues including gills, mantle, muscle, digestive tract, digestive glands and hemocyte. Further analysis results showed that AbFas ligand mRNA expression was highest in the the hemocyte. Then, the gills showed the second highest level of expression compared to that observed for hemocytes. Furthermore, in all tissues, the expression level was significantly ($p<0.05$) different to the expression observed in hemocytes. Finally, the AbFas ligand showed tissue-specific variation in abalone tissues.

2.3.2.3. Transcriptional regulation of Ab Fas ligand expression after bacteria, VHSV and LPS challenge

The inducibility and transcriptional regulation of the AbFas ligand was analyzed in gills and hemocytes after immune challenge of abalone by a mixture of bacteria (*V. alginolyticus, V. parahemolyticus,* and *L. monocytogenes*), VHSV and LPS. In gills, the AbFas ligand transcript level was slightly decreased at 6 h although, it was significantly up-regulated ($p<0.05$) after 12 h of bacteria challenge (Fig. 19B). AbFas ligand transcript level had decreased at 24 h and 48 h p.i. even though expression of those time points was significantly higher than the control group in gills. In bacteria challenged abalone hemocytes, Fas ligand transcripts were significantly induced after 12 h onwards (Fig. 19D). In VHSV challenged gills, AbFas ligand responded immediately and the transcript level was significantly ($p<0.05$) up-regulated at 3 h and gradually increased up to 24 h except for a slightly decreased expression observed at 6 h compared to 3 h p.i. The highest induced level (4.1 fold) of the AbFas ligand was observed at 24 h after VHSV infection (Fig. 19C). At 48 h of VHSV infection, the expression level was decreased 1.8-fold compared to the control. However, in VHSV challenged abalone hemocytes, it was induced only at 3 h (Fig 19D). In abalones challenged with LPS, the AbFas ligand was significantly ($p<0.05$) up-regulated in gills during the 48 h post challenge showing its highest level at 12 h with 2.6-fold expression. Then, expression level was gradually decreased up to 2.3 fold at 48 h.

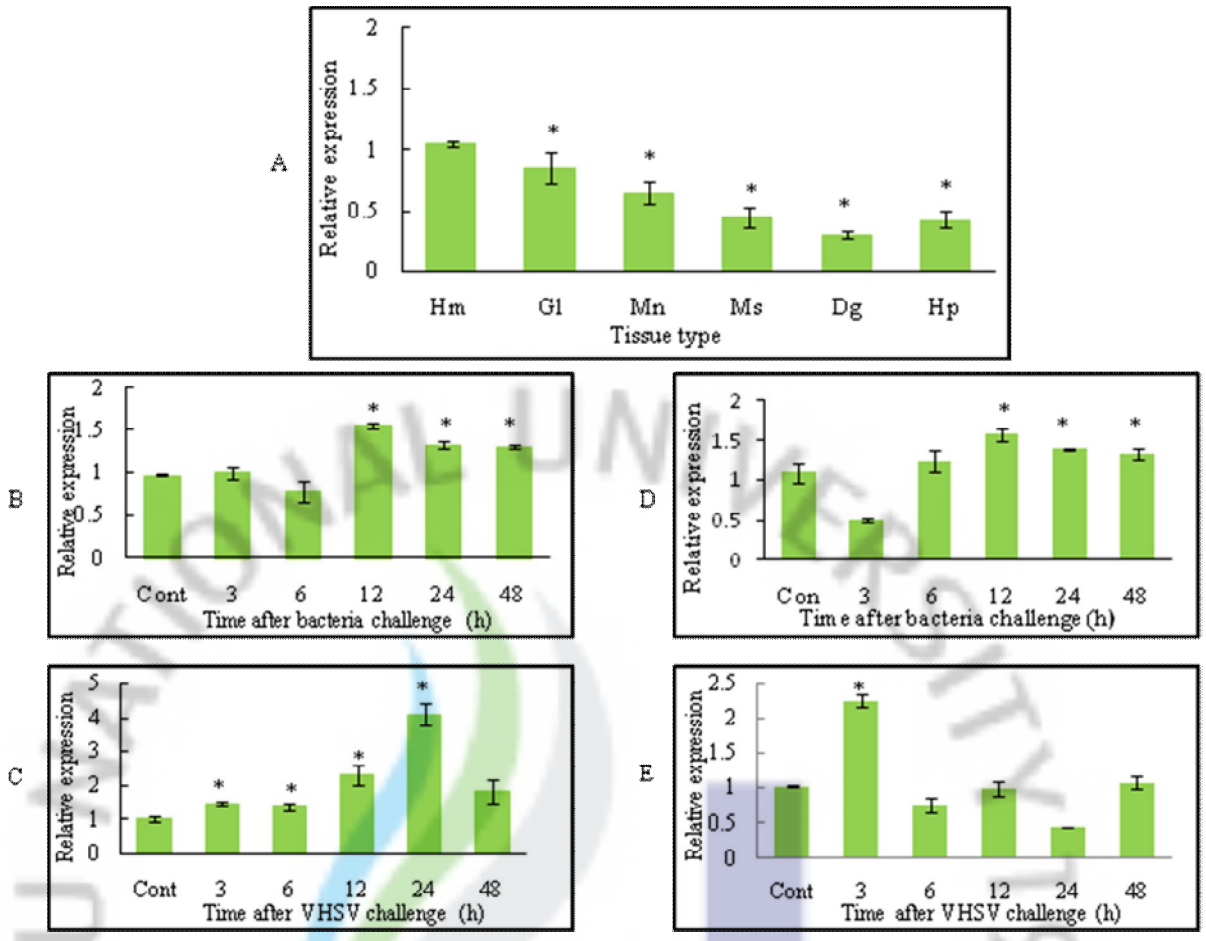

Fig. 19. Tissue expression analysis and transcriptional responses of AbFas ligand after bacteria and VHSV challenge by qRT-PCR. The relative AbFas ligand expression fold was calculated by the $2^{-\Delta\Delta CT}$ method using abalone ribosomal protein as a reference gene. Relative expression fold of each tissue was compared to that of hemocyte to determine the tissue specific expression. A) tissue expression analysis; B) bacteria challenged gills; C) bacteria challenged hemocytes; D) VHSV challenged gills; E) VHSV challenged hemocytes. Data are presented as mean relative expression ± standard deviation (SD) for three replicate real-time reactions from pooled tissue of three individual abalones at each time point. The bars represent the standard deviation (n=3). Gl-gill; Mn-mantle; Ms-muscle; Dg-digestive tract; Hp-hepatopancreas; Hm-hemocyte; Cont-control (PBS).

2.3.2.5. Overexpression and purification of recombinant abalone Fas ligand

The cloned AbFas ligand coding sequence was inserted into the *malE* gene, which encodes the MBP under the strong tac promoter and *malE* translation initiation signal of pMAL-c2X. The recombinant AbFas ligand protein was produced in the *E. coli* BL21 strain (DE3) by IPTG-driven induction. Aliquots of different fractions during the purification process were analyzed by SDS-PAGE gel with Coomassie Brilliant Blue (fig. 20). Data indicated a prominent band of approximately 77.5 kDa from the induced cells. Crude soluble protein fraction was obtained after cell lysis using sonication, followed by centrifugation. We observed a strong band in the crude protein extract (soluble) corresponding to the expected protein size. Thereafter, the recombinant AbFas ligand fusion protein was purified from the crude protein extract that showed this single protein band in the gel analysis. The molecular mass of the recombinant AbFas ligand was around 77.5 kDa, as determined by SDS-PAGE, which is in agreement with our predicted molecular mass of 35 kDa, since the molecular mass of the MBP is 42.5 kDa.

2.3.2.6. Biochemical properties of the recombinant AbFas ligand

In preliminary tests, the biological activity of the recombinant AbFas ligand was measured by evaluating its ability to induce apoptosis, and generate intracellular reactive oxygen species (ROS) such as O^-_2 in hemocytes and human leukemia THP-1 cells using flow cytometry. We examined whether the AbFas ligand could induce apoptosis in THP-1 cells by analyzing the phosphatidylserine on the cell surface using annexin-V staining. However, AbFas ligand treatment did not induce the apoptosis pathway in THP-1 cells (data not shown). As shown in fig. 21, intracellular O^-_2 level were increased in concentration-dependant manner after 2 h in the abalone hemocytes and THP-1 cells treated with recombinant AbFas ligand ranging from 0.5-3.0μg/mL. Control cells (without recombinant AbFas ligand or only with MBP) showed the almost similar intracellular O^-_2 levels lower than that of recombinant AbFas ligand.

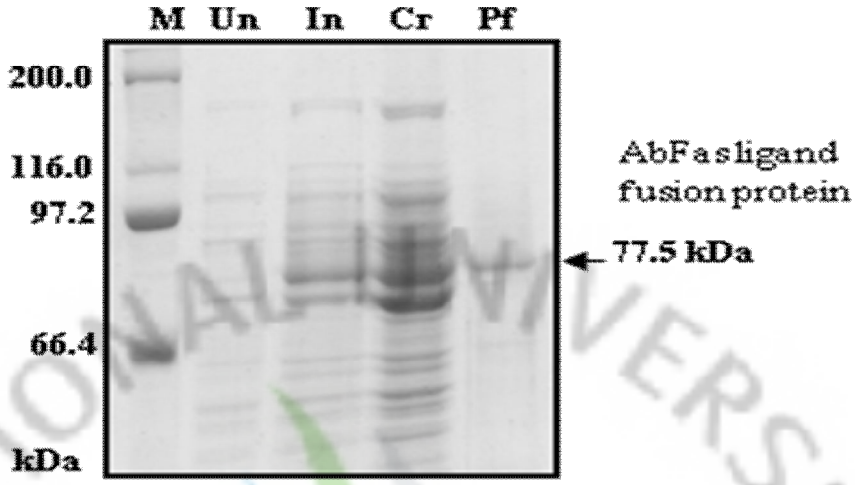

Fig. 20. Over expression and purification of recombinant AbFas ligand fusion protein. Protein samples are separated by 12% SDS-PAGE and stained with Coomassie brilliant blue. M: protein marker (TaKaRa, Japan). Un: total cellular extract from *E. coli* BL21(DE3) before induction; In: total cellular extract after induction with 1 mM IPTG at 12 ^{o}C for 16 hr; Cr: soluble crude extract after induction; Pf: purified recombinant AbFas ligand fusion protein.

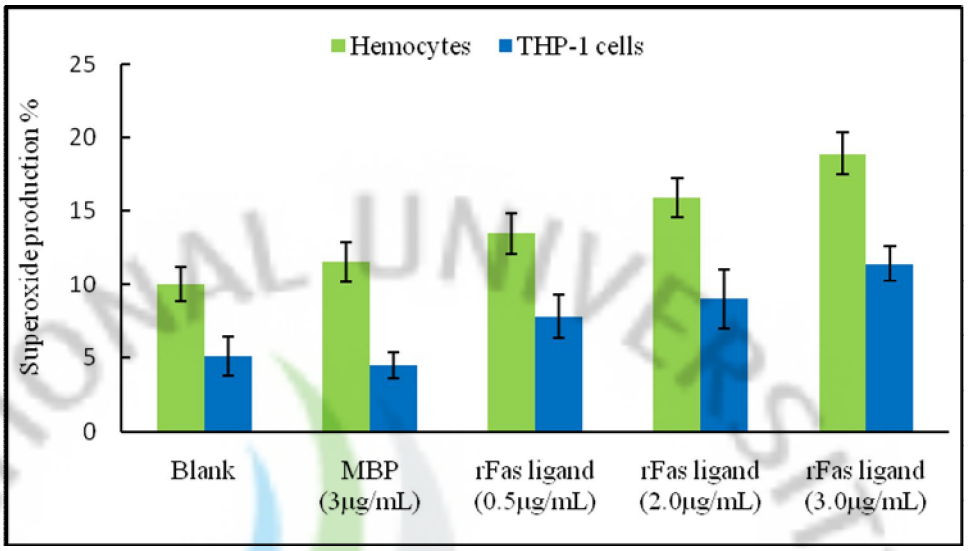

Fig. 21. Analysis of intracellular ROS generation (represented by O^{-}_{2}) by recombinant abalone Fas ligand. Abalone hemocytes or THP-1 cells were treated with different concentration of recombinant Fas-ligand for 2 h followed by addition of 2 μM HE for 30 min at 18°C (hemocytes) or 37°C (THP-1 cells). Cells were analyzed for flow cytometry considering 10000 events for each sample. The fluorescence intensity percentage (%) of cells stained by HE (FL2-H) are represented in X axis.

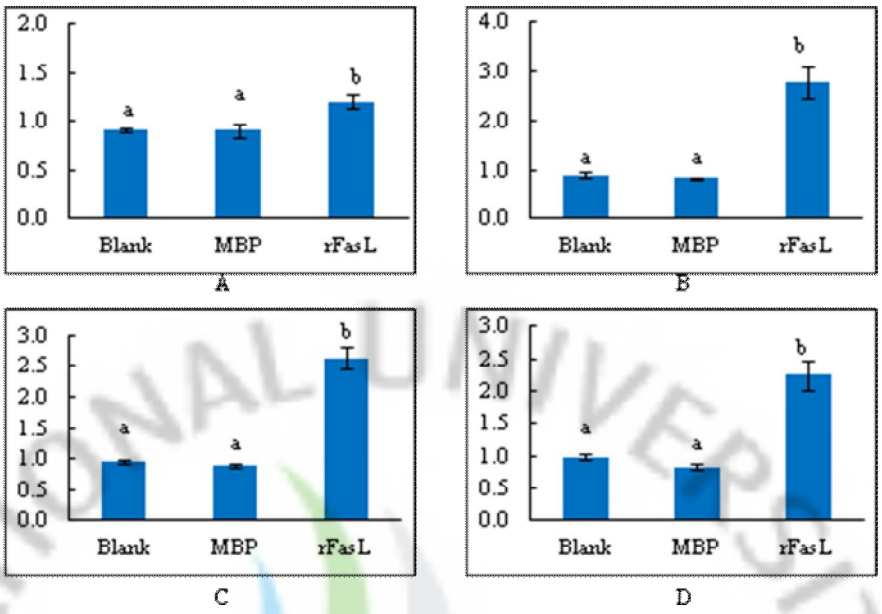

Fig. 22. Transcriptional analysis of different immune-relavant genes in abalone hemocytes after treatment of rFas ligand by qRT-PCR. Abalone hemocytes were treated with 2.5 μg/mL rFas ligand and incubated for 3 h at 18 °C. The relative expression fold was calculated by the $2^{-\Delta\Delta CT}$ method using abalone ribosomal protein as a reference gene. Relative expression fold of each gene was compared to that of blank (no protein) and MBP. A) NF-kB; B) caspase 8; C) catalase; D) SOCS-2. Data are presented as mean relative expression ± SD for three replicate real-time reactions from pooled tissue of three individual abalones at each time point. The bars represent the standard deviation (n=3).

2.3.2.7. Discussion

Several previous studies pointed out that fish TNF and cytokines showed lower identity to their mammalian counterparts (Goetz et al, 2004). For example, Japanese flounder Fas ligand (JF-Fas ligand) showed 26.1, 24.5 and 23.0% amino acid identity to human Fas ligand, TNF-α, and LT-α, respectively (Kurobe et al., 2007). Similarly, the Ab-Fas ligand described herein showed 22.0, 16.1 and 14.5% amino acid identity to human Fas ligand, TNF-α, and LT-α, respectively. Furthermore, the AbFas ligand shows lower identity to other mammalian and fish Fas ligand counterparts as well. Therefore, we compared the identity, similarity and gap percentages of AbFas ligand with Fas-ligand, TNF-α and LT-α from different species of organisms. The AbFas ligand shows the higher identity, similarity and lower gap percentages to other Fas ligands than the TNF-α and LT- α analyzed in this study. It has been described that Fas ligand is the only member of TNF superfamily containing a proline-rich domain (PRD) in the N-terminus. JF-Fas ligand contains a PRD with a 25% (9/36) proline ratio (Kurobe et al., 2007). In contrast, the AbFas ligand contains a lower proline ratio (5/54, 9%) in its N-terminus. The lower proline ratio is due to a longer cytoplasmic region of AbFas ligand than JF-Fas ligand. Moreover, our analysis results showed that zebrafish also has lower proline ratio (9/63, 14%) than the JF-Fas ligand. Sequence characterization of the AbFas ligand indicated that it has a predicted transmembrane region but no signal peptide similar to mammalian and fish Fas ligands. A potential single N-glycosylation site is seen in the AbFas ligand, which is commonly present in the extracellular portion of the transmembrane proteins as reported previously (Spiro et al., 2002). Phylogenetic analysis indicates that the AbFas ligand belongs to the invertebrate TNF family, and it differs greatly from vertebrate TNF-α and LT-α, but shows a closer similarity to vertebrate Fas ligand counterparts. These data herein have provided significant information regarding the phylogenetic linkage between vertebrate and invertebrate Fas ligands. Based on the above characteristic features, it could be suggested that abalone Fas ligand is a homologue of Fas ligand belonging to the TNF superfamily. Furthermore, we would like to emphasize that analysis of phylogenetic relationship of this study was restricted by limited number of Fas ligand sequences available from lower order species.

Constitutive expression of different TNF superfamily transcripts such as Fas ligand, TNF-α and LT-α have been detected in a variety of tissues and cells including liver, head kidney, spleen, thymus, intestine, gills, skin, muscle, leukocytes and macrophages from various healthy fish (Kono et al., 2006). Although, the Fas/FasL system was originally

described in the context of lymphocyte-mediated apoptosis, new data have shown that Fas and Fas ligand transcripts are widely expressed and function in many tissues outside the immune system (Song et al., 2000). Japanese flounder Fas ligand transcripts have been detected in the thymus, kidney, spleen, gills and stomach from healthy fish. Similarly, AbFas ligand transcripts are expressed in diversified tissues such as hemocyte, gills, mantle, muscle, digestive and digestive glands. Gills tissue showed the highest constitutive AbFas ligand expression among all selected tissues. It was observed that the AbFas ligand expression pattern was similar to that of disk abalone TNF-α in our previous study (De Zoysa et al., 2009). It is difficult at this time to understand the precise reason for the similar tissue distribution profile of AbTNF-α and AbFas ligand. However, we can suggest that in abalone, TNF family members may have common tissue expression patterns since their tissue-function specificity is less compared to vertebrates. Higher constitutive expression in gills may be associated with the abalone filter-feeding feature and frequent exposure to contaminants and pathogens, which are coming through the environment water and feeding materials.

Identification of expression responses of these cytokines will be useful for better understanding of host immune defense mechanisms against various pathogens. However, the expression of Fas ligand induced by immune stimulants has not been investigated even in fish, though some other TNF genes have been induced by different immune stimulants (Laing et al., 2001). It was pointed out that apoptosis induced by bacteria may play an important role in pathogenesis (Shao et al., 2004). Furthermore, LPS is a structural component of the Gram negative bacterial outer membrane that has shown different effects on the host immune system. Moreover, LPS is widely used as a potent immune stimulant for inducing different TNF superfamily genes (Xiang et al., 2008). Hence, we conducted further expression studies on the responses of AbFas ligand to different immune stimulants including bacteria, virus infection and LPS induction.

It was reported that Fas ligand is involved in inflammation and anti-bacterial innate immune responses by the direct killing of target cells after release from NCC or by the recruitment of phagocytic cells (Kaur et al., 2004). Apoptosis is also induced by cytotoxic cells during the removal of virus-infected cells or tumor cells. In contrast, Fas ligand can activate non-apoptotic signaling pathways as well (Wajant et al., 2003). Our results show that AbFas ligand mRNA level is induced by bacteria (*V. alginolyticus*, *V. parahemolyticus* and *L. monocytogenes*), VHSV and LPS stimulation in abalone gills. However, AbFas ligand expression was lower at 6 h p.i than at 3 h in all three immune stimulation experiments. The

reason for this is not clear at the moment. In general, AbFas ligand mRNA was induced in abalone gills by a mixture of pathogenic bacteria, VHSV and LPS showing a specific expression profile to each immune stimulation or challenge done in this study. The most important outcome of this immune stimulation is the inducibility of AbFas ligand transcripts. Thus, AbFas ligand may be involved in the inflammatory or immune defense responses against pathogens and immune stimulants.

We successfully purified the soluble AbFas ligand fusion protein using an *E. coli* expression system. It is well known that the O^-_2 anion has been involved in respiratory burst activity, important in immune defense by killing invading pathogens. Uenobe and his group reported that crude extract of ayu fish recombinant TNF induced the O^-_2 in ayu kidney cells (Uenobe et al., 2007). Therefore, we investigated the effect of the recombinant AbFas ligand on intracellular ROS induction. Interestingly, recombinant AbFas ligand showed its biological activity by inducing O^-_2 in hemocytes and human THP-1 cells in a concentration-dependant manner. These results could be correlated with the up-regulation of AbFas ligand transcripts by immune stimulation using bacteria, VHSV and LPS. In this role, up-regulation of the AbFas ligand transcripts may allow for continued synthesis of its protein and thereby induce the excessive O^-_2, which may have the effect of preventing, controlling or killing invading pathogens. However, the exact molecular mechanism involved in these activities requires further investigation. In contrast, purified AbFas ligand was not able to induce apoptosis in human THP-1 cells. It has been reported that the TNF superfamily ligands use different pathways to activate caspases in fruit flies versus mammals (Eimon et al., 2004). Therefore, no apoptotic signal in the THP-1 cells may be due to evolved differences between vertebrate and invertebrate apoptosis signaling pathways. This study does suggest that it may be worthwhile assessing further functional activity of the AbFas ligand using different assay systems.

In conclusion, sequence characterization and phylogenetic analysis of the cloned gene shows more similarity to known Fas ligands, and thus indicate that the abalone protein is indeed a Fas ligand. The data in summary, transcriptional up-regulation against bacteria, virus and LPS with biological activity of its recombinant protein (inducing O^-_2) would suggest that the AbFas ligand plays an important role in the abalone when responding to a microbial challenge.

CHAPTER 3

Immune regulatory transcription factors from disk abalone: Lipopolysaccharide-induced TNF-α factor (LITAF) and Rel family nuclear factor kappa B (Rel/NF-kB)

ABSTRACT

The lipopolysaccharide-induced TNF-α factor (LITAF) and Rel family nuclear factor kappa B (Rel/NF-kB) are two important transcription factors which play major role in the regulating inflammatory cytokines, apoptosis and immune related genes. Here, we repot the discovery of disk abalone LITAF (AbLITAF) and Rel/NF-kB (AbRel/NF-kB) homologues and their immune responses. Full-length cDNA of AbLITAF consists of 441 bp open reading frame (ORF) that translates into putative peptide of 147 aa. Analysis of AbLITAF sequence shows that it shares characteristic LITAF (Zn^{+2}) binding domain with two CXXC motifs (^{82}CPHC^{85} and ^{134}CPNC^{137}). Phylogenetic analysis results further confirms that AbLITAF is a member of LITAF family proteins. AbRel/NF-kB consists of 1752 bp length ORF that encodes 584 aa protein. It shares numerous signature motifs such as Rel homology domain (RHD), Rel protein signature (^{107}FRYECR^{112}), DNA binding motif (^{103}RGLRFFRYEC^{101}), nuclear localization signal (NLS) and transcription factor immunoglobulin –like fold (TIG) similar to their invertebrate and vertebrate counterparts.

Tissue specific analysis results showed that both AbLITAF and AbRel/NF-kB mRNA is expressed ubiquitously in all selected tissues in constitutive manner. However, constitutive expression of AbLITAF is higher than AbRel/NF-kB in all tissues except mantle. Upon immune challenged by bacteria (*V. alginolyticus, V. parahemolyticus and L. monocytogenes*) and VHSV, AbLITAF showed the significant up-regulation in gills while AbRel/NF-kB transcription was not change significantly. Based on transcriptional response against immune challenge we could suggest that regulation of TNF-α expression may occurred mainly by LITAF activation rather than NF-kB in disk abalone. The cumulative data from other molluscs and present results with reference to TNF-α, LITAF, Rel/NF-kB from disk abalone provide strong evidence that LITAF and NF-kB are independent pathways likely to occur throughout the Phylum mollusca.

3.1. Introduction

Cytokines are soluble, secreted molecules which act as components of cell to cell signaling network. The effect of cytokines on target cells may be enhanced or inhibited by other cytokines (Germano et al., 2008). TNF-α, IL-1 and IL-6 are classical pro-inflammatory cytokines (stimuli) which could control the expression of large number of inflammatory mediators together with chemokines (Sebban et al., 2006). When the inflammatory reaction occurs at high intensity, the level of cytokines is increased while they are released into the cellular environment and initiate the status called "acute phase response". On the other hand, large numbers of studies have proved extensively that TNF superfamily members (ligands and receptors) and other inflammatory cytokines are associated with cell proliferation, apoptosis, mediating immune systems in vertebrates (Pasparakis et al., 1996). In mammals, TNF-α is one of the most pleiotropic cytokines and mediator of large number of genes including cytokines, transcription factors, adhesion molecules and structural proteins (Goetz et al., 2004). It was reported that TNF-α expression is mainly regulated by the transcription factor NF-kB which is presents as an inactive cytoplasmic form bound to the inhibitor of NF-kB (IkB) under normal conditions (Karin et al., 2000). Upon TNF-α signaling, Ik-B leads to undergo its degradation by phosphorylation for releasing and immediate translocation of NF-kB into nucleus and binds the NF-kB binding site (^{5}GGGRNNYYCC^{3}) available in the promoter region of responsive gene (Hayden et al., 2004). On the other hand, over production of TNF-α can be lethal to host and thereby it has been postulated that TNF-α gene expression must be tightly regulated (Myokai et al., 1996). Moreover, Rel/NF-kB family members that regulate the expression of a large number of target genes involved with physiological processes such as immune response, programmed cell death (apoptosis), inflammation, and progression of the cell cycle in different organisms (Li and Verma, 2002).

Myokai et al., 1996 propose a new mechanism by introducing a novel LPS-induced transcription factor (named as LITAF) which regulates the human TNF-α transcription. Later, Tang et al., 2005 described the role for LITAF and signal transducer and activator of transcription (STAT-6B) as a co-factor in the regulation of inflammatory cytokines with response to LPS stimulation in mammalian cells. Upon LPS induction, the human LITAF was translocated into nucleus through formation of a complex with STAT6B which binds to the DNA sequence CTCCC present in the human TNF-α promoter and regulate its expression (Tang et al., 2005). However, Takashiba et al., 1995 emphasized that the nature of the nuclear factors involved in human TNF-α gene regulation is still unknown.

In contrast to vertebrates, relatively little is known about mollusc TNF superfamily members, and their transcription factors such as LITAF and NF-kB. The first mollusc LITAF and Rel/NF-kB were cloned from scallop *Chlamys farreri* (Yu et al., 2007) and Pacific oyster *Crassostrea gigas* (Montagnani et al., 2004), respectively. Recently, Pacific oyster (Park et al., 2008), Pearl oyster, *Pinctada fucata* (Zhang et al., 2009) LITAF homologues and abalone *H.*

diversicolor supertexta Rel/NF-Kb (Jiang et al., 2007) cDNAs were cloned and shown further evidence for existing different signaling pathways of TNF-α regulation. More importantly, the first molluscan homologue of TNF-α was cloned and characterized from disk abalone *H. discus discus* (named as AbTNF-α) in our previous study (De Zoysa et al., 2009). Moreover, Zhang et al., (2009) have identified the IkB homologue from pearl oyster. IkB is important member of NF-kB pathways which prevents the nuclear translocation of NF-kB by forming inactive form in the cytoplasm under normal conditions. Currently, no information available related to regulatory pathway of TNF-α expression, relationship between LITAF and Rel/NF-kB expression at transcriptional level in disk abalone. Therefore, it is very important to determine the role of LITAF and Rel/NF-kB as two transcription factors which involved in signaling pathway of TNF-α expression as well as regulation of other inflammatory, apoptosis and immune-related gene expression.

Herein, we report the identification and characterization of disk abalone *H. discus discus* LITAF (AbLITAF) and Rel/NF-kB (AbRel/NF-kB) homologues that share characteristic features of respective transcription factors in vertebrates and invertebrate counterparts. Also, transcriptional responses of LITAF and Rel/NF-kB were analyzed after abalone challenged with pathogenic bacteria and virus to understand inflammatory-apoptosis and immune related responses. Finally, we introduce molecular evidence for existing of LITAF and Rel/NF-kB as evolutionally conserved two different transcription factors which may function in signaling pathways for regulating inflammatory, apoptosis and immune-related gene expression in abalone.

3.2. Materials and methods

3.2.1. Identification and sequence characterization of the AbLITAF and AbRel/NF-kB

Partial sequence of abalone AbLITAF and AbRel/NF-kB were identified by BLAST analysis of abalone ESTs from cDNA library. Initially, two partial sequences showed the homology to known LITAF and Rel/NF-kB sequences. Full length cDNA sequence of AbLITAF was obtained by two consecutive internal sequencing reactions using two forward primers (LITAF-F1; LITAF-F2). Complete coding sequence of AbRel/NF-kB was obtained by single internal sequencing of identified EST clone (by primer Rel/NF-kB- F1) followed by further PCR cloning step (for 3′) using primers designed based on the partial sequence (Rel/NF-kB-F2) of *H. discus discus* and *H. diversicolor supertexta* Rel/NF-kB sequence (Rel/NF-kB-R1) (Table 1). We used cDNA synthesized from disk abalone gills to clone 3′ of coding sequence. Briefly, PCR was performed under the following conditions: initial denaturation at 94 °C for 3 min, followed by 25 cycles of amplification (94 °C for 30 s; 55 °C for 30 s; 72 °C for 90 s) and one cycle at 72 °C for 5 min. PCR product was run on 1.5% agarose gel. The expected band was gel-purified using AccuPrep® Gel purification Kit (Bioneer Corporation, Korea), and then subcloned into pGEM T easy cloning vector (Pomega). The cloned product was transformed into *Escherichia coli* DH5α competent cells and sequenced (Macrogen, Korea) in both direction of (M13 forward and reverse primers) pGEM T easy cloning vector.

3.2.2. Sequence characterization and phylogenetic analysis

Bioinformatics tools and methods used for sequence characterization and phylogenetic analysis were described in section 1.2.12.

3.2.3. Immune challenge and Transcriptional analysis of AbLITAF and AbRel/NF-kB

Abalone used for this study was described in section 1.2.2. To determine the immune responses of AbLITAF and AbRel/NF-kB, bacteria mixture and VHSV were used and experimental conditions have been described under the sections of 1.2.3, 1.2.4, 1.2.5, 1.2.6, 1.2.9, 1.2.10 and 1.2.11. Transcriptional analysis of AbLITAF and AbRel/NF-kB were analyzed by qRT-PCR using AbLITAF-F3 and AbLITAF-R1 gene specific primers (Table 1). Tissue-specific mRNA expression was analyzed in abalone hemocytes, gills, mantle, muscle, digestive tract and hepatopancrese. The AbLITAF and AbRel/NF-kB transcriptional responses were determined in gills and hemocytes in time frame analysis.

3.3. Results and discussion

3.3.1. Identification and characterization of the AbLITAF cDNA sequence

The Disk abalone full-length AbLITAF (GenBank accession no: GQ903762) consists of 1872 bp (fig.23). The ORF was composed of 441 bp that translate into a putative peptide of 147 amino acid residues. Sequence analysis indicated a 43 bp length 5' untranslated region (5' UTR) and 1388 bp 3' UTR, which contains two RNA instability motifs (^{890}ATTTA^{894} and ^{1470}ATTTA^{1474}) with a typical polyadenylation signal (^{1609}AATAAA^{1614}). The AbLITAF polypeptide has shown a putative molecular mass of 16 kDa with 8.6 isoelectric point (p*I*). Additionally, a characteristic LITAF domain (60-146 aa) and two CXXC motifs (^{82}CPHC^{85} and ^{134}CPNC^{137}) were identified with in the amino acid sequence. Moreover, it was identified one C-terminal microbodies targeting signal (^{145}SRM^{147}). Also, signal peptide prediction results showed that there was no putative signal peptide in the AbLITAF.

The AbLITAF amino acid identity and similarity percentages were calculated using FASTA program. Results showed that AbLITAF has the highest identity (48%) and similarity (62%) to scallop LITAF. Furthermore, results yielded on the variation of AbLITAF identity from 25-48% compared to other LITAF homologues including human, mouse, zebrafish, Atlanitic salmon, Pacific and pearl oysters. ClustalW multiple alignment results revealed that C-terminal region of AbLITAF was more conserved among other LITAF counterpart sequences. Also, two CXXC motifs of AbLITAF were highly conserved among all the selected sequences in this study. Multiple alignment results showed that eight cysteine residues in AbLITAF were completely conserved with invertebrates (scallop, Pacific oyster, pearl oyster) and vertebrates (Atlantic salmon, rainbow trout, mouse and human) LITAF sequences. We were interested to determine the phylogenetic relationship of the AbLITAF with known LITAF sequences by neighbor-joining method using human and zebrafish cell death induced protein sequences as an out-group (fig. 24). We can clearly distinguish two clusters of LITAF proteins from this tree. Cluster one includes vertebrate LITAF members while cluster 2 consists invertebrate molluscs LITAF proteins. Fish LITAF were positioned as a sub-cluster of vertebrate cluster. As expected, disk abalone LITAF was positioned with mollusc LITAF protein family.

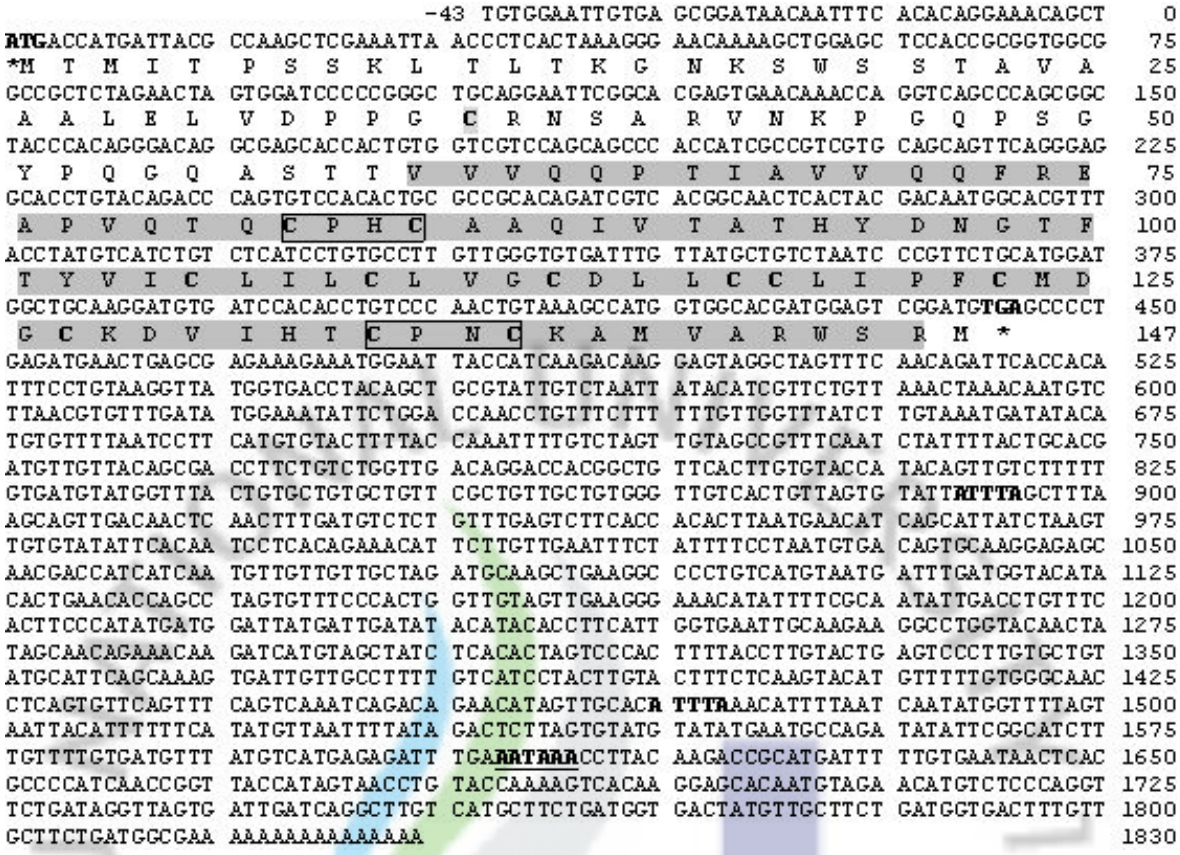

Fig. 23. The nucleotide and deduced amino acid sequences of disk abalone lipopolysaccharide induced TNF-α factor (LITAF). The start (ATG) and stop (TGA) codons are in boldfaces with asterisks (*). The predicted LITAF domain is shaded. The two CXXC motifs (^{82}CPHC^{85} and ^{134}CPNC^{137}) are in shaded boxes. Twelve cytenine residues are indicated in shaded bold face. Two mRNA instability motifs (ATTTA) in the 3′ UTR region are shown in bold. The polyadenylation signal is underlined and bold.

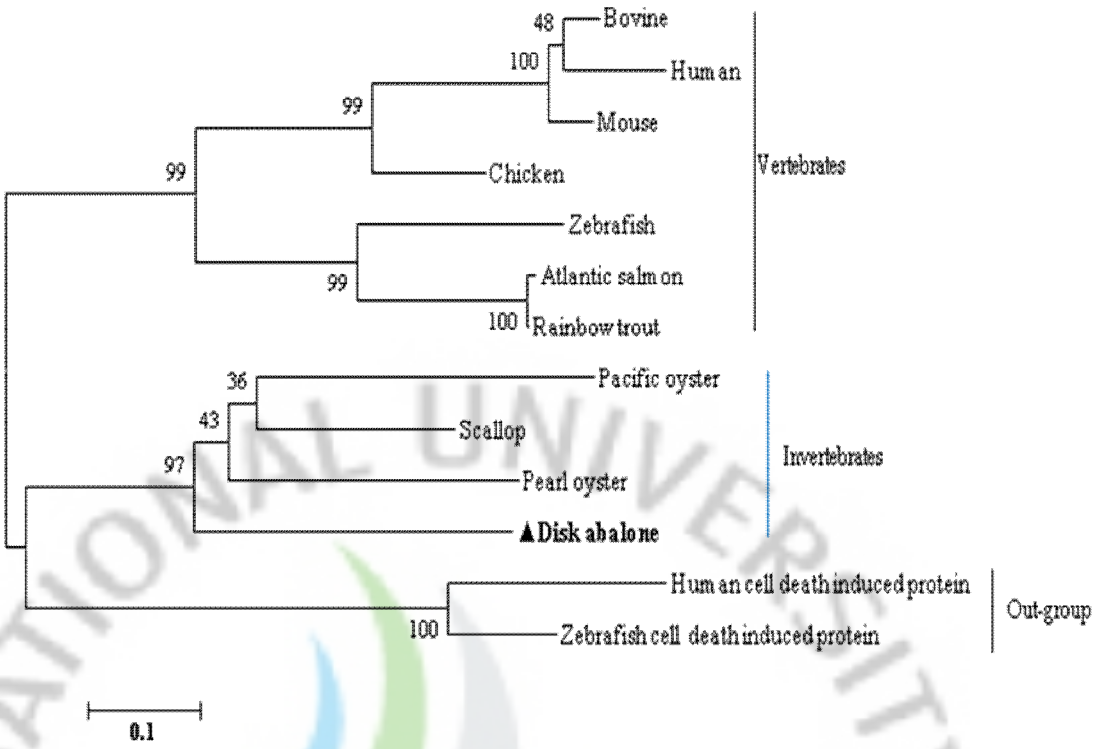

Fig. 24. Phylogenetic relationship of disk abalone LITAF. The number at each node indicates the percentage of bootstrapping after 1000 replications. The GenBank accession numbers of selected LITAF sequences are as follows: scallop (ABI79459), Pacific oyster (ABO70331), pearl oyster (ACN7008), disk abalone (GQ903762), Atlantic salmon (ACI67257), rainbow trout (ACO09164), zebrafish (NP_001002184), chicken (NP_989598), mouse (NP_064364), bovine (NP_001039717), human (NM_004862). Cell death induced proteins from human (NP_037531) and zebrafish (NP_001092712) were selected as out-group members.

3.3.2. Cloning and characterization of the AbRel/NF-kB cDNA sequence

The disk abalone Rel/NF-kB sequence (GenBank accession no: GQ903762**)** consists of 1752 bp length ORF that encodes a protein of 584 amino acids (Fig. 25). Amino acid sequence analysis revealed that AbRel/NF-kB processes the characteristic features of Rel/NF-kB family proteins. More specifically, the AbRel/NF-kB contains an N-terminal Rel homology domain (RHD) and transcription factor immunoglobulin-like folds (TIG residues from 267-366). Within the AbRel/NF-kB amino acid sequence, DNA binding motif (^{103}RGLRFRYEC^{101}), Rel protein signature (^{107}FRYECE^{112}) and the nuclear localization signal (^{404}KRKR^{407}) were identified as highly conserved characteristic motifs of Rel family proteins. No signal peptide was detected from AbRel/NF-kB sequence. The Rel/NF-kB family transcription factors are composed of a set of structurally related and evolutionary conserved DNA binding proteins (Baldwin et al., 1996). To distinguish the AbRel/NF-kB among other Rel family proteins, we analyzed the pair-wise identity using clustalW program. Results revealed AbRel/NF-kB to be 90%, 45% and 44% identical to mollusc abalone *H. diversicolor supertexta*, pearl oyster and Pacific oyster, respectively. Furthermore, it was shown that AbRel/NF-kB has 28-33% identity to RelA/p65, 27-30% to RelB, 26-28% to c-Rel, 17-24% to p53/p100, in vertebrates and 30-33% dorsal homologues of insects. Also, we aligned the characteristic regions of AbRel/NF-kB including Rel protein signature (RYXCE), DNA binding motif (RXXRXRXXC) and NLS with similar regions of representative Rel proteins (Fig. 26). It was shown that in the most conserved region of RHD in AbRel/NF-kB has higher identity ranged from 75-94% to Rel proteins of other molluscs, fruitfly, zebrafish, amphibian and human. Moreover, NLS of the AbRel/NF-kB has 100% and 89% amino acid identity to NLS of the *H. diversicolor supertexta* and human, respectively. In order to confirm the relationship between AbRel/NF-kB and other Rel proteins, we constructed a neighbor-joining phylogenetic tree using vertebrate and invertebrate Rel transcription factors (RelA/p65, RelB, c-Rel, p52, p50, dorsal) and sea urchin NF-kB as an out-group. Our results showed that all invertebrates Rel transcription factors grouped in one main cluster (Fig. 27). As expected disk abalone Rel/NF-kB clearly related with the abalone *H. diversicolor supertexta* (bootstrap of 100) in mollusc sub-cluster. Our results further illustrated that vertebrate RelA/p65, RelB, c-Rel, p50 and p52 were positioned in separate sub-clusters while insect dorsal proteins (homologue to vertebrate Rel) were in a separate sub-cluster.

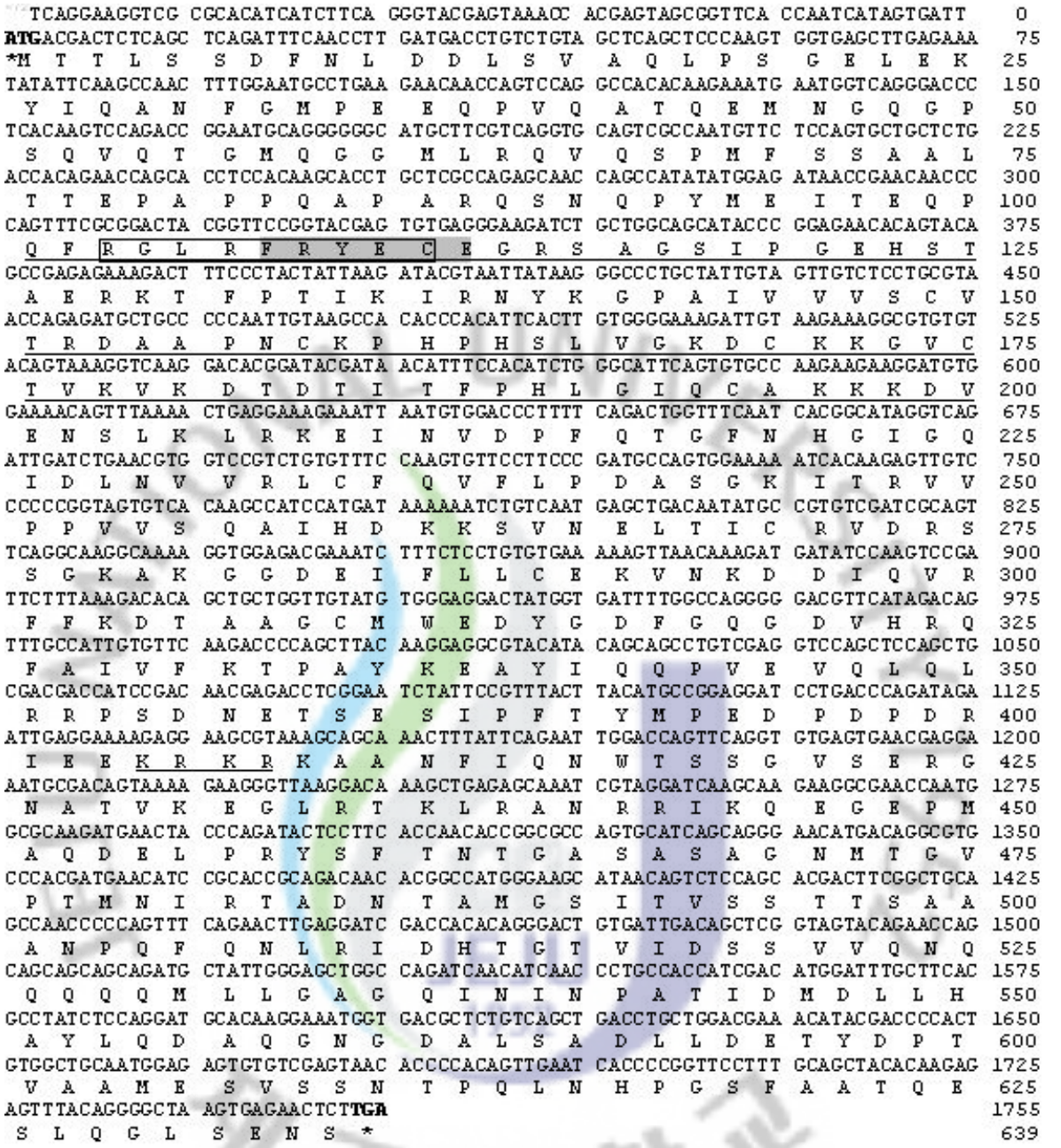

Fig.25. The nucleotide and deduced amino acid sequences of disk abalone Rel/NF-kB genes. The start (ATG) and stop (TGA) codons are in boldfaces with asterisks (*). The AbRel/NF-kB (GenBank accession no GQ903763) cDNA sequence. The predicted NF-kB/Rel/dorsal signature profile including the Rel homology domain (RHD) is underlined. Rel protein signature ^{107}FRYECE^{112} is shaded and DNA binding motif ^{103}RGLRFRYEC^{111} is shown in a box. The NLS (^{404}KRKR^{407}) is double underlined.

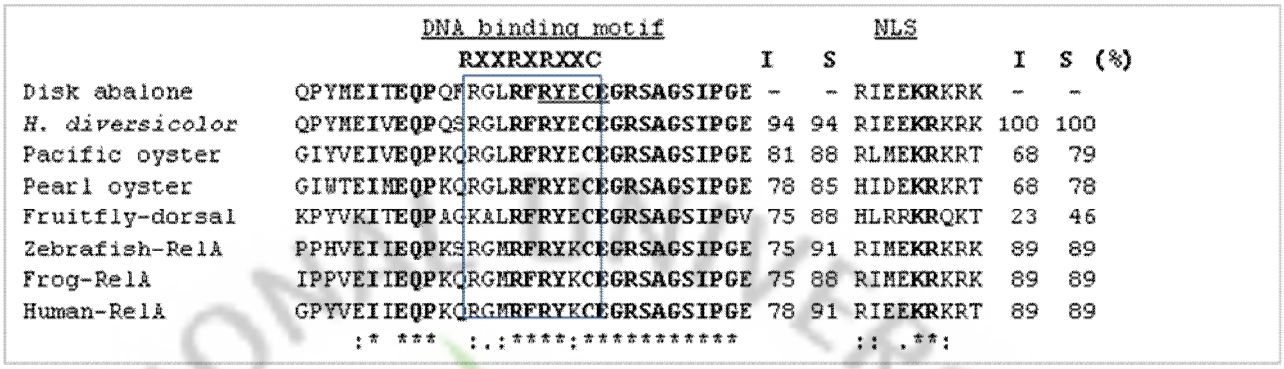

Fig. 26. Alignments of AbRel/NF-kB with characteristic motifs of other Rel proteins. The surrounding sequence range of RHD and NLS are used to align. The Rel protein signature (RYXCE) is underlined, consensus DNA binding motif (RXXRXRXXC) elements covered by a box. NLS is shown separately. Identical amino acids are indicated by bold with asterisks (*). Identity (I) and similarity (S) percentage of selected Rel domain and NLS are indicated at the right of each sequence. Alignment was performed with representative Rel proteins from Abalone *H. diversicolor* (AAW33559), Pacific oyster (AAK72690), pearl oyster (ABL63469), *Drosophila* dorsal (AAA28479), zebrafish (AY163839), frog (M60785), human (M62399) by clustalW.

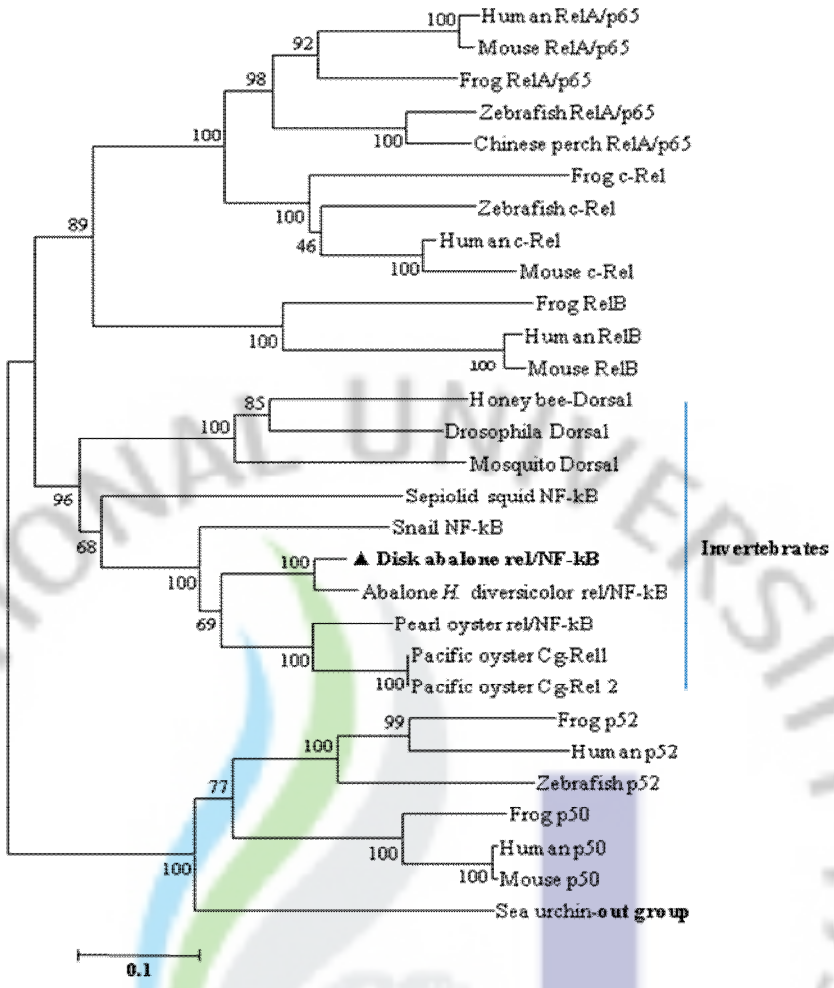

Fig. 27. Phylogenetic relationship of disk abalone Rel/NF-kB. The number at each node indicates the percentage of bootstrapping after 1000 replications. The GenBank accession numbers of selected Rel/NF-kB sequences are as follows: Human RelA/p65 (M62399), RelB (NM_006509), c-Rel (X75042), p50 (M55643), p52 (NM_002502), mouse RelA/p65 (M61909), RelB (M83380), c-Rel (X15842), p50 (NM_008689), Frog RelA/p65 (M60785), RelB (BAA09646), c-Rel (AF053060), p50 (AAH81252), p52 (ABO02629), zebrafish RelA/p65 (AY163839), c-Rel (AY163837), p52 (ABO26403), Chinease pearch RelA/p65 (ABW84004), Honey bee dorsal (NP_001011577), *Drosophila* dorsal (AAA28479), mosquito dorsal (CAA65156), sepiolid squid NF-kB (AAY27981), snail NF-kB (ACN73461), disk abalone Rel/NF-kB (GQ903763), *H. diversicolor supertexta* Rel/NF-kB (AAW33559), pearl oyster Rel/NF-kB (ABL63469), Pacific oyster Cg-Rel1 (AAK72690), Cg-Rel2 (AAK72691). Sea urchin NF-kB (O96458) was selected as an out-group.

3.3.3. Tissue distribution of disk abalone LITAF and Rel/NF-kB

To determine the tissue-specific mRNA expression of AbLITAF and AbRel/NF-kB, qRT-PCR was carried out using different abalone tissues. Relative expression fold of AbLITAF and AbRel/NF-kB in different tissues was further compared with hemocytes expression fold to display tissue specific variation (Fig. 28). Expression results revealed that both AbLITAF and AbRel/NF-kB transcripts were ubiquitously expressed in all analyzed tissues namely hemocytes, gills, mantle, muscle, digestive tract and hepatopancrese. Interestingly, AbLITAF (3.8-fold) and AbRel/NF-kB (2.1-fold) genes have shown the highest transcriptional expression in hepatopancrease compared to all the tissues analysis. AbLITAF and Rel/NF-kB expression was not significantly ($p<0.05$) different in hemocyte and gills. However, AbLITAF expressed at higher level in muscle, digestive and hepatopancrease than the hemocyte and gills. Furthermore, constitutive level of AbLITAF was higher than that of AbRel/NF-kB level in all analyzed tissues except in mantle. When compared the expression folds of AbLITAF and AbRel/NF-kB two transcription factors as tissue basis, significant difference were observed only in mantle, muscle, digestive and hepatopancrease tissues.

3.3.4. Transcriptional responses of LITAF and Rel/NF-kB after bacteria and VHSV challenge

Abalones were injected with three bacteria mixture (*L. monocytogenes, V. alginolyticus V.* and *parahemolyticus*) and VHSV. Expression profiles were determined in gills and hemocytes using qRT-PCR. Following the bacterial infection, AbLITAF mRNA was gradually up-regulated in gills and showed the highest induced state (3.2-fold) at 12 h and then decreased to 2.6-fold at 48 h p.i . Interestingly, AbLITAF was up-regulated significantly ($p<0.05$) in all the time points (during the 48 h) in gills (Fig. 29A). In contrast, no consistent changers in AbRel/NF-kB transcript levels were seen following bacterial infection (48 h). However, transcriptional level of AbRel/NF-kB was lower than level of PBS control. More similar to bacterial infection, AbLITAF expression was significantly ($p<0.05$) up-regulated after VHSV challenge. Furthermore, AbLITAF was significantly increased at early stage of infection while detected maximal (5.6-fold) at 24 h and decreased at 48 h below to basal level. In contrast to AbLITAF induction, VHSV injection could only induce the AbRel/NF-kB (1.4-fold) at 24 h while all other time points it was shown reduced level compared to PBS control Moreover, AbLITAF and AbRel/NF-kB levels were decreased below the basal level of respective controls at 48 h pi. Interestingly, AbLITAF has shown dominated role in transcription (except VHSV at 48 h) than AbRel/NF-kB upon bacteria and VHSV challenge.

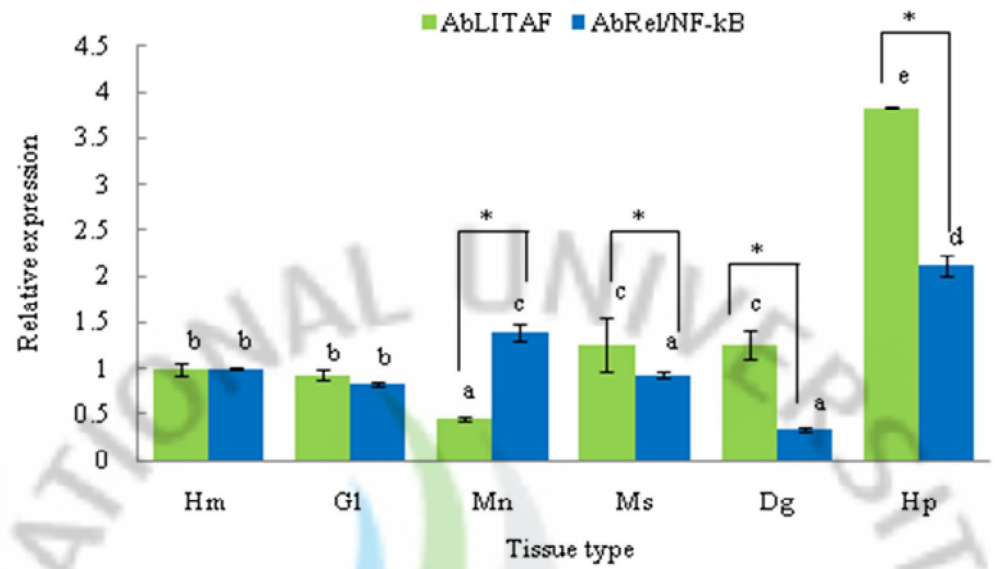

Fig. 28. Tissue expression profile of abalone LITAF and Rel/NF-kB. Analysis of mRNA was done by quantitative real-time PCR. The relative expression fold was calculated by the $2^{-\Delta\Delta CT}$ method using abalone ribosomal protein as a reference gene. Expression fold of each tissue was compared to that of hemocyte for determining the tissue specific expression. Each bar represents the mean of three replicates. Data are presented as mean relative expression ± SD for three replicate real-time reactions from pooled tissue of three individual abalones at each time point. Hm-hemocyte; Gl-gill; Mn-mantle; Ms-muscle; Dg-digestive tract; Hp-hepatopancreas. Asterisks (*) indicate significant difference of AbLITAF and AbRel/NF-kB mRNA expression in different tissues at $p<0.05$.

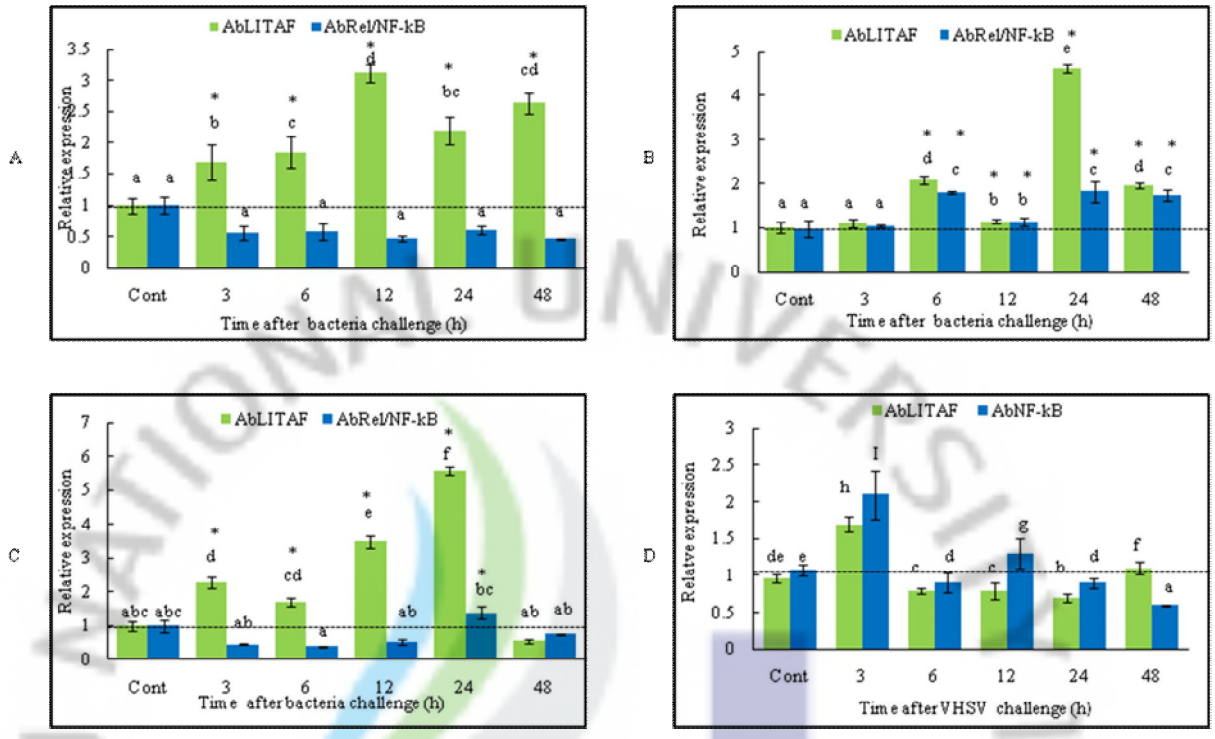

Fig.29. Transcriptional responses of AbLITAF and AbRel/NF-kB after bacteria and VHSV challenge by qRT-PCR. The expression fold was calculated by the $2^{-\Delta\Delta CT}$ method using abalone ribosomal protein as a reference gene. Relative fold of each time point was compared to that of PBS of each immune infection. A) bacteria challenged gills; B) bacteria challenged hemocytes; C) VHSV challenged gills; D) VHSV challenged hemocytes. Data are presented as mean relative expression ± standard deviation (SD) for three replicate real-time reactions from pooled tissue of three individual abalones at each time point. Statistical analysis was performed by one-way ANOVA followed by Duncan's Multiple Range test using SPSS 11.5 program. Asterisks (*) indicate significant increase mRNA expression when compared to PBS control group at $p<0.05$.

3.3.5. Discussion

In this study, we introduce disk abalone LITAF and Rel/NF-kB as two important transcription factors which has reported their vital role in inflammation, apoptosis and immune responses in many organisms. The isolated disk abalone LITAF full-length cDNA sequence and encoding polypeptide that share the characteristic organization such as i) molecular mass (16.0 kDa); ii) LITAF (Zn^{+2}) binding domain; iii) two CXXC motifs; iv) presence of mRNA instability motifs in 3′ UTR; v) higher homology in C-terminal. Most of these characteristics which match with previously reported LITAF family proteins from human (Myokai et al., 2004), mouse (Bolcato-Bellemin et al., 2004), chicken (Hong et al., 2006), scallop (Yu et al., 2007), Pacific oyster (Park et al., 2008) and pearl oyster (Zhang et al., 2009). Pairwise analysis results revealed that AbLITAF has the highest identity 48% to scallop LITAF while it shows 25-48% identity range among invertebrate and vertebrate LITAF proteins. Similar result has been reported from Pacific oyster which showed the highest identity 56% to scallop and its overall identity range remain in between 35-56% among other LITAF proteins (Park et al., 2008). Also, recently identified LITAF from pearl oyster has 33-50% identity range to the other known LITAF sequences (Zhang et al., 2009). Multiple alignment shows the highly conserved eight cysteine residues present in AbLITAF and other LITAF counterparts of scallop, oyster, Atlantic salmon, rainbow trout mouse, and human. Also, the phylogenetic relationship obtained from this study further strengthened that cloned abalone sequence is a homologue of LITAF family proteins.

On the other hand, the family of NF-kB transcription factors is one of the widely studied transcriptions factors in biology due to its broad spectrum of role in immunity, inflammation, apoptosis, development and differentiation (Hoffmann et al, 2006). NF-kB pathway is evolutionary conserved from *Drosophila* to human (Wang et al., 2006) although components of this pathway has been recently identified in mollusc species (Montagnani et al., 2004; Jiang et al., 2007; Zhang et al., 2009). Interestingly, NF-kB pathway is not functional in the *Caenorhabditis elegans* immune system (Wang et al., 2006). Therefore, understand the evolutional origin of NF-kB pathway could allow comparison of the immune systems in vertebrates and invertebrates. Primary sequence analysis results showed that cloned Rel/NF-kB from disk abalone shares the main characteristic features of Rel proteins including i) Rel domain with Rel protein signature and DNA binding motif; ii) NLS; iii) TIG signature. We compared the AbRel/NF-kB with various Rel family members including Rel/NF-kB, RelA/p65, RelB, c-Rel, p52/p100, dorsal (insects). Based on the AbRel/NF-kB

identity range, it has 44-90% identity with mollusc Rel/NF-kB followed by 28-33% to RelA/p65. It also showed comparatively higher identity range (30-33%) with insect dorsal Rel proteins as well. In Pacific oyster Cg-Rel has shown 17-31% overall sequence identity with known Rel proteins while the identity in the most conserved regions ranged from 35-55% (Montagnani et al., 2004). Disk abalone Rel/NF-kB has shown 17-90% identity range among all analyzed Rel proteins in this study while it has over 75% and 50% identity with mollusc RHD (32 bp partial conserved region) and NLS, respectively. However, it is difficult to make clear classification of AbRel/NF-kB only with the identity comparison. Hence, we conducted phylogenetic relationship using various Rel proteins. Phylogenetic tree constructed in this study gives us a clear clade division between vertebrate and invertebrate Rel/NF-kB. More specifically, disk abalone Rel/NF-kB is clustered with the other molluscs showing clear evidence that Rel family proteins are evolutionally conserved from mollusc to human. There are two structural classes (I and II) of NF-kB proteins. Both classes of proteins contain N-terminal DNA binding domain while only class I NF-kB proteins contain a several ankyrin repeats for transrepression activity (Gilmore et al., 2006). C-terminal of AbRel/NF-kB does not contain ankyrin-repeat domain suggested that it could be grouped in to a class II similar to some of the Rel family members such as p100 and p105 (Beinke et al., 2004). Altogether, these results showed that AbRel/NF-kB is a member of class II Rel/NF-kB transcription factor family which shares more homology with mollusc Rel proteins.

In order to better understand the biological role of LITAF and Rel/NF-kB, we analyzed the transcriptional expression in various abalone tissues. In vertebrates, LITAF mRNA is constitutively expressed in several tissues such as in human spleen, blood leukocytes (Myokai et al., 1999); in mice liver, heart, kidney, spleen, lung (Bolcato-Bellemin et al., 2004); in chicken spleen, intestinal intraepithelial lymphocytes (Hong et al., 2006). In contrast to vertebrates, constrictive expression of LITAF mRNA is detected in hemocyte, gills, mantle, muscle, digestive gland, digestive tract and gonad tissues from scallop (Yu et al., 2007), Pacific oyster (Park et al., 2008) and pearl oyster (Zhang et al., 2009). Disk abalone LITAF also expressed widely in all selected tissues and showed more or less similar pattern with other reported mollusc expression profiles.

AbRel/NF-kB also ubiquitously expressed in all examined tissues (hemocytes, gills, mantle, muscle, digestive tract and hepatopancrease) in disk abalone which is consistent with the tissue expression of Cg-Rel observed in Pacific oyster and abalone *Haliotis diversicolor supertexta* (Jiang et al., 2007). Also, NF-kB was constitutively expressed in hemocytes of

horseshoe crab *Carcinoscorpius rotundicauda* (Wang et al., 2006). One of the important results obtained in this study is higher constitutive expression of AbLITAF than AbRel/NF-kb in several organs suggested that AbLITAF may play key role as an active transcription factor in innate immune defense in abalone. Although, exact reason for higher constitutive expression of AbRel/NF-kB is not clear at the moment and further studies are required to clarify the issue.

For last few years, we are conducting research on identifying immune related genes and their inter-related functions in disk abalone. Recently, we discovered first molluscan TNF-α homologue from abalone and this discovery led us to hypothesis that existing of cell signaling molecules related to regulation of TNF-α pathway. TNF-α is one of the most pleiotropic inflammatory cytokines in mammals which responses against bacteria, virus and parasite infections (Hong et al, 2006). We also showed disk abalone TNF-α is induced upon bacteria (*V. alginolyticus and V. parahemolyticus* and *L. monocytogenes*), virus (VHSV) and LPS injection (De Zoysa et al., 2009). Thus, transcriptional responses of AbLITAF and AbNF-kB were studied upon the similar bacterial and virus challenged experiment for understanding the mechanism behind the transcriptional activation of TNF-α. Hoffmann and Baltimore (2006) have proposed that LPS like stimuli activate the NF-kB as well as other signaling pathways that may coordinately regulate the activity of other transcription factors to specific gene expression and cellular responses. Hong et al., 2006 reported that induction of chicken LITAF mRNA in macrophage cells by bacteria endotoxin (*Escherichia coli* or *Salmonella typhimurium*) as well as different species of *Eimeria* (parasite) infection. In addition to bacterial induction, present results have shown that non bacterial component such as VHSV is also capable of inducing abalone LITAF expression. Our results are more consistences with up-regulation of LITAF transcripts in scallop hemocytes against LPS (Yu et al., 2007), Pacific oyster hemocytes against bacterial infection (Park et al., 2008) and pearl oyster gills, digestive tract after LPS stimulation (Zhang et al., 2009). Taking together we could assume that upon infection or immune stimulation of pathogenic bacteria such as *V. alginolyticus and V. parahemolyticus and L. monocytogenes* and VHSV could activate the transcription factor LITAF and related pathway (yet unknown) to connect the regulation of TNF-α expression in disk abalone.

No significant expression change of Rel/NF-kB was detected in disk abalone gills against bacterial infection although slight elevated expression observed only at 24 h VHSV pi. In other molluscs also Rel/NF-kB activation has not shown at transcription level against

different immune challenge or induction. Transcription level of NF-kB was not induced in Pacific oyster (Cg-rel) hemocytes after challenged with pathogenic bacteria mixture (Montagnani et al., 2004) and in hemocytes of abalone *H. d. supertexta* against LPS stimulation from 0-9 h. However, DNA binding capacity of NF-kB has increased in *H. d. supertexta* hemocytes by LPS induction (Park et al., 2008). It was reported that activation of NF-kB signaling pathway in *Drosophila* may vary depending on type of bacteria such as Gram (G)-positive or negative (Wang et al., 2006). Hence, present study used the bacteria mixture including G positive and negative strains may have possibility to have affected on activation of abalone Ral/NF-kB. (Tang et al., 2005) investigated whether LITAF production depends on NF-kB activity in mice macrophages and concluded that LITAF and NF-kB have separate induction pathways and that are not affected by each other. Further, NF-kB expression has not changed significantly in response to over expression of LITAF in macrophages in mice and confirmed that LITAF signaling pathway is separate from NF-kB and involve in the regulation of various inflammatory cytokine. Based on overall results on transcriptional response against bacteria and virus challenge we could suggest that regulation of TNF-α expression may occurred mainly by LITAF activation rather than NF-kB in disk abalone. The transcripts described in the present study can be used to propose two putative pathways for regulating TNF-α in disk abalone. Taken together, the data with reference to TNF-α, LITAF and NF-kB for disk abalone and other previous data from several molluscs provide strong evidence that LITAF and NF-kB pathway is likely to occur throughout the Phylum mollusca.

CHAPTER 4

Antimicrobial peptides (AMPs) from disk abalone: Defensin and “Abhisin” a histone H2A derived AMP

ABSTRACT

Gene-encoded AMPs such as defensin and histone H2A derived peptides are important components of the host innate immune response against microorbial invasion. Abalone defensin was isolated from normalized cDNA library (ESTs) constructed from whole tissues of disk abalone. Abalone defensin (pro-defensin) consists of 198-bp coding sequence of putative 66 amino acids which includes the 48 amino acids mature peptide. The present of invertebrate defensin family domain, arrangement of six cysteine residues and their disulfide linage in C_1-C_4, C_2-C_5, and C_3-C_6, α-helix in three dimensional structure and phylogenetic relationship suggest that abalone defensin could be a new member of invertebrate defensin family more-related to arthropod defensins. In non-stimulated abalone, defensin transcripts were constitutively expressed in all examined tissues including hemocytes, gills, mantle, muscle, digestive tract and hepatopancreas. Also, abalone defensin transcripts were significantly induced in hemocytes, gills and digestive tract upon bacterial challenge of *V. alginolyticus, V. parahemolyticus* and *L. monocytogenes.*

In the second section of this study, a histone H2A full length cDNA was cloned from disk abalone. We identified a 40-amino acid AMP designated as "Abhisin" from the N-terminus of the abalone histone H2A sequence. Abhisin shows the characteristic features of AMPs including net positive charge (+13), higher hydrophobic residues (27%) and 2.82 Kcal/mol protein binding potential. Our results showed the growth inhibition of *L. monocytogenes*, *Vibrio ichthyoenteri* bacteria, and fungi (yeast) *Pityrosporum ovale*by synthetic abhisin at 250 µg/mL. However, stronger activity was displayed against the G+ than G- bacteria. Additionally, scanning electron microscope (SEM) observation results confirmed that *P. ovale* cells were damaged by abhisin treatment. Interestingly, abhisin treatment (50 µg/mL) decreased the viability of THP-1 leukemia cancer cells approximately by 25% but there was no effect on the normal vero cells, suggesting that abhisin has cytotoxicity against cancer cells than normal cells. qRT-PCR results revealed that histone H2A transcription was significantly induced at 3 h post challenge of bacteria in gills and digestive tract. Our overall results suggest that defensin and precursor histone H2A or its N-terminal peptide (abhisin) are potent AMPs in disk abalone that could involve in immune defense reactions to increase protection against infections.

4.1. Introduction

AMPs in invertebrates are described as key molecules in their innate immune defense mechanisms. Most AMPs are membrane-active, hydrophobic and positively charged (cationic) molecules of less than 10 kDa in molecular mass. The net positive charges of AMPs promote their binding to the membranes of microbes, which generally have an overall negative charge (Bulet et al., 2004). Recent studies have demonstrated the importance of AMPs based on their high biochemical diversity, broad specificity against microorganisms (Cho et al., 2009), anticancer activities (Lee et al., 2008), wound healing effects (Murphy et al., 1993), regulation of cell proliferation, extra cellular matrix production, anti-endotoxin activities and cellular immune responses by inducing gene expression (Mookherjee et al., 2007).

Defensins are a group of small AMPs, which provide the first line of host defense against invading pathogens (Selsted et al., 2005). They are present in plants, invertebrates and vertebrates which have shown antimicrobial activities against bacteria, fungi and certain viruses (Bullet et al., 2004). In general, defensin family consists of three sub-families namely α, β and θ based on the connectivity of disulfide bonds between six cysteine residues (Klotman et al., 2006). Although, vertebrate and invertebrate defensins have a similar antibacterial mode of action, they share lower structural or sequence homology. Froy and Gurevitz (2003) have described that arthropod and mollusk defensins exhibit common characteristics on sequence, structure and bioactivity and they are genetically related. However, it was shown that organization of defensin gene is extremely variable due to exon-shuffling and integrated downstream of unrelated leader sequence during evolution. Moreover, defensins are the most diversified family of AMPs in invertebrates, and over 70 different defensins have been isolated in arthropods and mollusks (Bullet et al., 2004). Despite this, no sequence or immune responses of abalone *H. discus discus* defensin have been described upto date.

On the other hand, several reports have shown that histone protein or histone-derived peptides process antimicrobial activity in vertebrates including human (Hirsch et al., 1958; Kim et al., 2002), amphibian (Kim et al., 1996; Park et al., 1996) and fish (Fernandes et al., 2002; Birkemo et al., 2003). The first histone antimicrobial activity was demonstrated from calf thymus in 1958 (Hirsch et al., 1958). Buforin I was the first histone H2A-derived AMP from the Asian toad (Park et al., 1996). However, very few histone-derived AMPs have been identified from invertebrates such as pacific white shrimp (Patat et al., 2004) and scallop

Chlamys farreri (Li et al., 2007).

Abalone-like invertebrates require strong innate immune defense systems mainly because they do not have well-established adaptive immune components. For that reason, having a wide range of AMPs could be highly beneficial in invertebrates for immune defense against pathogens. Therefore, the study of different AMPs and their growth inhibition capacity of specific pathogens could diversify our understanding of mollusk immune systems.

Thus, knowledge of the AMPs like defensin and histone H2A-derived AMPs could be a great interest to understand the host defense mechanisms of abalone and the phylogenetic relation of these molecules during the evolution. This chapter includes the molecular characterization, immune responses and functional activites of abalone defensin and histone H2A-derived AMP named as “abhisin”.

4.2. Materials and methods

4.2.1. Identification of abalone defensin

The complete coding sequence of abalone defensin was identified from the disk abalone normalized cDNA library (EST data base). Basic procedure of normalized cDNA library construction, and EST analysis were described in our previous report (De Zoysa et al., 2008).

4.2.2. Experimental abalone and bacteria challenge

Abalone used for this study was described in section 1.2.2. To determine the immune responses of abalone defensin, bacteria mixture (*V. alginolyticus, V. parahemolyticus* and *L. monocytogenes*) was used and experimental conditions have been described under the sections of 1.2.3, 1.2.4 and 1.2.9.

4.2.3. Transcriptional analysis of abalone defensin by quantitative real time RT-PCR

Transcriptional analysis of abalone defensin was analyzed by qRT-PCR using gene specific primers (defensin-1F and defensin-1R). For that total RNA was extracted from hemocytes gills and digestive tract of three abalones using Tri Reagent™ (Sigma, USA) according to the manufacturer's protocol. Sample of 2.5 μg RNA was used to synthesize cDNA from each tissue using a Cloned AMV first-strand cDNA synthesis kit (Invitrogen, USA) as described in section 1.2.11. qRT-PCR was carried using a Chromo4^{TM} real-time PCR detector (TaKaRa Japan) as described in section 1.2.12.

4.2.4. Cloning of histone H2A and synthesis of the synthetic abhisin peptide

Partial sequence of abalone histone H2A was identified during the screening of the abalone cDNA library (EST) database. Full-length sequence of abalone histone H2A was determined by an internal sequencing reaction using primer (Histone H2A-F1) by terminator reaction kit, Big Dye, and ABI 3700 sequencer (Macrogen, Korea). A 40-amino acid length abhisin peptide (^{1}MSGRGKGGKTKAKAKSRSSRAGLQFPVGRIHRLLRKGNYA^{40}) was synthesized by solid-phase peptide synthesis method (AnyGen Co., Korea). After synthesis, the peptide was purified by reverse phase HPLC by performing a Shimadzu 20A, 6A gradient system (Shimadzu Japan). Data were collected by using an SPD-20A detector at 230 nm. Homogeneity was assessed by matrix assisted laser desorption ionization mass spectrometry (MALDI MS). Purity of the peptide was determined as 88.4%. Purified synthetic peptide was dissolved in DEPC-treated, nuclease-free deionized water.

4.2.5. Antimicrobial assays

For antimicrobial assays and bacterial challenge experiment, several bacteria strains and one fungi (yeast) were obtained from the Korean Collection for Type Cultures including (G+) *L. monocytogenes* (KCTC3710), (G-) *V. alginolyticus* (KCTC2472), *V. parahemolyticus* (KCTC2729), *V.* (KCCM40870), and yeast *P. ovale* (KCCM 11894). Antimicrobial activity of synthetic abhisin towards selected bacteria and yeast was monitored by a modified liquid growth inhibition assay described by Cai and Wu (1996) and an agar disc diffusion assay described by Meena and Sethi (1994). In the liquid growth inhibition assay, selected bacteria and yeast were grown in optimal media and culture conditions overnight. After overnight incubation, bacteria and yeast were serially diluted to 1-5x10^5 cells/mL. Then, 100 µL of bacteria or yeast cells were added to a 96-well microtiter plate with 250 µg/mL of synthetic abhisin or respective negative and positive controls. Ampicillin and DEPC-treated nuclease-free deionized water were used as positive and negative controls, respectively. Plates were then, incubated at 30 ^oC for 24 h. The inhibition of bacterial growth was determined by measuring the optical density (OD) at 600 nm using a microtiter plate reader (Tecan, Switzerland). In an agar disc diffusion assay, bacteria or yeast were inoculated on appropriate agar plates (100 mm, petri-dish) by spreading overnight culture using sterile cotton tipped swabs. Subsequently, sterilized filter paper discs (Whatman, 6 mm) were immediately placed on the inoculated plates. Then, different quantities of synthetic abhisin (0, 25, 50, 100 µg) or 100 µg of ampicillin were applied on the discs of separately grown bacteria and yeast plates. The same volume of DEPC treated, nuclease-free deionized water was applied as a negative control to a separate disc. The plates were incubated at 30 ^oC for 24 h. The diameter of inhibition zone (DIZ) was measured (including the paper disc diameter) and expressed in millimeters (mm).

4.2.6. Scanning electron microscope (SEM) observation

The yeast *P. ovale* cells were grown in brain heart infusion (BHI) broth at 30 ^oC for 14-16 h then cells were serially diluted to 1-5x10^5 cells/mL. The suspension was divided equally into two tubes. The synthetic abhisin (500 µg/mL) sample was added into one tube and incubated at 30 ^oC for 24 h. The other tube was used as a control. After the incubation, cells from both tubes were harvested by light centrifugation and prefixed with a 2.5% glutaraldehyde solution in 0.1 M Na-cacodylate buffer (pH 7.2) overnight at 4 ^oC. Next, samples were dehydrated rapidly with ethanol series (30%, 50%, 70%, 90% and 100%)

followed by substitution processes using the same concentration series of isoamyl acetate. The samples were dried with liquid CO_2 at a critical point followed by platinum coating by a sputter coater at 10 mA for 2 min. Finally, morphology differences of yeast cells after abhisin treatment were observed on field emission SEM (JEOL, Japan) and compared against the respective non-treated control.

4.2.7. Determination of cytotoxicity effect of synthetic abhisin peptide

The cytotoxicity of abhisin was evaluated using a normal monkey kidney fibroblast cell line (vero) and a human monocytic leukemia cancer cell line (THP-1). Briefly, vero and THP-1 cells were cultured in DMEM and RPMI 1640 media, respectively, both containing 10% heat inactivated FBS at 37 °C in a 5% CO_2 humidified incubator. Additionally, both media were supplemented with 100 U/mL penicillin and 100 µg/mL streptomycin. Then, 1 mL of vero or THP-1 cells (1.0 x 10^5 cells/mL) were seeded in 6 well plates separately and exposed to different concentrations (0, 10, 20, 30, 40, 50 µg/mL) of abhisin for 48 h at 37 °C in a 5% CO_2 incubator. Samples of cells were maintained without abhisin as controls. Then, cell viability was determined by a 3-(4,5-dimethyl-2-thiazolyl)-2.5-diphenyl-2H-tetrazolium bromide (MTT) assay. In brief, 50 µL (2 mg/mL) of MTT was added to 1 mL of 1x10^5/mL cell suspension and incubated for 4 h. Then, the cells were collected after centrifugation. The cell pellets were dissolved in dimethyl sulfoxide (DMSO) and 200 µL was transferred into 96 well plates. The absorbance was measured using a microplate reader at 595 nm OD. Cell viability percentage (%) was calculated for each concentration relative to control cells and data were the means of a minimum of three replicates.

4.2.8. Immune responses of histone H2A

To determine the immune responses of histone H2A, change of transcriptional level was analyzed upon abalones challenge with bacterial mixture including *L. monocytogenes, V. alginolyticus and V. parahemolyticus* using qRT-PCR. The gene-specific primers (Histone H2A-F2 and Histone H2A-R1) used for qRT-PCR is shown in table 2. RNA isolation, cDNA synthesis and qRT-PCR reaction conditions are similar to procedures described under the sections of 1.2.3, 1.2.4, 1.2.5, 1.2.9 and 1.2.10.

4.2.9. Sequence characterization and phylogenetic analysis

Bioinformatics tools and methods used for sequence characterization and phylogenetic analysis of abalone defensin and Histome H2A were described in section 1.2.12.

4.3. Results and discussion

4.3.1. Abalone defensin

4.3.1.1 Identification and characterization of disk abalone defensin cDNA

Analysis of abalone defensin (GenBank FJ864724**)** nucleotide and corresponding amino acid sequences results showed that identified gene consisted with basic characteristics of defensin family members (fig. 30). The complete coding sequence of abalone defensin consisted with 198-bp encoding a pro-peptide of 66 amino acids. It showed 60-bp 5' untranslated region (5'UTR) and 56-bp long 3' UTR with slightly modified polyadnylation signal (ATTAAA). The putative signal peptide (^{1}MKFLLLCLVIAFVGMSDA^{18}) was identified at the N-terminal sequence with the cleavage site at 18 amino acid position. PROSITE program illustrated that abalone defensin consisted a characteristic invertebrate defensin family domain (24-66 aa).

The defenisn mature peptide (49 amino acids) was analyzed using antimicrobial peptide predictor program. The results showed that abalone defensin has characteristic features of AMPs including net positive charge (+5), higher hydrophobic residues (46%) and molecular mass of 4.9 kDa. The amino acid sequence of abalone defensin was aligned with mollusks and arthropods defensins available at Genbank. Figure 31 shows the CLUSTALW multiple alignments of mollusk and arthropod defensins. Mainly the cysteine residues were shown as identical residues among all the sequences. Results showed that disk abalone defensin was well conserved with abalone *H. discus hannai* defensin precursor but not at higher level with other mollusk and arthropod counterparts. Moreover, six cysteine residues present in abalone defensin were well conserved with arthropod defensin sequences. In contrast, only five cysteine residues from abalone defensin were conserved among other mollusk defensins. The abalone defensin amino acid sequence displays the highest amino acid identity (88.4%) to abalone *Haliotis discus hannai* defensin precursor (ABV60391). However, disk abalone defensin showed greater identities to insect defensins (30%-40%) than mollusk defensins (20-25%).

We compared the predicted 3D structure of abalone defenisn with available structures of defensins using Swiss-PdbViewer program (fig. 32). The 3D structure of abalone was more similar to that of mosquito *Anopheles gambiae* defensin (PDBe Entry:2e3eA) with 42.8% sequence identity. In that abalone defensin molecule was consisted with α-helical part (AHCLVK) and three cross-linked disulfide bonds at $^{27}C_1$-C_4^{58}, $^{44}C_2$-C_5^{63}, and $^{48}C_3$-C_6^{65}.

In the phylogenetic tree, selected defensin sequences were divided into two major groups as invertebrate and vertebrate defensins (fig. 33). Invertebrate defensins were further

sub-grouped into two clusters. One cluster was mainly consisted with various insect defensins together with two abalone defensins (*H. discus discus and H. discus hanni*) while all other mollusk defensins formed the second cluster of invertebrate group. Our phylogenetic results revealed that disk abalone defensin was strongly (98 bootstrap values) related to abalone *H. discus hanni* defensin precursor and both were closely related to insect/arthropod defensin counterparts than other reported mollusk defensins. Meanwhile, vertebrate group was consisted with fish and mammalian defensins used in this study.

Fig. 30. The complete nucleotide and deduced amino acid sequences of the disk abalone defensin cDNA. The start (ATG) are stop (TAA) codons are underlined. The predicted signal peptide is bold underlined. The predicted invertebrate defensin family domain is shaded. Cysteine residues are boxed and bold shaded.

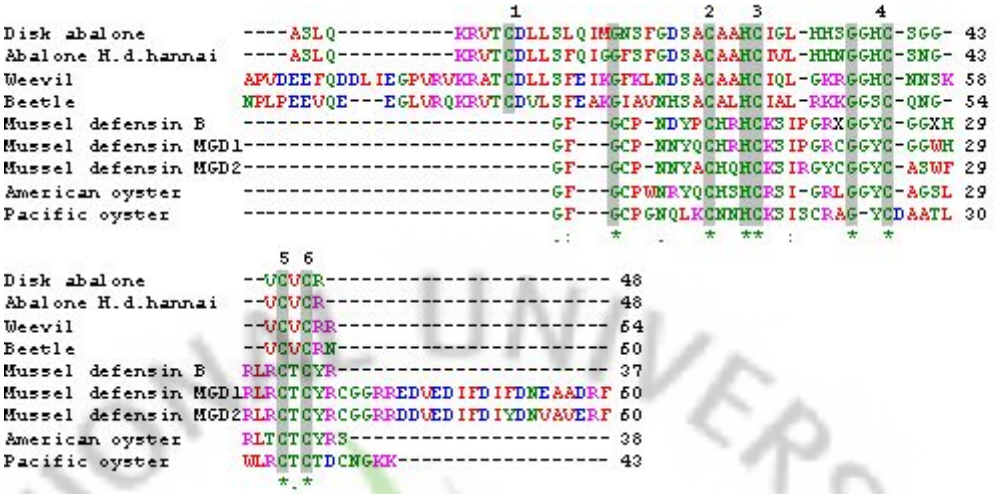

Fig. 31. Multiple sequence alignment of the disk abalone defensin mature peptide with the selected mollusk and insect defensin family members. Identical amino acid residues are shaded and indicated by asterisks (*). Six cysteine residues in the abalone defensin are numbered as 1-6 and completely conserved cysteine residues are bold shaded. The dashes indicate the gaps introduced to maximize the alignment.

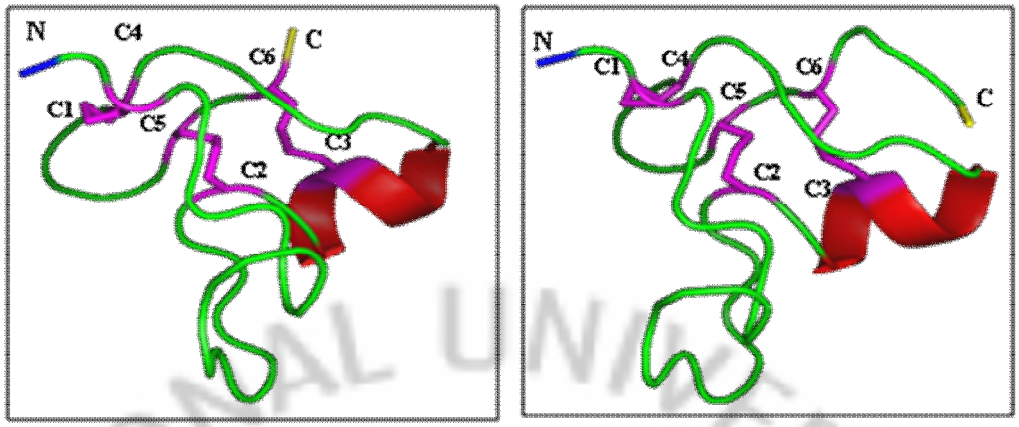

Fig. 32. The predicted three-dimensional structure of disk abalone defensin with selected arthropod defensin from mosquito *Anopheles gambiae*. Predicted cysteine bridges (in pink) are numbered. The amphipathic α-helix structure is in red. The N- and C-terminals are indicated in blue and yellow colors, respectively.

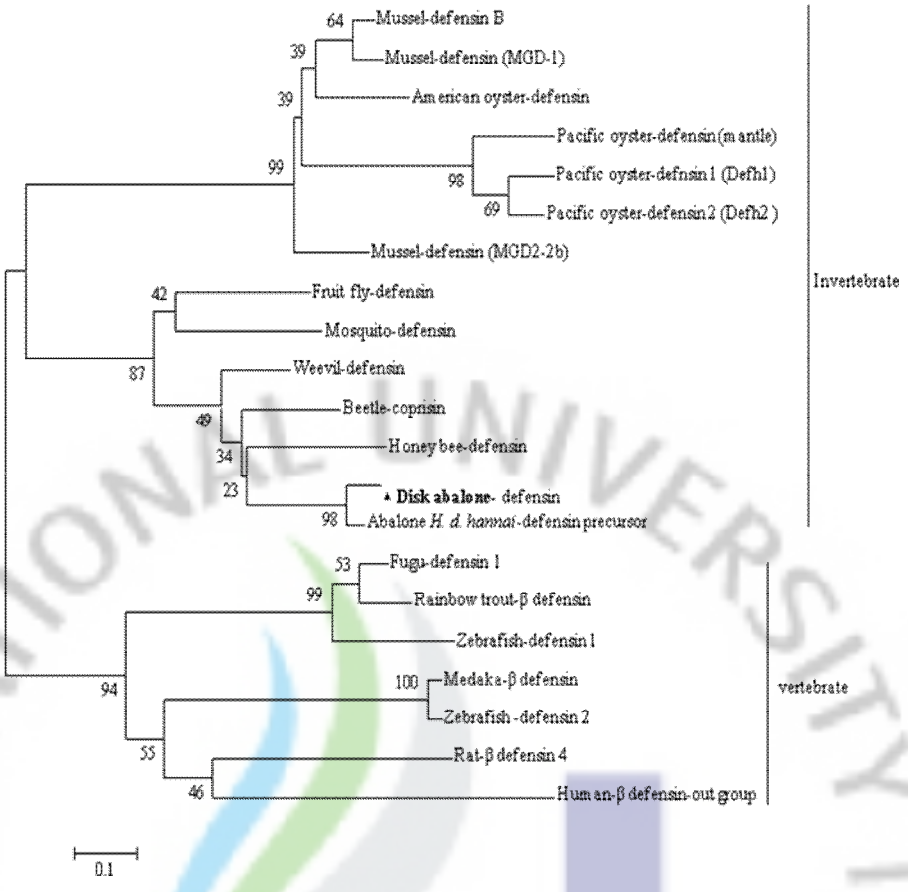

Fig. 33. Phylogenetic relationship of abalone defensin with different defensin family members. Phylogenetic analysis was done by the neighbor-joining algorithm within the MEGA program version 3.1 based on ClustalW (1.81) alignment using pro-defensin amino acid sequences. Numbers at tree nodes indicate the bootstrap confidence values from 1000 replicates. Human β-defensin (NP_005209) was used as out-group. The accession numbers are disk abalone *Haliotis discus discus* defensin (FJ864724); mussel *Mytilus edulis* defensin B (P81611); MGD-1 (P80571); Mediterranean mussel *Mytilus galloprovincialis* MGD-2b (AAD52660); American oyster *Crassostrea virginica* defensin (P85008); Pacific oyster *Crassostrea gigas* defensin mantle (AJ565499); Defh1 (DQ400101); Defh2 (DQ400102); fruit fly *Drosophila melanogaster* defensin (NP_523672); mosquito *Anopheles gambiae* defensin (Q17027); weevil *Sitophilus zeamais* defensin (ABZ80665); beetle *Copris tripartitus* coprisin (ABP97087); honey bee *Apis cerana defensin* (ACH96385); abalone *H. discus hannai* defensin precursor (ABF69125); Fugu *Takifugu rubripes* defensin 1 (Zoe at al., 2007); rainbow trout *Oncorhynchus mykiss* defensin (ABR68250); Zebrafish *Danio rerio* defensin 1 (AM181358); defensin 2 (NP_001075033); Japanese medaka *Oryzias latipes* β-defensin (EU676010) and rat *Rattus norvegicus* β-defensin 4 (NP_071989).

4.3.1.2. Tissue expression profile and transcriptional responses of abalone defensin after bacteria challenge by qRT-PCR

To examine whether defensin mRNA was constitutively expressed as in other mollusks, qRT-PCR was used to analyze 108 bp fragment of abalone defensin. The transcripts of abalone defensin were detected in all the tissues examined including hemocytes, gills, mantle, muscle, digestive tract and hepatopancrease (fig. 34A). The highest constitutive expression (8.5-fold) of abalone defensin was detected in mantle compared to that of hemocytes. Defensin mRNA expression was significantly ($p<0.05$) higher in mantle and hepatopancrease than other analyzed tissues. After healthy abalones were experimentally challenged with bacteria, (*V. alginolyticus, V. parahemolyticus* and *L. monocytogenes*) transcriptional response of defensin was determined in hemocytes, gills and digestive tract by quantitative real time RT-PCR (fig. 34 B,C,D). Transcriptional level of defensin was up-regulated significantly ($p<0.05$) in hemocytes during 48 h p.i. (except at 12 h) of bacteria mixture. The highest defensin induction-fold (3.8) was detected in hemocyte at 24 h p. i. compared to PBS control at 3 h. In hemocytes, defensin transcriptional up-regulation was higher at 24 and 48 h p.i than early stage. Neither the gill nor the digestive tract was induced defensin transcripts significantly at early stage (before 24 h) of p.i. In gills defensin transcripts were significantly induced (1.4-fold) only at 24 h while digestive tract showed the late phase response with highest expression fold (2.3-fold) at 48 h p.i. of bacteria. Even though, the transcriptional response was different in hemocytes, gills and digestive tract, present results have shown that abalone defensin expression could be induced by bacteria infection.

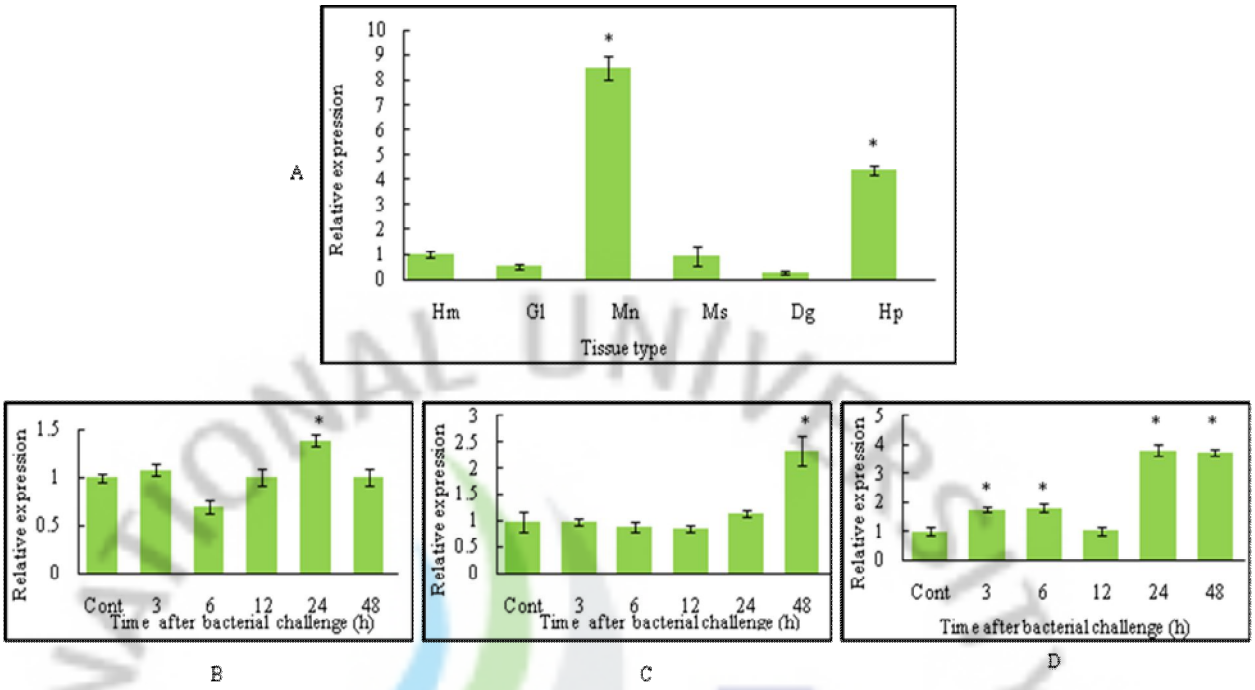

Fig. 34. Tissue expression profile and transcriptional responses of abalone defensin after bacteria challenge by qRT-PCR. The relative defensin expression fold was calculated by the $2^{-\Delta\Delta CT}$ method using abalone ribosomal protein as a reference gene. Relative expression fold of each tissue was compared to that of hemocyte to determine the tissue specific expression. A) tissue expression analysis; B) gills; C) digestive tract; D) hemocytes; Data are presented as mean relative expression ± standard deviation (SD) for three replicate real-time reactions from pooled tissue of three individual abalones at each time point. The bars represent the standard deviation (n=3). Gl-gill; Mn-mantle; Ms-muscle; Dg-digestive tract; Hp-hepatopancreas; Hm-hemocyte; cont-control (PBS).

4.3.1.4. Discussion

In the present study, we report the identification and molecular characterization of a defensin cDNA from disk abalone. The defensin family peptides share several characteristic features of small cationic AMPs, including molecular mass below 10 kDa, net positive (+) charge, high hydrophobic ratio, amphipathic structure (α helix, β sheet or α helix/ β sheet structure) and three to four disulfide bonds that all collectively to be important for their antibacterial action (Froy et al., 2003; Bulet et al., 2004). In agreement with the general features of AMPs, the abalone defensin amino acid sequence displays a typical distribution of positive charge (+5), hydrophobic residue ratio (46%), lower molecular mass (4.9 kDa) and α helical structure. It was described (Froy et al., 2003) that, invertebrate defensins consist of six cysteine residues in a pattern of C-X_{5-16}-C-X_3-C-X_{9-10}-C-X_{4-7}-C-X_1 (Xio et a;., 2004) and which are formed disulfide linkages of C_1-C_4, C_2-C_5 and C_3-C_6.We found that six cysteine residues presented in abalone defensin are arranged in the pattern of C-X_{16}-C-X_3-C-X_9-C-X_4-C-X_1 which is in agreement with the consensus invertebrate defensin. Additionally, abalone defensins shares the classical disulfide linkage structure (C_1-C_4, C_2-C_5, C_3-C_6) similar to invertebrate defensins. However, the number of cysteine residue presented in abalone defensin is in contrast to that of mussel defensins (MGD1 and MGD2), oyster defensin (CgDef) due to two additional cysteine residues present in those peptide sequences. Froy and Gurevits (2003) showed that high degree of identity among mature defensins from mollusk and arthropods. Multiple and pairwise sequence analysis results from present study also reveals that abalone defensin shares higher homology to arthropod defensin family than that of mollusks. The presence of invertebrate defensin family domain, sequence similarity, phylogenetic relationship and other common features suggest that abalone defensin could be a new member of invertebrate defensin family and closely related to arthropod defensins.

Several reports described that AMPs are expressed either constitutively or induced upon pathogenic challenge (Iwanaga et al., 1998; Imler et al., 2000). In lower order vertebrate zebrafish, several β-defensin homologues were constitutively expressed in gills, gonad, gut, kidney, muscle, skin and spleen (Zou et al., 2007). In Pacific oyster, the expression of *Cg-defh1* is considerably low while *Cg-defh2* is constitutively expressed in gills and mantle than the hemocytes (Gonzales ey al., 2004). The highest expression of Pacific oyster *Cg-Def* has been shown in mantle at a higher mRNA level (20-60-fold). In our results also mantle appears as the prominent tissue for expressing defensin in non-stimulated abalones. Additionally, abalone defensins expression is detected in various tissues such as hemocyte, gills, muscle,

digestive tract and hepatopancreas and it is more similar to *Cg-Def* expression in gills, hemocytes, muscle. The expression results of abalone defensin and *Cg-Def* are in contrast with those reported in mussel (*M. galloprovencialis*) defensin, which is only produced in hemocytes (Mitta et al., 1999). Selsted and Ouellet (Selsted et al., 2005) have been discussed that in early life forms, defensins and other AMP provided simple but efficient mechanisms for host resistance to microbial infection and during the gene diversification organism retained specific genes, which their products have additional advantages to the host. In general, expression of the genes encoding AMPs is induced by bacterial challenge (Hoffmann et al., 1996). Up-regulation of defensin transcripts were detected in scallop *Argopecten irradians* hemolymph (Zhao et al., 2007), *C. gigas* (*Cg-defh2*) in gills and mantle (Gonzales et al., 2007), *M. galloprovincialis* gills and mantle (Hubert et al., 1996), *C. verginica* gills (Seo et al., 2004) by bacterial challenge. For an example, expression of the scallop defensin transcripts in hemolymph has been gradually increased during 4-32 h post challenge of *Vibrio anguilarum*. Eventhough the induced level (fold) and the time points are not perfectly matched; these results are consistent with the transcriptional induction of abalone defenisn in hemocytes, gill and digestive tract. This could be due to variation of infected bacterial dose, physiological status of animal, culturing conditions during the bacterial challenge and level of constitutive expression before the bacterial challenge. There are few observations on either decrease or no change of transcriptional responses of mollusk defensins against bacterial infection. For an example, *C. gigas Cg-defh2* (hemocyte) was significantly decreased after bacterial challenge (Gonzales et al., 2007), while *C. gigas* mantle *Cg-Def* transcript level was unaffected by bacteria challenge (Gueguen et al., 2006). Similar to those at some extent abalone defensin transcription level has been decreased in hemocytes at 12 h p.i. This may be due to mobilization effect of hemocytes towards the bacterial colonization or infected site. Present study results indicate that transcription of abalone defensin is un-changed at early stages in gills and digestive tract after bacterial infection. This preliminary result would suggest that transcriptional change of abalone defensin in gills and digestive tract is not highly responded to bacterial mixture used in this study. Hence, more detailed study of abalone defensin gene expression with response to various microbial challenges is required to understand the tissue specific differences of transcriptional regulation. The constitutive and ubiquitous expression of abalone defensin in hemocytes as well as other tissues with transcriptional up-regulation against bacterial infection would suggest that it has an important immune function in host defense against pathogens.

4.3.2. Results-abalone abhisin

4.3.2.1. Identification and characterization of full-length histone H2A from disk abalone

Initially partial histone H2A cDNA sequence was isolated from a disk abalone normalized cDNA library. Abalone histone H2A (GenBank **EF103384)** full-length sequence consists of 898-bp (fig. 35). The open reading frame was composed of 408-bp that translate into a putative peptide of 136 amino acid residues. There was a 72-bp 5' untranslated region (5'UTR) and 418-bp long 3' UTR, which contains two RNA instability motifs (^{644}ATTTA^{648} and ^{651}ATTTA^{655}). Also, a characteristic histone H2A signature domain (^{21}AGLQFPV^{27}) was predicted by the motif scan program. Pair wise amino acid alignment results showed that abalone histone H2A has the highest identity (88.2%) to brine shrimp (*Artemia franciscana*) histone H2A (ABV60391).

4.3.2.2 Identification and characterization of abhisin peptide sequence from histone H2A

Based on the previous reports on antimicrobial activities of histone and histone-derived peptides (Bulet et al., 2004; Lee et al., 2008; Kim et al., 1996; Fernandes et al., 2002), we were interested to analyze the abalone histone H2A sequence using an antimicrobial peptide predictor program (Wang et al., 2004). Peptide analysis results showed that N-terminal domain of abalone histone H2A has significant similarity with histone-derived AMPs such as buforin I and hipposin. Therefore, 40 amino acids from the N-terminus of histone H2A was selected as a potential histone-derived AMP and named as abhisin. Comparison of abhisin with other histone-derived AMPs is shown in Table 11. The predicted abhisin showed characteristic features of AMPs including remarkably higher overall positive charge (+13), hydrophobic residues (27%) and 2.82 Kcal/mol protein binding potential. Additionally, abhisin has exceptionally higher percentage (6/40=15%) of both arginine and lysine residues. Interestingly, there was no negatively charged aspartate or glutamate residue within the abhisin peptide. The predicted molecular mass of abhisin was 4.32 kDa. Abhisin showed the highest amino acid identity (92%) to scallop histone H2A-derived AMP. Furthermore, it showed 80% and 67% identity to buforin I and hipposin, respectively. ClustalW multiple alignment results showed that 32 residues from abhisin were completely matched with scallop AMP, buforin II and hipposin, which all are H2A-derived peptides (fig. 36). Schiffer-Edmundson helical wheel modeling was employed to predict secondary structure of abhisin (fig. 37). These results demonstrated that abhisin is a linear α-helical molecule, having hydrophobic and hydrophilic residues on opposing sides.

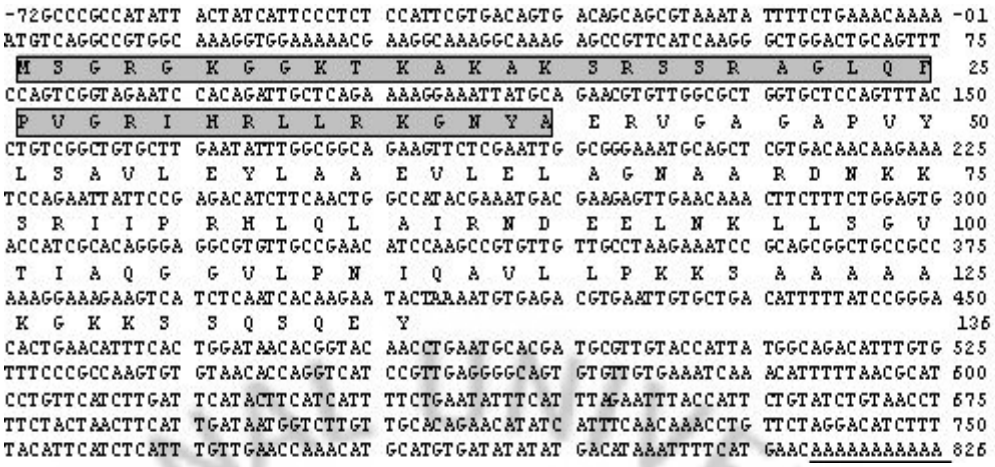

Fig. 35. The complete nucleotide and deduced amino acid sequences of the disk abalone histone H2A cDNA. The nucleotide sequence has been deposited in GenBank under accession number EF103384. The start (ATG) and stop (TAA) codons are in boldface. The predicted N-terminal 40 amino acid sequence, which is used to derive the synthetic abhisin peptide, is in the shaded box. The poly (A) tail is underlined at the end of sequence.

4.3.2.3 Identification and characterization of abhisin peptide sequence from histone H2A

Based on the previous reports on antimicrobial activities of histone and histone-derived peptides (Bulet et al., 2004; Lee et al., 2008; Kim et al., 1996; Fernandes et al., 2002), we were interested to analyze the abalone histone H2A sequence using an antimicrobial peptide predictor program (Wang et al., 2004). Peptide analysis results showed that N-terminal domain of abalone histone H2A has significant similarity with histone-derived AMPs such as buforin I and hipposin. Therefore, 40 amino acids from the N-terminus of histone H2A was selected as a potential histone-derived AMP and named as abhisin. Comparison of abhisin with other histone-derived AMPs is shown in Table 1. The predicted abhisin showed characteristic features of AMPs including remarkably higher overall positive charge (+13), hydrophobic residues (27%) and 2.82 Kcal/mol protein binding potential. Additionally, abhisin has exceptionally higher percentage (6/40=15%) of both arginine and lysine residues. Interestingly, there was no negatively charged aspartate or glutamate residue within the abhisin peptide. The predicted molecular mass of abhisin was 4.32 kDa. Abhisin showed the highest amino acid identity (92%) to scallop histone H2A-derived AMP. Furthermore, it showed 80% and 67% identity to buforin I and hipposin, respectively. ClustalW multiple alignment results showed that 32 residues from abhisin were completely matched with scallop AMP, buforin II and hipposin, which all are H2A-derived peptides (fig. 36). Schiffer-Edmundson helical wheel modeling was employed to predict secondary structure of abhisin (fig. 37). These results demonstrated that abhisin is a linear α-helical molecule, having hydrophobic and hydrophilic residues on opposing sides.

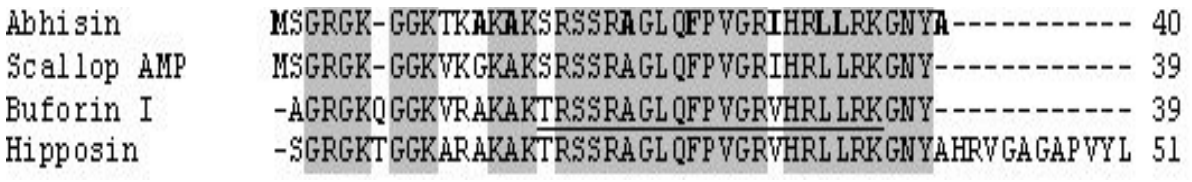

Fig. 36. ClustalW multiple alignment of abhisin with known H2A derived AMPs. Alignment was done with scallop AMP (*Chlamys farreri*), buforin I (*Bufo bufo gargarizans*) and hipposin (*A. halibut*). Hydrophobic residues present in the abhisin are in bold. Buforin II (21 amino acids) derived from buforin I is underlined. The dashes indicate the gaps introduced to maximize the alignment.

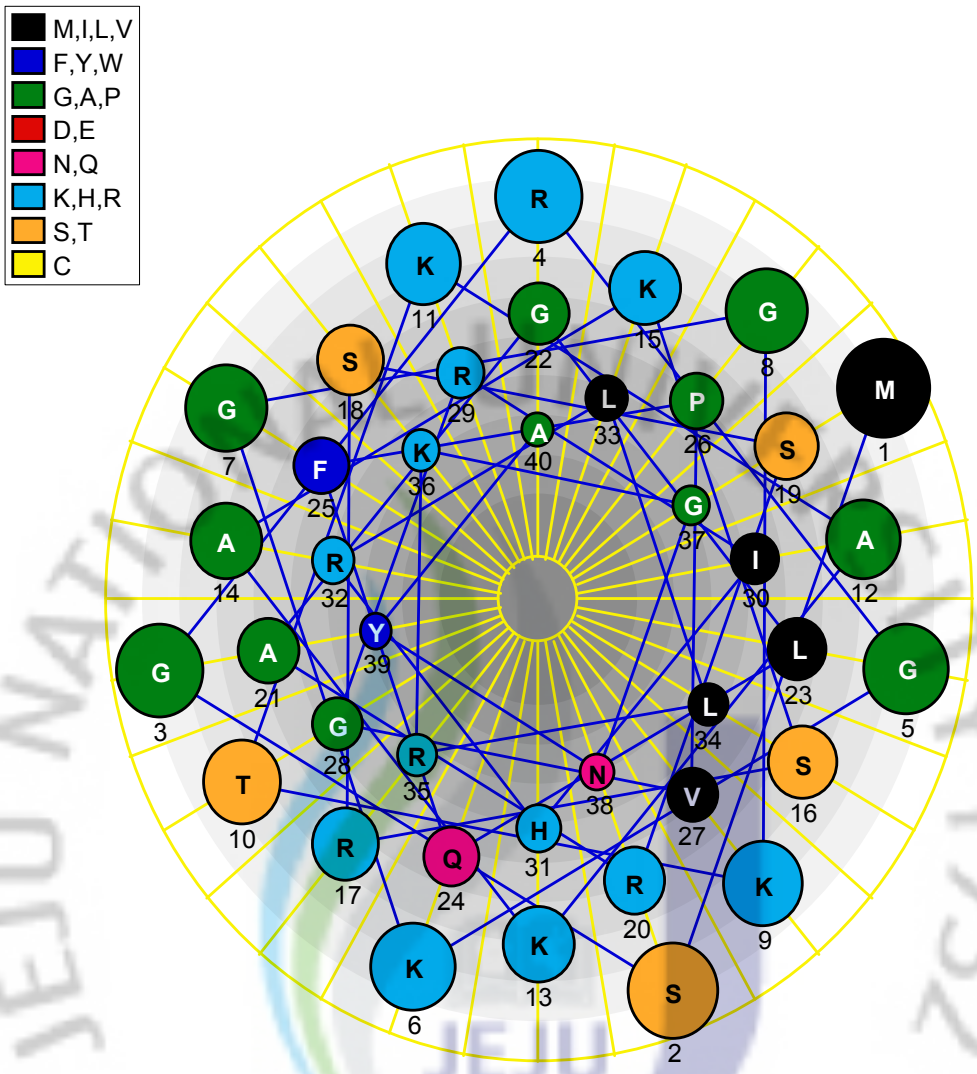

Fig. 37. Predicted α-helical secondary structure of disk abalone abhisin. The α-helical secondary structure was predicted from the N-terminal 40-amino acid length of abalone histone H2A sequence using the DNAstar program and Schiffer-Edmundson helical wheel modeling. Helical wheel shows the amino acid arrangement and residue numbers are counted from the amino (N) terminal of the abhisin.

4.3.2.4. Antimicrobial activity of synthetic abhisin

The antimicrobial effect of the synthetic abhisin was determined against different types of microorganisms, including G+, G- bacteria, and yeast by a liquid growth inhibition assay and an agar disc diffusion assay. Water was used as a control in both assays. The liquid growth inhibition assay results showed that statistically significant ($p<0.05$) growth inhibition of *L. monocytogenes*, *V. ichthyoenteri*, and yeast *P. ovale* by abhisin treatment at 250 µg/mL (fig. 38A). However, abhisin was not able to inhibit the growth of several other G- pathogenic bacteria such as *V. alginolyticus* and *V. parahemolyticus* at 250 µg/mL (data not shown). Interestingly, the highest growth inhibition was observed against yeast *P. ovale* than all of the bacteria tested in this study. Furthermore, ampicillin (positive control) has been shown significant ($p<0.05$) growth inhibition against all the selected microorganisms than control as well as abhisin.

In addition, we checked the antimicrobial effect of abhisin under different concentration by the agar disc diffusion assay. Since there was no significant effect from water in the liquid growth inhibition assay; water treated disc was used as a control in the disc diffusion assay (fig. 38B). Our results showed that growth of *L. monocytogenes*, and yeast *P. ovale* was significantly ($p<0.05$) inhibited by abhisin in a concentration-dependant manner (fig. 38B). However, there was no significant ($p<0.05$) growth inhibition of *V. ichthyoenteri* at 100 µg /disc. It was observed that abhisin elicited the highest DIZ with 15 mm towards *P. ovale* compared to that of *L. monocytogenes* (12 mm) at 100 µg /disc. Furthermore, it was revealed that yeast *P. ovale* was more sensitive to abhisin compared to bacteria *L. monocytogenes* since *P. ovale* growth was significantly ($p<0.05$) inhibited at 50 µg /disc but not the *L. monocytogenes*. The morphology change of *P. ovale* after abhisin treatment was determined by SEM image observation. The results showed that significant destructive effects occurred affecting the integrity of *P. ovale* cells in treated samples compared to un-treated cells as shown in fig. 39.

(A)

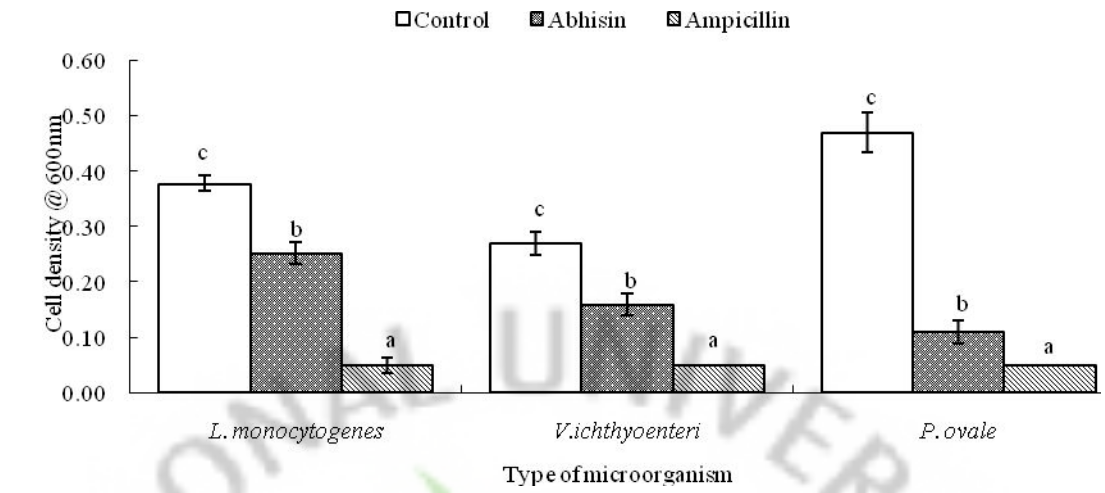

(B)

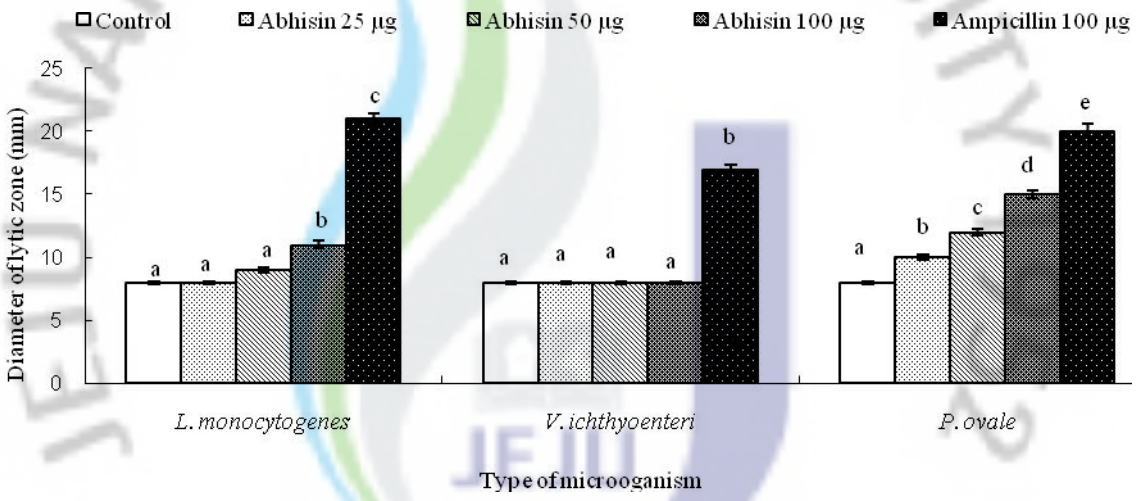

Fig. 38. Comparison of antimicrobial activities of synthetic abhisin against *L. monocytogenes*, *V. ichthyoenteri*, and *P. ovale*. A) In a liquid growth inhibition assay, cell growth was assessed after treatment with abhisin (250 μg/mL) at 30 °C for 24 h by measuring the OD at 600 nm. The cells treated with water and ampicillin (250 μg/mL) were used as negative and positive controls, respectively. B) In an agar disc diffusion assay, serial dilution (0-100 μg) of synthetic abhisin was added on paper disc and plates were incubated at 30 °C for 24 h. The diameter of the clear zone was measured in mm with the diameter of disc (6 mm). The bars indicate the mean ± S.D (n=3). Means with the different letters are significantly different at $p<0.05$ level.

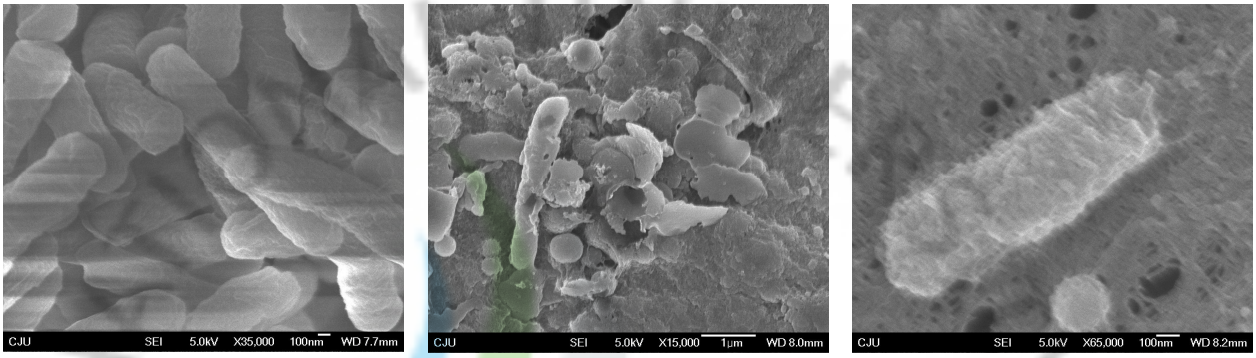

A: Untreated cells B: Treated cells C: Treated single cell

Fig. 39. Scanning electron microscope image of *P. ovale* after treated with synthetic abhisin peptide. Cells were treated with 500 μg/mL abhisin and incubated at 30 ^{o}C for 24 h before the preparation for SEM.

4.3.2.5 Transcriptional responses of abalone histone H2A after bacterial infection

The transcriptional response of histone H2A in gills and digestive tract was analyzed after abalones were infected by pathogenic bacteria mixture including (G+) *L. monocytogenes* and (G-) *V. alginolyticus* and *V. parahemolyticus*. Transcriptional responses of disk abalone histone H2A after bacterial infection are shown in Fig. 12. In gills, histone H2A transcripts were significantly ($p<0.05$) induced (2.2-fold increase) at 3 h, then it was decreased and leveled off to basal level by 48 h (fig. 40A). Furthermore, in gills expression level from 3-12 h was significantly ($p<0.05$) higher than the control group. Histone H2A expression was slightly increased (1.2-fold) only at 3 h in digestive tract and gradually decreased below the basal level after bacterial infection, compared to un-induced abalones (fig. 40B). The highest induced level (1.2-fold increase) of histone H2A was observed in digestive tract tissue at 3 h after bacterial infection. Interestingly, the transcriptional response pattern of histone H2A was similar in both tissues showing the highest level at 3 h. At 48 h post- bacterial infection, expression level was significantly ($p<0.05$) decreased to below the basal (control) level in both gills and digestive tract. However, digestive tract showed significant ($p<0.05$) decrease of histone H2A transcripts in digestive tract than gills.

4.3.2.6. Effect of synthetic abhisin peptide on cell viability

The cytotoxicity of abhisin peptide was tested using normal monkey kidney fibroblast (vero) and human monocytic leukemia cancer (THP-1) cells by MTT assay. As shown in fig. 441, there was no significant ($p<0.05$) cell death occurred in vero cells by abhisin treatment at concentration ranging between 0-50 µg/mL. In contrast, treatment with abhisin at concentration ranging between 10-50 µg/mL resulted the significant ($p<0.05$) dose-dependent decrease of cell viability in THP-1 cancer cells. Furthermore, THP-1 cell viability was decreased approximately by 25% with abhisin treatment at 50 µg/mL.

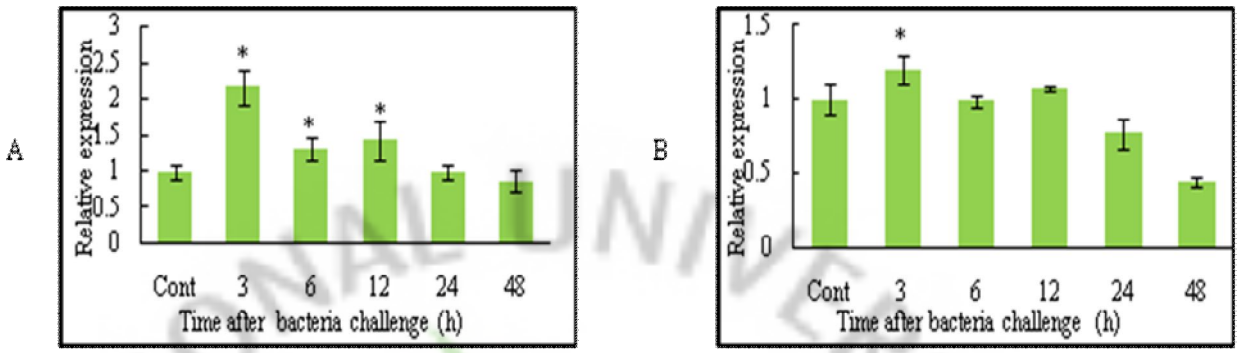

Fig. 40. Transcriptional responses of Histone H2A after bacteria challenge by qRT-PCR. A) gills; B) digestive tract. The relative mRNA expression was calculated by a $2^{-\Delta\Delta CT}$ method using abalone ribosomal protein as a reference gene and relative to a PBS control. Data are presented as mean relative expression ± SD for three replicate real-time reactions from pooled tissue of three individual abalones at each time point. Statistical analysis was performed by one-way ANOVA followed by Duncan's Multiple Range test using SPSS 11.5 program. Differences were considered statistically significant at $P<0.05$ and double asterisk (*) used to indicate the significant induction compared to control.

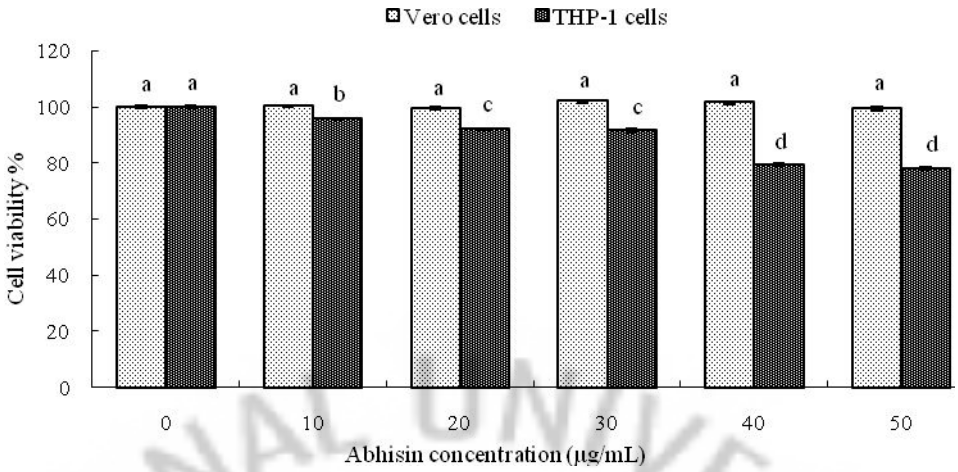

Fig. 41. Effect of synthetic abhisin peptide on cell viability of normal monkey kidney fibroblast (vero) and human monocytic leukemia cancer (THP-1) cells. Vero and THP-1 cells were incubated with synthetic abhisin peptide concentrations (0-50 μg/mL) at 37 ^{o}C for 48 h. Cell viability was determined by MTT assays and represented as percentage respective to the control. The bars indicate the mean ± S.D. (n=3). Means with the different letters are significantly different at $p<0.05$ level.

Table 13: A comparison of abhisin with selected histone-derived AMPs.

AMP property	Abhisin	Scallop AMP [19]	Buforin I [13]	Hipposin [15]
Number of amino acids	40	39	39	51
Amino acid identity to abhisin	-	92%	80%	67%
Total hydrophobic ratio	27%	25%	28%	31%
Total net charge	+13	+13	+13	+15
Protein-binding potential (Boman index) kcal/mol	2.82	2.79	3.08	2.43
Activity	Gram (G)+,G- bacteria, fungi	G+, G- bacteria, fungi	G+, G-bacteria, fungi	G+, G- bacteria
Source	Disk abalone N-terminal domain of histon H2A	Scallop N-terminal domain of histon H2A	Asian toad N-terminal domain of histon H2A	Atlantic halibut N-terminal domain of histon

Antimicrobial peptide sequences were analyzed using an antimicrobial peptide database (APD) (Wang et al., 2004). APD reference numbers of buforin, hipposin are AP00307 and AP00489, respectively.

4.3.2.4. Discussion

In the present study, we described the antimicrobial activity and cytotoxicity of a histone H2A-derived antimicrobial peptide from disk abalone, which is designated as abhisin. Further, we analyzed the transcriptional responses of histone H2A against bacterial infection. In eukaryotic cells, the genome is packed with histone H2A, H2B, H3 and H4 as core histones to form nucleosomes, which are associated with DNA packaging and regulation of transcription (Wyrick et al., 2009). Cloned abalone histone H2A has the characteristic H2A signature domain and over 80% amino acid identities to known H2A counterparts such as *Artemia franciscana* (ABV60391) and *Mytilus californianus* (AY267759). Therefore, based on the identified characteristic features, we could safely define abhisin as a histone H2A derived peptide.

The antimicrobial properties of histones or histone-derived fragments have been described for various vertebrate species. However, there is only one previous report of an antimicrobial peptide derived from mollusk histone H2A in scallop *Chlamys farreri* (Li et al., 2007). Most AMPs share several characteristics, such as a molecular mass of less than 10 kDa, overall net positive charge, hydrophobic and membrane active molecules with multiple arginine and lysine residues (Reddy et al., 2004; Maloy et al., 1995). Similarly, abhisin shows the characteristic features including 4.32 kDa molecular mass, +13 net positive charges, 27% hydrophobic ratio, 2.82 Kcal/mol protein binding potential and 6 arginine and lysine residues each. Also, The characteristic similarities of abhisin with other AMPs (as shown in Table 1) adds weight to evidence that vertebrate and invertebrate H2A-derived AMPs have a common ancestral gene.

Based on the NMR structures and sequence analysis, AMPs are broadly classified into five groups, namely α-helical, cysteine rich, β-sheet, AMPs rich in regular amino acids (histidine, proline, tryptophan) and AMPs with rare modified amino acids (Reddy et al., 20044). Buforin II is a 21 amino acid peptide, which is derived from buforin I. Structural analysis of buforin II showed that it is a linear amphipathic α-helical peptide without any cysteine residues. In addition, buforin II belongs to a major AMP group with cecropins, magainins and dermaseptin. Furthermore, a proline (Pro_{11}) residue is the main structural component of the α-helix structure of buforin II, which is required for its cell penetration properties (Park et al., 1998). Interestingly, only 2 amino acids difference (19/21) was noticed when comparing the buforin II and counterpart sequence of the abhisin peptide. Moreover, abhisin shows similar characteristics to buforin II by containing a single proline residue

(Pro_{26}) and the lack of any cysteine residues. The secondary structure of abhisin was solved using Schiffer-Edmundson helical wheel modeling, and it could be clearly classified as a linear α-helical AMP without cysteine.

As a preliminary experiment, we purified the recombinant abhisin as a MBP using the *E. coli* pMaL protein purification system and assayed for its antimicrobial activity. However, we did not observe significant antimicrobial activity from recombinant abhisin (data not shown). This may be due to neutralization of positive charge (by MBP) of abhisin, which is one of the most important characteristics of AMPs. Interestingly, it was reported that there were no differences in antimicrobial activities between natural and synthetic buforin II (Park et al., 1996). Hence, we focused to check the antimicrobial activity using synthetic abhisin. More importantly, molecular mass of the purified synthetic peptide (4.32 kDa) is in perfect agreement with the predicted peptide by DNAssist. The results obtained herein showed that synthetic abhisin exhibited antimicrobial activity especially at higher concentrations against pathogenic *L. monocytogenes*, *V. ichthyoenteri*, and *P. ovale*, which are representing the G+, G- bacteria and fungi, respectively. The results are consistent with previous studies of scallop AMP, buforin I, and hipposin as summarized in table 11. However, abhisin does not show stronger antimicrobial activity against a wide range of microorganisms as previously reported for H2A-derived AMPs. For example, buforin exhibits stronger antimicrobial activity with very low minimal inhibitory concentrations (MICs) ranging from 0.25-4.0 μg/mL, against G+ and G- bacteria [Cho et al., 2009]. Therefore, a reasonable question arises why the abhisin shows low antimicrobial activity even though it has almost 80% amino acid identity to buforin I. This result may be due to absence of post translational modifications in the synthetic molecule. Li et al., (2007) described that scallop histone H2A-derived AMP has 2.5 times more antibacterial activity against G^+ bacteria than that observed against G^- bacteria. The present study also showed that the G^+ bacteria are more sensitive than G^- bacteria since some *Vibrio* species growth was not inhibited by abhisin treatment. The SEM observation proved that synthetic abhisin could cause considerable morphological damage to treated yeast cells. The damage to the yeast cell wall and cytoplasmic membrane may cause to loss structural integrity, leading to loss of cell content and cell death. However, several possible mechanisms of action were proposed with respect to AMPs against various microorganisms. Park et al., (1998) have shown that buforin II inhibits *Escherichia coli* growth by binding to DNA and RNA of cells, after penetrating the cell membranes. Another AMP named as magainin 2 inhibits bacterial growth by pore-forming activity on the cell membrane, which

operates via a different mechanism than buforin II, even though both are linear amphipathic α-helical peptides (Matsuzaki et al., 1997). Therefore, it seems different mechanisms of action may exist within the same structural groups of AMPs, which highlights the importance of finding the mechanism of antimicrobial activity of abhisin in the near future. However, based on our results, we could suggest that mode of action of abhisin may be similar to either buforin or magainin 2.

Fernandes et al., (2002) suggested that rainbow trout H2A is involved in protection of the cells against bacterial infection. Furthermore, it has been described that an excessive amount of histone H2A is synthesized in toad (*B. bufo gargarizans*) gastric mucosal cells, and the protein is processed by pepsin to derive buforin I. It makes a protective layer of mucous on the stomach surface which provides antimicrobial effects against pathogens (Cho et al., 2009). The conversion of toad histone H2A into buforin I was processed using a specific pepsin by cleaving the amino acid sequence between tyrosine (Y^{39}) and alanine (A^{40}) (Kim et al., 2000). Interestingly, abalone histone H2A has Y^{39} and A^{40} residues at exactly the same positions as reported in toad, suggesting that similar protease cleavage may occur in abalone. To explore this idea, we analyzed the transcriptional responses of histone H2A in abalone gills and digestive tract after bacterial infection. Results showed that histone H2A transcription was induced in gill and digestive tract tissues after the early stages (3 h) of bacterial infection. Therefore, it could be suggested that induction of histone H2A may have defensive role against bacteria accumulating in abalone by direct immune response of histone H2A, or its derived peptide like abhisin. However, it is still unknown how proteolysis of histone H2A occurs in vivo to form an abhisin-like AMP in abalone. In contrast, scallop H2A expression was not induced in hemocytes by bacterial infection with *Micrococcus luteus* and *Vibrio splendidus* (Li et al., 2007). Therefore, a more detailed study of H2A gene expression in response to various microbial challenges is required to gain insight into the role of histone H2A in mollusk immunity.

Lee et al., (2008) described that histone H2A-derived buforin IIb is cytotoxic to cancer cells, but not to normal eukaryotic cells. Similarly, synthetic abhisin has shown cytotoxic effects by reducing cell viability in leukemia cancer (THP-1) cells but not in normal fibroblast vero cells. The outer surface of the plasma membranes of cancer cells contain negatively charged gangliosides while the surface of normal plasma membrane of mammalian cells are generally composed of neutral zwitter-ionic phospholipids and sterols (Lehrer et al., 1993). The selective cytotoxicity against cancer cells was explained as an

interaction of positively charged buforin IIb and negatively charged gangliosides. A similar mechanism may be involved for abhisin in reducing cell viability of THP-1 cellss since both abhisin and buforin IIb have similar peptide residues.

In conclusion, our results clearly demonstrate the first endogenous AMP derived from the N-terminal region of histone H2A in disk abalone. Abhisin is a linear α-helical AMP without cysteine, which represents the main characteristic features of net positive charge and higher hydrophobic residues similar to vertebrate and invertebrate histone H2A derived AMPs. Synthetic abhisin shows antimicrobial activity against pathogenic bacteria and fungi. However, stronger antimicrobial activity was displayed against fungi than bacteria. Abhisin treatment (50 μg/mL) decreased the viability of THP-1 leukemia cells approximately by 25% but not in normal fibroblast vero cells, suggesting that abhisin may have selective cytotoxicity to cancer cells than normal cells. Histone H2A transcription was significantly induced in abalone gills and digestive tract tissues at early stage (3 h) of bacterial challenge then decreased to basal level or below that at 48 h. These results suggest that abhisin is a potential antimicrobial agent and its precursor histone H2A may be involved in the innate immune defense system in abalone.

Finally, identification and characterization of defensin and abhisin as two endogeneous AMPs will expand the understanding of immune systems and their diversity in abalone-like mollusks, as well as it could permit the development of new AMP templates for therapeutic agents in many fields, including medicine and aquaculture.

CHAPTER 5

Antioxidant genes in disk abalone:

Immune responses against bacteria and VHSV challenge

ABSTRACT

ROS are known mediators of intracellular signaling cascades. Generation of ROS cascade starts with the production of $O_2^{\cdot -}$ anion by NADPH oxidase (NOX) complexes. The $O_2^{\cdot -}$ anion is precauser to a variety of ROS that are generally believed to participate in the killing of bacteria, parasite, and other pathogenic invaders during phagocytosis and the respiratory burst. Therefore, diverse antioxidant and immune defense systems are essential for marine invertebrates to overcome oxidative stress ad well as fine tune of immune reactions. This study describes the transcriptional analysis of antioxidant enzymes in gills of un-induced as well as abalone challenged with bacterial (*V. alginolyticus, V. parahemolyticus,* and *L. monocytogenes)* and VHSV using qRT-PCR. All selected antioxidant enzymes were shown constitutive (basal) expression in un-induced abalone gills indicating they all are protecting cells from lethal effects of excessive ROS formation. Abalone catalase showed the highest level expression in among all six antioxidants.

Upon bacteria and VHSV challenge, MnSOD, CuZnSOD, catalase, TPx, SeGPx, and TRx-2 expression levels were regulated differently in the gills, suggesting that they respond collectively as a classical enzymatic antioxidant defense system in abalone. Comparative analysis of expression profiles indicated that MnSOD, catalase and SeGPx transcripts were induced by bacteria and VHSV challenge during 48 h at different levels. CuZnSOD showed immediate down regulation at 3 h and then up-regulation during both bacteria and VHSV challenge. In contrast to CuZnSOD, TPx was immediately up-regulated until 12 h bacteria challenge and then decreased to basal level while it did not show significant change during VHSV challenge. TRx-2 transcription was down-regulated in response to bacterial challenge until 12 h and then increased up-to basal level by bacterial challenge while it was slightly up-regulated against VHSV challenges at all the time points. One of the most significant outcomes of this study was over 5-fold induction of SeGPx, against bacteria and VHSV challenge suggesting that SeGPx is a potential immune marker among antioxidant enzymes, under pathogenic conditions.

Based upon these results, we postulate that abalones may activate the phagocytosis and respiratory burst activity by excessive production of ROS during the bacteria and VHSV challenge. To balance the excessive ROS, abalones utilize antioxidant enzymes to reduce the oxidative stress caused during pathogenic conditions.

5.1. Introduction

Marine organisms are frequently exposed to bacteria, virus and pathogenic infections that enhance the formation of ROS, like superoxide anion ($O_2^{\cdot-}$), hydrogen peroxide (H_2O_2), alkyl peroxides, singlet oxygen ($^1O_2$), and hydroxyl radicals ($OH^{\cdot}$) (Van der Oost et al., 2003). Involvement of ROS in immune response was first characterized in the vertebrate polymophonuclear leukocytes (PMN) (Babior et al., 1973). Ingestion of foreign material through phagocytosis by PMN triggers O_2 uptake and induces rapid and strong production of ROS. Phagocytosis by neutrophils is accompanied by a burst of oxygen consumption known as 'respiratory burst'. This is non-mitochondrial respiration that is accomplished by the NADPH oxidase, a protein complex that assemble in the wall of the phagocytic vacuole and produces $O_2^{\cdot-}$ in the vacuole (Segal, 2005). Also, it has been known that the respiratory burst generates H2O2 that is microbicidal when combined with myeloperoxidase (Iyer et al., 1961).

Oxidative activity is considered as one of the main mechanisms involved in mollusk immune response against invading pathogens. Oxidative mechanisms were reported in the different mollusks including oysters, scallop, mussels, Manila clam (Donaghy et al., 2009). Exposuere of extracellular products from pathogenic *Vibrio aestuarianus* strain was shown to induce ROS production in hemocytes of *C. gigas* (Labreuche et al., 2006). Also, ROS are known mediators of intracellular signaling cascades. On the other hand, excessive production of ROS may lead to oxidative stress, loss cellular function, and ultimately apoptosis and necrosis (Di-Giulio et al., 1989). Therefore, ROS could help to promote the host immune system as well as cellular damage. To get the maximum benefit of ROS organism need to fine balance of ROS level.

Cells possess a complex defense system to protect themselves from oxidative damage due to ROS, using non-enzymatic scavengers and a range of antioxidant enzymes, including SOD, catalase, GPx, TPx and TRx (Roch, 1999). SODs are metal-containing enzymes that catalyze the removal of $O_2^{\cdot-}$, producing H_2O_2 and water as final by-products. Catalases are heme-containing enzymes that catalyze the conversion of H_2O_2 into water and molecular O_2. TPx and PRx are recently discovered enzymes that are capable of reducing peroxides, such as H_2O_2 and alkyl hydroperoxides. GPx removes the H_2O_2 by coupling its reduction with the oxidation of glutathione (GSH) as a substrate. It also can reduce other peroxides, like fatty acids and other hydroperoxides. A thiol-specific TRx antioxidant system plays a vital role among antioxidant defense systems, along with other components like thioredoxin reductase (TRxR). TRx reduces the intracellular disulfides induced by ROS, and

directly lowers ROS levels (Chae et al., 1999; Nordberg and Arner, 2001). Therefore, a defense system that has a diverse array of antioxidant enzymes must exist to reduce the oxidative stress caused by pathogenic infection.

Over the last few years, we have identified and characterized different anti-oxidant genes from disk abalone, allowing us to study their various responses and interactions at a molecular level. In this study, we describe the transcriptional responses of selected antioxidant enzymes in disk abalone gill against bacteria and VHSV challenge.

Table 14: Descriptions of the disk abalone antioxidant genes analyzed in this study

Gene	Basic function	Cellular localization	Reference
Mn-SOD	Detoxification of $O_2^{\cdot-}$	Mitochondria	Ekanayake et al., 2006
Cu,Zn-SOD	Detoxification of $O_2^{\cdot-}$	Cytoplasm	De Zoysa et al., 2009
Catalase	Detoxification of H_2O_2	Cytoplasm, mitochondria, nucleus	Ekanayake et al., 2008
TPx	Detoxification of H_2O_2	Cytoplasm, mitochondria, nucleus	Wickramaarachchilage et al., 2008
SeGPx	Detoxification of H_2O_2	All cell compartments	De Zoysa et al., 2008
TRx-2	Detoxification of H_2O_2	Mitochondria	De Zoysa et al., 2008

5.2. Materials and methods

5.2.1. Identification of abalone antioxidant cDNAs

Abalone antioxidant genes namely Mn-SOD, Cu,Zn-SOD, Catalase, TPx, SeGPx, TRx-2 were identified from abalone cDNA library and functionally characterized in previous studies (table 14).

5.2.2. Experimental abalone and immune challenge

Abalone used for this study was described in section 1.2.2. To determine the immune responses of antioxidant enzymes, three pathogenic bacteria mixture and VHSV were used as in time course experiments. Experimental conditions of abalone challenged with bacteria, and VHSV have been described under the sections of 1.2.3, 1.2.4, 1.2.5, 1.2.6, 1.2.9, 1.2.10 and 1.2.11.

5.2.3. Transcriptional analysis of antioxidant enzymes by qRT-PCR

For this total RNA was extracted from hemocytes, gills and digestive tract using Tri Reagent™ Kit (Sigma, USA) according to manufacturer's protocol (section 1.2.6). Sample of 2.5 μg RNA was used to synthesize cDNA from each tissue using a Cloned AMV first-strand cDNA synthesis kit (Invitrogen, USA) as described in section 1.2.11. Transcriptional analysis was analyzed by qRT-PCR using gene-specific primers of selected antioxidant genes as shown in table. qRT-PCR was carried using a Chromo4^{TM} real-time PCR detector (TaKaRa Japan) as described in section 1.2.11.

5.3. Results

5.3.1. Constitutive expression of abalone antioxidant genes in abalone gills

Basal transcriptional levels of six antioxidant enzymes were investigated in healthy abalone gills under habitat culture conditions. The relative expression of each transcript was normalized to that of MnSOD for the comparison. The results showed that transcripts of all the selected genes were expressed in the gills, though at significantly different levels (fig. 42). More specifically, catalase was expressed at the highest level (6.6 times higher than the level for MnSOD), while SeGPx exhibited the lowest relative level ($p<0.05$). The three antioxidant enzymes - MnSOD, SeGPx and TRx-2 were less expressed than most other enzymes (roughly the same level as for MnSOD) with no significant difference between them. Meanwhile, the expression levels for CuZnSOD and TPx, were significantly higher than for MnSOD, SeGPx and TRx-2.

5.3.2. Transcriptional responses of antioxidant genes against bacteria and VHSV challenge

Expression profiles indicated that MnSOD, catalase and SeGPx transcripts were induced by bacteria and VHSV challenge during the entire 48 h at different levels. In bacterial challenge, MnSOD, catalase and SeGPx showed the highest induction level at 48 h with 1.7, 1.5, 16.1-fold, respectively. On the other hand, in bacterial challenge MnSOD, catalase and SeGPx were shown the highest induction at 12 h (2-fold), 48 h (1.5-fold), 24 h (6.6-fold), respectively (fig 43 ACF). CuZnSOD showed immediate down regulation at 3 h and then up-regulation during both bacteria and VHSV challenge (fig. 43B). The highest transcriptional induction (1.5-fold) of CuZnSOD was detected at 12 h and 24 in VHSV and bacteria challenged gills, respectively. In contrast to CuZnSOD, TPx was immediately up-regulated until 12 h bacteria challenge and then decreased to basal level while it did not show significant change during VHSV challenge (fig 43-D). SeGPx showed remarkably higher up-regulation showing the highest level (6.6-fold) at 24 h in VHSV and (16.1-fold) at 48 h in bacterial challenge (fig 43E). Among all the selected antioxidant genes, SeGPx has shown the most sensitive gene with highest expression difference compared to basal level expression. TRx-2 transcription was down-regulated in response to bacterial challenge until 12 h and then increased up-to basal level by bacterial challenge while it was slightly up-regulated against VHSV challenges at all the time points (fig 43F).

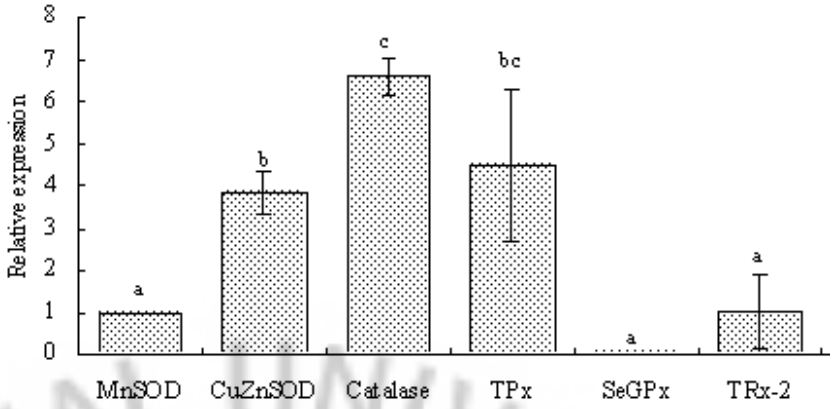

Fig. 42. Transcriptional analysis of abalone antioxidant enzymes in gills. Relative mRNA expression was calculated via the Livak method ($2^{-\Delta\Delta CT}$) using abalone ribosomal protein as a reference gene. The relative expression of each gene was normalized to the expression level of MnSOD. Data are presented as mean relative expression ± SD for three replicate real-time reactions from pooled tissue of three individual abalones. Statistical analysis was performed by one-way ANOVA followed by Duncan's Multiple Range test, using SPSS version 11.5. Differences were considered statistically significant at $p < 0.05$.

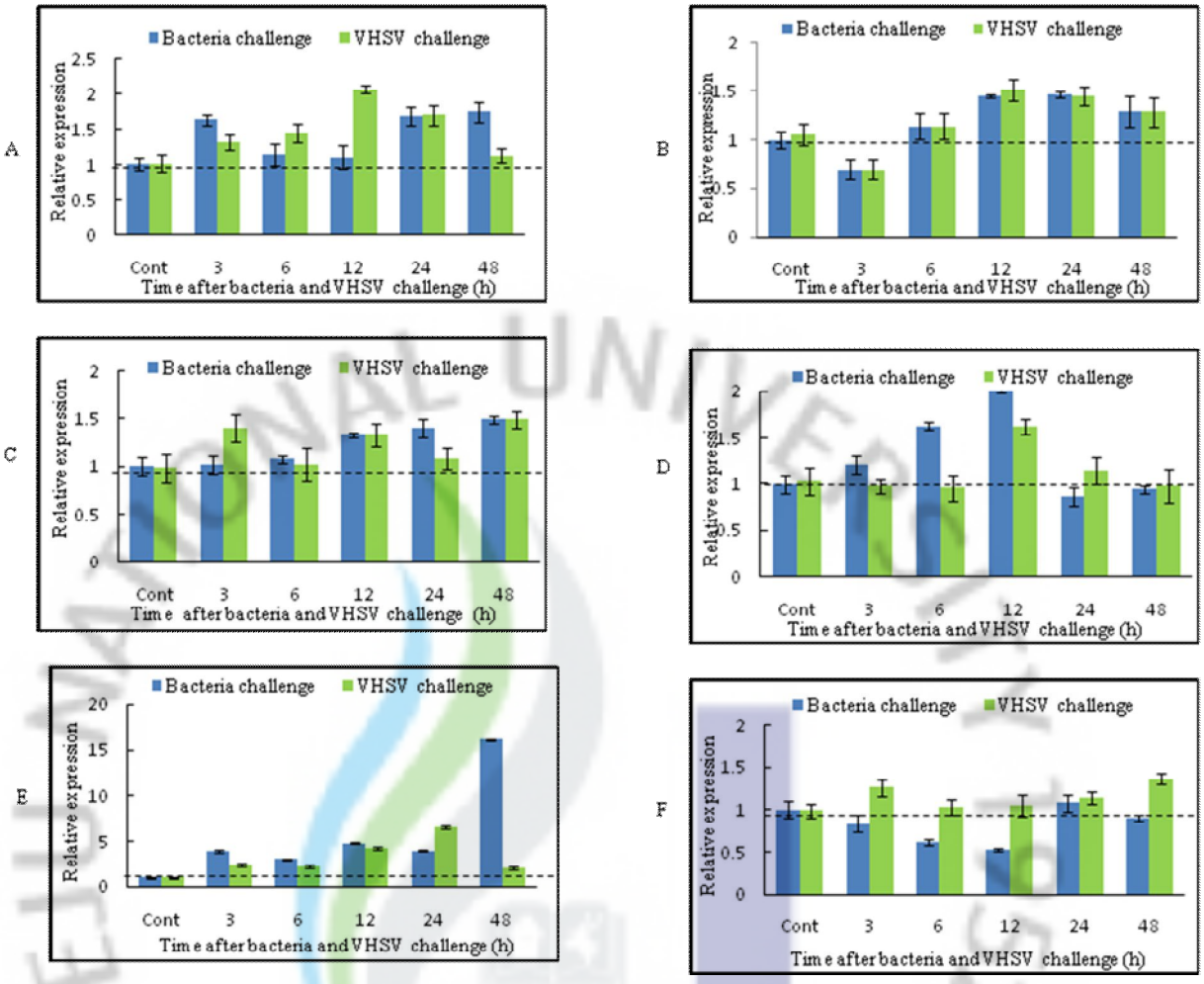

Fig. 43. Transcriptional responses of abalone antioxidant enzymes after bacteria and VHSV challenge by qRT-PCR. The expression fold was calculated by the $2^{-\Delta\Delta CT}$ method using abalone ribosomal protein as a reference gene. Relative fold of each time point was compared to that of control of each immune infection. A) Mn-SOD; B) CuZn-SOD; C) catalase; D) TPx; E) SeGPx; F) TRx-2. Data are presented as mean relative expression ± standard deviation (SD) for three replicate real-time reactions from pooled tissue of three individual abalones at each time point. Dotted line indicates the basal expression level of each gene.

5.3.3. Comparative analysis of antioxidant genes against the bacteria and VHSV challenge

The objective of the comparative analysis was to identify genes with similar responses, so as to better understand stress-immune interactions and select potential genes as immune-markers of pathogenic conditions. Genes were classified into four categories, based upon their expression profiles, using transcriptional regulation. These four categories were: (1) completely up-regulated; (2) completely down-regulated; (3) mixed regulation (up and down-regulated); and (4) no response. MnSOD, catalase, and SeGPx genes were completely up-regulated by both bacterial and VHSV challenge. Among three genes SeGPx showed the highest expression change compared to basal level. In contrast, no gene was completely down regulated by two microbial treatments. Furthermore, expression of CuZn-SOD and TPx was shown mixed responses with up and down regulation during 48 h bacterial and VHSV challenge. Notably, TRx-2 showed down regulation in bacteria challenge except at 24 h. Interestingly, there was no any gene which belongs to not responded group suggesting that all abalone antioxidant genes are sensitive to stress created by pathogen.

5.4. Discussion

Cadenas (1989) described a classical antioxidant defense system that consists of SOD, catalase, thioredoxin, GPx, glutathione reductase and glutathione S-transferase. The presence of SOD, catalase, GPx, and GST enzymatic activity has been reported in the gills of the bivalve *Pinna nobilis* (Box et al., 2009). In our previous reports, we have functionally characterized the MnSOD, CuZnSOD, catalase, TPx, SeGPx and TRx-2, antioxidant enzymes (Table 11). Hence, we introduce all these antioxidant enzymes that collectively represent a classical antioxidant defense system in disk abalone.

The variation in tissue responses to ROS is related to the metabolic capacity of the tissue as well as its antioxidant content. Two authors, Box (2009) and Regoli et al., (1997) have described how mollusk gill requires an efficient antioxidant defense system, since oxygen transfer occurs at the surface of the gill, where there is a greater potential to accumulate excessive ROS. Also, gill is in continuous contact with water, and slight environmental changes could be transferred easily to cellular defense systems. Moreover, our previous results have shown that the most striking changes in antioxidant gene expression occur at this site; hence, we chose gill for our analysis of transcriptional responses. In the present study, the basal expression levels of the various abalone antioxidant enzymes were found to be different in gill tissue. This could be related to the production of ROS via the non-linear function of the electron transport system, as stated by Brand (2000). Taken together, it appears that abalone has an efficient antioxidant system with signaling pathways to prevent the accumulation of excessive ROS by converting $O_2^{\cdot-} \rightarrow H_2O_2$ (MnSOD and CuZnSOD) and $H_2O_2 \rightarrow H_2O + O_2$ (catalase, TPx, SeGPx), and the use of excessive H_2O_2 to oxidize other substrates like reduced glutathione (TPx, SeGPx, TRx). Other than the above reactions, the system also can remove different alkyl (PRx) and lipid peroxides (Se-GPx). Furthermore, it could be suggested that abalone has a lower risk of forming highly toxic $OH^{\bullet}$ radicals from H_2O_2 via a Fenton reaction, because several H_2O_2 removing enzymes (catalase, TPx, SeGPx) exist in gill.

It was reported that increased $O_2^{\cdot-}$ level in shrimp (*L. vannamei*) injected with bacteria *V. alginolyticus* and *V. angularum* (Munoz et al., 2000). In addition SOD activity has been significantly increased in shrimp after injecting *V. alginolyticus*. Also, shrimp GPx transcription was increased significantly at 12 h after *V. alginolyticus* infection (Liu et al., 2007). The increased ROS production by viral infection was associated with changers in the expression of the thioredoxin (Elbim et al., 2001). Present study also has shown upregulation

of different antioxidant enzymes by bacteria and VHSV challenge suggests that it could be direct result of excessive ROS generated by microbial challenge.

The overall conclusion of this study is that abalones have a well-balanced antioxidant enzyme defense system that is sensitive to bacteria and VHSV challenge. It is evident that the transcription of MnSOD, catalase, and SeGPx is up-regulated against bacteria and VHSV challenge. Among the antioxidant enzymes, SeGPx exhibits prominent up-regulation of the transcripts against bacteria and VHSV challenge, suggesting that it has potential use as an immune marker of pathogenic infection. Based upon these results, we postulate that abalones may activate the phagocytosis and respiratory burst activity by excessive production of ROS during the bacteria and VHSV challenge. To balance the excessive ROS, abalones utilize antioxidant enzymes to reduce the oxidative stress caused during pathogenic conditions. Finally, the outcomes of this study could be extended towards a further understanding of stress-antioxidant-immune responses at a transcriptional level.

GENERAL DICUSSION AND CONCLUSION

cDNA microarrays have become a common tool to analyze gene expression profiles in response to stimulation. Generally, these analyses are used for genome-wide screening or for screening large numbers of immune response genes spotted on dedicated microarrays. Incorporation of disk abalone ESTs for constructing a cDNA microarray followed by transcriptional analysis has been resulted to screen novel immune response genes which have not identified previously from mollusks or invertebrates.

The immune genes identified from abalone cDNA library and microarray analysis representing several sub-components of innate immune system of disk abalone. These immune components are classified as immune regulatory pattern recognition proteins, transcription factors, antimicrobial peptides, inflammatory and apoptosis related proteins, IFN and cytokine regulatory proteins, antioxidant enzymes, serine protease inhibitors with other immune relevant genes (Table 15). We found a significant up-regulation of several apparently important genes that represent major immune defense pathway even though other genes in the same pathway have not significantly responded upon bacteria and VHSV challenge. We hypothesized that those genes do not induce immune responses since their high level of constitutive expression to maintain efficient innate immune system in abalone like mollusk.

Our microarray analysis results raveled that it could be used for initial identification of immune relevant genes. Collectively, results from this study show that bacteria and virus (VHSV) modulates the expression of several genes that are implicated in recognition and subsequent downstream signaling through transduction pathways leading to the induction of an innate immune defense response in abalone. Careful analysis of microarray data and further transcriptional conformation by dose dependant and time series immune stimulations/challengers with proper controls can lead to the isolation of genes that are genuinely related to the immune response reactions.

Over all outcome of this research study has potential in molecular understanding of abalone immune system and as well as applications in abalone aquaculture.

1. Many new candidate gene sequences identified from this study greatly enable future studies of immune defense mechanisms in marine mollusks.
2. Resulted immune responded genes could be used as templates for cloning of previously unknown genes in other invertebrate species.

3. Selection of immune marker genes for immunological studies under various immune modulations.
4. Final results would give sound basement for research community to deeper investigation of these mechanisms and comparative analysis in different invertebrate species.
5. Identified genes encoding antimicrobial peptides could be useful for pharmaceutical applications. Ex. Abhisin antimicrobial peptides.

In conclusion, the approach to combine the abalone ESTs with cDNA microarray analysis has been resulted for the screening of abalone genes involved in the defense reaction upon a bacteria and VHSV challenge. This approach has good potential for identifying genes as immune markers involved in abalone defenses against different pathogens. Present study clearly showed abalone innate immune system has a number of diversified gene families under different host defense components. Genes and their proteins involved in the disk abalone immunity include sets of TNF-α, Fas ligand, caspase like inflammatory and apoptosis regulators; NF-kB, LITAF, NFIL-3 C-Jun like transcription factors; SOCS-2 and IFN-44 like cytokine regulators; defensin and histone H2A like AMPs and classical set of enzymatic antioxidant genes. Final outcome of this study provides the linkage of evolutional relationship of immune functional genes between invertebrates and vertebrates with better insight into abalone immune defense as a highly complex and diversified system. Further functional studies on these selected immune response genes involved in the abalone host defense mechanisms have to be initiated in future.

Table 15: Components of immune systems with immune-related genes of disk abalone

Immune system component	Representing genes	Genbank number
Pattern recognition proteins (PRP)	β-1,3 binding protein	EF103355
	Lectin (c type)	ABO26595
Transcription factors	Rel/NF-kB	GQ903763
	LITAF	GQ903762
	NFIL-3	ACJ65688
	AP-1 (C-jun family protein)	ACJ65689
Antimicrobial peptides	Defensin	FJ864724
	Histone AMP	EF103384
	Mx	DQ821495
Inflammatory and apoptosis related	TNF- α	EU863217
	Fas ligand	ACJ12607
	Caspase 8	FJ864721
	Caspase 3 like	FJ864720
	Allograft inflammatory factor	ACJ65689
	Archeron	ACJ65686
IFN and cytokine regulatory proteins	γ-IFN inducible lysosomal thiol reductase	DQ821495
	IFN inducible protein 44	DQ821497
	Suppressor of cytokine signaling (SOCS-2)	FJ380205
Antioxidant enzymes	Mn-superoxide dismutase	DQ821491
	Cu,Zn-Superoxide dismutase	DQ821492
	Catalase	DQ821496
	Thioredoxin peroxidase	EF103376
	Glutathione peroxidase (SeGPx)	EF103379
	Mitochondrial thioredoxin-2	EF103378
	Peroxiredoxin 6	EF103356
Serine protease inhibitors	Antistasin like protein	FJ380206
	Kazal-type proteinase inhibitor	bankit1285369
	Serpin super family protein	bankit1285369
Other immune response proteins	Ferritin	DQ821493
	Leukocyte cell derived chemotaxin 1	FJ864723
	Macrophage migration inhibitory factor	ACJ65690
	Hematopoietic stem cell protein	bankit1285362
	Von Willebrand factor type A	bankit1285360
	Muscle LIM protein	ACJ65685
	Calmodulin	EF103391

References

Abbas AK, Lichtman AH, Pallai S. 2007. Cellular and molecular immunology. 6th ed., Elsevier, Saunders.Aguilar R, Jedlicka AE, Mintz M, Mahairaki V, Scott AL, Dimopoulos G. 2005. Global gene expression analysis of *Anopheles gambiae* response to microbial challenge. Insect Biochem Mol Biol **35**:709-19.

Akira S, Uematsu S, Takeuchi O. 2006. Pathogen recognition and innate immmunity. Cell **124**:783:801.

Altschul SF, Gish W, Miller W, Myers EW, Lipman DJ. 1990. Basic alignment search tool. J Mol Biol **27**:12-7.

Babior BM, Kipnes RS, Curnutte JT. 1973. Biological defense mechanisms: the production by leukocytes of superoxide, a potential bactericidal agent. J Clin Invest **52**:741-744.

Bairoch A, Bucher P, Hofmann K. 1997. The PROSITE data base, its status in 1997. Nucleic Acids Res **25**:217-21.

Baldwin AS Jr. 1996. The NF-kB and IkB proteins: New discoveries and insights. Annu Rev Immunol **14**:649-81.

Bangs P, Franc N, White K. 2000. Molecular mechanisms of cell death and phagocytosis in *Drosophila.* Cell Death Diffren **7**:1027-34.

Bartee E, Mohamed MR, McFadden G. 2008. Tumor necrosis factor and interferon:cytokine in harmony. Curr Opin Microbiol **11**:378-83.

Bassuk AG, Leiden JM. 1997. The role of Ets transcription factors in the development and function of the mammalian immune system. Ad Immunol **64**:65–104.

Birkemo GA, Luders T, Andersen O, Nes IF, Nissen-Meyer J. 2003. Hipposin, a histone derived antimicrobial peptide in Atlantic halibut (*Hippoglossus hippoglossus* L). Biochim BioPhys Acta **1646**:207-15.

Bolcato-Bellemin AL. Mattei MG, Fenton M, Amar S. 2004. Molecular cloning and characterization of mouse LITAF cDNA: role in the regulation of tumor necrosis factor-alpha (TNF-alpha) gene expression. J Endotoxin Res **10**:15-23.

Bridle AR, Morrison RN, Nowak BF. 2006. The expression of immune regulatory genes in rainbow trout, *Oncorhynchus mykiss*, during amoebic gill disease (AGD). Fish Shellfish Immunol **20**:346-64.

Bryant PA, Venter D, Browns RR, Curtis N. 2004. Chips with every thing: DNA microarray in infectious diseases. Infectious Diseases **4**:100-111.

Bulet P, Stocklin R, Menin L. 2004. Anti-microbial peptides: from invertebrates to vertebrates. Immunol Rev **198**:169-84.

Cai J, Wang Z, Cai C, Zhou Y. 2008. Characterization and identification of virulent *Klebsiella oxytoca* isolated from abalone (*Haliotis diversicolor supertexta*) postlarvae with mass mortality in Fujian, China. J Invertbr Pathol **97**:70-5.

Cai L, Wu CD. 1996. Compounds from *Syzygium aromaticum* processing growth inhibitory activity against oral pathogens. J Nat Prod **59**:987-90.

Caput D, Beutler B, Hartog K, Thayer R, Brown Shimer S, Cerami A. 1986. Identification of a common nucleotide sequence in the 3 untranslated region of mRNA molecules specifying inflammatory mediators. Proc Natl Acad Sci USA **83**:1670-74.

Chanchevalp S, Nandan MO, McConnell BB, Charrier L, Merlin D, Katz JP, Yang VW. 2006 KLF-like factor 5 is an important mediator for proinflamatory lipopolysaccharide-induced in intestinal cells. Nucleic Acids Res **34**:1216-23.

Chang PH, Kuo ST, Lai SH, Yang HS, Ting YY, Hsu CL, Chen HC. 2005. Herpes-like virus infection causing mortality of cultured abalone *Haliotis diversicolor supertexta* in Taiwan. Dis Aquat Org **65**:23-7.

Cheng W, Hsiao IS, Hsu CH, Chen JC. 2004. Change in water temperature on the immune response of Taiwan abalone *Haliotis diversicolor supertexta* and its susceptibility to *Vibrio parahaemolyticus*. Fish Shellfish Immunol **17**:235-43.

Cheng W, Juang FM, Chen JC. 2004. The immune response of Taiwan abalone *Haliotis diversicolor supertexta* and its susceptibitlity to *Vibrio parahaemolyticus* at different salinity levels. Fish Shellfish Immunol **16**:295-306.

Cheng W, Li CH, Chen JC. 2004. Effect of dissolved oxygen on the immune response of *Haliotis diversicolor supertexta* and its susceptibility to *Vibrio parahaemolyticus*. Aquaculture **232**:103-15.

Cheng TC, 1996. Hemocytes:forms and functions. In Kennedy VS, NeWell, RIE Eble AF, (Eds), The Eastern Oyster Crassostrea virginica. Maryland Sea Grant Book. College Park MD, USA, pp 299-333. Cho JH, Sung BH, Kim SC. Buforins: 2009. Histone H2A derived antimicrobial peptides from toad stomach. Biochim Biophys Acta **1788**:1564-69.

Cserzo M, Wallin E, Simon I, Vonheijne G, Elofsson A. 1997. Prediction of transmembrane Alpha helices in prokaryotic membrane proteins: Application of the dense alignment surface method. Prot Eng **10**:673-76.

Curtin JF, Cotter TG. 2003. Live and let die : regulatory mechanisms in Fas-mediated apoptosis. Cell Signal **15**:983-92.

Dang DT, Pevsner J, Yang VW. 2000. The biology of the mammalian Krüppell-like family of transcription factors. Int J Biochem Cell Biol **32**:1103-21.

Dhar AK, Dettori A, Roux MM, Klimpel KR, Read B. 2003. Identification of differently expressed genes in shrimp (*Penaeus stylirostris*) infected with white spot syndrome virus by cDNA microarrays. Arch Virol **148**:2381-96.

Dhein J, Walczak H, Baumler C, Debatin KM, Krammer PH. 1995. Autocrine T-cell suicide mediated by APO-1/(Fas/CD95). Nature **373**:438-41.

Dhiman N, Bonilla R, O'Kane JD, Poland GA. 2001. Gene expression microarraysa 21st century tool for directed vaccine design. Vaccine **20**:22-30.

De Zoysa M, Lee J. 2009. Suppressor of cytokine signaling 2 (SOCS-2) homologue in disk abalone: Cloning, sequence characterization and expression analysis. Fish Shellfish Immunol **26**:500-8.

De Zoysa M, Sungju Jung, Jehee Lee. 2009. First molluscan TNF-α homologue of the TNF superfamily in disk abalone molecular characterization and expression analysis Fish Shellfish Immunol **26**:625-31.

De Zoysa M, Nikapitiya C, Moon DO, Whang I, Kim GY, Lee J. 2009. A novel Fas ligand in mollusk abalone: Molecular characterization, immune responses and biological activity of the recombinant protein. Fish Shellfish Immunol **27**:423-32.

De Zoysa M, Pushmamali WA, Whang I, Kim SJ, Lee J. 2008. Mitochondrial thioredoxin-2

from disk abalone (*Haliotis discus discus*): Molecular characterization, tissue expression and DNA protection activity of its recombinant protein. Comp Biochem Physiol **49B**:630-39.

De Zoysa M, Kang HS, Song YB, Jee Y, Lee YD, Lee J. 2007. First report of invertebrate Mx: Cloning, characterization and expression analysis of Mx cDNA in disk abalone (*Haliotis discus discus*). Fish Shellfish Immunol **23**:86-96.

De Zoysa M, Lee J. 2007. Molecular cloning and expression analysis of interferon-γ inducible lysosomal thiol reductase (GILT)-like cDNA from disk abalone (*Haliotis discus discus*).J Invert Pathol **96**:221–9.

Donaghy L, Lambert C, Choi KS, Soudant P. Hemocytes of the carpet shell clam (*Ruditapes decussatus*) and the Manila clam (*Ruditapes philippinarum*): Current knowledge and future prospects. Aquaculture in Press. Eimon PM, Kratz E, Varfolomeev E, Hymowitz SG, Stern H, Zha J, Ashkenazi A. 2006.Delineation of the cell-extrinsic apoptosis pathway in the zebrafish. Cell Death Differ **13**:1619-30.

Ellis A.E. 2001. Innate host defense mechanisms of fish against viruses and bacteria. Dev Comp Immunol **25**:827-39.

Elston RA, Lockwood GS. 1983. Pathogenesis of vibriosis in cultured juvenile red abalone, *Haliotis rufescens* Swainson. J of Fish Dis **6**:111-28.

Eum JH, Seo YR, Yoe SM, Kang SW, Han SS. 2007. Analysis of the immune-inducible genes of *Plutella xylostella* using expressed sequence tags and cDNA microarray. Dev Comp Immunol **31**:1107-20.

Fang Y, Huang YY, Yan JH. 2002. Isolation and observation of "virus disease" of abalone in Dongshan, Fugian. Journal of Oceanography in Taiwan Strait, **21**:199-202.

Feldmann M, Steinman L. 2005. Design of effective immunotherapy for human autoimmunity. Nature **435**:612-19.

Fernandes JMO, Kemp GD, Molle MG, Smith VJ. 2002. Anti-microbial properties of histone H2A from skin secretions of rainbow trout, *Oncorhynchus mykiss*. Biochem J **368**:611-20. Friedman AD. 2002. Transcriptional regulation of granulocyte and monocyte development. Oncogene **21**:3377–90.

Froy O, Gurevitz M. 2003. Arthropod and mollusk defensins-evolution by exon-shuffling. Trends Genetics **19**:684-7.

Furnes C. Seppola M, Robertsen B. 2009. Molecular characterization and expression analysis of interferon gamma in Atlantic cod (*Gadus morhua*). Fish Shellfish Immuol **26**:285-92.

Garcia-Castillo J, Pelegrin P, Mulero V, Meseguer J. 2002. Molecular cloning and expression analysis of tumor necrosis factor alpha from a marine fish reveal its constitutive expression and ubiquitous nature. Immuogenetics **54**:200-7.

Germano G, Allavena P, Mantovani A. 2008. Cytokines as a key component of cancer-related inflammation. Cytokine **43**:374-9.

Gilmore T.D. 2006. Introduction to NF-kB: players, pathways, perspectives. Oncogene **25**:6680-4.

Goetz FW, Planas JV, MacKenzie S. 2004. Tumor necrosis factors. Dev Comp Immunol **28**: 487-97. Goggin CL, Lester RJG. 1995. Perkinsus, a protistan parasite of abalone in Australia: A review. Mar Freshwater Res **46**:639-46.

Gonzales M, Gueguen Y, Desserre G, de Lorgeril J, Romestand B, Bachere E. 2007. Molecular characterization of two isoforms of defensin from hemocytes of the oyster *Crassostrea gigas.* Dev Comp Immunol **31**:332-9.

Gueguen Y, Herpin A, Aumelas A, Garnier J, Fievet J, Escoubas JM, Bulet P, Gonzalez M, Lelong C, Favrel P, Bachere E. 2006. Characterization of a defensin from the Oyster *Crassostrea gigas*. J Biol Chem **281**:313-23.

Han J, Brown T, Beutler B. 1990. Endotoxin-responsive sequences control cachectin/tumor necrosis factor biosynthesis at the translational level. J Exp Med **171**:465-75.

Hancock REW, Brown KL, Mookherjee N. 2006. Host defense peptides from invertebrates-emerging antimicrobial strategies. Immunobiology **211**:315-22. Hayden MS, Ghosh S. 2004. Signaling to NF-kappa B. Genes Dev **18**:2195-224.

Hibino T, Loza-Coll M, Messier C, Majeske AJ, Cohen AH, et al., 2006. The immune gene repertoire encoded in the purple sea urchin genome. Develop Biol **300**:349-65.

Hirono I, Nam BH, Kurobe T, Aoki T. 2000. Molecular cloning, characterization and expression of TNF cDNA and gene from Japanese flounder, *Paralychthys olivaceus.* Immunol **165**:4423-27.

Hirsch JG. 1958. Bactericidal action of histone. J Exp Med **108**:925-44.

Hoffmann A, Baltimore D. 2006. Circuitry of nuclear factor kB signaling. Immunol Rev **210**:171-86.

Hoffmann JA, Reichhart JM, Hetru C. 1996. Innate immunity in higher insects. Curr Opin Immunol **8**:8-13.

Hong YH, Lillehoj HS, Lee SH, Park DW, Lillehoj EP. 2006. Molecular cloning and characterization of chicken lipopolysaccharide-induced TNF-α factor (LITAF). Deve Comp Immunol **30**:919-29.

Hooper C, Day R, Slocombe R, Handlinger J, Benkendorff K. 2007. Stress and immune responses in abalone: Limitations in current knowledge and investigative methods based on other models. Fish Shellfish Immunol **22**:363-79.

Hubert F, Noel T, Roch P. 1996. A member of the arthropod defensin family from edible Mediterranean mussels (*Mytilus galloprovincialis).* Eur J Biochem **240**:302-6. Hughes TK, Smith EM, Chin R, Cadet P, Sinisterra J, Leung MK, et al., 1990. Interaction of Immnoreactive monokines (interleukin 1 and tumor necrosis factor) in the bivalve mollusc *Mytilus edulis*. Proc Natl Acad Sci USA **87**:4426-29.

Igaki T, Kanda H, Yamamoto-Goto Y, Kanuka H, Kuranaga E, Aigaki T, et al. 2002. Eiger, a TNF superfamily ligand that triggers the Drosophila JNK pathway. EMBO J **21**:3009-18. Imler JL, Hoffmann JA. 2000. Signaling mechanisms in the antimicrobial host defense of *Drosophila*. Curr Opin Microbial **3**:16-22.

Iwanaga S, Lee BL. 2005. Recent advances in the innate immunity of invertebrate animals. J Biochem Mol Biol **38**:128-50.

Iwanaga S, Kawabata S. 1998. Evolution and phylogeney of defense molecules associated with innate immunity in horseshoe crab. Front Biosci D973-D984.Jeneway CA, Medzhitov R. 2002. Innate immune recognition. Ann Rev Immunol **20**:197-216.

Jenny MJ, Chapman RW, Mancia A, Chen YA, McKillen DJ, Trent H, Lang P, et al., A cDNA microarray for *Crassostrea virginica* and *C. gigas*. 2007. Mar Biotechnol **9**:577-91.

Jiang Y, Wu X. 2007. Characterization of a Rel/NF-kB homologue in a gastropod abalone, *Haliotis diversicolor supertexta*. Fish Shellfish Immunol **31**:121-31.

Johansson KC, Metzendorf C, Söderhäll K. 2005. Microarray analysis of immune challenged Drosophila hemocytes. Expt Cell Res **305**:145-55.

Kanda H, Igaki T, Kanuka H, Yagi T, Miura M. 2002. Wengen, a member of the *Drosophila* tumor necrosis factor receptor superfamily, is required for Eiger signaling. J Biol Chem **277**:28372-75.

Karin M, Ben-Neriah Y. 2000. Phosphorylation meets ubiquitination: The control of NF-kB activity. Annu Rev Immunol **18**:621-63.

Kaur H, Jaso-Friedmann L, Evans DL. 2004. Single base oligodeoxyguanosine up-regulates Fas ligand release by nonspecific cytotoxic cells. Dev Comp Immunol **28**:571-9.

Kerr JF, Wyllie AH, Currie AR. 1972. Apoptosis: a basic biological phenomenon with wide-ranging implications in tissue kinetics. Br J Cancer **26**:239-57.

Kim HS, Cho JH, Park HW, Yoon H, Kim MS, Kim SC. 2002. Endotoxin-neutralizing antimicrobial proteins of the human placenta. J Immunol **168**:2356-64.

Kim HS, Park CB, Kim MS, Kim SC. 1996. cDNA cloning and characterization of Buforin I, an antimicrobial peptide: A cleavage product of histone H2A. Biochem Biophy Res Comm **229**:381-87.

Klotman ME, Chang TL. 2006. Defensins in innate antiviral immunity. Nat Rev Immunol **6**:447-56. Kono T, Zou J, Bird S, Savan R, Sakai M, Secombes CJ. 2006. Identification and expression analysis of lymphotoxin beta like homologues in rainbow trout *Oncorhynchus mykiss*. Mol Immunol **43**;1390-1401.

Kruys V, Kemmer K, Shakhov A, Jongeneel V, Beutler B. 1992. Constitutive activity of the tumor necrosis factor promoter is cancelled by the 3' untranslated region in non macrophage cell lines; a trans-dominant factor overcomes this suppressive effect. Proc Natl Acad Sci USA **89**:673-77.

Kurobe T, Hirono I, Kondo H, SaitoTaki T, Aoki T. 2007. Molecular cloning, characterization expression and functional analysis of Japanese flounder *Paralichthys olivaceus* Fas ligand. Dev Comp Immunol **31**:687-95.

Laing KJ, Wang T, Zou J, Holland J, Hong S, Bols N, Hirono I, Aoki T, Secombes CJ. 2001.Cloning and expression analysis of rainbow trout *Oncorhynchus mykiss* tumor necrosis factor-alpha. Eur J Biochem **268**:1315-22.

Lamartine J. 2006. The benefits of DNA microarray in fundamental and applied bio-medicine. Material Science and Engineering C **26**:354-359.

Lang RP, Bayne CJ, Camara MD, Cunningham C, Jenny MJ, Langdon CJ. 2009. Transcriptome profiling of selectively bred Pacific oyster *Crassostrea gigas* families that differ in tolerance of heat shock. Mar Biotechnol **11**:650-68.

Lee HS, Park CB, Kim JM, Jang SA, Park IY, Kim MS, Cho JH, Kim SC. 2008. Mechanisms of anticancer activity of buforin IIb, a histone H2A derived peptide. Cancer Lett **271**:47-55.

Li C, Song L, Zhao J, Zhu L, Zou H, Zhang H, Wang H, Cai Z. 2007. Preliminary study on a potential antibacterial peptide derived from histone H2A in hemocytes of scallop *Chlamys farreri*. Fish Shellfish Immunol **22**:663-72.

Li TW, Ding M, Xiang J, Liu R. 1997. Immunological studies on *Haliotis discus hannai*

with *Vibrio fluvialia II*. Oceanologia et Limnologia Sinica **28**:27-32.
Livak KJ, Schmittgen TD. 2001. Analysis of relative gene expression data using real time quantitative PCR and the $2^{-\Delta\Delta CT}$ method. Methods **25**:402-8.
Liu CH, Tseng MC, Cheng W. 2007. Identification and cloning of the antioxidant enzyme, glutathione peroxidase, of white shrimp, *Litopenaeus vannamei*, and its expression following *Vibrio alginolyticus* infection. Fish Shellfish Immunol **23**:34-45.
Liu PC, Chen YC, Lee KK. 2001. Pathogenicity of *Vibrio alginolyticus* isolated from diseased small abalone, *Haliotis diversicolor supertexta*. Microbes **104**:71-7.
Liu PC, Chen YC, Huang CY, Lee KK. 2000. Virulence of Vibrio parahaemolyticus isolated from cultured small abalone, Haliotis diversicolor supertexta with withering syndrome. Lett Appl Microbiol **31**:433-37.
Li Q, Verma IM. 2002. NF-kappa B regulation in the immune system. Nat Rev Immunol **2**:725–34.
Loker ES, Adema CM, Zhang SM, Kepler TB. 2004. Invertebrate immune systems-not homogeneous, not simple, not well understood. Immunol Rev **198**:10-24.
Mah SA, Moy GW, Swanson WJ, Vacquier VD. 2004. A perforin-like protein from a marine mollusk. Biochem Biophys Res Commun **316**:468-75.
Matsuzaki K, Sugishita K, Harada M, Fujii N, Miyajima K. 1997. Interactions of an antibacterial peptide, magainin 2, with outer and inner membranes of Gram-negative bacteria. Biochim Biophys Acta **1327**:119-30.
Meena MR, Sethi V. 1994. Antimicrobial activity of essential oils from spices. J Food Sci Technol **31**:68-70.
McBride SC. 1998. Current status of abalone aquaculture in the Californias. J of Shellfish Res. **17(3)**:593-600.
McGuire K, Glass EJ. 2005. The expanding role of microarrays in the investigation of macrophage responses to pathogen. Vet Immunol Immunopathol **105**:259-75.
Mitta G, Vandenbulcke F, Hubert F, Roch P. 1999. Mussel defensins are synthesized and processed in granulocytes then released into the plasma after bacterial challenge. J Cell Sci **112**:4233-42.
Montagnani C, Kappler C, Reichhart JM, Escoubas JM. 2004. Cg-Rel, the first Rel/NF-kB homolog characterized in a mollusk, the Pacific oyster *Crassostrea gigas*. FEBS Lett **561**:75-82.
Mookherjee N, Hancock REW. 2007. Cationic host defense peptides: Innate immune regulatory peptides as a novel approach for treating infections. Cell Mol Life Sci **64**:922-33.
Morrison RN, Zou J, Secombes CJ, Scapigliati G, Adams MB, Nowak BF. 2007. Molecular cloning and expression analysis of tumor necrosis factor-α in amoebic gill disease (AGD)-affected Atlantic salmon (*Salmo salar L.*) Fish Shellfish Immunol **23**:1015-31.
Munasinghe H, Kang HS, Lee J. 2006. Analysis of digestive gland expressed sequence tag library from the disk abalone, *Haliotis discus discus*. J World Aquac Soc **37**:96-106.
Muta T and Iwanagat S. 1996. The role of hemolymph coagulation in innate immunity Curr Opin Immunol **8**:41-7.
Murphy CJ, Foster BA, Mannis MJ, Selsted ME, Reid TW. 1993. Defensins are mitogenic

for epithelial cells and fibroblasts. J Cell Physiol **155**:408-13.

Myokai F, Takashiba S, Lebo R, Amar S. 1999. A novel lipopolysaccharide-induced transcription factor regulating tumor necrosis factor gene expression: Molecular cloning, sequencing, characterization, and chromosomal assignment. Proc Natl Acad Sci USA **96**:4518-23.

Nishimori E, Hasegawa O, Numata T, Wakabayashi H. 1998. *Vibrio carcharia (harveyi)* causes mass mortalities in Japanese abalone, *Sulculus diversicolor supertexta*. Fish Pathol **33**:495-502.

Nakatsugawa T, Nagai T, Hiya K, Nishizawa T, Muroga K. 1999. A virus isolated from juvenile Japanese black abalone *Nordotis discus discus* affected with amyotrophia. Dis Aquat Org **36**:159-161.

NakatsugawaT. 1990. Infectious nature of a disease in cultured juvenile abalone with muscular atrophy. Fish Pathol **25**:207–11.

Nicolas JL, Basuyaux O, Mazurie J, Bault A. 2002. The *Vibrio carchariae*, a pathogen of the abalone *Haliotis tuberculata*. Dis Aquat Org **50**:35-43.

Nikapitiya N, De Zoysa M, Lee J. 2008. Molecular characterization and gene expression analysis of a pattern recognition protein from disk abalone, *Haliotis discus discus*. Fish Shellfish Immunol **25**:638-47.

Oikawa T, Yamada T. 2003. Molecular biology of the Ets family of transcription factors. Gene **303**:11-34.

Ordas MC, Costa MM, Roca FJ, Lopez-Castejon G, Mulero V, Meseguer J, Figueras A, Novoa B. 2007. Turbot TNFα gene: Molecular characterization and biological activity of the recombinant protein. Mol Immunol **44**:389-400.

Ottaviani E, Franchini A. Franceschi C. 1993. Presence of several cytokine-like molecules in molluscan hemocytes. Biochem Biophys Res Commun **195**:984-8.

Park CB, Kim MS, Kim SC. 1996. A novel antimicrobial peptide from *Bufo bufo gargarizans*. Biochem Biophy Res Comm **218**:408-13.

Park CB, HS Kim, Kim SC. 1998. Mechanism of action of the antimicrobial peptide buforin II: buforin II kills microorganisms by penetrating the cell membrane and inhibiting cellular functions. Biochem Biophys Res Commun **244**:253-7.

Park, EM, Kim YO, Nam BH, Kong HJ, Kim WJ, Lee SJ, Kong IS, Choi TJ. 2008. Cloning, characterization and expression analysis of the gene for a putative lipopolysaccharide-induced TNF-ά factor of the Pacific oyster, *Crassostrea gigas*. Fish Shellfish Immunol **24**:11-7.

Pasparakis M, Alexopoulou L, Douni E, Kollias G. 1996. Tumor necrosis factors in immune regulation: Everything that's interesting is …new. Cytokine Growth Factor Rev **7**:223-9.

Patat SA, Carnegie RB, Kingsbury C, Gross PS, Chapman R, Schey KL. 2004. Antimicrobial activity of histones from hemocytes of the Pacific white shrimp. Eur J Biochem **271**:4825-33.

Paillard C, Roux FL, Borrego JJ. **2004**. Bacterial disease in marine bivalves, a review of recent studies: Trends and evolution. Aquat Living Resour **17**:477-98.

Pal S, Wu J, Wu LP. 2008. Microarray analysis reveal distinct roles for Rel proteins in the *Drosophila* immune response. Dev Comp Immunol **32**:50-60.

Renault T, Novoa B. 2004. Viruses infecting bivalve molliscs. Aquat Living Resour **17**:397-409. Roch P. 1999. Defense mechanisms and disease prevention in farmed invertebrates. Aquaculture **172**:125-45.

Rothstein TL, Wang JK, Panka DJ, Foote LC, Wang Z, Stanger B, Cui H, Ju ST, Marshak-Rothstein A. 1995. Protection against Fas-dependent Th1-mediated apoptosis by antigen receptor engagement in B cells. Nature **374**:163-5.

Saeij JPJ, Stet RJM, De Vries BJ, Van Muiswinkel WB, Wiegertjes GF. 2003. Molecular and functional characterization of carp TNF: a link between TNF polymorphism and trypanotolerance? Dev Comp Immunol **27**:29-41.

Sawabe T, Setoguchi N, Inoue S, Tanaka R, Ootsubo M, Yoshimizu M, Ezura Y. 2003. Acetic acid production of *Vibrio halioticoli* from algibnate: a possible role for establishment of abalone–*V. halioticoli* association. Aquaculture **219**:671-79.

Schena M, Shalon D, Davis RW, Brown PO. 1995. Quantitiaitve monitoring of gene expression patterns with a complementarotry DNA microarray. Science **270**:467.

Sebban H, Courtois G. 2006. NF-kB and inflammation in genetic disease. Biochem Pharmacol **72**:1153-60.

Segal A. 2008. The function of the NADPH oxidase of phagocytes and its relationship to other NOXs in plants, invertebrates, and mammals. Int J Biochem Cell Biol **40**:604-618.

Selsted ME, Ouellette AJ. 2005. Mammalian defensins in the antimicrobial immune response. Nat Immunol **6**:551-7.

Seo JK, Crawford JM, Stone KL, Noga EJ. 2005. Purification of a novel arthropod defenisn from the American oyster, *Crassostrea virginica*. Biochem Biophys Res Commun **338**: 98-104.

Shao JZ, Liu J, Xiang LX. 2004. *Aeromonas hydrophila* induces apoptosis in *Carassius auratus* lymphocytes in vitro. Aquaculture **229**:11-3.

Shepheerd SA, Huchette S. 1997. Studies on southern Australian abalone (genus Haliotis). XVIII. ring formation in *H. scalaris*. Molluscan Res **18**:247-52.

Sigh J, Lindenstrom T, Buchmann K. 2004. Expression of pro-inflammatory cytokines in rainbow trout (*Oncorhynchus mykiss*) during an infection with *Ichthyophthirius multifiliis*. Fish Shellfish Immunol **17**:75-86.

Song J, Sapi E, Brown W, Nilsen J, Tartaro K, Kacinski BM, Craft J, Naftolin F, Mor G. 2000. Roles of Fas and Fas ligand during mammary gland remodeling. J Clin Invest **106**:1209-20.

Spiro RG. 2002. Protein glycosylation: nature, distribution, enzymatic formation, and disease implications of glycopeptides bonds. Glycobiology **12**:43-56.

Suzuki S, Hosono N, Kusuda R. 1997. Detection of aquatic birnavirus gene from marine fish using a combination of reverse transcription, nested PCR. J Mar Biotechnol **5**:2005-209.

Suzuki S, Kamakura M, Kusuda R. 1998. Isolation of birnavirus from Japanese pearl oyster *Pinctada fucata* Fish Sci **64**:342-43.

Tang X, Marciano DL, Leeman SE, Amar S. 2005. LPS induces the interaction of a transcription factor, LPS-induced TNF-α factor, and STAT6(B) with effects on multiple cytokines. Proc Natl Acad Sci USA **102**:5132-7.

Takashiba S, Van Dyke TE, Shapira L, Amar S. 1995. Lipopolysaccharide-inducible and salicylate-sensitive nuclear factor(s) on human tumor necrosis factor alpha promoter. Infect Immun **63**:1529-34.

Thanawongnuwech R, Thacker B, Halbur P, Thacker EL. 2004. Increased production of proinflamatory cytokines following infection with porcine reproductive and respiratory syndrome virus and *Mycoplasma hyopneumoniae*. Clin Diagnos Lab Immunol **11**:901-08.

Tafalla C, Coll J, Secombes CJ. 2005. Expression of genes related to the early immune response in rainbow trout (*Oncorhynchus mykiss*) after viral haemorrhagic septicemia virus (VHSV) infection. Dev Comp Immunol **29**:615-26.

Thompson JD, Higgins DG, Gibson TJ. 1994. CLUSTALW: improving the sensitivity of progressive multiple sequence alignment through sequence weighting, position-specific gap penalties and weight matrix choice. Nucleic Acids Res **22**:4673- 80.

Travers MA, Goic NL, Huchette S, Koken M, Paillard C. 2008. Summer immune depression associated with increased susceptibility of the European abalone, *Haliotis tuberculata* to *Vibrio harveyi* infection. Fish Shellfish Immunol **25**:800-8.

Tsai EY, Falvo JV, Tsytsykova AV, Barczak AK, Reimold AM, Glimcher LH, Fenton MJ, Gordon DC, Dunn IF, Goldfeld AE. 2000. A lipopolysaccharide-specific enhancer complex involving Ets, Elk-1, Sp1; and CREB binding protein and p300 is reqruted to the tumor necrosis factor alpha promoter in vivo. Mol Cell Biol **20**:6084–94.

Tincu JA, Taylor SW. 2004. Antibacterial Peptides from Marine Invertebrates. Antimicro Agen Chemothe **48**:3645-54.

Uenobe M, Kohchi C, Yoshioka N, Yuasa A, Inagawa, H, Morii K, Nishizawa, T,Takahashi Y, Soma GI. 2007. Cloning and characterization of a TNF-like Protein of *Plecoglossus altivelis* (Ayu fish). Mol Immunol **44**:1115-22.

Villena AJ. 2003. Applications and needs of fish and shellfish cell culture for disease control in aquaculture. Rev Fish Biol Fish **13**:111-40.

Xiang LX, Peng B, Dong WR, Yang ZF, Shao JZ. 2008. Lipopolysaccharide induces apoptosis in *Carassius auratus* lymphocytes, a possible role in pathogenesis of bacterial infection in fish. Dev Comp Immunol **32**:992-1001.

Xiao Y, Hughes AL, Ando J, Matsuda Y, Cheng JF, Skinner-Noble D. Zhang G. 2004. A genome-wide screen identifies a single beta-defensin gene cluster in the chicken: implications for the origin and evolution of mammalian defensins.BMC Genomics **5**:56.

Yang ZF, Ho DW, Lau CK, Lam CT, Lum CT, Poon RTP, Fan ST. 2005. Allograft inflammatory factor-1 (AIF-1) is crucial for the survival and pro-inflammatory activity of macrophages. Int Immunol 1-7.

Yazawa R, Kondo H, Hirono I, Aoki T. 2007. Cloning and characterization of the Ik-Bα gene from Japanese flounder, *Paralichthys olivaceus*. Fish Shellfish Immunol **23**:808–14.

Yu JH, Wang PH, Li CY, Xu GR, Chang YQ. 2007. Study on ultrastructure of Juvenile abalone *Haliotis discus hanni* with amyotrophia. Marine Environ Sci **26:**461-65.

Yu Y, Qiu L, Song L, Zhao J, Ni D, Zhang Y, Xu W. 2007. Molecular cloning and characterization of a putative lipopolysaccharide-induced TNF-ά factor (LITAF) gene homologue from Zhikong scallop *Chlamys farreri*. Fish Shellfish Immunol

23:419-29.

Wang Z, Wang G. ADP: 2004. the Antimicrobial Peptide Database. Nucleic Acids Res **32**:590-92. Wajant H, Pfizenmaier K, Scheuich P. 2003. Non-apoptotic Fas signaling. Cytokine Growth Factor Rev **14**:53-66.

Wang KJ, Ren HL, Xu DD, Cai L, Yang M. 2008. Identification of the up-regulated expressiongenes in hemocytes of variously colored abalone (*Haliotis diversicolor* Reeve, 1846) challenged with bacteria. Dev Comp Immunol **32**:1326-47.

Wan Q, Whang I, Lee J. 2008. Molecular characterization of mu class glutathione-S-transferase from disk abalone (*Haliotis discus discus*), a potential biomarker of endocrine-disrupting chemicals. Comp Biochem Physiol **150B**:187-99.

Wang N, Whang I, Lee J. 2008. A novel C-type lectin from abalone, *Haliotis discus discus*, agglutinates *Vibrio alginolyticus*. Dev Comp Immunol **32**:1034-40.

Wang B, Li X, Gou C. 1997. Infection of spherical viruses from *Haliotis discus hannai* Ino.*Virologica Sinica*,**12**:360–63.

Wang Z, Wang G. ADP: the Antimicrobial Peptide Database. 2004. Nucleic Acids Res.**32**:590-92.

Wang XW, Tan NS, Ho B, Ding JL. 2006. Evidence for the ancient origin of the NF-kB/IkB cascade: Its archaic role in pathogen infection and immunity. Proc Natl Acad Sci USA **103**:4204-09.

Watano K, Iwabuchi K, Fujii S, Ishimori N, Mitsuhashi S, Ato M, Kitabatake A, Onoé K. 2001. Allograft inflammatory factor-1 augments production of interleukin-6, -10 and -12 by a mouse macrophage line. Immunology **104**:307-16.

Wickramaarachchilage AP, De Zoysa M, Kang HS, Oh C, Whang I, Kim SJ, Lee J. 2008 Comparative study of two thioredoxin peroxidases from disk abalone (*Haliotis discus discus*): Cloning, recombinant protein purification, characterization of antioxidant activities and expression analysis. Fish Shellfish Immunol **24**:294-307.

Wyrick JJ, Parra MA. 2009.The role of histone H2A and H2B post-translational modifications in transcription:A genomic perspective. Biochem Biophys Res Commun **1789**:37-44.

Zhang A, Wu Y, Lai HWL, Yew DT. 2005. Apoptosis- A Brief Review. Neuroembryology **3**:47-59.

Zhang X, Luan W, Jin S, Xiang J. 2008. A novel tumor necrosis factor ligand superfamily member (CsTL) from *Ciona savignyi*: Molecular identification and expression analysis. Dev Comp Immunol **32**:1362-73.

Zhang D, Jiang J, Jinag S, Ma J, Su T, Qiu L, Zhu C, Xu X. 2009. Molecular characterization and expression analysis of a putative LPS-induced TNF-ά factor (LITAF) from pearl oyster *Pinctada fucata*. Fish Shellfish Immunol **27**:391-6.

Zhang D, Jiang S, Qiu L, Su T, Wu K, Li Y, Zhu C, Xu X. 2009. Molecular characterization and expression analysis of the IkB gene from pearl oyster *Pinctada fucata*. Fish Shellfish Immunol **26**:84-90.

Zou J, Mercier C, Koussounadis A, Secombes C. 2007. Discovery of multiple beta -defensin like homologues in teleost fish. Mol Immunol **44**:638-647.

Zou J, Secombes CJ, Long S, Miller N, Clem LW, Chinchar VG. 2003. Molecular identification and expression analysis of tumor necrosis factor in channel catfish

(*Ictalurus punctatus)*. Dev Comp Immunol **27**:845-58.

ACKNOWLEDGEMENT

I am sincerely grateful to acadmic supervisor Professor Jehee Lee for giving me an opportunity to study in Molecular Genetic Laboratory with excellent guidance, strong encouragement and kind help always to reach my goal during last 5 years. Secondly, I wish to express my gratitude to thesis Director Prof. Gi-Young Kim and members of the thesis committee Prof. Choon-Bok Song, Prof. Moon-Soo Heo, and Prof. Joon Bum Jeong for helpful suggestions, necessary guidance and allowing me to use their laboratory resources. I owe Prof. Ki-Wan Lee, Prof. Kwang-Sik Choi, Prof. Young-Don Lee, Prof. You-Jin Jeon, Prof. In-Kyu Yeo, Prof. Kyeong-Jun Lee for teaching and facilitating their laboratory resources.

My special “remembrance” and thanks go to Dr. Nalin Siriwardhana and Dr. Prashani Ekanayake for introducing me to Prof. Jehee Lee and converting my carrier as a successful researcher.

Also, I wish to give special thank to Dr. Rohan Karawita, Dr. Yasantha Athukorala, Dr. Mahinda Senevirathna, Mrs. Priyantha Samaraweera and Janaka Wijesinghe who helped me numeraous ways during last five years.

I greatly appreciate the unique support given by past and present lab members, Mrs. Ilson Whang, Dr. Chulhong Oh, Dr. Hyun-Sil Kang, Dr. Chamilani Nikapitiya, Dr. Wang-Ning, Young-Deuk Lee, Wan-Qiang, Kyoung-Im Kang, Ho-Jin Park, Su-Kyoung Lee, You-Chul Kim and Hyunjae Kim, Hyowan Kim, Minyoung Oh and Seongdo Lee. Also, I am thankfull and appreciate the support extended by past and present offices and colleagues of other laboratories, especially Dr. Dong-Oh Moon, Dr. Maeng-Jin Kim, Dr. Seon-Heui Cha, Hyun-Ki-Hong in the School of Biomedical Sciences. Also, I wish to thanks all foreign students in JNU for numerous supports.

Korea Research Foundation (KRF), Post BK21 and NURI programs are gratefully acknowledged for the scholarship for my studies and financial support for participating conferences. Also, I am thankfull to Prof. Yeung-Joo Kang Dean of the Graduate School, staff members of Gaduate School and International affairs for kind co-operation and unique service during my period in JNU.

Finally, I owed my humble gratitude to loving parents, relatives, wife Thushari and kids (Maneesha, Manora and Manosha) for being strengthened and stand behind me always to complete my studies successfully.